The University of Nottingham
UK · China · Malaysia

Investigation of NGO1152 and NGO0206 as potential vaccine antigens against *Neisseria gonorrhoeae*

Ali M A Almughrbi

B.Sc., M.Sc.

Thesis submitted in fulfilment of the requirements for the degree of Doctor of Philosophy

March 2025

Molecular Bacteriology and Immunology Group

School of Life Sciences

Faculty of Medicine and Health Sciences

The University of Nottingham, UK

Declaration

I hereby affirm that, except for properly cited works of others, which have been duly acknowledged, the research presented in this PhD thesis is the result of my own research and is entirely my own. Unless explicitly stated otherwise in the text, this work has not been submitted, in whole or in part, for any degree or qualification at any other institution of higher education.

Signature: Ali M A Almughrbi

12th March /2025

PhD Student.
Department: Molecular Bacteriology and Immunology Group.
School of Life Sciences.
University of Nottingham, UK.
Student ID: 20212507

Abstract

Gonorrhoea, caused by *Neisseria gonorrhoeae*, is the second most common bacterial STI worldwide, with the WHO estimating ~82 million new cases in 2020 among individuals aged 15–49 years. Cases in England continue to rise, and surveillance in 2025 reported a sharp increase in ceftriaxone-resistant strains. Growing resistance and the absence of a vaccine complicate disease control. Vaccine development is limited by the scarcity of conserved antigens, lack of human correlates of protection, antigenic variability, and inadequate animal models. Moreover, differences between in *vivo* and in *vitro* gene expression complicate antigen evaluation.

ATP-binding cassette (ABC) transporters are a highly conserved protein family in prokaryotes and eukaryotes. Using ATP hydrolysis, they transport substrates such as metal ions and proteins across membranes, acting as toxin exporters or nutrient importers. Their conservation, essential roles, and surface accessibility make them strong vaccine candidates. NGO1152 and NGO0206 are predicted SBPs of distinct ABC transporters in *N. gonorrhoeae* FA1090. NGO1152 (~30 kDa) is a putative histidine-binding protein with a meningococcal orthologue (NMB1612/NMC1533), while NGO0206 (~41 kDa) is a putative polyamine-binding SBP homologous to NMB0623/NMC0567. Both genes were previously deleted from FA1090, and recombinant His-tagged proteins were expressed, purified, and used to generate rabbit polyclonal antibodies. Although SBPs are typically periplasmic, evidence from *N. meningitidis* MetQ indicates some may be surface exposed. This research evaluated the vaccine potential of NGO1152 and NGO0206.

Hence, Δ*ngo1152* or Δ*ngo0206* mutant strains were complemented by reintroducing *ngo1152* or *ngo0206* at the *iga-trpB* intergenic region under either a constitutive P_{opaB} (pMR32) or an IPTG-inducible promoter (pMR33). PCR confirmed genotypes. Phenotypic analysis by immunoblotting with anti-NGO1152 and anti-NGO0206 antibodies revealed reactive bands at 30 kDa and 46 kDa, respectively, consistent with NGO1152 and NGO0206. IPTG induction restored protein expression in MR331152 and MR330206 to WT-FA1090 levels within 2 h. Unexpectedly, P_{opaB}-driven strains failed to express protein due to upstream transcription defects. *In vitro* growth analyses showed no significant

differences among the WT-FA1090, mutant, and complemented strains, irrespective of IPTG induction.

To evaluate conservation and prevalence, immunoblotting confirmed NGO1152 and NGO0206 expression across 28 clinical isolates. Complementary bioinformatic analysis of 7,327 clinical-isolate genomes from PubMLST found *ngo1152* in 100% of isolates (99.97% predicted to encode a functional protein), whereas ngo0206 was present in 87.9% (87.8% predicted functional); despite its lower prevalence, ngo0206 exhibited limited sequence variability. Pairwise alignment showed limited overall similarity between NGO1152 and NGO0206 (246 residues overlap; 24% identity, 36.6% similarity, 32.9% gaps), but conservation of the N-terminal signal peptide, lipobox and short motifs (*e.g.* YAVPYF/FSDPYF, GFDVDL/GKSGYD), which likely support folding, epitope presentation and reciprocal cross-reactivity of anti-NGO1152 and anti-NGO0206 antibodies. NGO1152 is nearly identical to its *N. meningitidis* orthologue NMB1612 (98.1% identity), confirming its conserved role as an ABC transporter SBP and highlighting its potential as a cross-species vaccine target. By contrast, NGO0206 is more divergent, retaining N-terminal conservation and suggesting functional specialisation relative to NGO1152 and NMB1612.

Surface exposure of NGO1152 and NGO0206 was confirmed by immuno-dot blot analysis, which showed antibody binding to intact WT-FA1090 and IPTG-induced complemented strains, but not to the corresponding mutants. Subcellular fractionation coupled with immunoblotting detected NGO1152 and NGO0206 in outer membrane (OM), cytoplasmic (C), and cytoplasmic membrane (CM) fractions, but not in the periplasmic (PP) fraction. Both proteins were expressed in IPTG-induced complemented strains at levels comparable to WT-FA109 and were absent in mutant and uninduced strains. Whole-cell ELISA (WC-ELISA) showed strong antibody binding to WT-FA1090 and complemented strains, with significantly reduced binding in mutant and uninduced strains and similar patterns were observed across 7 additional clinical isolates. Finally, serum bactericidal activity (SBA) revealed that antisera against NGO1152 and NGO0206 mediated human complement-dependent killing of WT-FA1090. Antisera against NGO0206 exhibited titres of 1:1024–1:2048, whereas antisera against NGO1152 induced even higher titres, up to 1:8192. In

both cases, bactericidal activity was markedly reduced against the corresponding mutant strains. Collectively, these findings demonstrate that NGO1152 and NGO0206 are surface-accessible, conserved, and capable of eliciting human complement-mediated killing of *N. gonorrhoeae*, strongly supporting their potential as vaccine candidates.

Acknowledgements

I begin with profound and humble gratitude to ALLAH, the most merciful, whose infinite wisdom and boundless grace have sustained me throughout this journey. It is by His divine strength and guidance that I have been able to overcome myriad challenges and bring this degree to fruition.

I am deeply indebted to my supervisors, Dr. David Turner and Dr. Neil Oldfield, whose unwavering dedication and exemplary mentorship have been pivotal to my development as a scientist. Their expert guidance, patience, and steadfast commitment throughout my research have profoundly enriched my academic experience. I am especially grateful to Dr. Neil Oldfield for the invaluable opportunity to train under his mentorship and to benefit from his extensive expertise and insightful counsel as part of the Molecular Bacteriology and Immunology Group (MBIG). My sincere thanks are also extended to my principal internal assessor, Dr. Christopher Penfold, whose insightful advice, constructive criticism, and unwavering support have been instrumental in shaping the direction and quality of this work. I would like to express my sincere thanks to Professor Myron Christodoulides, my external examiner from the University of Southampton, for his thoughtful feedback and constructive advice, and for making my viva voce both an encouraging and memorable experience. I am equally grateful to Dr Karl Wooldridge for his insightful advice, constructive feedback, and continued support, which have been instrumental throughout the course of my research.

I further acknowledge the diligent efforts of technician Tyler Harvey-Cowlishaw for her exceptional assistance in procuring materials and her vital technical support within the 97-laboratory of MBIG. I also wish to extend my gratitude to Professor Patrick Tighe for his invaluable mentorship in the laboratory and for the guidance and encouragement that have greatly contributed to both my professional and personal development.

I am deeply grateful to the Libyan Ministry of Higher Education for the generous scholarship and to the Libyan Cultural Attaché in London, UK, for their financial and administrative support, which enabled me to pursue my PhD at the University of Nottingham and my Master's degree at Nottingham Trent

University. With heartfelt appreciation, I also honour my homeland, Libya**,** and my cherished hometown, Benghazi**,** for nurturing my academic aspirations and providing the foundation for my educational journey.

Most of all, I owe an immeasurable debt of gratitude to my beloved parents, Halima and Mohammed, whose prayers, steadfast faith, and steadfast support have been an unceasing source of strength throughout this arduous endeavour. Their nurturing guidance and wisdom have instilled within me a lifelong passion for learning.

To my brothers: Abu Baker, Abudalkarim, Emarajiea, Khalid, Ahmed, Mahmoud, and Saleh and my sisters: Zahra, Haniya, Aisha, and Salmeen, I offer my deepest thanks for their enduring companionship, encouragement, and joyful spirit. This achievement is dedicated to each of you as a testament to your boundless love and support, which have sustained me at every step. I would also like to express my heartfelt gratitude to Azoof for her unwavering support and encouragement throughout my research journey. Special thanks are due to my cherished niece, Fatma, whose constant love and inspiration have been a beacon of light.

I remain profoundly grateful to my Master's supervisor, Dr. Felix Calse, whose encouragement and provision of research opportunities first ignited my passion for scientific inquiry. Through his guidance and example, I developed a lasting commitment to research that continues to shape my academic trajectory and underpins my pursuit of doctoral studies in microbiology. To my closest friends, especially my dearest companion Halim, Shahrukh Khan, and the wider community, I extend my sincere appreciation for their constant encouragement and support. Their kindness has brought me immeasurable joy, comfort, and a profound sense of purpose beyond the academic realm.

Finally, I glorify ALLAH, the source of all my strength and wisdom, for His eternal guidance through every achievement and trial; this accomplishment stands as a living testament to His limitless grace.

List of Presentations

As part of this research project, the key findings and progress were disseminated through the following presentations:

1. **Oral presentation**: **Ali Almughrbi**.
   Substrate binding proteins of ABC transporter systems as vaccine antigens against *N. gonorrhoeae*.
   Presented at the School of Life Science PGR Symposium on July 13, 2023, University of Nottingham, NG7 2RD, UK.

2. **Poster presentation**: **Ali Almughrbi**.
   Substrate binding proteins of ABC transporter systems as vaccine antigens against *N. gonorrhoeae.*
   Presented at the School of Life Science PGR Symposium on July 13, 2022, University of Nottingham, NG7 2RD, UK.

Table of Contents

List of Figures

List of Tables

List of Abbreviations

Abbreviation	Full form
%	Percentage
°C	degrees Celsius
<	Less than
>	Greater than
≥	More than or equal to
~	Approximately
α	Alpha
λ	Lambda
Δ	Delta (deleted/missing)
::	Denote an insertion or integration of a gene of interest
OH	Hydroxyl radical
v/v	Volume/volume
w/v	Weight/Volume
ABC	Adenosine triphosphate (ATP)-binding cassette ABC
(Al (OH)3)	Aluminium hydroxide
AMR	Antimicrobial resistance
ATCC	American-type culture collection
APS	Ammonium Persulfate
BamA	β-barrel assembly machinery A
BCIP	5-bromo-4-chloro-3-indolyl phosphate
BHI	Brain Heart Infusion
BHI-V	Brain Heart Infusion with 1% (v/v) Vitox
BSA	Bovine serum albumin
C	Cytoplasmic
ca.	Approximately
C3	Complement component 3
$CaCl_2$	Calcium chloride
CD	Cluster of Differentiation
CD4+	CD4+: Cluster of Differentiation 4+ (+ sign indicates the presence of the CD4 protein on the cell surface)
CDC	Centre for Disease Control and Prevention
CEACAM	Carcinoembryonic antigen-related cell adhesion molecule
CEACAM-1	Carcinoembryonic antigen-related to cellular adhesion molecule 1 (also known as CD66a)
CO_2	Carbon dioxide
CM	Cytoplasmic membrane
CFU	Colony-forming unit
CPS	Capsular polysaccharides

ECDC	European Centre for Disease Prevention and Control
EDTA	Ethylenediaminetetraacetic acid
ELISA	Enzyme-Linked Immunosorbent Assay
DGI	Disseminated gonococcal infection
DNA	Deoxyribonucleic acid
dATP	Deoxyadenosine triphosphate
dNTP	Deoxynucleoside triphosphate
DUS	DNA uptake sequence
ECF	Energy-coupling factor
EcMetQ	MetQ SBP from *E. coli*
ermC	Erythromycin resistance marker
ESCs	Extended-spectrum cephalosporin
EU	European Union
e.g.	exempli gratia (for example)
FASTA	Fast alignment search tool-all
FBA	Fructose-1,6-bisphosphate aldolase
FDA	Food and Drug Administration (US)
Fe^{2+}	Ferrous
Fe^{3+}	Ferric
FetA	Ferric enterobactin transporter A
fH	Factor H
fHbp	Factor H-binding protein
Fur	Ferric uptake regulator
g	Gram
g/L	Grams per litre
GAPDH	Glyceraldehyde 3-phosphate dehydrogenase
GASP	Gonococcal antimicrobial surveillance programme
GC-B	Gonococcal broth
GC-Hb-V	Gonococcal base agar with 1% (w/v) soluble haemoglobin and 1% (v/v) Vitox.
GRASP	Gonococcal resistance to antimicrobials surveillance programme
Hb	Haemoglobin
H_2O_2	Hydrogen peroxide
dH_2O	Deionized water
HCl	Hydrochloric acid
HIV	Human immunodeficiency virus
hSBA	Human serum bactericidal assay
IFNγ	interferon-γ (IFNγ)
IgA	Immunoglobulin A
IgM1	Immunoglobulin M1
IM	Inner membrane

IPTG	Isopropyl β-D-1-thiogalactopyranoside
iTRAQ	Isobaric Tags for Relative and Absolute Quantitation
Kan^R	Kanamycin resistance cassette
kb	Kilo base pair
kDa	Kilo Dalton
lacI^Q	A mutation in *lac* operon causes the expression of *lac*
lacPOPO	Tandem promoter/operator for gene expression in *Neisseria*
LB	LB Luria-Bertani broth or agar
LOS	Lipo-oligosaccharide
Lpp	Braun lipoprotein
LPS	Lipopolysaccharide
m	Milli- (10^{-3})
M	Molar
mL	Millilitre 10^{-3} moles per litre
mL^{-1}	per millilitre
Mbp	Mega base pairs
MDR	Multidrug-resistant
MenB	Meningococcal serogroup B
MetQ	Methionine-binding periplasmic protein
mg	Milligram
$MgCl_2$	Magnesium chloride
MIC	Minimum inhibitory concentration
min	Minute
MLST	Multilocus sequence typing
mM	Millimolar
MS	Mass spectroscopy
MSM	Men who have sex with men
MsrA/B	Methionine sulfoxide reductase A/B
1min/kb	min per kilobase
NadA	Nada: Neisseria adhesion A
NBD	Nucleotide-binding domain
NCBI	National Centre for Biotechnology Information
Ng	*Neisseria gonorrhoeae*
NG-MAST	*N. gonorrhoeae* multiantigen sequence typing
NgMetQ	*N. gonorrhoeae*- MetQ
NHBA	Neisserial heparin-binding antigen
Nl	*Neisseria lactamica*
Nm	*Neisseria meningitidis*
NmMetQ	*N. meningitidis*- Methionine-binding protein Q
NspA	Neisserial surface protein A
nm	Nanometer

OD	Optical density
OH-	Hydroxide ion
OM	Outer membrane
OmpA	Outer membrane protein A
OMP	Outer membrane proteins
OMV	Outer membrane vesicle
Opa	Opacity-associated adhesin proteins
ORF	Open reading frame
p	Probability value
bp	Base pair
PBP	Periplasmic binding proteins
PP	Periplasmic
PBS	Phosphate buffer saline
PBST	PBS with 0.05% Tween 20
pQE30	plasmid QuikChange Expression Vector 30
PCR	Polymerase chain reaction
pH	Unit of acidity/alkalinity
PHE	Public Health England
PorA/B	Porin A/B
Rmp	Reduction modifiable protein
ROS	Reactive oxygen species
rpm	Revolutions per minute
RT	Room temperature
s	Second
SBA	Serum bactericidal activity
SBP	Substrate-binding protein
SD	Standard deviation
SDS	Sodium dodecyl sulphate
SEM	Standard Error of the Mean
SOC	Super optimal broth with catabolite repression
STI	Sexually transmitted infection
STIRL	STI Reference Laboratory (STIRL)
SHS	Sexual health services
T0/30	Time 0/30 minutes
T4P	Type IV pili
Taq	*Thermus aquaticus* thermostable polymerase
TBDT	Two-Component TonB-Dependent Transporters
TbpA	Transferrin-binding protein A
TbpB	Transferrin-binding protein B
Tbp	Transferrin binding protein
TGF-β	Transforming growth factor-beta
Th2	Type 2 helper T-cell

TMD	Transmembrane domain
TNF-α	Tumour necrosis factor-alpha (TNF-α)
UK	United Kingdom
UKHSA	United Kingdom Health Security Agency
US	United States
UoN.UK	University of Nottingham, UK
V	Volt
VvMetQ	*Vibrio vulnificus*- MetQ
v/v	volume/volume
WHO	World Health Organisation
wt-OMVs	Wild-type outer membrane vesicles
WT	Wild type
XDR	Extensively drug-resistant
× *g*	The centrifugal force is applied as multiples of the earth's gravity (g) (The "g" in "× *g* " represents the acceleration due to gravity, approximately 9.8 m/s² on Earth)
Zur	Zinc uptake regulator
µg	Microgram
µg·mL^{-1}	Micrograms per millilitre
µL	Microlitre
µm	Micrometre

Chapter 1: General introduction

1.1. Family *Neisseriaceae*

The family *Neisseriaceae* consists of the genus *Neisseria* and several heterogeneous genera, including *Moraxella*, *Kingella*, *Eikenella*, *Alysiella*, *Simonsiella*, and *Acinetobacter*, all classified as β-proteobacteria (Rossau *et al.*, 1989). Over the years, *Moraxella* and *Acinetobacter* have been reclassified into the *Moraxellaceae* family based on 16S rRNA gene sequence analysis and whole genome sequencing (Harmsen *et al.*, 2001; Rossau *et al.*, 1986). Members of *Neisseriaceae* are non-spore-forming, Gram-negative, oxidase-positive, and catalase-positive organisms. They can be either aerobic or facultative anaerobes and are typically rod-shaped or coccoid.

The genus *Neisseria*, named after Albert Neisser, who discovered *Neisseria gonorrhoeae* in 1879, is a prominent genus in the family *Neisseriaceae*. It consists of several commensal species and two major human pathogens, *N. gonorrhoeae* and *Neisseria meningitidis* (Johnson, 1983). Members of *Neisseria* are non-motile, diplococci with flattened sides. These bacteria exhibit optimal growth between 35-37°C in the presence of sufficient CO_2 (Platt, 1976). They are known for utilising carbohydrates such as glucose or maltose, producing acid, and reducing nitrite to nitric oxide, except *Neisseria mucosa*, which reduces nitrate to nitrite and breaks down sucrose to polysaccharides (Knapp, 1988).

Currently, the genus *Neisseria* comprises 35 Gram-negative species (Parte, 2018), which predominantly grow under aerobic conditions at temperatures of 35-37°C. Most *Neisseria* species are cocci with a diameter of up to 2 μm, and they typically appear as single bacteria or in pairs (diplococci) (Jorgensen and Turnidge, 2015). The genus includes several species isolated from humans, such as *N. gonorrhoeae*, *N. meningitidis*, *N. cinerea*, *N. elongata*, *N. flavescens*, *N. lactamica*, *N. mucosa*, *N. polysaccharea*, *N. sicca*, and *N. subflava*. Additionally, the genus also contains animal-associated species like *N. animalis*, *N. animaloris*, *N. zoodegmatis* (cats and dogs), *N. denitrificans* (guinea pigs),

N. dentiae (domestic cows), *N. macacae* (rhesus monkeys), and *N. weaveri* (dogs) (Jorgensen and Turnidge, 2015; Liu *et al.*, 2015).

Although most human *Neisseria* species are commensals of the upper respiratory tract and typically cause opportunistic infections in immunocompromised hosts, species of animal origin are rarely associated with human disease, although infections can occur in human wounds following animal bites (Diallo *et al.*, 2019).

The two most clinically relevant species in the genus *Neisseria* are *N. gonorrhoeae* (gonococcus or GC), the causative agent of gonorrhoea, and *N. meningitidis* (meningococcus), which can cause cerebrospinal meningitis and septicaemia. *N. gonorrhoeae* is constantly considered a transmitted pathogen, whereas *N. meningitidis*, a commensal of the human oropharynx, can cause acute disease in otherwise healthy individuals (Harrison *et al.*, 2013).

N. meningitidis is the only *Neisseria* species that expresses a polysaccharide capsule, and it is classified into 12 distinct serogroups based on structural differences between capsular polysaccharides (Harrison *et al.*, 2013).

However, *N. gonorrhoeae* and *N. meningitidis* are fastidious bacteria, requiring specific growth conditions and exhibiting sensitivity to environmental stresses such as extreme temperatures, desiccation, and variations in pH. In contrast, other *Neisseria* species are less nutritionally demanding (e Silva, 2021).

All species in the *Neisseria* genus are naturally competent for DNA uptake and exhibit a high frequency of horizontal gene transfer (HGT), which plays a crucial role in their adaptability and survival under changing environmental conditions (e Silva, 2021).

1.1.1. *N. gonorrhoeae*

Gonorrhoea is a sexually transmitted infection (STI) caused by the bacterium *N. gonorrhoeae.* There were approximately 376 million new bacterial STI cases diagnosed in 2019 worldwide, according to the World Health Organisation (WHO) (Aggarwal *et al.*, 2022). STIs attributable to *N. gonorrhoeae* alone numbered 86.9 million new cases in 2016 (WHO, 2016). This was an increase from the estimated 78 million new cases reported in 2012

(WHO, 2012). Gonorrhoea is most common in the 15 to 49 age group, black Caribbean men and men who have sex with men (MSM) (WHO, 2016).

In 2020, the WHO estimates, there were approximately 82.4 million [47.7 million-130.4 million] new cases of gonorrhoea among adolescents and adults aged 15 to 49 years worldwide (WHO, 2021). This corresponds to an incidence rate of 19 new cases per 1,000 women and 23 new cases per 1,000 men. Most of these cases were reported in the WHO African Region and the Western Pacific Region, highlighting significant geographical disparities in incidence rates (WHO, 2024). In 2020, the Centre for Disease Control and Prevention (CDC) reported a total of 677,769 cases of *N. gonorrhoeae* infections in the United States (US), representing a 10% increase from 2019 and a 45% increase since 2016 (CDC, 2022). Over half of the gonococcal isolates in 2020 were resistant to at least one class of antibiotics, underscoring rising concerns about antimicrobial resistance (AMR).

In 2022, the European Centre for Disease Prevention and Control (ECDC) reported 70,881 confirmed cases of gonorrhoea across 28 European Union/European Economic Area (EU/EEA) countries, corresponding to a notification rate of 17.9 per 100,000 people (Biała *et al.*, 2024; ECDC, 2023). This represents a 48% increase from 2021 and a 59% rise since 2018. The 2022 rate is the highest recorded since European STI surveillance began in 2009 (Biała *et al.*, 2024; ECDC, 2023). In 2022, infection rates varied widely across countries, with some reporting less than one case per 100,000, while others exceeded 75 cases per 100,000. The highest age-specific rates were observed in the 20-24 age group, particularly for men (99.6 per 100,000) and women (48.1 per 100,000), with women in this age bracket experiencing a 63% increase over the previous year. Furthermore, MSM accounted for 60% of reported cases (Biała *et al.*, 2024; ECDC, 2023).

The epidemiological patterns of gonorrhoea in England from 2012 to 2023 demonstrated significant fluctuations, reflecting the intricate dynamics of public health related to STIs (Figure 1.1). In 2012, the number of diagnosed cases was 26,895 per 100,000 population. The diagnostic rate increased consistently over the following years: rising by 15.85% to 31,177 cases in 2013, by 19.50% to 37,150 cases in 2014, and by 11.09% to 41,290 cases in 2015. However, a

notable decline occurred in 2016, with the number of diagnoses decreasing by 11.38% to 36,545 cases. This decline was followed by a significant recovery: in 2017, diagnoses increased by 22.38% to 44,839 cases, in 2018, the number increased by 26.12% to 56,690 cases, and in 2019, it surged by 25.85% to 71,133 cases. The COVID-19 pandemic in 2020 had a major impact, leading to a substantial decrease of 28.80% to 50,678 cases. This downward trend continued into 2021, with a further reduction of 3.87% to 49,321 cases.

In 2022, there was a dramatic rebound, with the number of diagnoses increasing by 60.21% to 79,268 cases. This upward trend continued into 2023, with the number rising by an additional 8.90% to 85,223 cases, which is the highest number since records began in 1918 (UKHSA, 2024).

The incidence of *N. gonorrhoeae* infections in England showed a significant increase between 2018 and 2019, with the total number of reported cases rising from 56,690 to 71,133 (Figure 1.1). The most substantial increase was observed among men who engage in same-sex relationships, with cases rising from 26,864 to 33,853, corresponding to a 26% increase.

A significant rise was also noted among heterosexual women, with cases increasing from 14,167 to 17,826, reflecting a 25.8% increase. As well, the number of cases among heterosexual men increased from 13,036 to 15,253, representing a 17% increase (Wise, 2020).

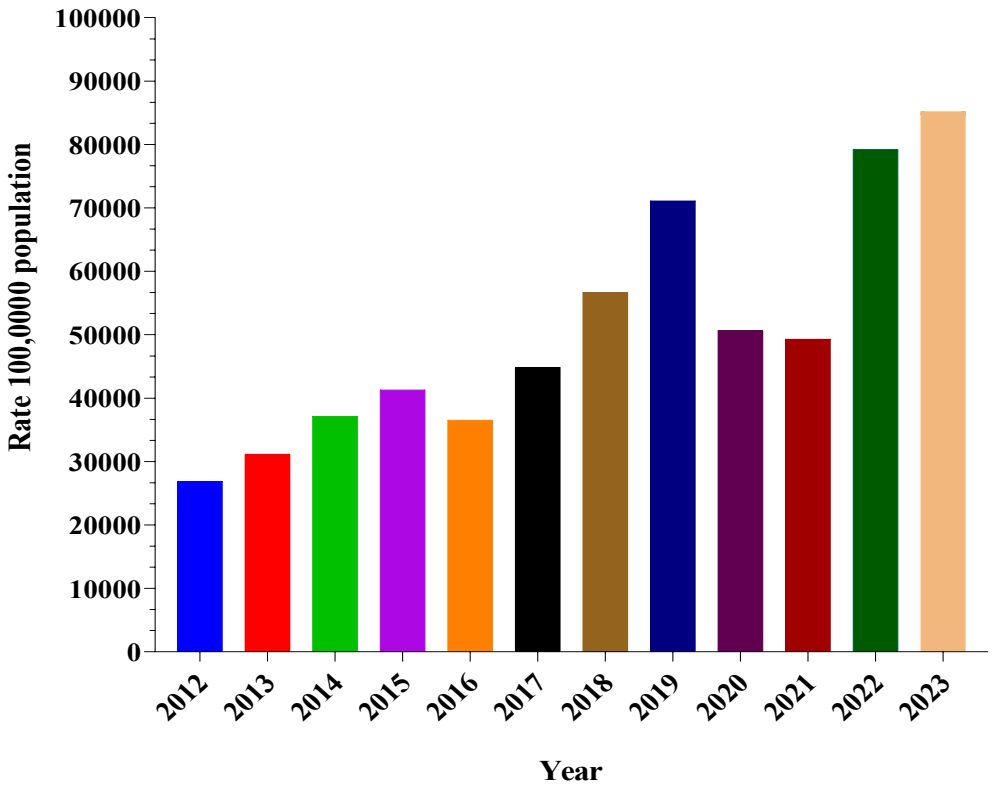

Figure 1.1. Gonorrhoea diagnostic rate per 100,000 population in England between 2012 and 2023, according to the UK Health Security Agency (UKHSA).
The data that were used to generate this figure were adapted from (UKHSA, 2024). Available at: https://fingertips.phe.org.uk/profile/sexualhealth/data#page/4/gid/8000057/pat/159/par/K02000001/ati/15/are/E92000001/iid/90759/age/1/sex/4/cat/-1/ctp/-1/yrr/1/cid/4/tbm/1/page-options/tre-do-1.

These epidemiological data emphasise the need for continuous surveillance and adaptive public health strategies to effectively manage STIs (Elendu *et al.*, 2024). Continuous monitoring and responsive measures are essential to mitigate the impact of healthcare disruptions and public health emergencies on the diagnosis and treatment of gonorrhoea. Several worldwide organisations have categorised *N. gonorrhoeae* as a global threat, particularly with the detection of gonococcal strains that are resistant to the current dual-antibiotic treatment of azithromycin and the extended-spectrum cephalosporins (ESCs), such as ceftriaxone (Unemo *et al.*, 2024).

Amendment to current treatment guidelines for gonorrhoea. Ceftriaxone (a cephalosporin) is now the sole recommended treatment for uncomplicated gonorrhoea, as per updated CDC (2020) and the British Association for Sexual Health and HIV BASHH (2019) guidelines (BASHH, 2019; Cyr, 2020).

Administered as a single 500–1000 mg intramuscular dose, it replaces the previous dual therapy with azithromycin due to rising antimicrobial resistance and emerging azithromycin-resistant *N. gonorrhoeae* strains (BASHH, 2025).

A concerning increase in the number of cases of ceftriaxone-resistant *N. gonorrhoeae* infections has been reported in England. Most cases with ceftriaxone-resistant *N. gonorrhoeae* infections are linked with international travel, especially to and from the Asia-Pacific region, where resistance levels have been documented in up to 30% of isolates in certain countries (UKHSA, 2025).

However, in April 2025, 3 cases of ceftriaxone-resistant *N. gonorrhoeae* were identified in England without any history of international travel: 2 involved heterosexual men who reported sexual contact with sex workers in Leeds, and the third was a female sex worker from the same city (UKHSA, 2025). These isolates exhibited resistance to cefixime, penicillin, ciprofloxacin, and tetracycline, but remained below the EUCAST epidemiological cut-off value (ECOFF) for azithromycin, thus qualifying as multidrug-resistant (MDR). The origin of these infections remains undetermined, raising concerns about additional, undetected cases in Leeds or other parts of the UK. In response, the UKHSA has assembled a local incident management team to oversee the public health investigation and response (UKHSA, 2025).

1.1.2. Pathogenesis of *N. gonorrhoeae*

N. gonorrhoeae is primarily transmitted through vaginal, oral, or anal sex. The bacteria adhere to columnar epithelial cells, penetrate them, and proliferate on the basement membrane, facilitated by pili and Opa proteins (Walker *et al.*, 2023). *N. gonorrhoeae* lipooligosaccharides (LOS) stimulate the production of tumour necrosis factor, which results in cell damage. The bacteria can disseminate via the bloodstream, and strains responsible for disseminated infections often exhibit resistance to serum and complement killing or opsonin-facilitated phagocytosis of the gonococcus (Walker *et al.*, 2023). *N. gonorrhoeae* is a human-restricted pathogen that infects the lower genital tract, pharynx, and rectum, with varying degrees of complications depending on the sex of the patient. Most women with gonorrhoea, between 50% and 80% of cases, are

asymptomatic; however, when symptoms do occur, vaginal discharge is commonly observed (Unemo and Jensen, 2017). Conversely, approximately 90% of gonorrhoea cases in males are symptomatic, typically presenting with purulent penile discharge (Li *et al.*, 2020).

In females, *N. gonorrhoeae* primarily infects the cervix, causing cervicitis, whereas in males, the anterior urethra is the main site of infection, resulting in urethritis. Additionally, the bacteria have also been detected in rectal, conjunctival, and pharyngeal mucosa. *N. gonorrhoeae* has several mechanisms to evade the immune system and colonise cells within the urogenital tract. Spread to other parts of the body, causing pustular skin lesions, septic arthritis, or bacteraemia (referred to as disseminated gonococcal infection [DGI]) has been observed in less than 3% of cases (Jefferson *et al.*, 2021). Although gonorrhoea is most commonly observed in young individuals aged 15–24 years, it can affect any sexually active individual (Li *et al.*, 2020).

Symptoms of gonorrhoea include purulent cervical or urethral discharge, discomfort, dysuria, urethritis, or cervicitis. If left untreated, cervical infection may ascend to the upper genital tract, leading to severe reproductive health issues such as pelvic inflammatory disease (PID), chronic pelvic pain, ectopic pregnancy, and tubal infertility (Lovett and Duncan, 2019). Outcomes may also encompass adverse birth outcomes, ophthalmia neonatorum, various eye disorders, *N. gonorrhoeae* associated with human immunodeficiency virus (Pillai *et al.*, 2012) infections, and other conditions such as epididymitis, proctitis, disseminated gonococcal infection, or male infertility (Lyu *et al.*, 2024). The PID has also been associated with STIs caused by *Chlamydia trachomatis*, the causative agent of chlamydia, and coinfection with *N. gonorrhoeae* frequently (Reekie *et al.*, 2018).

However, PID caused by gonococcal infections typically presents with more severe symptoms (Taylor *et al.*, 2011). Vertical transmission is a significant concern for pregnant women infected with *N. gonorrhoeae*, as it can result in chorioamnionitis, septic abortion, premature rupture, preterm delivery, and sight-threatening neonatal conjunctivitis (Vallely *et al.*, 2021).

In males, untreated urethritis can lead to rare complications such as penile oedema, urethral stricture, epididymitis, or prostatitis. Untreated urogenital gonorrhoea can occasionally disseminate to extragenital sites, causing septic arthritis, endocarditis, and skin manifestations in both sexes (Hakenberg *et al.*, 2017). Additionally, *N. gonorrhoeae* infection increases the risk of acquiring and transmitting other STIs, particularly HIV (Omori *et al.*, 2024).

1.1.3. Immune responses to *N. gonorrhoeae* infection: innate and adaptive

N. gonorrhoeae is known to be significantly adapted to the human host and able to avoid and modify innate and adaptive immune responses (Figure 1.2). Patients can be infected repeatedly and yet develop no immunological memory; this results in recurrent infections (Fung *et al.*, 2007). These infections can be symptomatic or asymptomatic, with the discharge present in symptomatic infection consisting of bacteria and neutrophil granulocytes. As humans are the only natural hosts, this has made laboratory investigations more challenging. Nevertheless, there have been attempts to model *N. gonorrhoeae* modulation and evasion of the immune system. Such research has used an oestrogen-modified murine infection model and immortalised human and murine cell lines (Jerse *et al.*, 2011; Rice *et al.*, 2017).

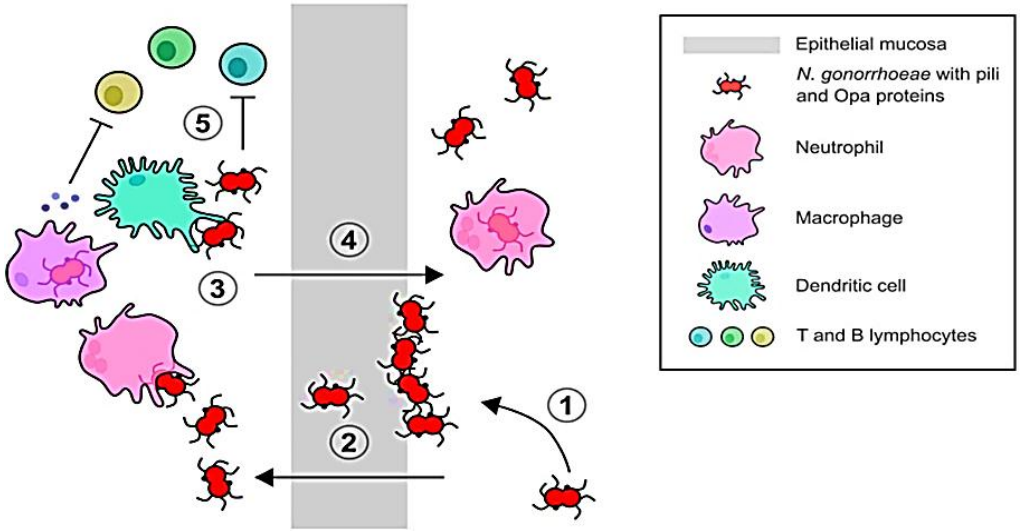

Figure 1.2. Schematic diagram revealing the infection process, transmission pathways, and host immunity modulation by *N. gonorrhoeae*.
1) Bacterial attachment and colonisation are mediated by Opacity (Opa) proteins and Type IV pili (T4P). 2) The host epithelium is colonised and invaded, with transcytosis through the epithelial mucosa. 3) Local mucosal immune cells are stimulated, prompting the host to mount an immune response. 4) Bacteria are discharged via a neutrophil-rich exudate. 5) The T and B lymphocyte immune response is modulated. That response occurs when phagocytic cells stimulate proinflammatory cytokines and chemokines, thus suppressing a Type 1 helper T-cell (Th1) or Type 2 helper T-cell (Th2) immune response and elevating a Type 17 helper T-cell response (Haese *et al.*, 2021). Th1 cells promote cellular immune response, and inhibition of the macrophage stimulation leads to the activation of the B cells to produce IgM and IgG1. Furthermore, the Th2 activation humoral immune response induces B cell proliferation and antibody production of interleukin-4 (IL-4) (Winer *et al.*, 2011). Figure adapted from (Haese *et al.*, 2021).

There are various mechanisms by which *N. gonorrhoeae* evades and modulates the host's immune system. One well-documented way is via antigenic and phase variation of surface exposed Opa proteins and T4P in the outer membrane (OM) (Cahoon and Seifert, 2011). Additional strategies involve LOS epitope mimicry and subversion of phagosomal processes (Huynh *et al.*, 2007). The Opa52 protein from the *N. gonorrhoeae* MS11 strain, commonly known as Opa5, is one of the 10 to 12 Opa proteins found in *N. gonorrhoeae*. It has been shown to bind to a specific molecule on activated human Cluster of Differentiation 4 (CD4+) T lymphocytes: the carcinoembryonic antigen-related to cellular adhesion molecule 1 (CEACAM-1, also known as CD66a). CD4 is found on the surface of immune cells such as T helper cells, monocytes, macrophages, and dendritic

cells (Hilligan and Ronchese, 2020). The Opa interaction causes downregulation of antigenic activation and proliferation of CD4+ lymphocytes. Nevertheless, an interesting finding (Zariri *et al.*, 2013) demonstrated that Opa-CEACAM-1 binding did not affect the host's immune response against outer membrane vesicles (OMVs), even though it reduced Opa-specific antibody titres in a human-CEACAM-1 transgenic mouse model. As such, this type of binding may not affect a future gonococcal vaccine.

The host's immune responses are also modified by the interaction of *N. gonorrhoeae* with local mucosal immune cells. The key OM porin B (PorB), in a manner like Opa proteins, inhibits the dendritic cell stimulation of CD4+ T cells, downregulating their proliferation (Zhu *et al.*, 2018). Bacterial replication is not controlled by either resident mucosal macrophages or recruited monocytes and neutrophils, which fail to control *N. gonorrhoeae* replication during an infection (Escobar *et al.*, 2018). It is thought that inflammatory and immunosuppressive responses are elevated by *N. gonorrhoeae*. That elicits increased expression of tumour necrosis factor-alpha (TNF-α), a pro-inflammatory cytokine, in human macrophages (Château and Seifert, 2016).
N. gonorrhoeae may also stimulate the expression of the immunoregulatory cytokines interleukin-1 (IL-1), (IL-6), (IL-8), (IL-10) and TNF-α in human macrophages. The T cell-stimulating factor interleukin-12 (IL-12), which plays a crucial role in the Type 1 helper T cell (Th1) response, was exclusively detected in human monocyte-derived macrophages (MDMs) that had been subjected to gonococcal challenge (Château and Seifert, 2016).

In murine models, infected macrophages were found to express transforming growth factor-beta (TGF-β) and IL-10; these are both immunoregulatory cytokines, but proinflammatory cytokine TNF-α was not detected (Escobar *et al.*, 2013). Additionally, there was no evidence of increased co-stimulatory CD86 nor up-regulation of major histocompatibility complex class II molecules (Escobar *et al.*, 2013), suggesting that the antigen-presenting cells may have developed a tolerogenic phenotype. In addition, IL-12, a T-cell-stimulating factor that is integral to the Th1 response, was found only within infection-challenged macrophages obtained from MDM (Château and Seifert, 2016).

In addition, the MDM challenged with *N. gonorrhoeae* have also been reported to differentiate toward a macrophage 2 (M2) profile (Tramont and Boslego, 1985). When a host is exposed to gonorrhoeal infection, macrophage 1 (M1) macrophages become divided between the typical pro-inflammatory M1 type or the anti-inflammatory and pre-resolving M2 type, influenced by factors such as the pathogen virulence and mediation by the host immune system (Viola *et al.*, 2019). The Th1 response is generated by the M1 phenotype, which has effective tumoricidal and microbicidal properties (Sica and Mantovani, 2012). The M2 phenotype promotes immunoregulatory activities such as reducing inflammation, clearance of infection, remodelling of tissues and regression of tumours (Escobar *et al.*, 2018). The MDM has been found to gravitate towards the M2 profile when exposed to gonococcal infection (Ortiz *et al.*, 2015).

During infection, *N. gonorrhoeae* may contribute to poor host immunity by stimulating a Th17 response while suppressing Th1 and Th2 responses in Figure 1.2. This immune profile is typically associated with neutrophil influx and the activation of non-protective inflammatory mechanisms (Feinen *et al.*, 2010; Liu *et al.*, 2012). Researchers have suggested that immunity could be affected by the presence of antibodies targeting the surface Reduction modifiable protein (Rmp) (also known as protein III), as these antibodies prevent gonococcal surface antigens from being targeted by bactericidal antibodies (Gulati *et al.*, 2015).

Thus, *N. gonorrhoeae* can evade and modulate the host immune system through multiple mechanisms. The result is that individuals fail to develop immunological memory of gonococcal infection and therefore remain vulnerable to repeated gonorrhoeal disease. That may in part explain the unsuccessful attempts to develop a protective vaccine against *N. gonorrhoeae*, with vaccines based on killed whole cells, PorB or a single antigen pilus, all proving ineffective (Colón Pérez *et al.*, 2024).

1.2. Treating *N. gonorrhoeae* with antibiotics: past and present treatment regimens

Gonorrhoea has been treated with various antibiotics since sulphonamides in the 1930s (Figure 1.3). Treatment changes have been driven by antibiotic resistance in *N. gonorrhoeae*, partly due to efflux pump overexpression and altered drug targets (Unemo, 2015).

Gonococcal strains resistant to all previous monotherapies, including penicillin, sulphonamides, first-generation cephalosporins, fluoroquinolones, tetracyclines and streptomycin, have emerged (Rice *et al.*, 2017). For example, mutations in the *fo1P* gene reduced binding between sulphonamide and its target, dihydropteroate synthase, leading to sulphonamide resistance (Rice *et al.*, 2017). Resistance to penicillin, which was used to treat gonorrhoea from the early to mid-20th century, arose with the emergence of *N. gonorrhoeae* strains that had a specific enzyme, plasmid-mediated β-lactamase, which deactivates β-lactam antibiotics. The utility of tetracycline was hampered by the emergence of *N. gonorrhoeae* strains that possessed a ribosomal protection protein, TetM (Rice *et al.*, 2017).

Fluoroquinolones were subsequently used, but genetic mutations in the *gyrA* and *parC* genes reduced drug binding to gyrase and topoisomerase IV; this resulted in *N. gonorrhoeae* strains that were resistant to ciprofloxacin. As depicted in Figure 1.3, the year 2007 saw the removal of fluoroquinolones from the ECDC guidelines (ECDC, 2012). Injectable ceftriaxone or oral cefixime represented the last attempt at single-drug therapy for gonorrhoea. In 2012, however, increasing antibiotic resistance saw the CDC move away from recommending cefixime (Pitasi *et al.*, 2019).

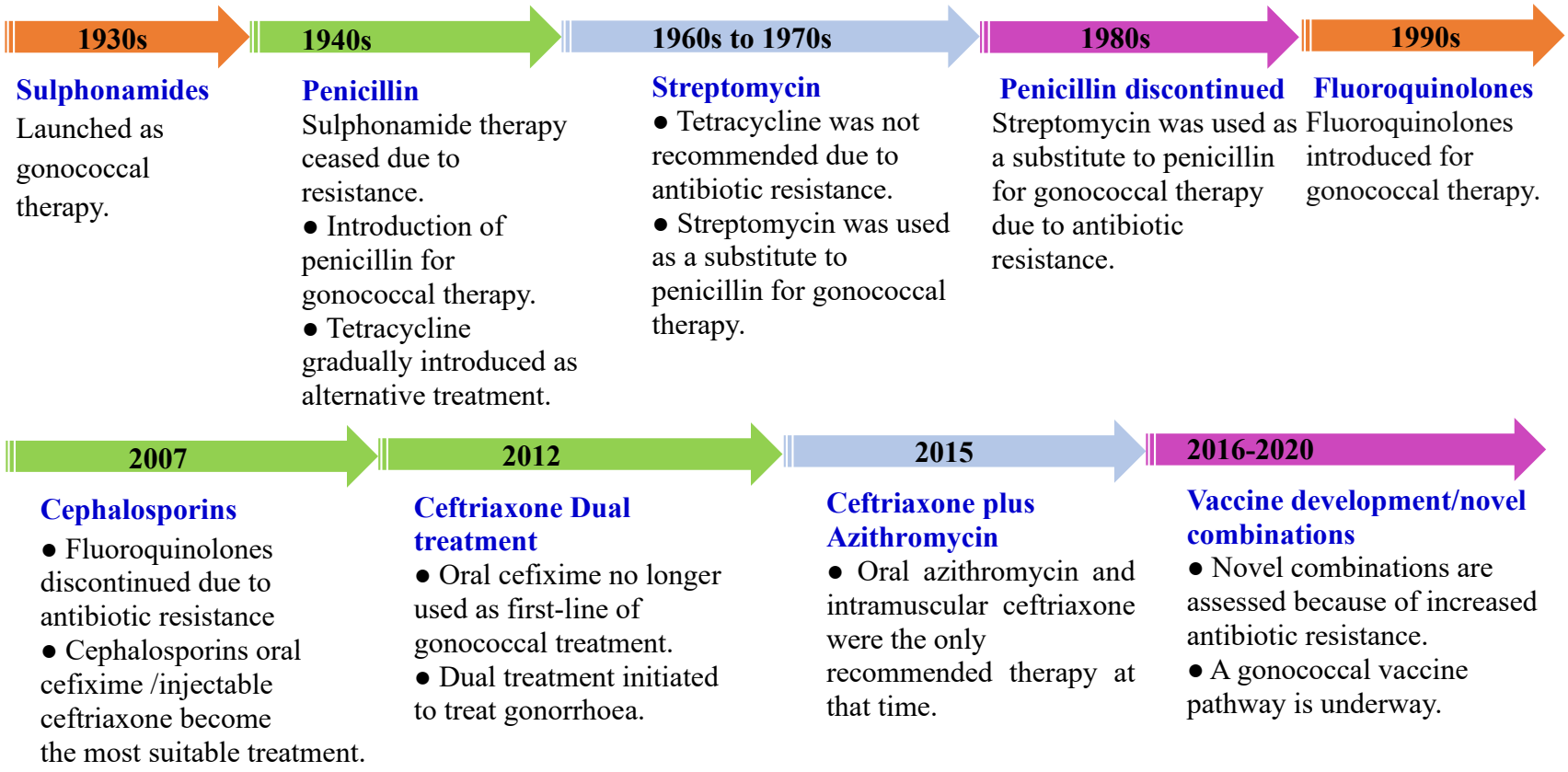

Figure 1.3. Drug treatments for *N. gonorrhoeae* infections over time.
The figure presents data adopted with modifications from (Jefferson *et al.*, 2021).

Furthermore, for several years, cefixime treatment failures have been recognised in Japan (Deguchi *et al.*, 2003; Tapsall *et al.*, 2009; Yokoi *et al.*, 2007), where cefixime was already excluded from treatment guidelines in 2006 (Tapsall *et al.*, 2009).

Effective antimicrobial therapy is essential for preventing *N. gonorrhoeae* infections. The rising incidence and prevalence of multidrug-resistant (MDR) and extensively drug-resistant (XDR) strains have heightened concerns regarding the potential for widespread, untreatable gonorrhoea (Unemo *et al.*, 2019). Treatment failures of oropharyngeal gonorrhoea with ceftriaxone monotherapy have been documented in various countries (Golparian *et al.*, 2014). For example, it has been recorded that the first high-level ceftriaxone-resistant gonococcal strain (H041) exhibits high resistance to cefixime (oral) and ceftriaxone (injectable), which are the last remaining options for first-line gonorrhoea monotherapy. H041 was isolated from the pharynx of a female commercial sex worker in Kyoto, Japan (Ohnishi *et al.*, 2011).

In addition, H041 exhibited a minimum inhibitory concentration (MIC) for ceftriaxone that was 4- to 8-fold higher, ranging from 2 to 4 μg/mL, indicating an exceedingly elevated level of resistance. Prior to this, only one isolate with an MIC of 0.5 μg/mL had been reported (Tanaka *et al.*, 2006). H041 is classified under the internationally spreading multilocus sequence typing (MLST), sequence type 7363 (ST7363). This sequence type is closely related to subclones that exhibit high-level resistance to the antibiotics cefixime and ceftriaxone, which have been particularly prevalent in Japan (Ohnishi *et al.*, 2010) and are now also being transmitted in Europe. It may be a subclone of ST7363 with additional resistance determinants, confirming decreased susceptibility and resistance to ESCs and MDR in many countries discussed below (Golparian *et al.*, 2010).

Historically, gonococcal AMR has predominantly emerged in the WHO Western Pacific Region (WPR) and, particularly, Japan has been a notable epicentre over the years. This resistance has spread rapidly, via sex tourists, long-distance truck drivers, and forced migration in the WPR, to the Pacific Rim countries, including

the US, Southeast and Central Asia, Europe, and on a global scale (Huang *et al.*, 2010).

Recent treatment failures for gonorrhoea with cefixime in Norway (Unemo *et al.*, 2010), Austria (Unemo *et al.*, 2011), and the UK (Ison *et al.*, 2011) were caused by the MLST ST1901 clone. This clone appears to have evolved into multiple different *N. gonorrhoeae* multiantigen sequence typing (NG-MAST) STs, which most likely originated in Japan and subsequently spread globally (Unemo *et al.*, 2012).

Strain F89, which is the second *N. gonorrhoeae* strain globally to demonstrate high-level resistance to ESCs such as cefixime and ceftriaxone, was isolated from a urethral specimen of a 50-year-old MSM during a test of cure in June 2010 in Quimper, France (Unemo *et al.*, 2012). Strain F89 also demonstrated resistance to nearly all antimicrobials previously utilised for gonorrhoea treatment, including fluoroquinolones, macrolides, tetracycline, trimethoprim-sulfamethoxazole, and chloramphenicol. Furthermore, F89 showed high-level resistance to cefixime (MIC = 4 μg/mL; actually, 3 μg/ mL according to the Etest method), ceftriaxone (MIC = 1 μg/mL [agar dilution] to 2 μg/mL [Etest, 1.5 μg/mL]), and all additional ESCs tested (Ohnishi *et al.*, 2011). Unexpectedly low MICs were observed for the β-lactam antibiotics, including penicillin G, ampicillin, piperacillin, and the carbapenems ertapenem and meropenem. The strain did not exhibit β-lactamase production. Additionally, F89 displayed susceptibility to spectinomycin, and its MIC values for aminoglycosides, tigecycline and rifampin were also relatively low. It should be noted that there are no established breakpoints for these antimicrobials, including ampicillin, piperacillin, and carbapenems (Ohnishi *et al.*, 2010).

In 2016, Japan reported the first case of treatment failure for oropharyngeal gonorrhoea using dual therapy, which combines ceftriaxone (an injectable cephalosporin antibiotic) and azithromycin (an oral macrolide antibiotic) (Fifer *et al.*, 2016). The international spread of MDR ceftriaxone-resistant gonococcal strains has since been confirmed in Japan (Nakayama *et al.*, 2016), Denmark (Terkelsen *et al.*, 2017), France (Poncin *et al.*, 2018), Australia (Lahra *et al.*, 2018), Canada (Lefebvre *et al.*, 2018) and the UK (Eyre *et al.*, 2019; Golparian *et al.*, 2018). In addition, the first XDR strain with ceftriaxone resistance and

high-level azithromycin resistance was isolated in England and Australia in 2018 (Eyre *et al.*, 2018; Jennison *et al.*, 2019; Whiley *et al.*, 2018).

The CDC, in 2020, moved away from recommending single-drug treatment for gonorrhoea. The preferred regimen for a simple case of urogenital and anorectal gonorrhoea is now a single 250 mg intramuscular dose of ceftriaxone administered with a single 1g oral dose of the macrolide azithromycin (Kesharwani *et al.*, 2020). In 2016, Fischer *et al*. reported the first isolated case from a patient with pharyngeal gonorrhoea treatment failure using dual therapy (ceftriaxone and azithromycin) due to a highly resistant strain of *N. gonorrhoeae*. The case involved a heterosexual man in the UK whose pharyngeal gonorrhoea did not respond to ceftriaxone (500 mg) and azithromycin (1 g). The isolated strain of *N. gonorrhoeae* exhibited high-level resistance to azithromycin and reduced susceptibility to ceftriaxone (Fischer *et al.*, 2016).

That represented the first recorded case of azithromycin and ceftriaxone failing to treat *N. gonorrhoeae* infection (Fifer *et al.*, 2016). In subsequent years, health monitoring initiatives in Australia and the UK have isolated MDR strains of *N. gonorrhoeae* that are resistant to azithromycin and ceftriaxone (Whiley *et al.*, 2018). It is thus likely that this dual antibiotic therapy will, in time, prove ineffective in its attempts to stave off antibiotic resistance (Unemo, 2015). The ever-present challenge of antibiotic resistance thus means that treating gonorrhoea will require the development of novel and effective drugs.

The number of bacterial drug targets is, however, limited. Consequently, the development and deployment of a protective vaccine may be the best long-term method of controlling the spread of *N. gonorrhoeae* (Williams *et al.*, 2022).

1.2.1. Increasing incidence of antibiotic-resistant gonorrhoea cases in England

In 2012, both the WHO and the ECDC introduced strategies to address the transmission and impact of AMR in *N. gonorrhoeae* (ECDC, 2019; WHO, 2012). To support these efforts in England, the Health Protection Agency, which transitioned to Public Health England (PHE) in 2013 and later became the United Kingdom Health Security Agency (UKHSA) in 2021, launched the Gonococcal Resistance to Antimicrobials Surveillance Programme Action Plan

(UKHSA, 2023). This plan aimed to guide national efforts in managing AMR in gonococcal infections (GRASP, 2013). Since 2000, the GRASP has collected sentinel surveillance data to track AMR in *N. gonorrhoeae*. GRASP encompasses a series of surveillance systems designed to detect and monitor AMR in *N. gonorrhoeae* and to document potential treatment failures according to the UKHSA (UKHSA, 2024).

Trend data were collected through the national sentinel surveillance system, which annually gathers gonococcal isolates from consecutive patients attending a network of 26 sexual health services (24 in England and 2 in Wales) over a two- to three-month period. These isolates are submitted to the UKHSA National STI Reference Laboratory (STIRL) for antimicrobial susceptibility testing. The results are linked with patient demographic, clinical, and behavioural information to analyse trends in AMR among patient sub-groups. Between 2021 and 2022, the percentage of isolates with decreased susceptibility to ceftriaxone (MIC >0.03 mg/L), the current first-line treatment, stayed low, reaching 0.21% in 2022 compared to 0.07% in 2021. This follows a continuous year-on-year decline since a high of 7.1% in 2018 (UKHSA, 2024).

However, no ceftriaxone resistance (MIC >0.125 mg/L) was detected within the sentinel program. However, 14 cases of ceftriaxone resistance were identified from January 2022 to June 2023 through direct referrals from primary diagnostic laboratories, as opposed to a total of 11 cases recorded between 2015 and 2021 (UKHSA, 2023). Most of these cases were associated with travel to the Asia-Pacific region, known for the highest global prevalence of ceftriaxone-resistant *N. gonorrhoeae* (Unemo *et al.*, 2021). Nonetheless, local transmission within the UK may still occur, as not all partners could be reached, and some cases had no travel history. A timeline of resistance trends starting in 2000 highlights the emergence of resistance to tetracycline, ciprofloxacin, penicillin, and spectinomycin, as shown in Figure 1.4. Resistance to azithromycin was noted in 2001, followed by resistance to cefixime in 2004.

Cefixime resistance (MIC >0.125 mg/L) remained low at 0.8% in 2022. However, isolates with an elevated MIC >0.06 mg/L have doubled yearly since 2019. Resistance to azithromycin (MIC >0.5 mg/L, using the previous European Committee on Antimicrobial Susceptibility Testing (EUCAST) breakpoint for

consistency) and ciprofloxacin (MIC >0.06 mg/L) continues to rise significantly. While penicillin resistance has remained stable with some minor variation, tetracycline resistance (MIC >1.0 mg/L, using the previous EUCAST breakpoint) declined for the first time after consecutive increases since 2016, despite not being used to treat gonorrhoea. As in previous years, no spectinomycin resistance (MIC >64 mg/L) was observed in 2022. For the first time in 2022, whole genome sequencing was performed on all isolates, showing that more than two-thirds of isolates belonged to 10 multi-locus sequence types. Increased MICs for cephalosporins were linked to the presence of mosaic *penA* alleles, especially *penA34* (UKHSA, 2023). Between June 2022 and May 2024, 15 cases of ceftriaxone-resistant gonorrhoea were detected in England, including 5 cases that were extensively drug-resistant (UKHSA, 2024). Since 2015, there have been 31 total cases, with 7 being extensively resistant. To date, all cases have been identified in heterosexuals, mainly in their 20s, with most infections acquired abroad. Limited local transmission has been observed, but the recent rise in cases raises concerns over potential wider spread and treatment challenges (UKHSA, 2024).

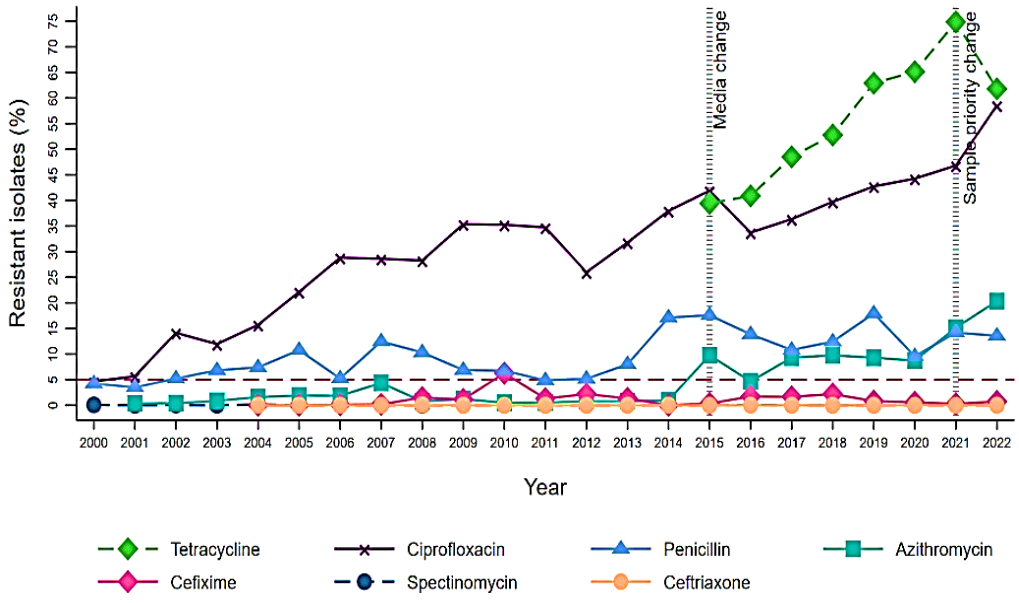

Figure 1.4. *N. gonorrhoeae* isolates ratio in the GRASP sentinel surveillance system that demonstrated resistance to selected antimicrobials in England and Wales from 2000 to 2022†.
This figure is adapted directly from (UKHSA, 2024).

1.2.2. Novel antibiotics for *N. gonorrhoeae* display reduced efficacy compared to established first line treatments

Despite extensive efforts by researchers and pharmaceutical companies, several promising investigational treatments in clinical trials have not demonstrated non-inferiority when compared to current first-line therapies (Raccagni *et al.*, 2023).

Solithromycin is a fluoro-ketolide antibiotic that has been evaluated in clinical trials for the treatment of gonorrhoea. It demonstrated significant effectiveness against various strains of *N. gonorrhoeae*, including those resistant to other treatments. However, its development was halted due to its failure to demonstrate non-inferiority compared to ceftriaxone (Lewis, 2019; Raccagni *et al.*, 2023).

In trials involving 261 volunteers treated with either solithromycin or a combination of ceftriaxone and azithromycin, 80% in the solithromycin group and 84% in the combination group achieved eradication of gonorrhoea, a difference not statistically significant enough to confirm non-inferiority.

The solithromycin group also reported a higher incidence of adverse effects, particularly diarrhoea and nausea. Consequently, a single 1000 mg dose of solithromycin is not recommended as a first-line treatment for gonorrhoea (Chen *et al.*, 2019).

Delafloxacin is a new broad-spectrum fluoroquinolone with improved potency and target affinity compared to older versions, demonstrating effectiveness against multidrug-resistant *N. gonorrhoeae*. Nevertheless, clinical trials indicate it is not a reliable option for treating urogenital gonorrhoea due to a high rate of treatment failures. In a study with 460 participants, delafloxacin had a urogenital cure rate of 85%, while ceftriaxone achieved a rate of 91%. This difference did not meet the non-inferiority margin, suggesting delafloxacin is not suitable as a first-line treatment (Hook III *et al.*, 2019).

1.2.3. Prospective novel antibiotic agents to treat gonorrhoea

Promising new treatments for gonorrhoea currently in advanced clinical development include zoliflodacin and gepotidacin, which are under investigation in ongoing clinical trials. Zoliflodacin is a novel topoisomerase inhibitor that effectively targets bacterial DNA biosynthesis, making it a promising option for treating uncomplicated gonorrhoea (Mancuso *et al.*, 2018). Its unique mechanism suggests potential efficacy against fluoroquinolone-resistant strains. In Phase II trials, participants were administered either 2 g or 3 g of zoliflodacin, with microbiologic cure rates reported at 96% for both doses, compared to a 100% cure rate with ceftriaxone. Although well tolerated, zoliflodacin was less effective against pharyngeal infections, with most reported side effects being mild gastrointestinal symptoms (Bradford *et al.*, 2020).

Gepotidacin, a triazaacenaphthylene antibiotic, exhibits bactericidal effects through the inhibition of DNA topoisomerase II activity. It has demonstrated low minimum MIC values against a range of gonococcal strains, including those resistant to ciprofloxacin. Phase II trials revealed a 95% success rate in treating uncomplicated genitourinary gonorrhoea, with microbiological eradication rates of 97% in the 1500 mg dosage group and 95% in the 3000 mg dosage group. However, no significant adverse effects were reported, highlighting gepotidacin's promise as an effective single-dose treatment for uncomplicated urogenital infections (Watkins *et al.*, 2023).

Corallopyronin A is an alpha-pyrone with demonstrated antibacterial activity, which is primarily attributed to its ability to selectively inhibit the RpoB subunit of bacterial RNA polymerase (Edwards *et al.*, 2022). It exhibits efficacy against both Gram-positive bacteria like *Staphylococcus aureus* and Gram-negative bacteria such as *Chlamydia* spp., making it a candidate for testing against *N. gonorrhoeae*. Studies have shown that its antibacterial activity is more pronounced when the expression of the Mtr-CDE efflux pumps is low, and conversely, less effective when these pumps are highly expressed (Colón Pérez *et al.*, 2024).

1.3. History of development of *N. gonorrhoeae* vaccine antigens

A protective vaccine remains the most promising strategy for controlling the spread of gonorrhoea. However, no gonorrhoea vaccine has yet been approved by the U.S. Food and Drug Administration (FDA). To enable vaccine development, appropriate antigens must be identified. These antigens should be highly conserved and present across most *N. gonorrhoeae* strains. Additionally, they must be immunogenic and capable of generating opsonic or bactericidal antibodies, or antibodies that inhibit vital physiological functions (Edwards *et al.*, 2018; Semchenko *et al.*, 2019).

One challenge is that *N. gonorrhoeae* does not express a surface capsule. This contrasts with the related *N. meningitidis* bacterium. In the case of *N. meningitidis*, the expressed surface capsule is used as an effective immunogenic target by several meningococcal vaccines, including Menveo, Menactra and Menomune, which have all been approved by the FDA (Berti *et al.*, 2021). In the case of *N. gonorrhoeae*, vaccine antigen research has been confined to proteinaceous targets; these have included surface accessible lipoproteins and OM proteins. Multiple *N. gonorrhoeae* surface structures have successfully elicited bactericidal antibodies in vaccinated animals and are thus possible vaccine targets (Jefferson *et al.*, 2021). These structures are often essential for *N. gonorrhoeae* survival, contributing to key processes such as mucosal epithelial cell invasion (Yuen *et al.*, 2019), iron acquisition and metabolism (Shewell *et al.*, 2013), protection against oxidative stress (Jen *et al.*, 2019), efflux of neutrophil-derived antimicrobial peptides (Kłyż and Piekarowicz, 2018), and immune evasion via serum complement resistance (Lewis *et al.*, 2019).

A crucial step in the development of gonorrhoea is the ability of *N. gonorrhoeae* to adhere to the mucosal lining of the human body. The search for a vaccine target has focused on proteins involved in adherence, including the Opa proteins, PorB and the T4P as possible vaccine antigens. Notably, both Opa proteins and T4P are expressed during infection and play a vital role in the bacterium's colonisation of epithelial cells within the genital tract (Kraus-Römer *et al.*, 2022). T4P enable the pathogen to attach to and colonise the surface of these epithelial cells.

Further interactions are subsequently mediated by adhesins such as OM Opa proteins, which enable *N. gonorrhoeae* to bind to CEACAM receptors on the surface of epithelial cells (Chen *et al.*, 1997). PorB also aids colonisation, helps facilitate serum complement resistance and is the most abundant protein in the OM (Ram *et al.*, 2001). Type IV pili, Opa and PorB could, therefore, be regarded as ideal vaccine antigen candidates: they are surface structures and are also required for optimal colonisation of human epithelial cells. The problem, however, is their inherent variability (Muenzner and Hauck, 2020).

For example, the occurrence of intrachromosomal recombination events at the expression locus of the major pilus subunit (PilE) results in the creation of distinct T4P variants (Huang *et al.*, 2020). Opa proteins also make a challenging antigen target: their genes undergo phase variation, which results in their expression being turned on and off (Song *et al.*, 2020). One suggestion, however, is worth noting: using cyclic peptides to target the more conserved semi-variable (Cole and Jerse, 2009) loop within Opa proteins may potentially elicit a humoral response, and this may result in antigenically separate Opa variants being recognised (Cole and Jerse, 2009).

The development of vaccines against *N. gonorrhoeae* has historically faced considerable challenges, primarily due to the organism's capacity for antigenic variation and immune evasion. Early vaccine strategies, initiated in the 1970s and 1980s, focused on surface exposed antigens, particularly type IV pili and OMPs, because of their roles in colonisation and pathogenesis (Boslego *et al.*, 1991; Tramont and Boslego, 1985). Initial pilus-based vaccines targeted the type IV pili, given their essential role in bacterial adhesion and colonisation. Although these vaccines elicited antibody responses against homologous strains with antigenically similar pili, they consistently failed to protect against heterologous strains in clinical trials. A study by Boslego *et al*. (1991) reported that a pilus vaccine composed of a single pilus type did not confer protection against heterologous gonococcal strains. This failure was attributed to the extensive antigenic variability of pilin proteins, which allows the bacteria to evade immune recognition and highlights a fundamental limitation of pilus-targeted vaccine approaches (Boslego *et al.*, 1991).

Subsequent strategies targeted OMPs such as PorB, which are relatively more conserved than pili. However, clinical trials of OMP-based vaccines showed limited bactericidal activity, and immunity was often short-lived (Rice *et al.*, 2017). The absence of a polysaccharide capsule, a feature exploited in successful meningococcal vaccines, further limited vaccine efficacy (Semchenko *et al.*, 2022; Unemo and Shafer, 2014). Despite these challenges, recent evidence suggests that OMV-based vaccines from *N. meningitidis* serogroup B, such as MeNZB, may provide partial cross-protection against gonorrheae, demonstrating a potential path forward for gonococcal vaccine development (Paynter *et al.*, 2019).

There has been a progression in identifying gonococcal antigens that have more significant conservation and stability of expression between and within *N. gonorrhoeae* strains and that also elicit antibodies in laboratory-based animals. These antigens, which represent potential vaccine targets, include MtrE (Multiple transferable resistance E protein) of the MtrCDE multidrug efflux system (Handing *et al.*, 2018; Wang *et al.*, 2018), Neisserial surface protein A (NspA**)** (Lewis *et al.*, 2019), transferrin-binding proteins A and B (TbpA and TbpB) (Shewell et al., 2013), nitrite reductase (AniA) (Shewell *et al.*, 2013), and methionine sulfoxide reductase A/B (MsrA/B) (Jen *et al.*, 2019). Among these, NspA and MtrE are particularly notable because they possess surface exposed epitopes and contribute to *N. gonorrhoeae* immune evasion. Their high degree of sequence conservation across diverse gonococcal strains further strengthens their candidacy as promising vaccine antigens (Handing *et al.*, 2018).

Moreover, target-specific bactericidal antibodies were elicited when mice were immunised with a recombinant plasmid encoding gonococcal NspA and with the surface exposed Loop 2 of MtrE. Moreover, MtrCDE itself is crucial to *N. gonorrhoeae* survival, as was demonstrated by a vaginal tract infection model in mice (Warner *et al.*, 2007). MtrCDE is a member of the hydrophobic and amphiphilic efflux resistance-nodulation-division family of efflux pumps. MtrCDE is upregulated in resistant strains, leading to an increase in the minimal inhibitory concentration (MIC) of antibiotics (Warner *et al.*, 2008).

One study has even suggested that the filamentous NgoΦfil bacteriophage (phage), which is found in gonococcal genomes, may represent a source of

potential vaccine antigen (Kłyż and Piekarowicz, 2018). This study demonstrated that surface phage proteins generated bactericidal antibodies in rabbits and that NgoΦfil protein antibodies could prevent *N. gonorrhoeae* from affixing or attaching to human endocervical cells.

1.4. Introduction to ATP-binding cassette (ABC) transporters

ABC transporters are a highly conserved and ubiquitous superfamily of transmembrane proteins found across all domains of life, including eukaryotes and prokaryotes. These transporters mechanochemically couple ATP-Mg^{2+} binding, ATP hydrolysis, and ADP/phosphate release to power the unidirectional translocation of a wide variety of substrates such as metal ions, proteins, toxins, and xenobiotics across cellular membranes (Akhtar and Turner, 2022; Rees *et al.*, 2009). Based on the direction of substrate movement, ABC transporters are typically classified as importers, exporters, or extruders (Tanaka *et al.*, 2018; Thomas and Tampé, 2018).

Exporters, which are universally distributed among all life forms, function to expel substances from the cytoplasm to the extracellular environment. Importers, on the other hand, facilitate the uptake of essential molecules like metal ions and proteins, and are predominantly found in prokaryotes and archaea, with limited representation in certain eukaryotic systems (Choi and Ford, 2021). The superfamily also includes less common subtypes such as non-canonical importers and non-transporting ABC proteins that lack transmembrane domains (Akhtar and Turner, 2022).

1.4.1. Structure and function of the ABC transporter in microorganisms

The movement of substrates across the cell membrane is managed by transport proteins. These include ABC transporters, which are present in all organisms, from bacteria to eukaryotic species. The import and export of substrates by ABC transporters are maintained in such a way as to provide the cell with vital nutrients while preventing possible substrate-induced toxicity. Exported substrates include proteins, lipids, and antibiotics; imported substrates include amino acids, metals, peptides, and sugars (Berntsson *et al.*, 2010). In bacteria and archaea, ABC transporters are used to import specific substrates into the

cytoplasm. This process of import and export across the cell membrane is facilitated by ATP-binding proteins and a hydrolysis mechanism (Higgins and Linton, 2004). Variations in the mechanisms and structures of ABC transport proteins have led to their classification into three main groups: Type I, Type II, and Type III transporters. Additionally, there is a specific subset of Type III transporters known as energy-coupling factor (ECF) transporters (Rice *et al.*, 2014). There are structural differences between the different classes of ABC transporters, as depicted in Figure 1.5. In both Type I and Type II ABC importers, substrates are identified and brought to the transporter with the help of a substrate-binding protein (SBP).

In Gram-positive bacteria, the SBP is anchored to the cytoplasmic membrane or directly associated with the transporter, whereas in Gram-negative bacteria, it resides in the periplasmic space (Van der Heide and Poolman, 2002). Although there are various categories of SBP, differentiated by variations in structure (Scheepers *et al.*, 2016), all SBPs have a minimum of two locations (or lobes) that, employing an interface pocket, enable binding with the substrate. Type I and II ABC transporters have, within the lipid bilayer, a transmembrane domain (TMD); these TMDs constitute the translocation channel, and the nucleotide-binding domain (NBD), by which ATP is hydrolysed. Among TMDs, there is limited sequence conservation. However, there are several conserved NBD motifs involved in ATP binding. In addition, there is some topological conservation between different ABC transporters.

For instance, the Type I class has five to six helices per TMD, whereas the Type II class has 10 to 12 helices per TMD. As shown in Figure 1.5A, NBDs and TMDs dimerise to form the core of an ABC importer, with the fifth component being the SBP (Higgins, 1992). In several importers, the NBD contains an accessory domain; this enables the regulation of substrate movement (Biemans-Oldehinkel *et al.*, 2006). Each ECF transporter contains a membrane-embedded SBP (known as the S or T component). The S-component of the ECF transporter is called EcfS. A pair of cytosolic ATPases (EcfA and EcfA') and a transmembrane component (EcfT) that connects the S-component to the EcfA-EcfA' subcomplex are the other components. EcfA-EcfA'-EcfT is a complex of EcfA, EcfA' and EcfT. The architecture of Type III, or ECF, transporters is

different. There are four aspects to ECF transporters: two NBD components (EcfA and EcfA'), the transmembrane component (EcfT) and the substrate-specific binding component (EcfS). Although EcfS is substrate-specific, EcfA, EcfA′ and EcfT, which make up the energising module, are conserved components as shown in Figure 1.5 B (ter Beek *et al.*, 2011). In ECF transporters, there is no need for the SBPs used by the Type I and II classes: the EcfS, which is within the lipid membrane, itself binds to substrates (Slotboom, 2014).

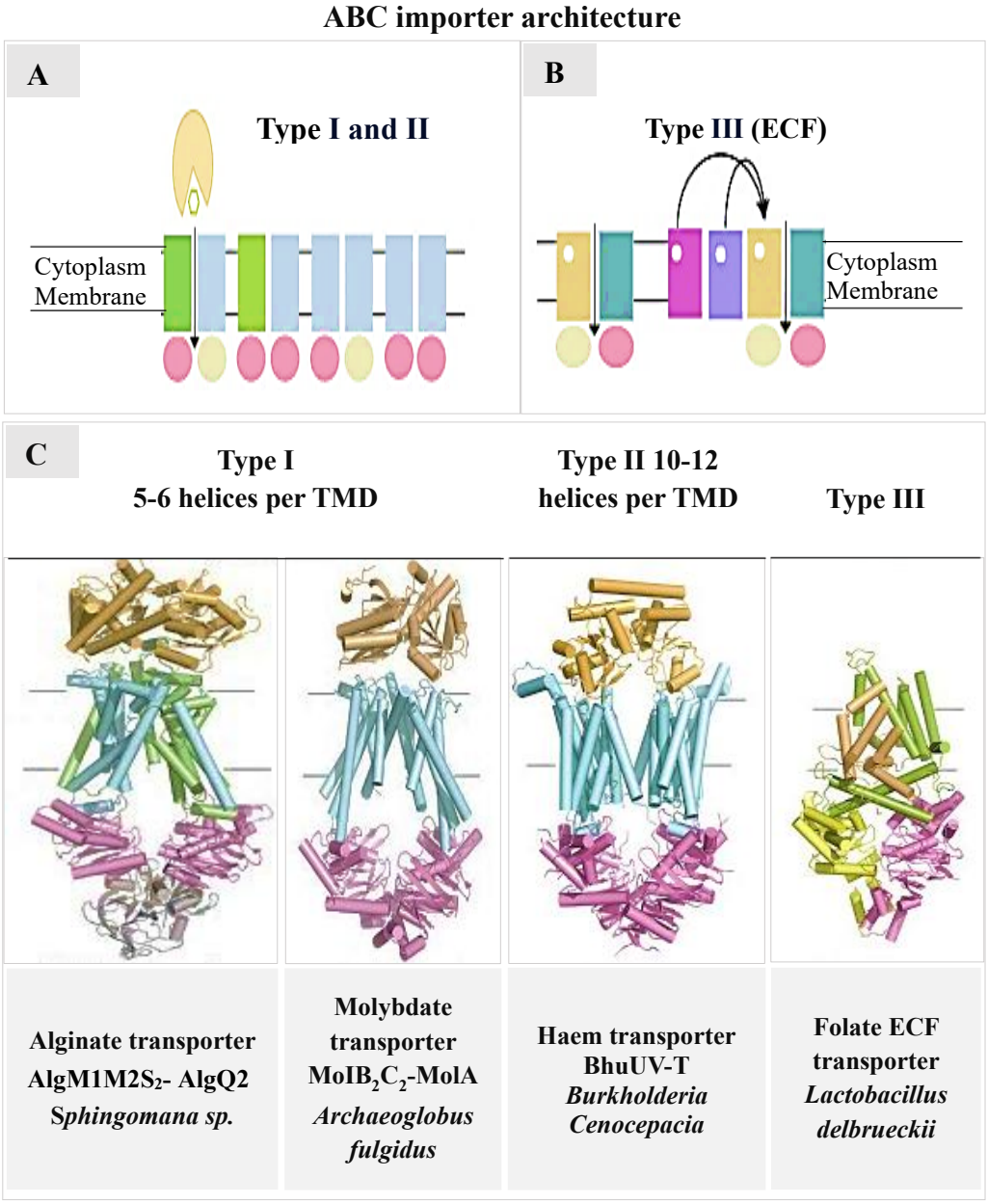

Figure 1.5. ABC transporters vary in assembly and architecture.
(A) shows the assembly of Type I and II importers. The NBD is represented with a rectangle; the TMD with an oval; and the SBP with a circle. The circle's triangular notch denotes the location of substrate binding. Such importers are

thus homo-and heterodimers of NBD and TMD. (B) shows ECF, or Type III, ABC transporters. These consist of the EcfS and the energising module, with the latter made up of EcfT, EcfA and EcfA′. In some cases, an energising module can serve different EcfS types. (C) presents examples of typical Type I, II and III ABC transporters. Type I is exemplified by the alginate transporter $AlgM1M2S_2$- AlgQ2 from *Sphingomonas sp*. (PDB ID: 4TQU) and the molybdate transporter $MolB_2C_2$- ModA from *Archaeoglobus fulgidus* (PDB ID: 2ONK). Type II is exemplified by the haem transporter $BhuU_2V_2$, which is in a complex with the SBP, BhuT, from *Burkholderia cenocepacia* (PDB ID: 5B58). In these images, TMDs are depicted in green or cyan, NBDs in pink or yellow, and SBPs in orange. In the Type I transporters, the accessory domains are pictured in grey. Type III is exemplified by the folate ECF transporter from *Lactobacillus delbrueckii.* The T-component is shown in yellow and pink, with NBD components in yellow, pink, and green, and the S-component in brown. The figure is adopted with modifications from (Tanaka *et al.*, 2018).

Classes of ABC transporters are also differentiated by their import and export mechanisms. In Type I and II transporters, although there is a degree of heterogeneity, unidirectional transport is primarily facilitated by TMD rearranging; this enables access to switch from one side of the internal and external surfaces of the cell's lipid bilayer to the other. Studies have shown that a given SBP will form a complex with the TMD of its cognate transporter, thereby enabling the conveyance of the selected substrate to the translocation pathway. A substrate is thus selected for transport by its binding with the SBP and by the formation of the SBP-transporter complex (Beis, 2015).

In ECF transporters, the S-component, after binding with the substrate, changes position; this transports the substrate across the cell's lipid bilayer (Xue and Ha, 2013). A particular subtype of ECF transporter can bind with multiple EcfS (Slotboom, 2014). Such transporters, depending on the substrate in question, can make use of different EcfS, as depicted in Figure 1.5B, the EcfA, EcfA′ and EcfT components (Eitinger *et al.*, 2011).

1.4.2. Role of ABC transporters in nutrient acquisition and pathogen virulence

Nutrient acquisition is crucial for all bacteria, whether commensal or pathogenic, to establish colonisation within a host. Various import systems play pivotal roles in nutrient uptake. For instance, ECF transporters for riboflavin are commonly found in *Listeria monocytogenes*, *Bacillus subtilis*, and *Clostridioides difficile,* while the Type I zinc importer ZnuABC is present in *B. abortus*, *Yersinia pestis*, and *Proteus mirabilis* (Gutiérrez-Preciado *et al.*, 2015). In 2016, *Clostridium difficile* was reclassified as *Clostridioides difficile* to reflect its distinct genetic and phenotypic characteristics (Guery *et al.*, 2019).

While various essential nutrients are necessary for bacterial survival, information linking these systems to pathogen virulence is often limited, primarily derived from the phenotypic characterisation of transporter mutants in animal infection models. Although many important transport systems are yet to be identified, some ABC importers are crucial for bacterial virulence, establishing them as key virulence factors (Table 1.1). These importers transport a range of substrates, including transition metals, peptides, and amino acids. Examines ABC importers as virulence determinants in pathogenic bacteria, with evidence often based on the loss of virulence following the genetic deletion of essential ABC transporter components (Tanaka *et al.*, 2018).

Table 1.1. Selected examples of ABC transporters in different bacterial strains that play a role in full virulence.

Type of substrate	Name	Organism name
Metal transporters		
Zinc	ZnuABC	*Brucella abortus*, *Salmonella enterica serovar Typhimuriu*m, *Campylobacter jejuni*, *Moraxella catarrhalis*, uropathogenic *E. coli*, *Acinetobacter baumannii, Yersinia pestis,* and *Proteus mirabilis* (Higgins and Linton, 2004)
Manganese and iron	SitABCD	Avian pathogenic *E. coli*, APEC O78 strain $_{X}$7122, and *B. henselae* (M. Liu *et al.*, 2013; Sabri *et al.*, 2008)
Manganese and zinc	MntABC	*S. Typhimurium* and *N. gonorrhoeae* (Boyer *et al.*, 2002)
Manganese and zinc	PsaABC	*S. pneumoniae* (Kehres *et al.*, 2002)
Nickel and cobalt	CntABCDF (formerly Opp1ABCDEF)	*S. aureus* (Remy *et al.*, 2013)
Amino acid transporter		
Glutamate	GltTM, SBP (NMB1964)	*N. meningitidis*
Glutamine	GlnHPQ	*S. Typhimurium, N. gonorrhoeae,* Group B, *Streptococci*, and *S. pneumoniae* (*spd1 098–1099*, *spd0411–0412*).
Alanine	DalS, SBP of putative D-alanine transporter	*S. Typhimurium*
Cysteine	CtaP, SBP of putative oligopeptide transporter	*L. monocytogenes*
Lysine, Ornithine	SBP1, SBP3, and SBPs are putative amino acid transporters	*M. catarrhalis* (Otsuka *et al.*, 2014)
Methionine	MetNIQ	*M. catarrhalis*
Methionine	MetQNP	*S. pneumoniae*
Peptide transporter		
Peptides	OppABCDF	*M. catarrhalis* and *B. thuringiensis*
AMPs	SapABCDF	*Nontypable H. influenzae* and *H. ducreyi*
AMPs	YejABEF	*B. melitensis* (*BMNI_I0006- BMNI_I000 10*) and *S. Typhimurium* (Tanaka *et al.*, 2018).

1.5. The role of nutritional immunity in suppressing *N. gonorrhoeae* pathogenesis

N. gonorrhoeae and *N. meningitidis* acquire all requisite nutrients from the human host (Awate *et al.*, 2024). Humans, however, have several mechanisms designed to isolate such nutrients into niches that cannot be easily accessed by pathogens (Bilitewski *et al.*, 2017). This phenomenon, known as nutritional immunity, deprives bacteria of the nutrients they need to grow. For example, lipocalins transport small hydrophobic compounds such as steroids, retinoids, lipids, and bilins (also known as bilichromes). Bilins are linear tetrapyrrole pigments derived from haem metabolism (Taniguchi and Lindsey, 2023).

Most lipocalins may also bind to complexed iron (through siderophores or flavonoids) and haem (Pérez Medina and Dillard, 2018). Lipocalin absorbs ferric siderophores, while lactoferrin absorbs iron, making them pivotal in iron sequestration (Miethke and Skerra, 2010). The proteins haemoglobin and transferrin have also been shown to keep levels of free iron low (Awate *et al.*, 2024). Bacterial growth is inhibited by the actions of these metal-chelating proteins, which prevent pathogens from acquiring the necessary quantities of iron (Crawford and Wilson, 2015).

A similar mechanism has been observed with zinc (Liuzzi *et al.*, 2005). A family of EF-hand proteins known as S100 proteins, such as calprotectin, effectively sequester zinc from invading pathogens. While these proteins primarily function in calcium sensing and chelation, they also exhibit high affinity for other divalent cations, including manganese and zinc (Zackular *et al.*, 2015).

1.6. ABC-mediated transport of metals essential to *N. gonorrhoeae* iron acquisition systems

N. gonorrhoeae requires iron to survive; iron is needed for bacterial cellular functions such as growth, DNA and RNA synthesis, and metabolism. It is, for example, used in the metabolic processes of oxidative phosphorylation and the tricarboxylic acid cycle (Choby and Skaar, 2016). As such, gonococci have multiple systems devoted to iron uptake. Iron is also vital to the human host. It can safeguard cells from oxidative stress: free radical-destroying peroxidases and catalases possess iron, and other enzymes and proteins also need iron for

optimal functioning (Zughaier *et al.*, 2014). Yet toxicity also results from an excess of free iron: the hydroxyl radicals produced by the Fenton reaction:

$Fe^{2+} + H_2O_2 \rightarrow Fe^{3+} + OH^- + \cdot OH$ cause oxidative stress. Therefore, high-affinity iron-binding proteins hold the majority of iron present in humans (Sritharan, 2016).

Iron-binding proteins in humans include lactoferrin, transferrin, ferritin, haemoglobin, haem and siderophores. *N. gonorrhoeae* has iron transport systems that enable it to use lactoferrin, transferrin and haemoglobin (Cornelissen and Hollander, 2011). The glycoproteins transferrin and lactoferrin have an extremely high affinity for ferric iron. Transferrin, which is present in serum, binds with two iron atoms to sequester and transport the metal (Cassat and Skaar, 2013). Lactoferrin, which is present in mucosal and lymph secretions, participates in iron chelation. Both proteins are used as an iron source by *N. gonorrhoeae* (Hood and Skaar, 2012). The pathogen is also known to make use of oxygen-transporting haemoglobin, which is found in red blood cells. Haemoglobin is a tetramer, and, as such, each of its subunits can bind with one haem molecule. Haem, which is cytotoxic in isolation and is largely found bound with haemoglobin, represents the most prolific source of bound iron in invertebrates; it is a protoporphyrin whose centre can bind with a single ferrous iron (Loss *et al.*, 2019). Although a dedicated haem uptake system has not been identified for *N. gonorrhoeae*, this type of transport system is present in most bacteria, as haem is required for several bacterial aerobic processes.

In vitro studies have demonstrated that *N. gonorrhoeae* utilises haemoglobin as a source of both iron and haem (Richard *et al.*, 2019). It is also worth considering the role of the cytoplasmic protein ferritin, which consists of 24 subunits and is capable of binding to thousands of iron ions, which is vital to iron storage within cells. The role of siderophores in iron acquisition by gonococci is an additional factor. *N. gonorrhoeae* does not produce its own siderophores, which are low molecular weight compounds secreted by microorganisms to scavenge and facilitate the uptake of iron. The pathogen can, however, use the siderophores produced by other bacteria (Bisht *et al.*, 2018). Siderophores, which are chelating agents, work by removing iron from the human host's iron-binding proteins and by engaging in high-affinity binding with ferric iron.

Microorganisms can therefore use a ferrated siderophore as a source of iron. *N. gonorrhoeae* has transport systems that enable the use of certain heterologous siderophores (Gokarn and Pal, 2018). Siderophores used by *N. gonorrhoeae* include enterobactin, aerobactin, and catecholates such as the dimers and trimers of dihydroxybenzoylserine and salmochelin S2 (Haschka *et al.*, 2021).

1.6.1. Ton-B Dependent Transporters (TBDTs)

TBDT is a nutrient-acquisition mechanism used by Gram-negative bacteria. The nutrients required by pathogens such as gonococci are usually larger than 600 Daltons, the maximum size of solutes that can be conveyed via non-specific, concentration-dependent, porin-mediated diffusion **(**Maurakis *et al.*, 2019**)**.

In contrast, TBDT facilitates the transport of larger molecules such as iron complexes, vitamin B12, carbohydrates, and nickel chelates **(**Gómez-Santos *et al.*, 2019**)**. The structure of a TBDT is that of a beta-barrel containing a folded globular plug domain, which binds with specific substrates, as well as 22 amphipathic beta-strands **(**Noinaj *et al.*, 2010**)**. A TBDT will interact with a cytoplasmic-membrane protein complex. This complex consists of ExbB and ExbD, which are rooted in the cytoplasmic membrane, and TonB, which bridges the outer and cytoplasmic membranes. Energy is harnessed from the cytoplasmic membrane's proton motive force by ExbB and ExbD; this energy is then transferred to TonB, conveying it to the OM transporter **(**Sverzhinsky *et al.*, 2015**)**.

ExbB and ExbD thus have a vital role in ensuring that TonB both communicates with the cytoplasmic membrane and gains the required energy from the proton motive force **(**Held and Postle, 2002**)**. This process enables a substrate to bind with relevant receptors, be conveyed through an appropriate channel, and interact with a suitable periplasmic binding protein. This binding protein then transfers the substrate to ABC transporters within the cytoplasmic membrane. From there, the substrate can be taken into the cytoplasm via an ABC transporter **(**Thomas and Tampé, 2020**)**.

1.6.2. Two-Component TonB-Dependent Transporters (TBDTs)

N. gonorrhoeae uses two-component TBDTs to acquire iron from lactoferrin, transferrin and haemoglobin, as is depicted in Figure 1.6. Two-component TBDTs differ in that they have a surface exposed companion lipoprotein as well as a beta-barrel transmembrane channel (Yadav *et al.*, 2020).

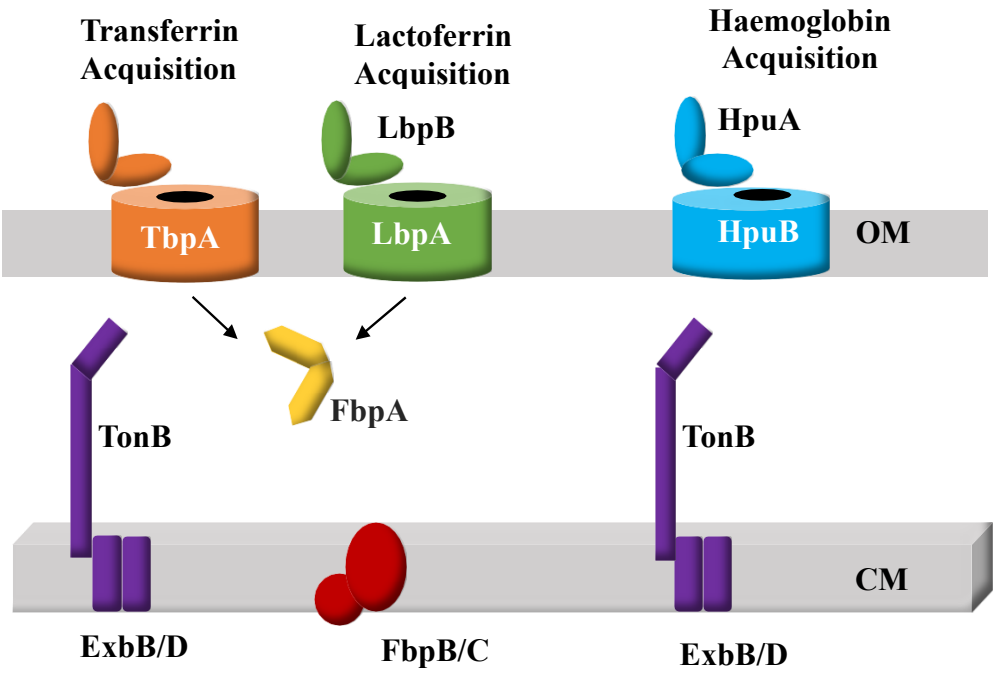

Figure 1.6. Two-Component TonB-Dependent Transporters diagram. This diagram demonstrates how two-component TBDTs are used in the acquisition of iron from transferrin, lactoferrin and haemoglobin. In these systems, the OM transporters, which span the outer membranes (captioned OM), are represented as cylinders. Attached to the OM are the companion lipoproteins, each shown next to its respective transporter. The purple ExbB, ExbD and TonB complex is shown within the cytoplasmic membrane (captioned CM); the periplasm is spanned by TonB. The ferric binding protein FbpA, which is shown in yellow, forms the periplasmic binding protein. The path taken by transported iron is shown by the direction of the arrows; these depict a route from transmembrane channels to the periplasmic binding protein. Within the cytoplasmic membrane is the cytoplasmic membrane permease, FbpB, shown in red with its linked ATPase FbpC. Finally, although the ExbB-ExbD-TonB complex is known to be used by haemoglobin receptors, thus far, researchers have not identified the periplasmic binding protein or the ABC transporter. The figure is adapted with modifications from (Cornelissen and Hollander, 2011; Silale, 2023).

1.6.3. Transferrin-mediated iron acquisition and transport

The most studied and best-understood means by which *N. gonorrhoeae* obtains iron is from transferrin. Thus far, every gonococcal strain examined has genes encoding for the OM proteins TbpA and TbpB. It has also been demonstrated that naturally acquired mucosal infection results in the expression of both *tbpA* and *tbpB* genes (DeRocco *et al.*, 2008) and, according to one study, a gonococcal strain containing a mutated transferrin receptor could not infect male human subjects (Noto and Cornelissen, 2008). Transferrin binding proteins are a potential vaccine candidate in that they are highly conserved, surface exposed, and needed for successful infection. Their immunogenicity would, however, need to be increased. A study found that antibodies against TbpA and TbpB, while present in natural infection, were not at levels significantly higher than in controls (Price *et al.*, 2007). The structure and function of the TbpA and TbpB are not identical. TbpA is a typical TBDT, made up of a globular plug domain and a transmembrane beta-barrel. The transferrin binding function of TbpA is dependent on two of its 11 surface exposed loops, namely numbers four and five (Yadav *et al.*, 2020). TbpB, however, is entirely surface exposed: it is a surface-tethered lipoprotein with two lobes capable of binding with transferrin (Fegan *et al.*, 2019).

Studies with *E. coli* found that pathogens expressing recombinant TpbA were able to bind with transferrin *in vivo,* but that mutant strains, unable to express TbpA, could not (Noinaj *et al.*, 2012). In contrast, mutant strains that could not express TbpB could nevertheless still bind with human transferrin; the degree of binding was, however, at around 50% of that observed with naturally occurring strains (Noto and Cornelissen, 2008). It is therefore assumed that TbpB increases the efficiency of transferrin-mediated iron acquisition, a process that is dependent on TbpA expression (DeRocco and Cornelissen, 2007). It has been proposed that TbpA and TbpB, after initially binding with ferrated transferrin, extract iron. This iron is prepared for transport by interacting with the TbpA plug domain. Transport is then initiated by TonB communicating with the plug domain. Iron is then relinquished by the plug and taken up by the periplasmic ferric binding protein, FbpA (Siburt *et al.*, 2012). Ferrated FbpA, which has reduced affinity to TbpA, can then proceed through the periplasm.

Liberated holo-FbpA then interacts with the cytoplasmic permease FbpB, which, utilising energy from the ATPase FbpC, conveys iron into the cytoplasm (Weerasinghe *et al.*, 2013). Energisation may also be achieved using other ATP-binding proteins that are predicted in the *N. gonorrhoeae* genome. That is suggested by research that demonstrated successful iron transport even in the absence of a working FbpC protein (Moreau *et al.*, 2017).

The ferric binding protein, FbpA, is responsible for drawing ferric iron into the periplasm (Pogoutse and Moraes, 2017). FbpA, a 37 kDa protein, has been termed bacterial transferrin. This is because the need for a synergistic anion and the way residues are managed resemble the binding undertaken by a transferrin lobe (Dhungana *et al.*, 2003). It has also been shown, through a modified H/D exchange technique, that FbpA engages in specific and direct TbpA binding (Siburt *et al.*, 2012). This enables increased efficiency in the transport process from the TpbA plug domain to the relevant apo-FbpA.

1.6.4. Lactoferrin-mediated iron acquisition

The process of iron acquisition from lactoferrin is believed to be analogous to transferrin acquisition. Although less is known about the lactoferrin system, the process involves lactoferrin binding protein A (LbpA), which is again a TBDT, and lactoferrin binding protein B (LbpB), a surface-tethered lipoprotein. It is thought that LbpB is not essential for the acquisition of iron from human lactoferrin, but that LbpA is vital (Holbein *et al.*, 2021). Analysis has revealed that among gonococcal isolates with both *lbpA* and *lbpB* genes, all express LbpA, but 70% fail to express LbpB; this may be due to phase variation within *lbpB* (Marjuki *et al.*, 2019).

About half of the *N. gonorrhoeae* strains lack functional lbpA and lbpB proteins due to gene deletions. The *lbpA* gene is partially deleted, and lbpB is completely absent, preventing lactoferrin-binding needed for iron uptake (Marjuki *et al.*, 2019). These deletions help the bacteria avoid detection by the immune system, which can recognise the lactoferrin-binding process (Diallo *et al.*, 2019). Genetic drift and mutations also contribute to these deletions, enhancing the bacteria's adaptability to different host environments (Marjuki *et al.*, 2019).

1.6.5. Haemoglobin-mediated iron acquisition

Acquisition of iron from haemoglobin requires the presence of both the HpuA and HpuB proteins, with HpuA forming a small surface-tethered lipoprotein and HpuB being the TBDT that spans the OM (Harrison *et al.*, 2013). In terms of size, HpuA is about half that of the other lipoproteins implicated in two-component TonB-mediated iron transport. The *hpuA* gene has a poly G tract that varies in length; the resultant frameshifting leads to slipped-strand mispairing and, therefore, phase variation in expression (Harrison *et al.*, 2013). Haemoglobin receptors are often in the "on" phase among early-cycle menstruating females, although receptors are largely in the "off" phase among laboratory strains. In contrast to the lactoferrin and transferrin systems, there is no species-dependent specificity in the binding between haemoglobin and HpuA and HpuB (Akinbosede, 2022).

1.7. Single-Component TonB-Dependent Transporters

Single-component TonB-dependent transporters (TBDTs) consist solely of a beta-barrel transmembrane channel and work without a surface exposed companion lipoprotein. In *N. gonorrhoeae*, these TBDTs facilitate iron acquisition from siderophores, as illustrated in Figure 1.7. While the role of these single-component TBDTs in siderophore-mediated iron uptake is established, many other TBDTs remain largely uncharacterised and have been identified primarily through bioinformatics predictions.

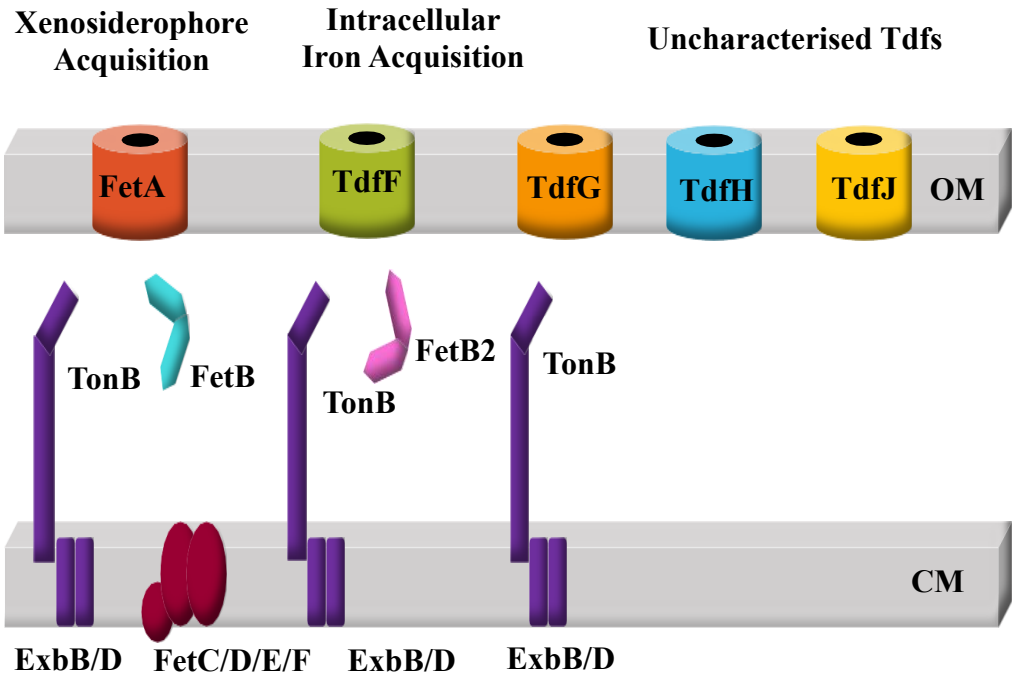

Figure 1.7. Diagram of Single-Component TonB-Dependent Transporters (TBDTs).
Five TBDT systems known to be made up of a single transmembrane channel are depicted in this diagram. Although these systems are generally uncharacterised, several xenosiderophores are thought to be transported by the single-component TBDT Ferric enterobactin transporter A (FetA). In this image, cylinders are used to depict the outer membrane transporters; these span the outer membrane (captioned OM). The ExbB-ExbD-TonB complex is shown in purple within the cytoplasmic membrane (captioned CM). TonB itself encompasses the periplasm. The periplasmic binding protein FetB, which is integral to the transport of siderophores, is depicted in aquamarine. This Fet system is thought to use the ABC transporter system FetC, D, E or F, shown in dark red. FetB2, a periplasmic binding protein encoded near the TonB-dependent receptor TdfF, is shown in pink. There is evidence for Fet-based systems. Strains that, due to mutations, were unable to express FetB were also less able to acquire iron from enterobactin (Cornelissen and Hollander, 2011). Furthermore, other catecholate siderophores, including the dimers and trimers of salmochelin S2 and dihydroxybenzoylserine, have been found to use FetA (Strange *et al.*, 2011). The figure is adapted with modifications from (Silale, 2023; Strange *et al.*, 2011).

Obtaining iron from enterobactin, a catelochate-type siderophore produced by bacteria such as *E. coli, Salmonella* and *Klebsiella* species, is facilitated by the single-component TBDT, Ferrin enterobactin transporter (FetA). The *fetA* gene is a phase variable and located upstream of those genes purportedly responsible for encoding an ABC transporter and also the periplasmic binding protein FetB (Rohde and Dyer, 2003).

Although iron is acquired from enterobactin via the single-component TBDT ferric enterobactin transporter (FetA), other uncharacterised single-component TBDTs have been identified using bioinformatics. Their resemblance to other TBDTs has resulted in them being named TonB-dependent function Tdf proteins. For example, TdfF has been detected in *N. gonorrhoeae* FA1090, MS11 and FA19 strains grown in a cell culture medium but with the presence of serum (Solger *et al.*, 2020). TdfF appears to be integral to vital intracellular functions (Quillin and Seifert, 2018) and so may also assist with the intracellular acquisition of iron once the host cell has been invaded.

A periplasmic binding protein, together with an associated gene, exists upstream of TdfF. The gene, thought to resemble *fetB*, has been termed *fetB2*. The iron-repressed and significantly larger 136 kDa TfdG is found in only 17% of *N. gonorrhoeae* strains, even though the *tdfG* gene is found in all gonococcal genomes. It is thought that, as there are two clades of the *tdfG* gene, the antibodies used to detect expressed TdfG can only identify specific types of this protein. The amino acid sequences of TdfG proteins resemble those of haem transporters, although a mutated TdfG-deficient variant was nevertheless able to obtain iron from haem alone (Zafar and Saier Jr, 2018). TdfH, which is sized at 104 kDa, has a sequence similar to haem transport systems in terms of its sequence (Rohde and Dyer, 2003). Mutated TdfH-deficient variants were again able to increase, even with haem as the only source of iron. This suggests that neither TdfG nor TdfH engage in haem transportation. TdfJ found within all *Neisseria* species differs in that it is iron-induced and smaller at 86 kDa; it does, however, resemble siderophore and haem transporters in terms of the sequence (Yadav *et al.*, 2020).

1.8. Cytoplasmic transport

Metallic nutrients, having been imported via TonB-mediated OM receptors, are transported into the cytoplasm. This is facilitated by employing periplasmic binding proteins (PBP), an ABC, and an inner membrane (IM) permease (Cockerell *et al.*, 2014).

The ABC transport system FbpABC, in which FbpA is the PBP, is specifically involved with the transport of iron from hTf and hLf into the periplasm. The hypothetical process is that once FbpA binding is released by Fe^{3+}, FbpA interacts with TbpA; this enables TbpA-mediated iron transport, facilitated by the binding affinity of TbpA $\sim 10^{-18}$ M for Fe^{3+} (Subashchandrabose and Mobley, 2015). It means that TbpA has an extremely high affinity for Fe^{3+}, binding it tightly even at extremely low concentrations. Specifically, a dissociation constant (Chidiac *et al.*, 2024) of 10^{-18} M indicates that the equilibrium concentration of free Fe^{3+} is exceedingly small when bound to TbpA. This high affinity is crucial for effective iron transport in biological systems, where iron is often scarce and tightly regulated (Subashchandrabose and Mobley, 2015).

Transport of enterobactin is facilitated by the ABC transport system FetC/D/E/F, which uses a separate PBP: FetB. Transport of haem is via a transport system that, while thought to exist, has not yet been definitively identified in *Neisseria* species. In *N. meningitidis*, Zur-regulated Zinc transport sees this metal transported into the cytoplasm by a PBP termed ZnuA, which is also required for gonococcal growth in calprotectin and S100A7 (Maurakis *et al.*, 2019).

1.8.1. Zinc acquisition

Zinc is integral to multiple enzymatic reactions, including nucleotide synthesis and oxidation-reduction, necessary for bacterial survival. Bacteria have many ways of maintaining a sufficient zinc supply (Puig *et al.*, 2017). Gonococci have two TdTs-TdfH and are involved in zinc acquisition (Kammerman *et al.*, 2020). These zinc-repressed TdTs, which do not possess a surface-tethered lipoprotein, are characteristic of zinc transporters. Two particular qualities, however, are worth noting: iron-replete conditions can induce TdfJ, while TdfH enables *N. gonorrhoeae* to fulfil its zinc requirements from *in vitro* human calprotectin (Jean *et al.*, 2016).

It is worth noting that the meningococcal homologue of TdfJ, termed Zinc uptake protein D (ZnuD), was put forward for potential inclusion in a meningococcal group B vaccine (Gasparini *et al.*, 2014). ZnuD is implicated in zinc acquisition (Maurakis *et al.*, 2019). It is also regulated by zinc and Ferric uptake regulators known as Zur and Fur proteins, respectively (Thomas and Tampé, 2020). Research has found that ZnuD, when expressed in *E. coli*, binds with haem, although a meningococcal variant with a mutated *znuD* could still make use of this iron source (Chan *et al.*, 2018). However, this mutant was also found to be less able to invade, adhere to, and survive within epithelial cells (Cornelissen, 2018). ZnuD may therefore be an excellent meningococcal vaccine candidate: it is present in most strains of group B meningococci, it is expressed during a course of infection, and, under zinc-limited conditions, ZnuD antibodies can spark the complement-mediated killing of these group B meningococci (Gasparini *et al.*, 2014).

1.9. Potential *N. meningitidis*, Methionine-binding protein Q (NmMetQ) vaccine antigen and its relevance to gonococcal vaccine development

In searching for a gonococcal vaccine candidate, it is worth examining a potential vaccine antigen for *N. meningitidis*, another human-specific pathogen from the *Neisseria* family. NmMetQ, which interacts with microvascular endothelial cells in the human brain, may also act as an adhesin, and it has been suggested that the surface exposure of SBPs in several pathogenic bacteria may be associated with extra functions such as adherence (Kovacs-Simon *et al.*, 2014).

The fact that NmMetQ resides on the cell's surface is significant, and this finding suggests that the SBPs of Gram-negative bacteria are not always located in the periplasm (Thomas and Tampé, 2020). This finding thus challenges the model of periplasm-based SBPs binding with substrates and then delivering them to the relevant ATP-ABC transporters in the cell's IM. As such, there are essential questions to be addressed. The first is exploring how and why NmMetQ is located on the surface of the bacterial OM. Thus far, the finding that NmMetQ is at the bacterial cell surface, despite SBPs not being membrane proteins, indicates that it is attached to the OM (Scheepers *et al.*, 2016). Furthermore,

whether NmMetQ has retained its IM-based ABC transporter-dependent role needs to be addressed.

SBPs in Gram-negative bacteria have traditionally been perceived as based in the periplasm, thereby freely diffusing between the OM and IM. This paradigm is based on the classic experiments of Heppel, who demonstrated that Gram-negative bacteria, when in osmotic shock, release SBPs (Heppel, 1969). The SBPs of Gram-negative bacteria are predominantly classed as secreted proteins (Yang *et al.*, 2010). However, several SBPs have been categorised as lipid-modified (Shi *et al.*, 2019). The existence of lipo-SBPs in Gram-negative bacteria needs to be explored to identify the possible effect of lipid modification on the surface-based localisation of NmMetQ. Numerous studies, which have investigated many different ABC transporter systems, have documented the transporter-dependent function of SBPs (De Boer *et al.*, 2019; Liu *et al.*, 2020; Sabrialabed *et al.*, 2020).

They have shown that SBPs have multiple conserved characteristics. These include being responsible for conveying substrates to ABC transporters and, in this way, also prompting transport-dependent ATPase action. According to structural research, SBPs attach to transporters TMD at their periplasmic surface. The SBP aligns with the translocation pathway of its corresponding transporter, facilitating the transport process (Bhattacharya *et al.*, 2022). However, some studies have found that several SBPs also display a so-called moonlighting function in that they display transporter-independent and transporter-dependent activity (Mächtel *et al.*, 2019).

The maltose-binding SBP within *E. coli*, for example, not only binds with the appropriate ABC transporter during the import of maltose (Mächtel *et al.*, 2019) but also serves as a chemotaxis receptor ligand, thus helping stimulate the signalling cascade associated with nutrient acquisition. Other examples of SBPs exhibiting functions independent of ABC transporters include the non-secreted periplasmic SBP (NspS) of *V. cholerae*. NspS, a homologue of ABC-type SBPs, mediates polyamine signal transduction independently of polyamine transport (Delepelaire, 2019). Notably, NspS does not participate in substrate transport (Cockerell *et al.*, 2014) but his implicated in the formation of biofilms (Young *et al.*, 2021).

1.9.1. Functional conservation of MetQ proteins is observed across species

The MetQ proteins, such as NgMetQ from *N. gonorrhoeae* and VvMetQ from *Vibrio vulnificus*, are thought to act as adhesins, respectively, involved in adhesion to epithelial cells in the human cervix (Semchenko *et al.*, 2019) and intestine (Yu *et al.*, 2011). There is no evidence that these NgMetQ and VvMetQ are also involved in binding with and stimulating their cognate ABC transporters. Consequently, the transporter-dependent functions of NgMetQ and VvMetQ, as well as NmMetQ, have not attracted significant studies. Most of the research on MetQ proteins has been undertaken in *E. coli.* This research has demonstrated that the methionine uptake system of *E. coli* involves the SBP EcMetQ and its associated ABC transporter, EcMetNI (Costa *et al.*, 2015). This transporter comprises two key components: MetN, the NBD responsible for ATP hydrolysis that powers substrate transport, and MetI, the integral membrane permease forming the translocation channel for methionine (Johnson *et al.*, 2012). Structural studies have examined these components both individually and as a functional complex, elucidating their coordinated role in methionine import. Within EcMetNI, there are two NBD involved in transport-related ATP binding and hydrolysis and two TMDs, which represent a translocation pathway for substrates.

The conformation of EcMetNI, if EcMetQ is not present, is inward facing: NBD separated and TMDs open to the cytoplasm. Meanwhile, the crystal structure of EcMetQ reveals a methionine-binding pocket, which is formed by two domains joined with a linker (Nguyen *et al.*, 2015). When together in a complex, EcNetNI faces outward with NBDs and TMDs close together; EcMetQ, with its binding pocket open to the central cavity, is attached to the TMDs' periplasmic surface (Nguyen *et al.*, 2018). These findings, together with the results of *in vivo* assays, suggest that EcMetQ is indeed integral to methionine transport that is facilitated by EcMetNI (Nguyen *et al.*, 2018). Radioactive palmitate labelling has also demonstrated that EcMetQ is a lipoprotein (Shi *et al.*, 2019). Notably, there is evidence that the EcMetQ-EcMetNI association may well depend on this SBP's N-terminal lipid. For instance, a study demonstrated that, when solubilised in peptidiscs and detergent, EcMetQ continued to associate with His-tagged and recombinantly expressed EcMetMI; when lipidation was prevented via mutation

of the N-terminal cysteine, this association did not occur (Carlson *et al.*, 2019). In the case of *N. meningitidis*, such a detailed investigation into the relationship between SBP and the ABC transporter is still needed. The ABC transporter NmMetNI, for example, has so far failed to attract structural or biochemical studies. There has, however, been a structural categorisation of NmMetQ in both a ligand-free state and when bound to either D-methionine or L-methionine. NmMetQ is, according to binding assays, likely to bind with greater affinity to L-methionine as compared to D-methionine (Nguyen *et al.*, 2019). This ligand binding is not thought to require an N-terminal signal sequence, as the tests involved the NmMetQ protein without this native sequence. It can thus be seen that there is only a limited understanding of how NmMetQ interacts with NmMetNI, of the SBP's post-translational changes, and its role in methionine transport. Both NmMetQ and NmMetNI still require full characterisation, including the native N-terminal signal sequence. The N-terminal signal sequence for NmMetQ does, however, suggest that this SBP may be a lipoprotein (Nguyen *et al.*, 2019).

Although this hypothesis has not been experimentally confirmed, there is supporting evidence from other lines of analysis. For example, a study that used site-directed mutagenesis and mass spectrometry concluded that full-length NmMetQ was a lipoprotein, named lipoNmMetQ, when recombinantly expressed within *E. coli* (Bolla *et al.*, 2014). According to functional assays, optimal stimulation of NmMetNi-ATPase activity requires both lipo-NmMetQ and L-methionine (Sharaf *et al.*, 2021). When these molecules were replaced with a combination of L-methionine and the NmMetQ preprotein, which has an unprocessed N-terminal signal peptide, this reduced the stimulation of NmMetNi. Reduced stimulation was also observed when lipo-NmMetQ was used in conjunction with analogues of methionine. When examined with single-particle electron cryo-microscopy (cryo-EM), the structure of NmMetNI could be determined at 6.4 Å in the presence of lipo-NmMetQ, and 3.3 Å in the absence of lipo-NmMetQ (Ingersol *et al.*, 2020).

Overall, MetQ proteins in *N. meningitidis* and *E. coli* are likely to be lipid-modified, and, according to bioinformatics-based analysis, this is likely to be the case for other MetQ proteins from Gram-negative bacteria (Zielke *et al.*, 2016).

GNA1946 (also called NMB1946) is a potential vaccine candidate against *N. meningitidis*. It is believed to be the methionine-binding component of an ABC transporter. NMB1946 is the gene name in the *N. meningitidis* MC58 strain, encoding the MetQ protein, which helps with methionine transport. NMB1946 and GNA1946 refer to the same gene *NmmetQ* but exist in different *N. meningitidis* strains (Pizza *et al.*, 2000). This surface expressed and surface exposed lipoprotein shows greater than 98% identity across its 287 amino acids, indicating strong conservation between strains (Jacobsson *et al.*, 2006).

Likewise, studies examining diverse *N. gonorrhoeae* strains via proteomics and bioinformatics (for example, PubMLST database) confirm widespread expression and conservation of the MetQ homologue (Zielke *et al.*, 2014). This conservation is critical for its candidacy as a vaccine antigen, supported by evidence that antibodies against MetQ inhibit bacterial adhesion and exhibit bactericidal activity in murine models (Sikora *et al.*, 2020). According to crystal structure analysis, the structure of GNA1946 also resembles the substrate binding components of methionine-uptake ABC transporters. The lipoprotein was crystallised with L-methionine, which is bound in the gap between its two globular lobes of lipoprotein (Jacobsson *et al.*, 2006). When antiserum from mice was raised against GNA1946, the antiserum showed a complement-mediated bactericidal action against heterologous strains of *N. meningitidis* (Pizza *et al.*, 2000). This finding is relevant for the development of a gonococcal vaccine. Although the most well-known methionine uptake system in bacteria is the MetNIQ transporter-SBP, an ABC transporter in *E. coli* with a methionine-binding component coded by the *metQ* gene (Merlin *et al.*, 2002), *N. gonorrhoeae* also has a homologue of GNA1946 in its OM. This homologue, produced by various strains of *N. gonorrhoeae*, including those examined in a study of 36 strains, participates in nutrient uptake and may play a critical role in the bacterium's ability to evade the host immune response. Furthermore, the study found that all examined strains expressed this homologue, which can trigger bactericidal antibodies (Zielke *et al.*, 2016). This suggests its potential utility as a target for vaccine development, as eliciting an immune response against this protein could enhance protection against gonococcal infections.

1.9.2. Innovative strategies are being employed to identify potential gonococcal vaccine antigens

Innovative strategies are also being employed to identify potential gonococcal vaccine antigens. One such initiative, which draws on bioinformatics research and high-throughput quantitative proteomics techniques, is reverse vaccinology antigen mining. For example, the gonococcal strain FA1090 was subjected to proteomic profiling after being grown under three conditions designed to replicate different microecological environments in humans (Zielke *et al.*, 2016). The conditions included normal human serum, serum with limited iron, and serum deprived of oxygen (anaerobiosis). This approach led to the discovery of MetQ (NGO2139), a functionally uncharacterised gonococcal lipoprotein. It was identified among a subset of ubiquitous proteins that retained expression across all three microecological conditions (Zielke *et al.*, 2016).

Experiments in rabbits using anti-NGO2139 antibodies demonstrated bactericidal activity and that NGO2139 was conserved across different isolates of *N. gonorrhoeae* (Zielke *et al.*, 2016). According to bioinformatics analysis, NGO2139 possesses a typical lipoprotein signal peptide, indicating its export to the OM (Zielke *et al.*, 2016). In a promising observation, MetQ homologs were found within the 14 gonococcal strains listed by the WHO in 2016 and were incidentally present when three *N. meningitidis* strains were analysed (El-Rami *et al.*, 2019; Zielke *et al.*, 2016).

In another study that utilised female mice to model gonococcal infection of the genital tract, it was shown that anti-MetQ polyclonal antibodies hindered gonococcal adhesion to epithelial cells and exhibited bactericidal activity (Sikora *et al.*, 2020). Researchers formulated a recombinant protein construct (rMetQ) using phylogenetically diverse alleles of MetQ with a CpG adjuvant. The mice received the resulting rMetQ-CpG construct once subcutaneously and three times intranasally. When exposed to gonococcal infection, these immunised mice cleared the pathogen significantly faster compared to controls (Sikora *et al.*, 2020). The study thus proposed that MetQ be considered for inclusion in a future broad-spectrum gonorrhoea vaccine.

1.10. Vaccine development and the potential role of TBDTs: advantages and disadvantages

Studies have suggested that TBDTs could be used to provide human hosts with immunity from infection (Wang *et al.*, 2021). As shown in Table 1.2, TBDTs possess various characteristics that make them suitable for inclusion within a gonococcal vaccine. However, their potential use is impeded by antigenic variation among several TBDTs (Wang *et al.*, 2021).

Table 1.2. Pros and cons associated with using TBDTs in a gonococcal vaccine.

Advantages	Disadvantages
• Surface exposed and broadly distributed in Gram-negative bacteria.	• Subject to antigenic variation, which can reduce vaccine efficacy.
• Expression is induced during infection, contributing to virulence and immunogenicity.	• A single TBDT antigen may not provide sufficient coverage for all gonococcal strains.
• Possess distinctive sequence features that allow reliable in *silico* annotation.	• High variability complicates the identification of universally conserved immunogenic epitopes.

Variation is frequent in certain TBDTs, attributed to them being under significant selection pressure. This selection pressure is associated with their significant role in virulence and with their surface location. Efforts to develop an effective gonococcal vaccine have been hampered by the antigenic variation that frequently occurs within the bacteria's surface structures. *N. gonorrhoeae* used two main mechanisms to generate antigen variation: the first is homologous recombination, which is used by pilin proteins (Criss *et al.*, 2005), and the second is slipped-strand mispairing, which is behind the differing expression of iron transport proteins such as FetA, HpuAB and LbpAB (Bayliss *et al.*, 2001). This frequent variation means that a single TBDT antigen is unlikely to offer sufficient protection against all *N. gonorrhoeae* strains (Sarkissian *et al.*, 2019). An effective vaccine may therefore require multiple TBDTs. Nevertheless, there are many TBDTs involved in nutrient transportation that may help spread Gram-negative bacterial infections. This type of molecule is thus likely to feature highly in future vaccine research (Wang *et al.*, 2021).

1.10.1. SBPs as potential vaccine targets for *N. gonorrhoeae*

SBPs are a potential vaccine target and perhaps a viable option in the quest to control gonorrhoea with vaccination rather than antibiotic treatment. SBPs and certain NBDs are classed as immunogenic ABC transporter proteins. Screening with immune sera, raised against bacterial cells, has identified these molecules as immunodominant proteins and, therefore, potential vaccine targets (Akhtar and Turner, 2022).

Research has found evidence of anti-SBP antibodies. For example, when sera from rabbits immunised with deactivated *Yersinia pestis* cells were analysed, four SBPs–oligopeptide-binding protein A (OppA), phosphate-specific transport system (PstS), YrbD and periplasmic iron uptake protein A (PiuA) were categorised as immunoreactive. Only OppA, however, increased survival time among mice subsequently challenged with the bacteria, which is known for being the cause of plague (Tanabe *et al.*, 2006). These mice, immunised with OppA, survived longer than controls following *Y. pestis* infection, and their mean time-to-death correlated with IgG levels. OppA is a conserved periplasmic SBP integral to the oligopeptide permease system, widely distributed among both Gram-negative and Gram-positive bacteria, including *E. coli*, *Listeria monocytogenes*, *Helicobacter pylori*, and *Yersinia pestis*. Due to its surface accessibility, evolutionary conservation, and immunogenicity, OppA has been increasingly recognised as a promising subunit vaccine candidate in various pathogens, notably *N. meningitidis* and *B. pseudomallei* (Singh *et al.*, 2020; Wang *et al.*, 2025). Another study showed that mice immunised with OppA exhibited a significant reduction in *Moraxella catarrhalis* colonisation in pulmonary clearance models (Yang *et al.*, 2011). Future work needs to focus on *oppA*-mediated virulence and explore how the OppA antibodies potentially provide bacterial immunity (Tanaka, 2019).

In addition, mice immunised with the lipoproteins PiuA and periplasmic iron-binding protein A (PiaA), binding components of the SBP-mediated iron transport system in *S. pneumoniae*, displayed a similar level of resistance to infection as those immunised with an established vaccine (Whalan *et al.*, 2005). Mice immunised with PiuA and PiaA, thought to be essential for virulence, also displayed additive protection when challenged with *S. pneumoniae* (Mahdi *et al.*,

2015). However, in conditions where iron was restricted, mechanistic studies found that polyclonal anti-PiaA and anti-PiaB rabbit antibodies did not prevent *S. pneumoniae* proliferation. This finding indicates that the immunised mice may have been protected by the mechanism of opsonophagocytosis rather than by preventing siderophore-binding OM protein (SBO)-mediated iron transport (Jomaa *et al.*, 2006).

A study that examined a human neutrophil cell line reached a similar conclusion (Abhilasha and Marathe, 2021). Mice immunised with the polyamine-binding protein PotD, which is again integral to virulence, were also protected from systemic *S. pneumoniae* infection (Shah and Swiatlo, 2006).

The periplasmic or surface exposed SBP of the manganese ABC transporter, MntC (Manganese-binding protein of the MntABC system), elicits a protective immune response. Mice immunised with recombinant MntC generated anti-MntC IgG sufficient to protect against *S. aureus* infection. Functional and structural studies demonstrated that monoclonal MntC antibodies interacted with the globular lobes of the protein, including the manganese-binding pocket, likely occluding the SBP–TMD interaction and preventing manganese uptake (Begier *et al.*, 2017). Clinical trials further suggest that a multicomponent *S. aureus* vaccine, incorporating MntC, can target multiple virulence pathways (Mohamed *et al.*, 2017).

1.10.2. Impact of *N. meningitidis* OMV vaccines on *N. gonorrhoeae* infection and vaccine development

Vaccine innovation for *N. gonorrhoeae* has faced significant challenges, as all vaccine candidates evaluated in clinical trials have failed to provide adequate protection. This is thought to be due to its numerous mechanisms, such as a lack of animal models that can mimic natural infection diseases and a lack of understanding of what immune response is required to induce protection (Edwards *et al.*, 2016; Rice *et al.*, 2017). Furthermore, the absence of suitable animal models that accurately replicate natural gonococcal infections, coupled with a limited understanding of the immune responses necessary for effective protection, complicates vaccine innovation (Edwards *et al.*, 2018). Despite causing distinct diseases, *N. meningitidis* and *N. gonorrhoeae* are genetically

and antigenically remarkably similar, with 80–90% nucleotide identity across the genome (Massari *et al.*, 2003).

OMVs, composed of spherical bi-layered membrane structures, are naturally released from the OM of Gram-negative bacteria and consist of a mixture of OM proteins, lipopolysaccharide (LPS) and phospholipid in their native conformations (Kulp and Kuehn, 2010; Van Der Pol *et al.*, 2015). PorA, PorB, and Opa protein C (OpcA) were found to be the most abundant proteins in meningococcal OMVs. These proteins are implicated in the adhesion of bacteria to host cells. They mediate the attachment of bacteria to the host epithelial cells and contribute to the bacteria's ability to evade the host immune response. This adhesive interaction is essential for the initiation and establishment of infection (Moore *et al.*, 2005). OMV-based vaccines have been used to protect individuals against meningococcal serogroup B disease.

The antigenically varied PorA is immunodominant and the primary target of serum bactericidal antibodies (Martin *et al.*, 2006). As such, meningococcal OMV-based vaccines have been used to contain outbreaks caused by strains with matching PorA types in countries such as Cuba (VA-MENINGOC-BC®) (Balboa *et al.*, 2009; Díaz *et al.*, 2021; Whelan *et al.*, 2016), Norway (MenBvac) and New Zealand (MeNZB), which was developed by Novartis (a global pharmaceutical company based in Switzerland) (Díaz *et al.*, 2021; Petousis-Harris *et al.*, 2017; Whelan *et al.*, 2016). The latter vaccine was developed in response to a nationwide outbreak of meningococcal serogroup B disease (B: P1.7-2,4), and more than 1 million people were vaccinated between 2004 and 2008 (Arnold *et al.*, 2011).

A retrospective observational case-control study involving 15- to 30-year-olds attending sexual health clinics in New Zealand suggested that individuals vaccinated with MeNZB may have had reduced incidence of gonorrhoea compared with unvaccinated controls, with an estimated vaccine efficacy of approximately 30%.

However, due to the observational design and potential confounding factors, these findings indicate a possible association rather than definitive evidence of vaccine efficacy against gonorrhoea (Petousis-Harris *et al.*, 2017). This study

demonstrated the biological plausibility of vaccine-mediated protection against *N. gonorrhoeae* infection and offered evidence of the concept that an effective *N. gonorrhoeae* vaccine could be possible (Edwards *et al.*, 2018).

This discovery was supported by evidence from studies in Canada, Norway, and Cuba, which showed that the *N. meningitidis* serogroup B OMV-containing vaccines reduced the incidence rate of gonorrhoea infection (Azze, 2019).

In order to widen coverage against serogroup B strains, recent MenB vaccines have been developed using advanced in *silico* reverse vaccinology and proteomic approaches, enabling comprehensive analysis of *Neisseria* genomes and their gene products (Pizza and Rappuoli, 2020; Rappuoli *et al.*, 2024).
In addition, the reverse vaccinology identified three (subcapsular MenB)-recombinant antigens that each play roles in meningococcal survival and/or virulence, including Neisseria Heparin-binding antigen (NHBA), factor H-binding protein (fHbp), and Neisseria adhesin A (NadA). Recombinant versions of these proteins in combination with the New Zealand MeNZB OMVs are the immunogens contained in the broad-spectrum serogroup B vaccine Bexsero® (Bettinger *et al.*, 2013). The EU authorised the use of the Bexsero vaccine in 2013 and recommended its use for infants in the UK (McNeil *et al.*, 2013; Pollard *et al.*, 2014).

With regards to cross-protection against gonorrhoea, a research study showed that the *N. gonorrhoeae* gene encoding NadA was absent (Hadad *et al.*, 2012); the gene encoding fHbp protein was present, but not associated with surface exposed protein (Muzzi *et al.*, 2013); and genes encoding NHBA, GNA2091 (fused to fHbp to increase immunogenicity), and GNA1030 (fused to NHBA) are present, but they have not been characterised in detail (Hadad *et al.*, 2012). NHBA was found to be present in 17/17 *N. gonorrhoeae* strains studied, with an average identity of 81.2% to NHBA-2 peptide in Bexsero (Muzzi *et al.*, 2013), and in 97/111 strains, *N. gonorrhoeae* had a 65.6% identity to the non-vaccine NHBA-3 peptide from *N. meningitidis* strain MC58 (Hadad *et al.*, 2012).

1.11. NGO1152 and NGO0206 are novel vaccine antigen candidates against *N. gonorrhoeae*

This study focuses on evaluating NGO1152 and NGO0206 as potential vaccine candidates. ABC transporters are proposed as promising vaccine candidates across various organisms due to their conserved amino acid sequences, structural similarities, anticipated surface exposure, and accessibility to antibodies. Additionally, their potential role in nutrient acquisition contributes to their significance in vaccine development.

According to bioinformatics data, the first candidate is a predicted 268-amino acid, 30 kDa protein, annotated as NGO1152 in the *N. gonorrhoeae* strain FA1090 genome (accession number YP_208231). NGO1152 is a putative SBP, predicted to function as a periplasmic histidine-binding lipoprotein component of an ABC transporter involved in the uptake of amino acids such as glutamine, glutamate, or aspartate. It has a known orthologue in *N. meningitidis* (NMB1612 / NMC1533), suggesting a conserved role in amino acid transport within the *Neisseria* genus. The initial identification of NGO1152 was made by Professor Myron Christodoulides at the University of Southampton, and this was first recorded in the PubMLST database, providing a foundation for its subsequent functional and immunological characterisation. Complementing this, bioinformatic analyses indicate that NGO1152 and NMB1612 are highly conserved orthologues, sharing 98% nucleotide sequence identity and differing by only five base substitutions, suggesting functional equivalence across *Neisseria* species.

However, recent research by Dijokaite-Guraliuc (2023) identified *ngo1152* in *N. gonorrhoeae* strain FA1090 as encoding the protein ArtJ, based on bioinformatics analyses and UniProt annotations. In the UniProtKB, ArtJ is classified as a periplasmic substrate-binding lipoprotein involved in arginine transport and annotated as an arginine-binding extracellular protein (Dijokaite-Guraliuc *et al.*, 2023).

The second candidate is NGO0206 (accession number YP_207371), predicted 378 amino acids, a ~40 kDa putative periplasmic SBP with an orthologue (NMB0623/NMC0567) in *N. meningitidis*. NGO0206 is a putative

spermidine/putrescine-binding lipoprotein ABC transporter according to the *N. gonorrhoeae* strain FA1090 genome. NGO0206 is a component of a polyamine transporter system known as PotFGHI that contains three putative periplasmic polyamine binding proteins encoded by *potF1* (NGO0206), *potF2* (NGO1253), and *potF3* (NGO1494) (Goytia and Shafer, 2010).

Additionally, Zielke *et al*. (2014) identified NGO0206 in membrane vesicles of different strains of *N. gonorrhoeae* F62, MS11, and 1291, using the Isobaric Tags for Relative and Absolute Quantitation (iTRAQ) technique (Zielke *et al.*, 2014). The iTRAQ is known as an advanced quantitative proteomics technique that enables the simultaneous identification and quantification of proteins across multiple biological samples within a single mass spectrometry (MS) experiment. Introduced in the early 2000s, iTRAQ has become widely used in comparative proteomic studies due to its high sensitivity, reproducibility, and multiplexing capability (Chang *et al.*, 2025).

Furthermore, NMB1612 is a 268-amino-acid protein with a predicted 20-amino-acid N-terminal signal peptide. The mature protein is thought to undergo lipidation at Cys21 through attachment of a fatty acid chain (Hung *et al.*, 2015). The NMB1612 protein is highly conserved in meningococci and gonococci, according to BLAST analysis, and it has a domain that is a member of the bacterial SBP 3 family (Hung *et al.*, 2015). However, NMB1612 in 131 strains of meningococci has been annotated by the National Centre for Biotechnology Information (NCBI) as ArtJ (Arginine transport) due to ~41% similarity to ArtJ in *E. coli*, which is a component of the ArtPIQMJ complex, a periplasmic transport mechanism for L-arginine (Hung *et al.*, 2015). In addition, the amino acid sequence of NMB1612 shows ~ 42% (106/231 residues) similarity with the ArtJ protein from *Geobacillus stearothermophilus*, for which a crystal structure has been produced (Vahedi-Faridi *et al.*, 2008) and also shows similarity to the ArtJ proteins from *C. trachomatis* and *C. pneumoniae* (De Boer *et al.*, 2019; Soriani *et al.*, 2010). The ArtJ proteins of *C. trachomatis* and *C. pneumoniae* were investigated as vaccine candidates and were shown to have amino acids exposed on the bacterial surface (Hung *et al.*, 2015; Soriani *et al.*, 2010; Tsolakos *et al.*, 2014).

The binding of recombinant ArtJ protein to the surface of human epithelial cells may play a role in bacterial adhesion to host cells during infection, providing further evidence of surface exposure. Murine polyclonal antibodies against the ArtJ domain 1 were able to partially reduce chlamydial elementary body infectivity *in vitro* (Soriani *et al.*, 2010). Data demonstrated that NMB1612 surface exposure is adequate to offer a target for the binding of bactericidal antibodies, and it is probable that NMB1612 has similar surface exposure of amino acid sequences in a putative domain 1 (Hung *et al.*, 2015).

In a study by Hung *et al*. (2015), the immunogenic potential of the *nmb1612* gene product was evaluated by cloning and expressing the gene in *E. coli*, which enabled the purification of recombinant NMB1612 (rNMB1612) (Hung *et al.*, 2015). This antigen was then formulated for immunisation in mice using aluminium hydroxide adjuvant, both alone and in combination with liposomes, with or without the addition of monophosphoryl lipid A (MPLA). The induced antiserum demonstrated bactericidal activity not only against the homologous strain MC58 (encoding Allele 62) but also against strains carrying distinct alleles (Alleles 1, 64, and 68), with comparable serum bactericidal activity (SBA) titres reported across these diverse targets (Hung *et al.*, 2015).

However, in a human serum bactericidal assay (hSBA), a notable inconsistency was observed: strain MC58 showed resistance to killing (titre <4) despite expressing the same allele as MC168, which was susceptible, with median hSBA titres between 16 and 64. This contrast underscores the influence of additional strain-specific factors that may affect susceptibility, highlighting the importance of evaluating candidate antigens across a broad panel of clinical isolates.

A broader sequence analysis of 4,351 *N. meningitidis* genomes in the pubmlst.org/*Neisseria* database, supplemented by data from 13 colonising and invasive isolates, revealed that antibodies targeting rNMB1612 could potentially confer protection against approximately 72% of MenB strains. Notably, in isolates collected from UK MenB cases between 2013 and 2015, over 91% harboured Allele 1 of *nmb1612*, suggesting a high potential for vaccine coverage in this population (Hung *et al.*, 2015). Taken together, the conserved nature of NMB1612, its surface exposure, and its capacity to elicit cross-protective

bactericidal responses support its candidacy for inclusion in future multicomponent meningococcal B vaccines.

Nonetheless, immuno-proteomics (Williams *et al.*, 2009) has demonstrated a link between elevated SBA, widely regarded as the primary correlate of protection against meningococcal disease (Vermont, 2002), and the presence of antibodies targeting various proteins, including the product of gene *nmb1612* (NEIS1533), which encodes a putative ABC transporter, specifically a periplasmic SBP. The ABC transporters are membrane-embedded protein complexes that use the energy from ATP hydrolysis to ADP to mediate active transport of small molecules (Bulut *et al.*, 2012). SBPs selectively bind to target molecules, such as amino acids, and engage with the extracellular component of the transporter complex to facilitate translocation across the bacterial membrane.

Martin *et al*. (1986) found that polyclonal antisera generated in mice against meningococci could also recognise surface exposed, immunogenic antigens on *N. gonorrhoeae* that were targeted by bactericidal antibodies (Cremieux *et al.*, 1984; Martin *et al.*, 1986). Through using these sera to screen a gonococcal genomic library, they identified a positive clone encoding a 268-amino acid protein homologous to the *hisJ* and *argT* gene products from *E. coli* and *Salmonella typhimurium*, both of which are involved in intracellular amino acid transport (Lavitola *et al.*, 1992). BLAST analysis revealed that this gonococcal protein shared 97% amino acid sequence identity with the meningococcal NMB1612 protein. Although the exact biochemical role of NMB1612 remains undefined, its involvement in pathogenesis has been proposed; disruption of *nmb1612* in meningococci led to diminished bacterial invasion in an infant rat infection model (Sun *et al.*, 2000).

1.11.1. Research background

Due to the high similarity between NMB1612 and NGO1152, it was hypothesised that NGO1152 may have a similar potential as a vaccine antigen against *N. gonorrhoeae*. Similarly, NGO0206, as an SBP-lipoprotein, may also have similar potential features to NGO1152.

In prior work conducted in our laboratory (Patel, 2019; Smith, 2019; Williams, 2018), both *ngo1152* and *ngo0206* genes were deleted from *N. gonorrhoeae* strain FA1090, resulting in deletion mutants designated FA1090Δ*ngo1152*kan^r-F and FA1090Δ*ngo0206*kan^r-F, respectively. As well, *ngo1152* and *ngo0206* were cloned into the pQE30 vector, and N-terminally 6xHis-tagged recombinant NGO1152 and NGO0206 proteins were expressed in *E. coli*. These proteins were then purified under native conditions using Ni-NTA affinity chromatography. The recombinant proteins (rNGO1152 and rNGO0206) were used to immunise New Zealand White rabbits to yield anti-NGO1152 and anti-NGO0206 monospecific polyclonal antibodies.

1.12. Aims and objectives of this research

The aim of this project is to evaluate the potential of NGO1152 and NGO0206 as candidate antigens for *N. gonorrhoeae* vaccine development by assessing: (i) their expression and surface exposure, (ii) immunological accessibility, (iii) prevalence and conservation across a diverse collection of clinical isolates, (iv) sequence conservation and allelic variation across 7327 clinical *N. gonorrhoeae* isolates, and (v) their capacity to elicit bactericidal activity.

In Chapter 3, complemented strains of the deletion mutants FA1090Δ*ngo1152*kan^r-F and FA1090Δ*ngo0206*kan^r-F were constructed by reintroducing the SBP-encoding genes under the control of either a strong constitutive P_{opaB} promoter or an IPTG-inducible *lacPOPO* promoter. Phenotypic changes associated with the deletion mutants and their complemented strains were characterised, alongside an examination of protein levels and immune cross-reactivity against the raised antibodies.

In Chapter 4, the presence and conservation of NGO1152 and NGO0206 proteins across a diverse panel of clinical *N. gonorrhoeae* isolates were explored. Additionally, bioinformatics analyses were conducted to determine the prevalence and conservation of *ngo1152* and *ngo0206* among representative gonococcal whole genome sequences from the PubMLST database.

In Chapter 5, the subcellular localisation of NGO1152 and NGO0206 within gonococcal cells was examined, and their surface accessibility on whole bacteria was determined. Finally, the ability of anti-NGO1152 and anti-NGO0206 antibodies to mediate bactericidal activity was assessed.

Chapter 2: Materials and Methods

2.1. Bacterial strains, media, and growth conditions

N. gonorrhoeae strains used in this research are displayed below (Tables 2.1 and 2.2). *N. gonorrhoeae* strains were grown on chocolate agar (Oxoid GC Agar Base CM0367) or Thayer-Martin Medium agar with 1% Vitox, or on GC agar base supplemented with 1% (w/v) soluble haemoglobin and 1% (v/v) Vitox (Thermo Fisher Scientific, Waltham, MA, USA), named as GC-Hb-V. Mutant and complemented strains were grown on GC-Hb-V agar plates containing kanamycin (80 μg mL^{-1}) and/or erythromycin (50 μg mL^{-1}) (Sigma-Aldrich, UK). All agar plates were incubated at 37°C in a humidified atmosphere with 5% (v/v) CO_2 for 16, 18, or 24 h, depending on the experimental conditions. When grown in suspension, gonococcal strains were grown in Brain Heart Infusion (BHI) broth (Oxoid™, Thermo Fisher Scientific, UK) pre-warmed to 37 °C, supplemented with 1% (v/v) Vitox (BHI-V), and incubated at 37 °C for 16 h with shaking at 250 rpm. *E. coli* strains used for plasmid propagation and cloning, as shown in Table 2.3, were grown either in Luria–Bertani (LB) broth or on LB agar (Fisher Scientific, UK). Antibiotics were added, when appropriate, at the following concentrations: kanamycin (80 μg mL^{-1}) and erythromycin (50 μg mL^{-1}). Cultures were grown aerobically at 37°C for 16 h (unless otherwise specified) and with shaking at 250 rpm, if in liquid media. Bacterial and plasmid strain stocks were preserved at −80°C using one of two cryopreservation methods: (Delaveris *et al.*, 2021) suspension in 2 mL cryovials containing 25 porous beads and cryoprotectant, or (2) mixing 500 μL bacterial culture broth with an equal volume of glycerol (1:1 ratio). All samples were homogenised by agitation before storage.

Table 2.1. List of *N. gonorrhoeae* strains used in this research.

Strain Name	Relevant characteristics	Relevant antibiotic resistance	Source/reference
N. gonorrhoeae FA1090	Wild-type strain isolated in 1983 from a male patient with disseminated gonococcal infection (DGI)	Streptomycin	ATCC (700825) (Nachamkin *et al.*, 1981)
N. gonorrhoeae DGI-18	Wild-type strain isolated in 1983 from a patient with DGI	-	ATCC (BAA-1844)
N. gonorrhoeae MS11	Wild-type strain isolated in 1960 from a patient with an uncomplicated gonococcal infection.	-	ATCC (BAA-1833)
FA1090Δ*ngo1152*kan^r-F (Δ*ngo1152*)	*ngo1152* replaced by Kanamycin cassette	Kanamycin	Dr. Neil Oldfield, UoN. UK
FA1090Δ*ngo0206*kan^r-F (Δ*ngo0206*)	*ngo0206* replaced by Kanamycin cassette	Kanamycin	Dr. Neil Oldfield, UoN. UK
MR321152	FA1090Δ*ngo1152*kan^r-F with P_{opaB}::NGO1152 at *iga-trpB*	Kanamycin & Erythromycin	This work
MR331152	FA1090Δ*ngo1152*kan^r-F with *lacPOPO*::NGO1152 at *iga-trpB*	Kanamycin & Erythromycin	This work
MR320206	FA1090Δ*ngo0206*kan^r-F with P_{opaB}::NGO0206 at *iga-trpB*	Kanamycin & Erythromycin	This work
MR330206	FA1090Δ*ngo0206*kan^r-F with *lacPOPO*::NGO0206 at *iga-trpB*	Kanamycin & Erythromycin	This work

Table 2.2. Clinical isolates of *N. gonorrhoeae* strains used in this project. All isolates were provided by Nottingham University Hospitals NHS Trust, UK (2017–2018).

Isolate ID number	Year of isolation	Gender	Specimen Site
17N0001	2017/18	Female	Cervical
17N0002	2017/18	Male	Other
17N0003	2017/18	Male	Urethral
17N0004	2017/18	Male	Urethral
17N0005	2017/18	Male	Urethral
17N0007	2017/18	Female	Cervical
17N0008	2017/18	Female	High Vaginal
17N0009	2017/18	Female	Cervical
17N0010	2017/18	Female	Cervical
17N0011	2017/18	Male	Urethral
17N0012	2017/18	Male	Rectal
17N0013	2017/18	Female	Cervical
17N0014	2017/18	Male	Rectal
17N0015	2017/18	Male	Rectal
17N0016	2017/18	Male	Urethral
17N0017	2017/18	Female	Cervical
17N0018	2017/18	Female	Urethral
17N0019	2017/18	Female	Urethral
17N0020	2017/18	Female	Rectal
17N0021	2017/18	Male	Urethral
17N0022	2017/18	Female	Cervical
17N0023	2017/18	Female	High Vaginal
17N0024	2017/18	Female	Cervical
17N0025	2017/18	Male	Rectal
17N0026	2017/18	Male	Urethral
17N0027	2017/18	Male	Urethral

Table 2.3. List of *E. coli* and plasmid strains used in this research.

Strain Name	Relevant characteristics	Relevant antibiotic resistance	Source/reference
E. coli JM109	Competent cells were used for cloning and plasmid propagation	-	Promega, Madison, WI, USA
E. coli TAM1 (pMR32)	Source of pMR32: *E. coli* TAMI harbours the pMR32 plasmid containing a strong constitutive *opaB* promoter from *N. gonorrhoeae* strain FA1090 (P_{opaB}) driving continuous expression of target genes	Kan^R (*E. coli* / Kanamycin) and *ermC* (*Neisseria* / Erythromycin) selection	(Ramsey *et al.*, 2012)
E. coli TAM1 (pMR33)	Source of pMR33: *E. coli* TAMI harbours the pMR33 plasmid containing the tandem *lac* promoter/operator (*lacPOPO*) and *lac* repressor ($lacI^q$) from pKH37, facilitating IPTG-inducible expression of target genes	Kan^R (*E. coli* / Kanamycin) and *ermC* (*Neisseria* / Erythromycin) selection	(Ramsey *et al.*, 2012)

2.2. DNA manipulation

2.2.1. Chromosomal DNA Extraction

Genomic DNA from *N. gonorrhoeae* strains was extracted and purified using the GenElute™ Bacterial Genomic DNA Kit (Sigma-Aldrich, UK), according to the manufacturer's instructions. Alternatively, bacterial genomic DNA was prepared following a previously published protocol (Dillard, 2011). *N. gonorrhoeae* strains were grown overnight on chocolate agar or GC-Hb-V plates at 37°C in a humidified atmosphere enriched with 5% (v/v) CO_2. Bacterial growth was scraped off the plates and resuspended in 100 µL of colony lysis solution in a PCR tube. The suspension was incubated at 94°C for 15 min, followed by 5 min at 25°C in a thermocycler (C1000 Touch™, Bio-Rad, UK). After incubation, 2.5–25 µL of the lysate was used as a template for PCR reactions.

2.2.2. Plasmid DNA extraction

Overnight cultures of *E. coli* containing the plasmid of interest were grown in 10 mL of LB broth at 37°C in a shaking incubator at 250 rpm. Cells were harvested by centrifugation at 3,939 × *g* (Megafuge S16 Centrifuge, ThermoFisher) for 10 min at 4°C, and the resulting pellets were resuspended in 200 µL of resuspension solution from the GenElute™ Plasmid Miniprep Kit (Sigma-Aldrich, UK). Lysis buffer (200 µL) was added, and the mixture was incubated at RT for 10 min, followed by the addition of 400 µL of neutralisation solution. After centrifugation, the supernatant was transferred to a GenElute™ column, and plasmid DNA was isolated according to the manufacturer's instructions. The DNA bound to the column was eluted in 100 µL of dH_2O. The resulting plasmid DNA was subsequently used for downstream applications such as PCR or cloning.

2.2.3. Analysis of DNA

In all cases, the purity and concentration of isolated DNA were assessed using a NanoDrop® ND-1000 spectrophotometer (Thermo Fisher Scientific™, Waltham, MA, USA) by measuring the absorbance at 260 nm. Purity was validated with a 260/280 nm ratio of ~1.8. All DNA products were stored at -20°C.

2.3. Polymerase Chain Reaction (PCR)

The PCR thermocycle was performed utilising either a C1000 (Bio-Rad) or Parma Alpher Cycler (Cole-Parmer) as described in sections 2.3.1 and 2.3.1.

2.3.1. Phusion High-Fidelity DNA Polymerase

A 50 µL reaction mixture typically contained 5 µL of 2 µM (2 pmol μL^{-1}) of each forward and reverse primer as stated in (Table 2.4), 5 µL of 2 mM deoxynucleotides (dNTPs), 1 µL of DNA template of *N. gonorrhoeae* strain FA1090 chromosomal (*ca*. 1 ng), 5 µL of 1 x Phusion® HF Buffer, 0.5 µL Phusion High-Fidelity DNA Polymerase made up to 50 µL by addition of dH_2O.

The PCR amplification program conditions for Phusion High-Fidelity DNA was performed under the following conditions: an initial denaturation at 98 °C for

30 s, followed by 30 cycles of denaturation at 98 °C for 10 s, annealing at 62–69 °C (depending on primer T_m) for 10 s, and extension at 72 °C for 1 min. A final extension was carried out at 72 °C for 5 min (or 1 min per kilobase of the expected product size). Reaction tubes containing PCR products were held at 4 °C in the thermocycler until removal. Samples were either used immediately after being mixed with 2 µL of 6× Purple Gel Loading Dye or stored at –20 °C for future use.

2.3.2. *Taq* polymerase

For other PCRs, 10 µL reaction mixtures typically contained 1 µL of 2 µM (2 pmol µL-^{1}) of each forward and reverse primer as stated in (Table 2.4), 1 µL of 2 mM dNTPs, 0.1 µL of *Taq* polymerase (NEB, UK), 1 µL of DNA template of *N. gonorrhoeae* strain FA1090 chromosomal DNA (*ca.* 1 ng), and 1 µL of 1X ThermoPol® Buffer (NEB, UK), and were made up to 10 µL using dH_2O.

The reaction conditions for the amplification program using *Taq* polymerase consisted of an initial denaturation step conducted for 5 min at 95°C, followed by 30× cycles of 95°C for 30 s, 67–69°C for 30 s (annealing temperature determined by the melting temperature of the primer pair), and 68°C for 1 min/kb of product. This was followed by a final incubation step for 5 min at 68°C. This was followed by a final incubation at 68°C for 5 min. Reaction tubes were held at 4°C in the thermocycler until removal, after which samples were either mixed with 2 µL of Gel Loading Dye, Purple 6X and used immediately or stored at -20°C for future use.

Table 2.4. List of oligonucleotide primers used in this study. All primers were synthesised by Sigma (UK). Restriction enzyme recognition sites are indicated in bold.

Primer	Oligonucleotide Sequence (5' – 3')	Restriction Enzyme Site
NGO1152F3	CGC**TTAATTAA**ATGAATATGAAAAA ATGGATTGCC	PacI
NGO1152R3	CGC**CCGCGG**TTATTTCGCAGCCTGTC CGC	SacII
NGO0206F4	CGC**TTAATTAA**ATGAAAAAAACACT GGTGGCGGC	PacI
NGO0206R3	CGC**CCGCGG**TTATTTGCCCGCTTTGA GCCCTTG	SacII
*Trp*B-forward	AGACGCGATGAACGAAGCGATGC	-
Iga-forward	ATTGACTTACTCTGACAGTCAGC	-

2.4. Restriction Digestion and Ligation

All DNA was digested using restriction enzymes, such as PacI, SacII, and NheI, in a 37°C water bath overnight as per the manufacturer's instructions. Subsequently, all digested products were purified using the GenElute DNA Cleanup Kit (Sigma Aldrich, UK). DNA fragments were subsequently ligated utilising T4 DNA Ligase for 18 h at 4°C according to the manufacturer's specifications. Heat shock transformation of *E. coli* JM109 was performed by transferring 10 µL (100 ng) of each ligation reaction into 80 µL aliquots of *E. coli* JM109 chemically competent cells (Promega, Madison, WI, USA) in an Eppendorf tube, followed by gentle mixing. All reaction tubes were then incubated on ice for 10 min, heat-shocked at 42°C for 45–50 s in a water bath and immediately transferred back to ice for 2 min before adding 900 µL of SOC medium (Sigma-Aldrich, UK). Aliquots were then spread onto LB agar plates containing kanamycin (80 µg mL^{-1}) and/or erythromycin (50 µg mL^{-1}) and incubated overnight at 37°C. Colonies were subsequently patch-plated onto fresh agar plates for storage and confirmation.

2.5. DNA Clean-up

Overnight cultures of *E. coli* containing the plasmid of interest were grown in 10 mL of LB broth at 37°C in a shaking incubator at 250 rpm. Cells were harvested by centrifugation at 3,939 × *g* (Megafuge S16 Centrifuge, ThermoFisher) for 10 min at 4°C, and the resulting pellets were resuspended in 200 µL of resuspension solution from the GenElute™ Plasmid Miniprep Kit (Sigma-Aldrich, UK). Lysis buffer (200 µL) was added, and the mixture was incubated at RT for 10 min, followed by the addition of 400 µL of neutralisation solution. After centrifugation, the supernatant was transferred to a GenElute™ column, and plasmid DNA was isolated according to the manufacturer's instructions. The DNA bound to the column was eluted in 100 µL of dH_2O. The resulting plasmid DNA was subsequently used for downstream applications such as PCR or cloning.

2.6. Agarose Gel Electrophoresis

Agarose gels 1% (w/v) were pre-stained with SYBR® Safe DNA gel stain (Invitrogen). Gels were run in gel tanks with 1x Tris-acetate-EDTA buffer (Fisher) at 110 volts for approximately 50 min. Each 10 µL of sample was mixed with 2 µL Gel Loading Dye, Purple 6X and was run in parallel to a 3 µL 1 kb DNA Ladder to estimate DNA fragment size. DNA bands were visualised using a Uvitec scanner (Bio-Rad) or a NuGenius (Syngene) imaging system.

2.7. DNA Sequencing

The integrity of all plasmids constructed in this study was verified by DNA sequencing by Genewiz, from Azenta Life Sciences (Germany). All DNA samples were submitted via the QMC Store at the University of Nottingham, UK.

2.8. Natural transformation of *N. gonorrhoeae*

A spot transformation procedure was used to transform gonococci (Dillard and Chan, 2024). Gonococcal strains were grown in a circular area for 5 h on appropriate GC-Hb-V agar plates before 1–10 µg of linearised plasmid DNA with NheI, suspended in 20 µL of dH_2O, was spotted onto the growth zone.

Plates were then dried out in a biosafety hood for 10 min to allow the DNA to be absorbed into the bacterial growth. The agar plates were then incubated for 18 h in a humidified atmosphere at 37°C with 5% (v/v) CO_2. The next day, a Dacron swab was used to transfer the growth onto agar plates containing kanamycin (80 µg mL^{-1}) and/or erythromycin (50 µg mL^{-1}) and incubated for 16 h. Individual transformant colonies were re-streaked onto fresh selective agar plates and incubated at 37°C in a humidified atmosphere with 5% (v/v) CO_2 for 16 h and subsequently screened.

2.9. Growth curve assays

Gonococcal strains were cultured in 20 mL of prewarmed BHI-V and incubated with shaking at 250 rpm at 37°C for 16 h. The bacterial cultures were then diluted by adding 10 mL of fresh prewarmed BHI-V to achieve an OD_{600} of 0.8 or 0.7. To start a new culture at a target OD_{600} of 0.205, from an overnight culture (OD_{600} = 0.664), was calculated using the formula:

$$\frac{OD^2 = \text{desired OD for the new culture } (e.g. OD^2 = 0.205)}{OD^1 = \text{ overnight culture } (e.g. OD^1{}_{600} = 0.664)} \times 20\ \text{mL} = 6.17\ \text{mL}$$

Overnight culture (6.17 mL) was mixed with 13.83 mL of fresh, prewarmed BHI-V to a final volume of 20 mL. The OD_{600} of the mixture was measured, and volumes were adjusted using the same formula as needed to achieve an OD_{600} of 0.205. Isopropyl β-D-1-thiogalactopyranoside (IPTG) (10µl 0.5 mM final concentration) was added at T0 to induce gene expression when appropriate (Ramsey *et al.*, 2012). All broth cultures were incubated at 37°C with shaking at 250 rpm, and the growth rate of the gonococcal strains was assessed by measuring the OD_{600} every hour for 8 h using an EVOLUTION 60S spectrophotometer (ThermoFisher Scientific, UK) with BHI serving as a blank. Experiments were performed on at least 5 independent occasions. The results were analysed using GraphPad Prism (version 10.1).

2.10. Proteomic assays

2.10.1. Preparation of whole cell lysates

During the growth curve assays, 1-3 mL of culture was collected at time zero (T0) and at 1, 2, 3, and 4-h time points, then centrifuged at 33,939 × *g* for 10 min at 4°C. Subsequently, the supernatant was removed, and the cell pellets were resuspended in 1× SDS-PAGE sample buffer (Appendix-1). Before adding the SDS-PAGE sample buffer, the required volume was calculated using the formula: [80 0.3 × OD_{600} of bacterial culture = volume of buffer (µL) required to resuspend per mL of cell pellet], and the volume was adjusted based on the OD_{600} of the culture to ensure equivalent protein concentrations across samples. The bacterial suspension was then boiled at 95°C for 10 min in a heat block to be ready for SDS-PAGE analysis.

2.10.2. A Sodium dodecyl sulfate-polyacrylamide gel electrophoresis (SDS- PAGE)

Ten % (w/v) acrylamide SDS-PAGE gels were prepared as described in (Appendix-1) and used to separate proteins based on their molecular weight alongside Colour-Plus Pre-stained Standard, Broad Range P7719S (10-250 kDa) (NEB, UK), which was used as the protein molecular weight markers. Gels were run in 1× SDS-PAGE running buffer (Appendix-1) at 124 V and 400 mA until the dye front had reached the bottom of the gel. Separation was followed by gel staining or immunoblotting.

2.10.3. Acrylamide gel staining

Gels were stained using SimplyBLUE™ SafeStain (Invitrogen) according to the manufacturer's instructions. Alternatively, gels were washed with dH_2O for 5 min and then stained by immersing them in 10 mL of Coomassie Blue solution. The mixture was heated up at 70°C for 30 s in a microwave and then incubated at RT for 20 min with shaking at 40 rpm. Subsequently, the staining solution was removed and replaced with dH_2O and heated at medium power for 1 min in the microwave. Subsequently, the gel was treated with 10 mL of a destaining solution (10% [v/v] methanol, 10% [v/v] acetic acid, and 80% [v/v] dH_2O) for 1

h with shaking at RT to remove excess stain. In another approach, gels were incubated with 10 mL of Coomassie Blue solution for 1 h at RT with shaking at 40 rpm, followed by incubation in the destaining solution under the same conditions overnight. Ultimately, the gels were rinsed with dH_2O and imaged using the NuGenius (Syngene) system or using other scanner apps.

2.10.4. Immunoblotting

Subsequent protein samples were separated on 10% SDS-PAGE gels. SDS-PAGE gels were soaked in a semi-dry blotting transfer buffer (Appendix-1) for 15 min with shaking at 20 rpm before being transferred. Proteins were then transferred to Amersham™ Protan™ 0.2 µm nitrocellulose membrane using a Trans-blot SD Semi-Dry Transfer Cell (Bio-Rad) apparatus for 20 min at 12V. The membranes were blocked with 20 mL of blocking buffer containing 5% (w/v) non-fat dry skimmed milk powder dissolved in phosphate-buffered saline (PBS, pH 7.2) containing 0.05% (w/v) Tween-20 (PBST) (Sigma-Aldrich, UK) and incubated either for 2 h or overnight with shaking at 20 rpm at RT. Subsequently, the blots were washed three times with 20 mL of PBST for 5 min each with shaking at 30 rpm. Subsequently, the blotting membranes were incubated with primary rabbit polyclonal antisera (Table 2. 5), diluted in 20 mL fresh blocking buffer, and incubated for over 2 h with shaking at 20 rpm at RT or overnight at 4°C. Afterwards, the blots were washed with 20 mL of PBST for 5 min each with shaking at 30 rpm. To detect the bound primary antibody, the membrane was probed for 2 h on an orbital shaker using a goat anti-rabbit IgG alkaline phosphatase-conjugated secondary antibody, which was diluted into 20 mL fresh blocking buffer and incubated with the blots for 2 h with shaking at 20 rpm at RT. The nitrocellulose membranes were washed with 20 mL of PBST for 5 min each with shaking at 30 rpm at RT. Immunological reactivity was detected at the final stage using 1-2 mL of 5-Bromo-4-chloro-3-indolyl phosphate/nitro blue tetrazolium liquid substrate system (BCIP/NB; Sigma-Aldrich, UK) reagent and shaking for 7 min in a dark place. The detection reaction was stopped via rinsing in dH_2O. Membranes were then dried and pictured using a NuGenius (Syngene) imaging system or scanner apps.

Table 2.5. Antibodies utilised in this research.

Name	Concentration	Protein Target	Source /reference
Primary antibodies			
Rabbit polyclonal anti-NGO1152	1:1,000 and 1:100,000 (Immunoblotting assay) 1:100,000 (WC-ELISA assay)	NGO1152	This study
Rabbit polyclonal anti-NGO0206		NGO0206	This study
Rabbit polyclonal anti-meningococcal PorA	1:1,000 (WC-ELISA assay)	Cross-reactive with gonococcal PorB	Dr. Neil Oldfield
Rabbit polyclonal anti-meningococcal Fructose-1,6-bisphosphate aldolase (FBA)	1:10 (Bactericidal activity assay)	Cross-reactive with gonococcal Fructose-1,6-bisphosphate aldolase (FBA)	(Shams *et al.*, 2016)
Secondary antibodies			
Goat anti-rabbit IgG–alkaline phosphatase conjugate	1:10,000 (Immunoblotting assay) 1:1,000 (WC-ELISA assay)	Primary antibody	Sigma, UK

2.10.5. Sub-cellular fractionation of gonococcal cells

Gonococcal cells' sub-cellular fractionation was performed using a modified approach as previously reported (Nossal and Heppel, 1966). Gonococcal strains were grown in 20 mL of BHI-V at 37°C with shaking for 16 h. The turbidity of the bacterial cultures was equilibrated to an OD_{600} of 0.2 at T0 in 20 mL BHI-V. IPTG was added at a final concentration of 0.5 mM to complement strains at T0 to induce protein expression (Ramsey *et al.*, 2012). Cultures were incubated at 37°C with agitation at 250 rpm for 4 or 7 h, or until mid-logarithmic growth was reached (OD600 ≈ 0.9). At various time points, gonococcal cell growth was harvested by centrifugation at 3,939 × *g* for 10 min at 4°C and pellets were resuspended in 1 mL of ice-cold PBS buffer. Cell pellets were then washed three times with 1 mL of ice-cold PBS buffer, then centrifuged at 6,280 × *g* for 1 min, and the supernatants were discarded. The cell pellets were re-suspended again in 1 mL of ice-cold PBS, followed by probe sonication with ten repeated cycles at 6 microns (MSE Soni prep 150) for 10 s each cycle, 10 s bursts, followed by 10 s cooling on ice to prevent protein degradation due to overheating.

Subsequently, the lysed suspension was centrifuged for 3 min at 2180 × *g,* and 900 µL was transferred to a new Eppendorf tube. Then, the residual cell pellets were centrifuged for 30 min at 17142 × *g* at 4°C and 200 µL of the supernatant containing the cytoplasmic membrane (CM) fraction was removed and stored at -20°C, followed by discarding the residual supernatant. Subsequently, the remaining pellet was re-suspended in 200 µL ice-cold 10 mM Tris-HCl (pH 7.5) containing 10 mM $MgCl_2$. Then, 200 µL of ice-cold 10 mM Tris-HCl (pH 7.5) and 10 mM $MgCl_2$ containing 2% (v/v) Triton X-100 was added. The suspension was then incubated at 37°C with agitation at 100 rpm for 30 min and centrifuged at 17142 × *g* for 30 min. Then, 200 µL of supernatant containing the cytoplasmic membrane (CM) fraction was transferred to a new tube and the residual liquid was discarded. The final pellets containing the outer membrane protein (OMP)-enriched fraction were resuspended in 500 µL ice-cold 10 mM Tris-HCl [pH 7.5], 10 mM $MgCl_2$, with 2% (v/v) Triton X-100 and resuspended by a brief sonication (5 to 10 s) to solubilise clumps. In the next step, the suspensions were incubated at 37°C with shaking at 100 rpm for 30 min, then centrifuged at 17142 × *g* for 30 min at 4°C, and the supernatant was discarded. The OMP pellet was resuspended in 200 µL ice-cold 10 mM Tris-HCl [pH 7.5]. Ultimately, appropriate volumes of 5× SDS-PAGE sample buffer were added to the harvested fractions, and samples were heated up at 95°C for 7 min and stored at -20°C.

To extract periplasmic proteins, a chloroform approach (Dhital *et al.*, 2022) was undertaken. From 20 mL of overnight BHI-V culture, bacterial cells were diluted in fresh BHI-V to obtain an OD_{600} of 0.2 at T0. IPTG was then added to a final concentration of 0.5 mM to the complemented strains at T0 to induce protein expression. Subsequently, the cultures were incubated at 37°C with shaking at 250 rpm for 4 or 7 h, until reaching the mid-log phase, corresponding to an OD_{600} of ≈ 0.9. All 20 mL of bacterial culture were harvested by centrifugation at 3,939 × *g* for 5 min, and the bacterial cell pellets were resuspended in 1 mL of ice-cold PBS buffer, gently vortexed, and transferred to an Eppendorf tube. The pellets were then washed three times with 1 mL of ice-cold PBS by centrifugation. After that, bacterial cell pellets were re-suspended in 20 µL of chloroform, then briefly vortexed and incubated for 15 min at RT. Subsequently,

100 µL of ice-cold 10 mM Tris solution (pH 7.5 or 8.5) was added to the suspension and briefly vortexed and centrifuged at 4,360 × *g* for 5 min. Approximately 100 µL from the top of the supernatant (enriched in periplasmic proteins) was transferred to a new tube and mixed with 25 µL of 5× SDS-PAGE sample buffer. Samples were heated up at 95°C for 7 min and stored at -20°C.

2.10.6. Immuno-dot blot assay

Gonococcal strains were grown in BHI-V at 37°C, with shaking for 16 h. The turbidity of the gonococcal cultures was then diluted to achieve an OD_{600} of 0.2. IPTG at 0.5 mM final concentration was added at T0 to the complemented strains to induce protein expression. Then the bacterial cultures were incubated at 37°C, with shaking at 250 rpm for 4 or 7 h. Bacterial growth was harvested by centrifugation at 3,939 × *g* for 10 min at 4°C, and supernatants were discarded. Gonococcal cell pellets were briefly vortexed and resuspended in 1.5 mL of ice-cold PBS, washed five times with the same solution by centrifugation at 6,280 × *g* for 1 min per wash, and the supernatants were discarded. Subsequently, 20 µL from the residual cell suspensions of intact cells were spotted on 0.45 µm nitrocellulose membranes and dried for 4 min at 37°C. The membranes were blocked with 5% (w/v) non-fat dry skimmed milk in phosphate-buffered saline PBS (pH 7.2) containing 0.05% (w/v) Tween-20 (PBST) (Sigma-Aldrich, UK) and incubated for 2 h with shaking at 40 rpm at RT. Subsequently, blots were washed three times for 5 min each with shaking. The blot membranes were probed with primary rabbit antiserum (Table 2.5), which was diluted in fresh blocking buffer and incubated with the membrane for over 2 h, with gentle shaking at 40 rpm at RT. Blots were washed three times for 5 min each with shaking. The bound primary antibody was detected using an anti-rabbit IgG–alkaline phosphatase-conjugated secondary antibody, diluted in fresh blocking buffer, and incubated for over 2 h with shaking at RT. The nitrocellulose membranes were washed three times in PBST for 5 min with shaking. Immunological reactivity was detected at the final stage using 1-2 mL of 5-Bromo-4-chloro-3-indolyl phosphate/nitro blue tetrazolium liquid substrate system (BCIP/NB; Sigma-Aldrich, UK) reagent. The detection reaction was stopped via rinsing in dH_2O.

2.10.7. Whole-Cell Enzyme-Linked Immunosorbent Assays (WC-ELISAs)

Gonococci were grown in prewarmed BHI-V and incubated at 37°C for 16 h with shaking. The next day, this culture was used to inoculate a fresh BHI-V culture to achieve an OD_{600} of 0.2. IPTG (0.5mM final concentration) was added, where appropriate, and cultures were incubated at 37°C with shaking for 4 h until the OD_{600} reached approximately 0.8–0.9. Bacterial cell pellets were harvested by centrifugation at 3,939 × *g* for 10 min at 4 °C, and the cell pellet was gently resuspended in 5 mL PBS (0.2 µm-filtered). The bacterial pellet was washed three times with PBS by centrifugation at 3,939 × *g* for 3 min each time. Finally, bacterial pellets were resuspended in 5 mL 0.2µm-filtered Carbonate buffer (0.1M $NaHCO_3$, 0.1M Na_2CO_3 at pH 9.4). The OD_{600} of the bacterial suspensions was equilibrated to achieve an OD_{600} of ≈ 0.3 in carbonate buffer to be ready for coating. Subsequently, 96-well ELISA microtiter plate wells (Nunc™ Immobiliser™ Amino 12×8 Strips, Thermo Fisher Scientific, UK) were filled with 150 µL of bacterial cell suspension, and the wells were air-dried in a laminar flow cabinet at 25 °C. The dried plates were heat-treated at 56 °C for 1 h (Jen *et al.*, 2019). The wells were then washed three times with PBST and blocked with 150 µL of PBST containing 1% (w/v) bovine serum albumin (1%BSA) (Sigma-Aldrich, UK) to reduce non-specific antibody binding. Plates were incubated at 4 °C overnight or for 2 h at RT, followed by times with PBS 3 times. Wells were then probed with 150 µL rabbit polyclonal antiserum (typically 1:5000 diluted) in PBST containing 1% BSA. Rabbit anti-meningococcal whole PorA (1:1000 dilution) was used as a positive control for surface exposure. Plates were incubated at 4°C overnight, followed by washing three times with PBS. Subsequently, 150 µL of goat anti-rabbit IgG–alkaline phosphatase conjugate (Sigma-Aldrich, UK), diluted 1:1000 in PBST containing 1% BSA (v/v), was added and incubated for 2 h at RT, followed by washing three times with PBS. Colour was developed by adding 150 µL per well of phosphatase substrate (Sigma; each tablet dissolved in 1.5 mL of glycine buffer [100 mM glycine, 1 mM $ZnCl_2$, 1 mM $MgCl_2$, pH 10.4]). All plate absorbance readings were taken at 405 nm using A GloMax® microplate reader (Promega, Madison, WI, USA) after 2 h of incubation in a dark place.

2.11. Serum Bactericidal Activity (SBA) assay

The SBA assay was performed according to the protocol described by Zhu *et al*. (2019), with some modifications (Zhu *et al.*, 2019). Gonococcal strains were grown overnight in prewarmed BHI-V at 37°C for 16 h with shaking. The following day, fresh pre-warmed BHI-V was added to equilibrate the cultures to achieve an OD_{600} of 0.2, and the cultures were incubated at 37°C with shaking for 4 h until the mid-logarithmic phase of growth reached an OD_{600} of 0.8 to 0.9. One mL of bacterial culture was harvested by centrifuging at 4,360 × *g* for 2 min, and the bacterial pellet was gently reconstituted in 1 mL of bactericidal buffer (Appendix-1).

The gonococci cell suspension was subsequently diluted in a bactericidal buffer to achieve ~ 8×10^4 CFU/mL. Separately, rabbit antisera to be tested were double diluted in bactericidal buffer to obtain 1:128, 1:256, 1:512, 1:1024, 1:2048, 1:4096 and 1:8192 dilutions. Rabbit polyclonal anti-meningococcal FBA antiserum (Shams *et al.*, 2016) was used at a 1:10 dilution in bactericidal buffer as a positive control for killing. All diluted antibody dilutions were decomplemented by heat-inactivation at 56°C for 30 min and stored at -20°C. As a T0 control for gonococcal cell viability, 10 µL of the diluted gonococcal cell suspension (8×10^2 CFU) was added to 30 µL bactericidal buffer in two wells of a sterile 96-well V-bottom microtiter plate and gently mixed by pipetting. Subsequently, 20 µL aliquots of these suspensions were taken and subjected to serial dilution with 20 µL of bactericidal buffer to achieve the following dilution series: 1:2, 1:4, 1:8, and 1:16. After that, 10 µL aliquots from each dilution were plated onto GC chocolate agar plates (Oxoid GC Agar Base CM0367) and incubated at 37°C in a humidified atmosphere with 5% CO_2 for 16 h. To calculate the viable count per well at T0, the dilution which yielded 3-30 colonies per 10 µL spot was utilised. The CFU per well was calculated using the formula: (colony count X dilution factor X 4), and the mean CFU count across the duplicate wells was calculated. As a T30 min control for gonococcal cell viability, 10 µL of the gonococcal cell suspension was added to 30 µL bactericidal buffer in two wells of a sterile 96-well V-bottom microtiter plate in 40 µL total volume and gently mixed by pipetting. Following 30 min incubation at 37°C, aliquots were subjected to serial dilution with bactericidal buffer,

subsequently plated onto GC agar plates, and incubated at 37°C in a humidified atmosphere with 5% CO_2 for 16 h. The resulting CFUs were counted, and the mean value was calculated as the number of viable colonies at T30 min. The SBA assay itself was initiated by adding 10 µL IgG/IgM-depleted pooled human complement serum (HC; Pel-Freez Biologicals, USA) to a well already containing 10 µL bacterial suspension and 20 µL of diluted polyclonal rabbit antibody. A complement-only control was included by adding 10 µL HC to a well already containing 10 µL bacteria and 20 µL bactericidal buffer. For antibody-only controls, wells containing 10 µL of bactericidal buffer, 10 µL bacteria and 20 µL test (1:128 diluted) or control (1:10 diluted) antibodies were used. All samples were mixed, and the plate was incubated for 30 min at 37°C in a humidified atmosphere with 5% CO_2. Following incubation, 20 µL of the wells were doubly diluted with 20 µL bactericidal buffer to achieve the following dilution series: 1:2, 1:4, 1:8, and 1:16. Diluted 10 µL aliquots of the suspensions were plated out onto chocolate agar and incubated at 37°C in a humidified atmosphere with 5% CO_2 for 16 h, and the number of surviving CFUs were enumerated.

To calculate the viable count per well, the dilution which typically yielded 3-30 colonies per 10 µL spot was utilised to yield the CFU count following 30 min incubation with 1:128, 1:256, 1:512, 1:1024, 1:2048, 1:4096 or 1:8192 diluted test sera (or controls) at 37°C in a humidified atmosphere with 5% CO_2. The SBA titre was defined as the lowest serum dilution which showed ≥50% killing after 30 min compared to the T0 CFU count (Dijokaite-Guraliuc *et al.*, 2023). Additionally, results were only considered valid if the % survival in the test reaction mixture divided by the percentage survival in the complement-only control was ≤50%, and there was ≥90% survival at 30 min in the complement-only control. All experiments were conducted on multiple separate occasions, with each sample being tested four times unless otherwise noted.

2.12. Bioinformatics analysis tools

2.12.1. Defining a list of *N. gonorrhoeae* isolates

A list of *N. gonorrhoeae* isolates, with associated provenance and phenotype information, was extracted from the Public Databases multilocus sequence typing (PubMLST) web server [https://pubmlst.org/bigsdb?db=pubmlst_neisseria_isolates&page=query] on 12th August 2022. The list was generated using the following settings: (i) under *Isolate provenance/primary metadata fields*, the option "year > = 2014" was selected; (Binker *et al.*, 2007) results were filtered such that the *Ribosomal MLST* (*multilocus sequencing typing ST*) *profile* was "complete"; (Agbodzi *et al.*, 2023; Bennett *et al.*, 2007; Jolley *et al.*, 2012) under the *Attribute values list*, the field: *species* (*Ribosomal MLST*) was selected, and the search was undertaken using the term '*Neisseria gonorrhoeae*'. The resulting dataset was exported in an Excel file format and included all relevant metadata associated with each isolate record (for example, country of isolation, continent of isolation, and multilocus sequence type).

2.12.2. Local alignment search tool (BLAST; Basic Local Alignment Search Tool) analyses

The BLAST feature embedded in PubMLST [https://pubmlst.org/bigsdb?db=pubmlst_*neisseria*_isolates&page=plugin&name=BLAST] was used to extract the closest sequence in each of the previously identified gonococcal isolates to the FA1090-NGO1152 or FA1090-NGO0206 sequence (Table 2. 6). Default settings were used, except to allow isolates with no matches to be displayed in the results (Jolley *et al.*, 2018). When completed, the Excel sheet (containing information for each isolate, such as percentage identity to the query sequence, alignment length, number of mismatches, and gaps) and the Fast alignment search tool-all (FASTA) with flanking sequence file were downloaded and saved for further analysis.

Table 2.6. The full amino acid sequences of NGO1152 and NGO0206 from *N. gonorrhoeae* FA1090, and NMB1612 from *N. meningitidis* MC58.
Amino acid residues are coloured according to their physicochemical properties: red (AVFPMILW; small hydrophobic, blue (DE; acidic), magenta (RK; with basic-H) and green (STYHCNGQ; hydroxyl, sulfhydryl, amine, and G).

Protein name	Amino acid sequence	Locus information	Predicted function
NGO1152 (268 amino acids), (accession number YP_208231) from *N. gonorrhoeae* strain FA1090	**>NGO1152** MNMKKWIAAALACSALALSAC GGQGKDAAAPAANPGKVYRVA SNAEFAPFESLDSKGNVEGFD VDLMNAMAKAGNFKIEFKHQP WDSLFPALNNGDADVVMSGVT ITDDRKQSMDFSDPYFEITQV VLVPKGKKVSSSEDLKKMNKV GVVTGHTGDFSVSKLLGNDNP KIARFENVPLIIKELENGGLD SVVSDSAVIANYVKNNPAKGM DFVTLPDFTTEHYGIAVRKGD EATVKMLNDALEKVRESGEYD KIYAKYFAKEGGQAAK*	NEIS1533 Aliases: In *N. meningitidis* NMB1612 NMC1533	Histidine-binding periplasmic SBP is involved in the transport of amino acids (*e.g.* glutamine, glutamate, or aspartate).
NGO0206 (378 amino acids), (Accession number YP_207371) from *N. gonorrhoeae* strain FA1090	>NGO0206 MKKTLVAAILSLALTACGGGS DTAAQTPSAKPEAEQSGKLNI YNWSDYVDPETVAAFEKETGI KMRSDYYDSNETLEAKVLTGK SGYDLTAPSIANVGRQIKAGA YQKIDKAQIPHYGNIDKDLLK MMEAVDPGNEYAVPYFWGINT LAINTRQVQKALGTDKLPENE WDLVFKPEYTAKLKSCGISYF DSAIEQIPLALHYLGKDPNSE NPEDIKAAVDMMKAVRGDVKR FSSSGYIDDMAAGNLCAAIGY GGDLNIAKTRAEEAANGVEIK VLTPKTGVGVWVDSFMIPRDA QNVANAHRYIDYTLRPEVAAK NGSFVTYAPASRPARELMDEK YTSDASIFPTKELMEKSFIVS PKSAESVKLGVKLWQGLKAG*	NEIS0567 Aliases: In *N. meningitidis* NMC0567 NMB0567	Putative polyamine permease periplasmic SBP.
NMB1612 (268 amino acids), (ID:2018662) from *N. meningitidis* serogroup B (strain ATCC BAA-335 / MC58)	>NMB1612 MNMKKWIAAALACSALALSAC GGQGKDTAAPAANPDKVYRVA SNAEFAPFESLDSKGNVEGFD VDLMNAMAKAGNFKIEFKHQP WDSLFPALNNGDADVVMSGVT ITDDRKQSMDFSDPYFEITQV VLVPKGKKVSSSEDLKNMNKV GVVTGYTGDFSVSKLLGNDNP KIARFENVPLIIKELENGGLD SVVSDSAVIANYVKNNPAKGM DFVTLPDFTTEHYGIAVRKGD EATVKMLNDALEKVRESGEYD KIYAKYFAKEDGQAAK*	Aliases: In *N. meningitidis* NMC1533	Putative amino acid ABC lipoprotein transporter, periplasmic SBP involved in gaining transport.

2.13. Further bioinformatics tools for sequence analysis

2.13.1.1. Translation of DNA sequences

The ExPASy translate tool [https://web.expasy.org/translate/] was used to obtain the amino acid sequences of proteins of interest using the DNA sequence provided in the FASTA with the flanking file. Truncated proteins (identified by their shorter alignment length, but high amino acid identity) were resolved by closely examining the DNA sequence and translated amino acid sequence for the presence of substitutions creating internal stop codons or insertions/deletions leading to frameshifts in the gene of interest. Alternatively, genes of interest were determined to span multiple contigs if the coding sequence was incomplete and no flanking sequence was present in the FASTA output.

2.13.2. Multiple sequence alignments

The multiple sequence alignment program Crustal Omega [https://www.ebi.ac.uk/Tools/msa/clustalo/] was used to compare multiple protein sequences and highlight amino acid differences within proteins of interest. This alignment tool allowed representative examples of all full-length sequences to be aligned for comparison to visualise the location and nature of amino acid substitutions. The National Centre for Biotechnology Information (NCBI) standard nucleotide BLAST [https://blast.ncbi.nlm.nih.gov/Blast.cgi?PROGRAM=blastn&PAGE_TYPE=blastsearch&LINK_LOC=blasthom] was used to identify low identity hits extracted from gonococcal isolates in the *N. gonorrhoeae* FA1090 complete genome.

2.13.3. Pairwise sequence alignment.

To assess the degree of sequence conservation between NGO0206 (378 amino acids) and NGO1152 (268 amino acids) or NMB1612 (268 amino acids).

The pairwise sequence alignment was performed using the EMBOSS Water program available from the European Bioinformatics Institute (Binker *et al.*, 2007) [https://www.ebi.ac.uk/jdispatcher/psa/emboss_water/]. EMBOSS Water applies the Smith-Waterman algorithm to identify optimal local alignments between sequences. The alignment was conducted using the EBLOSUM62

substitution matrix with a gap opening penalty of 10.0 and a gap extension penalty of 0.5. The resulting output included alignment length, percentage identity, similarity, and gap information, providing a detailed measure of sequence conservation.

2.14. Statistical analysis

GraphPad Prism (version 10.1) was used for all statistical analyses. Samples were analysed in quadruplicate, and each experiment was repeated at least four times. The built-in *t*-test, one-way ANOVA or two-way ANOVA were utilised to determine statistically significant differences between experimental results. A *p*-value of >0.05 was considered non-significant (ns), while values ≤0.05, ≤0.01, ≤0.001 or ≤0.0001 were considered significant (*), very significant (**), highly significant (***) and very highly significant (****), respectively.

Chapter 3: Functional complementation of *ngo1152* and *ngo0206* in *N. gonorrhoeae* FA1090

3.1. Introduction

Functional complementation is the reintroduction of a gene of interest into a mutant strain to investigate whether it restores a wild-type phenotype, thus excluding the possibility that any observed phenotypes in the mutant are due to undetected secondary mutations or polar effects. In *N. gonorrhoeae*, functional complementation is commonly achieved by reinserting a gene of interest into the chromosome at an ectopic site. *N. gonorrhoeae* exhibits an extraordinary capacity to acquire antibiotic resistance through both plasmid uptake and chromosomal mutations (Unemo and Shafer, 2014). Gonococci are naturally transformable and, in particular, readily take up DNA that contains a specific 10-bp *Neisseria* DNA uptake sequence (DUS), GCCGTCTGAA (Flemming, 2023). More recently, 12 bp sequences were identified as (AT-DUS: 5'-AT-GCCGTCTGAA-3'), which enhanced transformation efficiency (Miari *et al.*, 2024). Furthermore, variant DUS (Vdus 5'-GTCGTCTGAA-3') was present in the commensal *Neisseria* has also been described, with some species such as *N. mucosa* having > 3,000 copies (Marri *et al.*, 2010).

For efficient DNA uptake, plasmids or linear DNA fragments used in the transformation of *N. gonorrhoeae* should contain the DUS sequence. The DUS is commonly observed in the chromosomes of *N. gonorrhoeae* and other *Neisseria* species, typically appearing as a pair of inverted repeats, often occurring in multiple copies. In reality, an expanded 12-bp DUS sequence, specifically ATGCCGTCTGAA, was identified as the predominant form of DUS in *Neisseria* genomes (Carter *et al.*, 2022). This particular sequence has been found to enhance the efficiency of gonococcal transformation with plasmids twofold compared to those encompassing the 10-bp DUS (Ambur *et al.*, 2007). In contrast to many other transformable microbes, *N. gonorrhoeae* does not regulate transformation and retains the ability to undergo transformation at all stages of growth (Walker *et al.*, 2023). However, natural transformation occurs only in piliated gonococci, as piliation is a phase-variable

characteristic. Thus, it is important to carefully select piliated colonies for transformation.

Numerous chromosomal sites have been utilised for gene complementation in gonococci, including regions near the *iga* gene responsible for encoding IgA1 protease and an intergenic area located between *lctP* and *aspC* (Mehr *et al.*, 2000). While IgA protease is not crucial for the growth of *N. gonorrhoeae*, it could be disrupted without affecting *in vitro* characteristics (Koomey *et al.*, 1982). Intergenic insertions are often favoured as they are less likely to impact any observable traits. In principle, any location that does not disrupt genes or operons can be employed for this procedure.

However, significant effort has been devoted to developing *lctP-aspC*-based constructs for effective gonococcal complementation in the past. A set of plasmids was developed containing a polylinker, an antibiotic resistance marker and, in some cases, a regulatable promoter. Following the transformation of gonococci and subsequent selection for the antibiotic resistance marker, bacteria that integrated the construct via double crossover recombination were identified with the genes (including the antibiotic resistance marker) inserted between *lctP* and *aspC* (Dillard and Chan, 2024). Among these plasmids, pGCC6 stands out for its inclusion of two copies of the *lac* promoter-operator and the *lac* repressor gene (*lacI*^{q}) for inducible gene expression (Mehr *et al.*, 2000). The intergenic region between *lctP* and *aspC* has also been used in other studies for complementation, using a variety of constructs that have been engineered to facilitate direct gene insertion at this site (Hamilton *et al.*, 2005; Mehr *et al.*, 2000; Stohl *et al.*, 2003) as well as other chromosomal loci, such as *proB, iga*, and the *porin* pseudogene (Steichen *et al.*, 2011; Steichen *et al.*, 2008; Wolfgang *et al.*, 2000). However, collectively, the existing complementation constructs have substantial limitations. For instance, in the case of the *iga* and *porB* constructs, gene insertion takes place within an open reading frame (Steichen *et al.*, 2008; Wolfgang *et al.*, 2000), which introduces the potential risk of altering the organism's growth or pathogenicity.

Moreover, there are limitations in the availability of promoters for regulating gene expression. Typically, the gene of interest could be either cloned along with its native promoter or expressed from the promoter of an upstream antibiotic

resistance marker. The *lac* promoter is one of the few inducible systems that has been established for gene complementation in pathogenic *Neisseria* species (Dam and Bos, 2012; Dillard, 2011). This study will utilise a set of complementation constructs that contain regions of the *iga* and *trpB* genes, facilitating the direct insertion of genes into the *iga-trpB* intergenic region (Ramsey *et al.*, 2012). These constructs include two distinct promoters. pMR32 has a strong constitutive *opaB* promoter from *N. gonorrhoeae* strain FA1090 (P_{opaB}). In contrast, pMR33 contains the tandem *lac* promoter/operator (*lacPOPO*) and *lac* repressor ($lacI^q$) from pKH37 (Kohler *et al.*, 2007) (Figure 3.1).

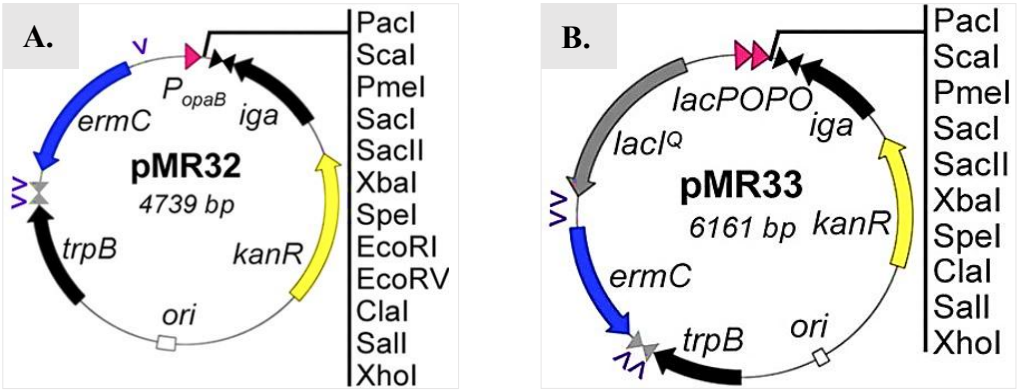

Figure 3.1. Complementation plasmids (pMR32 and pMR33) are used for constitutive and IPTG-inducible gene expression in *N. gonorrhoeae* and *N. meningitidis*.
(**A**) Plasmid map illustrating the genetic arrangement of the pMR32 (4,739 bp) *iga-trpB* complementation construct, which includes P_{opaB} constitutive *opaB* promoter (*P_{opaB}*) from *N. gonorrhoeae* FA1090. (**B**) Plasmid map illustrating the genetic arrangement and key elements of the pMR33 (4,739 bp) *iga-trpB* complementation construct, including *lacPOPO* and *lac* repressor (*lacI^q*), facilitating IPTG-inducible expression (Ramsey *et al.*, 2012). Black arrows in both show regions of homology with the meningococcal and gonococcal chromosomes. Both pMR32 and pMR33 are plasmids that utilise direct gene of interest insertion between (*trpB* and *iga*) and encode an erythromycin resistance marker (*ermC*; blue arrow) along with the cloned gene of interest and kanamycin resistance gene (*kanR*; yellow arrow) as a selectable marker for *E. coli* propagation. The pMR32 contains the strong constitutive promoter from the *opaB* gene of *N. gonorrhoeae* strain FA1090 (P_{opaB}), whilst the pMR33 contains tandem *lac* promoter/operator (*lacPOPO*) and *lac* repressor ($lacI^q$), facilitating IPTG-inducible expression. However, the transcriptional terminator is located in the chromosome between the *iga* and *trpB* genes, as indicated by the grey inverted triangles. Another transcriptional terminator from the *ermC* gene is denoted by (black inverted triangles), while unique restriction sites in the polylinkers are highlighted. DNA uptake sequences are represented by (purple arrowheads). The figure above is adapted from (Ramsey *et al.*, 2012).

In previous work, recombinant NGO1152 and NGO0206 proteins were expressed, purified, and used to raise rabbit polyclonal antibodies. Additionally, *ngo1152* and *ngo0206* were deleted in *N. gonorrhoeae* strain FA1090 and replaced with a kanamycin cassette.

The work described in this chapter aimed to functionally complement each gene by introducing *ngo1152* or *ngo0206* into the *iga-trpB* intergenic region of pMR32 and pMR33, before reintroducing *ngo1152* or *ngo0206* gene back into the Δ*ngo1152* or Δ*ngo0206* mutant chromosomes at the *iga-trpB* intergenic region, under the control of either the strong constitutive P_{opaB} or IPTG-inducible *lacPOPO* promoter, by natural transformation, followed by genotypic and phenotypic characterisation of the resulting strains.

3.2. Results

3.2.1. Amplification of *ngo1152* for cloning

The NGO1152-encoding gene was PCR amplified from the chromosomal DNA of *N. gonorrhoeae* FA1090 utilising the oligonucleotide primers NGO1152F3 and NGO1152R3 as described in Table 2.4. These primers were designed to incorporate PacI and SacII restriction enzyme sites at the 5' and 3' ends of the amplicon, respectively, and enable amplification from the ATG start codon to the TAA stop codon of the gene.

The PCR product was analysed on an agarose gel stained with SYBR Safe, confirming successful amplification of the gene encoding NGO1152. As expected, a single band of approximately 800 bp was observed (Figure 3.2).

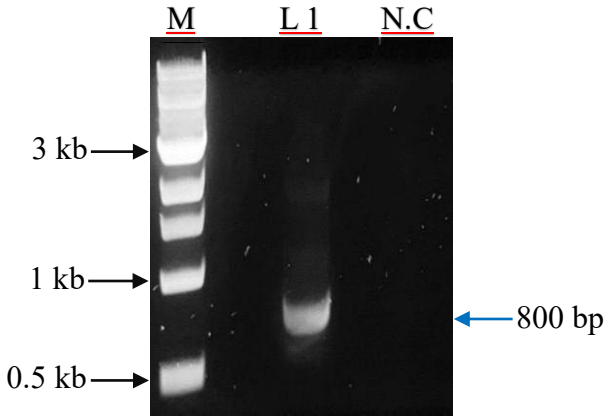

Figure 3.2. Successful amplification of *ngo1152* visualised via 1% agarose gel electrophoresis.
Genomic DNA of *N. gonorrhoeae* strain FA1090 was used as a template for the PCR amplification of *ngo1152*. Lane M: 1 kb DNA ladder marker used to indicate the size of the DNA fragments. Lane 1: shows an 800 bp amplified PCR product corresponding to the expected size of *ngo1152*. Lane N.C: negative control without DNA template.

3.2.1.1. Cloning *ngo1152* into pMR32 and pMR33 vectors

The *ngo1152* amplicon and pMR32 (or pMR33) were digested with PacI and SacII, subsequently ligated by T4 DNA ligase, and then transformed into *E. coli* JM109 competent cells. As a result, single putative transformant colonies were obtained following overnight incubation on LB agar containing erythromycin and kanamycin. Plasmid DNA extracted from selected transformant colonies was subjected to double digestion with PacI and SacII enzymes. The resulting fragments were then analysed by gel electrophoresis to confirm the insertion of *ngo1152* into the respective plasmid backbones. The analysis showed a band at *ca*. 4.7 kb (equivalent to the size of pMR32) and *ca*. 800 bp (corresponding to the expected size of the *ngo1152* insert) in one out of six screened *ngo1152*::pMR32 transformant clones (Figure 3.3A).

Additionally, 5 out of 6 selected *ngo1152*::pMR33 colonies revealed bands at *ca.* 6.1 kb (corresponding to pMR33) and another band at 800 bp (commensurate with *ngo1152*), confirming the successful ligation of *ngo1152* to the pMR33 vector (Figure 3.3B).

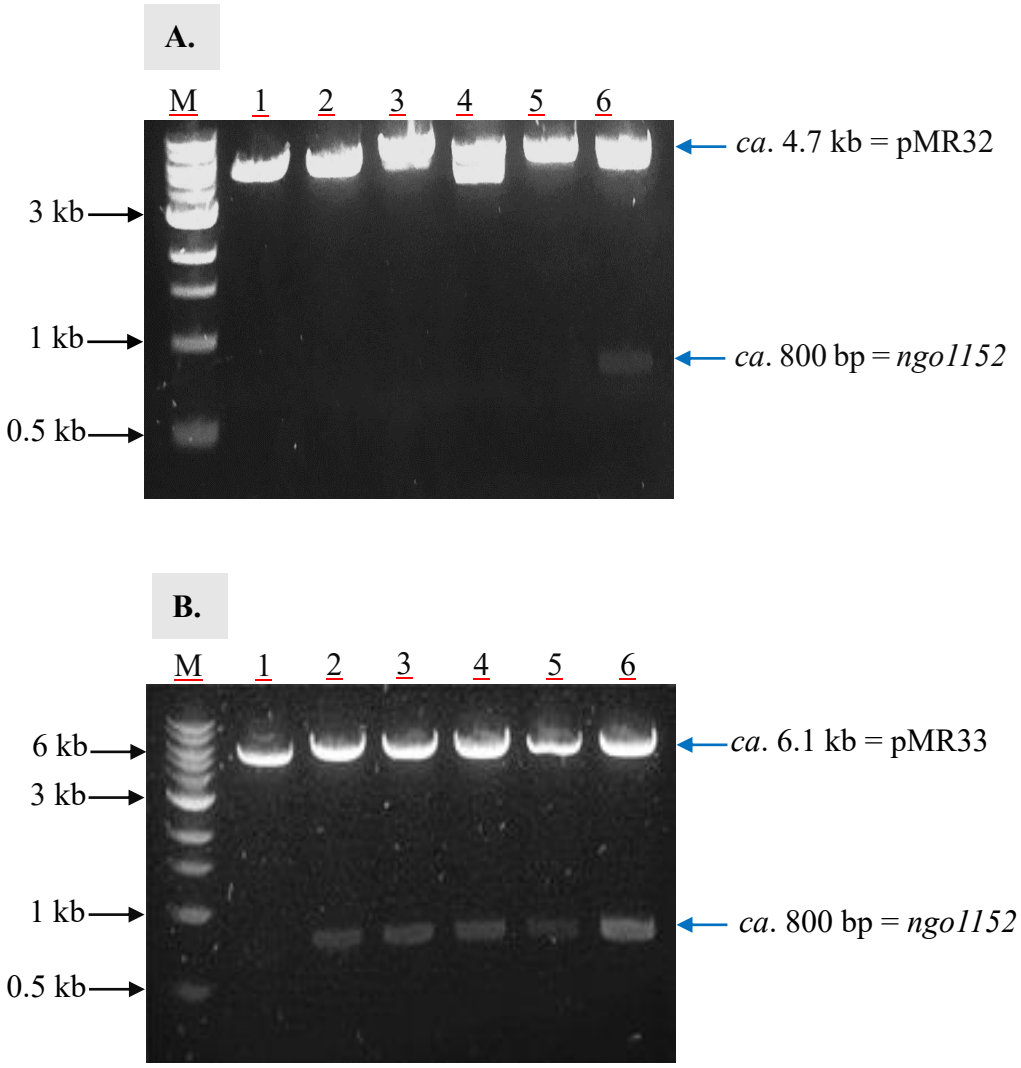

Figure 3.3. PacI and SacII double-digested plasmid DNA isolated from 12 selected *E. coli* JM109 transformant clones confirms the successful ligation of *ngo1152* into (A) pMR32 and (B) pMR33.
The agarose gel image in panel (A) shows the restriction profile of six independent clones potentially harbouring the *ngo1152*::pMR32 construct. Lane M: 1 kb DNA Ladder Marker. Lanes 1 to 6: a 4.7 kb band corresponding to the linearised pMR32 vector. Lane 6: shows an additional band at 800 bp, indicating the presence of the *ngo1152* insert, indicating successful ligation. Panel (B) depicts the restriction profile of six independent clones potentially harbouring the *ngo1152*::pMR33 construct. Lane M: 1 kb DNA Ladder Marker. Lane 1 to 6: a 6.1 kb band corresponding to the predicted sizes of the linearised pMR33 vector. Lanes 2, 3, 4, 5 and 6: display an additional 800 bp band corresponding to the *ngo1152* insert, indicating successful ligation.

To confirm the constructs, the pMR32-based plasmid shown in Figure 3.3A, Lane 6 (named pAA2), and the pMR33-based plasmid shown in Figure 3.3B, Lane 3 (named pAA4), were sent for DNA sequencing. The sequencing results confirmed successful cloning and the absence of any PCR-generated errors. Additionally, schematic diagrams of the pAA2 and pAA4 constructs, generated as part of this study, are presented below in Figure 3.4.

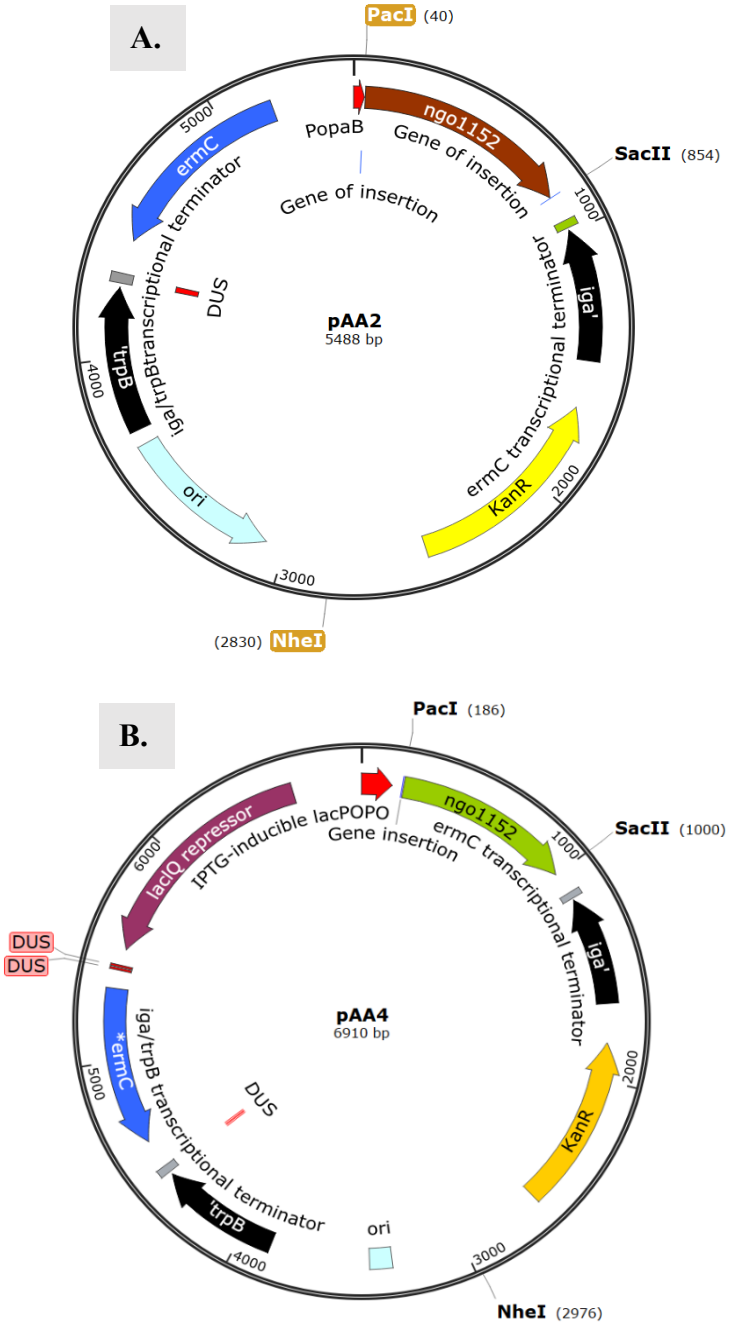

Figure 3.4. Schematic diagrams of *ngo1152* cloned into pMR32 or pMR33 vector to construct DNA yield pAA2 (A) or pAA4 (B), respectively. Maps were generated using SnapGene.

3.2.1.2. Natural transformation of FA1090Δ*ngo1152* with pAA2 and pAA4

NheI-linearised pAA2 and pAA4 plasmid DNA were spotted onto a fresh Δ*ngo1152* strain grown on agar plates containing kanamycin. Subsequently, the agar plates were incubated for 18 h at 37°C in a humidified atmosphere with 5% (v/v) CO_2. The following day, the growth was removed and streaked onto agar containing kanamycin and erythromycin and incubated for 18 h at 37°C in a humidified atmosphere with 5% (v/v) CO_2. Multiple colonies were obtained, and after resub-culturing, their chromosomal DNA was extracted for PCR analysis. Additionally, primers were designed to demonstrate the correct insertion of *ngo1152* (with promoter) and *ermC* between the *trpB* and *iga* genes following double crossover with the chromosome of FA10900Δ*ngo1152*. These primers were: a *trpB*-forward primer and an *iga*-forward primer, both of which anneal to the region of *trpB* (or *iga)* present in the FA1090 chromosome, but outside the regions contained in pMR32 and pMR33.

These primers were used together or in combination with the *ngo1152*-specific primer to confirm successful recombination (Figures 3.5A and 3.6). By using the *trpB* forward primer and the NGO1152R reverse primer, a *ca* 2.9 kb band was obtained from pAA2 transformants, whilst a band of *ca* 4.3 kb was observed from pAA4 transformants. As expected, no band was obtained from the chromosomal DNA of Δ*ngo1152* because no *ngo1152* gene was present downstream of *trpB.* Whereas the absence of any band observed in the negative control (no DNA template) indicated that the PCR mix was not contaminated (Figure 3.5A). To determine whether the gene with its promoter had been correctly integrated between the *trpB* and *iga* genes, primers were designed.

Two PCR strategies were used to demonstrate the correct insertion of *ngo1152* between the *trpB* and *iga* genes. One pair of primers was designed, *trpB*-forward and *iga*-forward, each annealing to the *trpB* (or *iga*) region that is present in the FA1090 chromosome. However, these primers anneal to regions outside those contained in pMR32/pMR33 plasmids.

These primers were used together or with other reverse primers of *ngo1152* to confirm successful recombination. The schematic diagram in Figure 3.5B describes the crossover of natural transformation of the constructed DNA of

pAA2 and pAA4 plasmids with the FA10900Δ*ngo1152* strain's chromosome to generate a complemented mutant (Figure 3.5B). Furthermore, the diagram shows an illustration of homologous recombination to facilitate the insertion of constructed DNA at the gonococcal *trpB-iga* intergenic region of the FA10900Δ*ngo1152* strain.

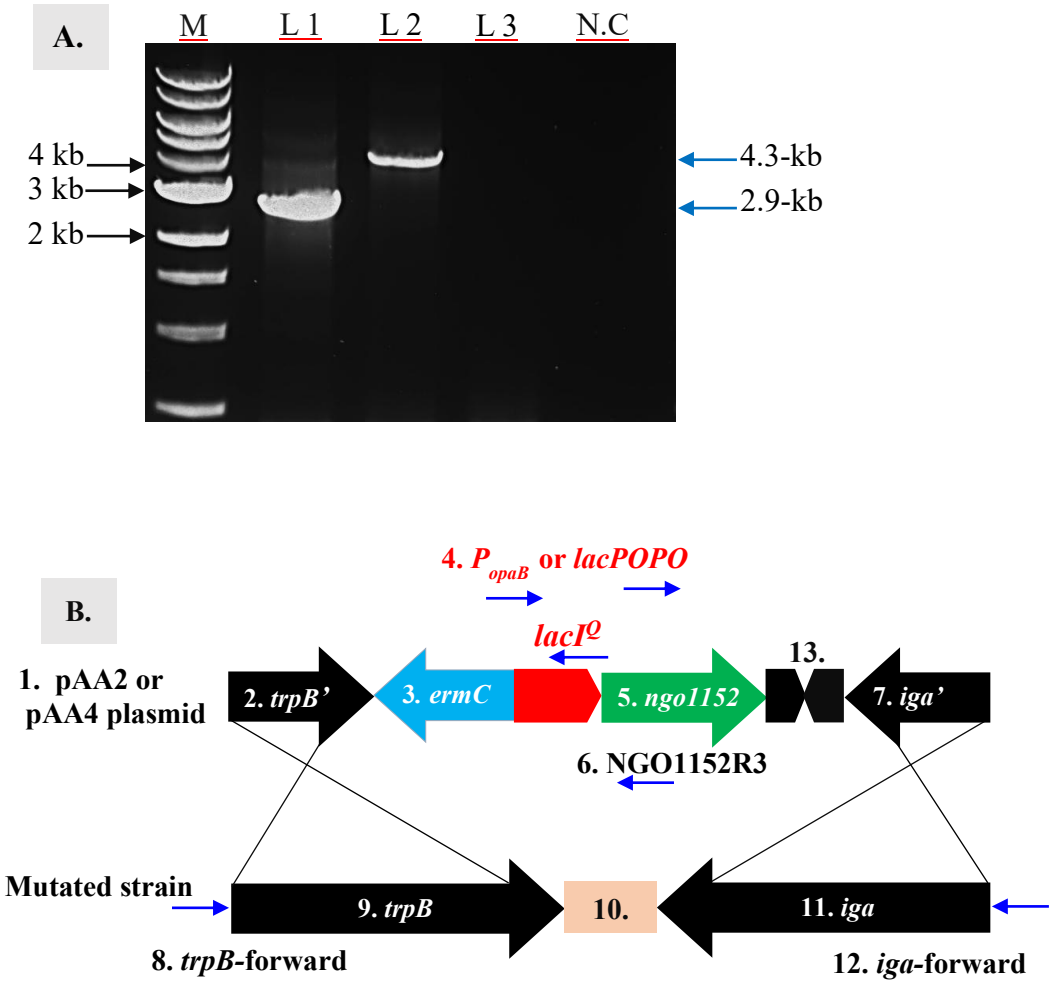

Figure 3.5. A. PCR products obtained using the *trpB*-forward and NGO1152R3 reverse primers confirm the insertion of *ngo1152* (with *opaB* or *lacPOPO* promoter) and *ermC* downstream of *trpB* in FA10900Δ*ngo1152*. B. Schematic diagram describing the crossover of natural transformation of Δ*ngo1152*.

A. Lane M: 1 kb DNA ladder marker. Lane **1**: shows a 2.9 kb band obtained from the transformation of Δ*ngo1152* with pAA2. Lane **2**: shows a 4.3 kb band obtained from the transformation of Δ*ngo1152* with pAA4. Lane **3**: Δ*ngo1152*, where the absence of a visible band in the mutant strain is due to the lack of *ngo1152* at the *trpB–iga* locus. Lane N.C: Negative control (no DNA template). **B**. Schematic diagram illustrating the insertion of elements present on pAA2 or pAA4-based plasmids constructed in this study into the Δ*ngo1152* chromosome. Numbered elements correspond to: **1**. pAA2 or pAA4 plasmid backbone. **2**. *trpB'* gene fragment present on pAA2 or pAA4 plasmid. **3**. *ermC* (erythromycin resistance cassette). **4**. P_{opaB} promoter; strong constitutive *opaB* promoter from *N. gonorrhoeae* strain FA1090 or tandem *lac* promoter/operator (*lacPOPO*) and *lac* repressor (*lacI*^{q}) from pKH37. **5**. *ngo1152*. **6**. Reverse primer NGO1152R3 annealing site. **7**. *iga'* gene fragment present on pAA2 or pAA4. **8**. *trpB*-forward primer annealing site. **9**. *trpB* is present in the FA1090 chromosome. **10**. *trpB-iga* intergenic region. 11. *iga* is present in the FA1090Δ*ngo1152*. **12**. *iga*-forward primer annealing site. **13**. The transcriptional terminator is located between *trpB* and *iga* on pAA2 or pAA4.

Using *trpB*-forward and *iga*-forward primers, the agarose gel revealed a single band at 3.5 kb in Δ*ngo1152* transformed with pAA2, and a *ca.* 5 kb band in Δ*ngo1152* transformed with pAA4 DNA. A band at 1.4 kb was obtained, as expected, from the parental Δ*ngo1152* strain, confirming the absence of any additional DNA between *trpB* and *iga* (Figure 3.6). Thus, these strains were renamed MR321152 (Δ*ngo1152* complemented with *ngo1152* under the strong constitutive *opaB* promoter at *iga-trpB*) and MR331152 (Δ*ngo1152* complemented with *ngo1152* under the IPTG-inducible promoter at *iga-trpB*), respectively.

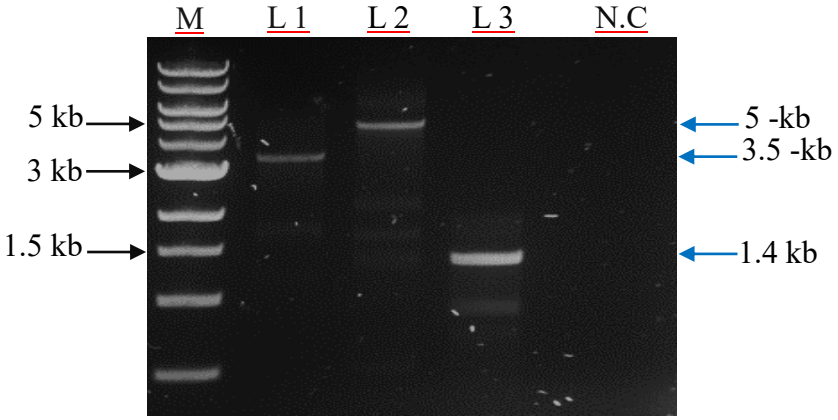

Figure 3.6. PCR products obtained using the *trpB* forward and *iga* forward primers confirm the insertion of *ngo1152* (with *opaB* or *lacPOPO* promoter) and *ermC* downstream of *trpB* in FA10900Δ*ngo1152*.
Lane M: 1 kb DNA ladder marker. Lane 1: shows a 3.5 kb band obtained from Δ*ngo1152* transformed with the pAA2 construct. Lane 2: shows a band of 5 kb obtained from the transformation of Δ*ngo1152* with the pAA4 construct. Lane 3: exhibited a band at 1.4 kb from the parental Δ*ngo1152* strain. Lane N.C: Negative control (no DNA template), indicating no PCR mix contamination.

3.2.2. Amplification of *ngo0206* for cloning

The gene encoding NGO0206 was amplified from the genomic DNA of *N. gonorrhoeae* FA1090 using the primers NGO0206F4 and NGO0206R3 as described in Table 2.4. The gel electrophoresis results demonstrated the successful amplification of the PCR product by showing a band at 1.1 kb that corresponds with the expected size of *ngo0206* in Figure 3.7.

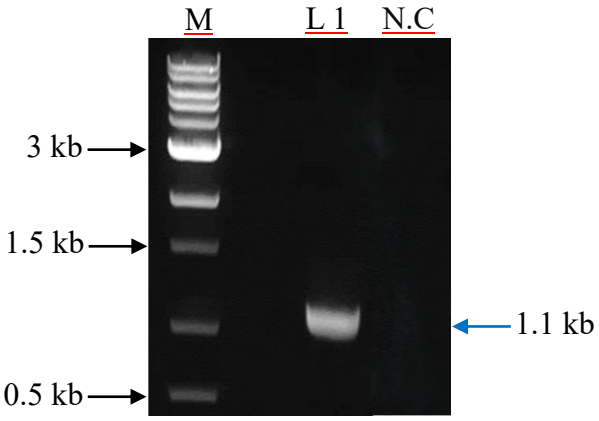

Figure 3.7. Successful amplification of *ngo0206* visualised via 1% agarose gel electrophoresis.
Genomic DNA of *N. gonorrhoeae* strain FA1090 was used as a template for the PCR amplification of *ngo0206*. Lane M: 1 kb DNA ladder. Lane 1: shows a 1.1 kb amplified PCR product corresponding to the expected size of *ngo0206*. Lane N.C: Negative control (no DNA template).

3.2.2.1. Cloning *ngo0206* into pMR32 and pMR33 vectors

In order to insert *ngo0206* into the pMR32 and pMR33 vectors, an identical approach was used as described in cloning *ngo1152* into pMR32 and pMR33. Both PCR fragments and vectors were digested with PacI and SacII, ligated and transformed into *E. coli* JM109. Plasmids were extracted from sub-cultured colonies and screened using PacI and SacII digestion (Figure 3.8). One of the six plasmids digested yielded two separate bands at 4.7 kb (commensurate with the pMR32 vector) and 1.1 kb corresponding to the *ngo0206* gene in Figure 3.8A. Likewise, one of the six digested plasmids yielded bands of 6.1 kb (commensurate with pMR33) and 1.1 kb (corresponding to *ngo0206*) (Figure 3.8B), confirming the success of the cloning process. From the screened colonies, the pMR32-based construct shown in Figure 3.8A (lane 1) and the pMR33-based construct shown in Figure 3.8B (lane 5) were sent for DNA sequencing. This analysis confirmed the success of the cloning process and the absence of any PCR-generated errors.

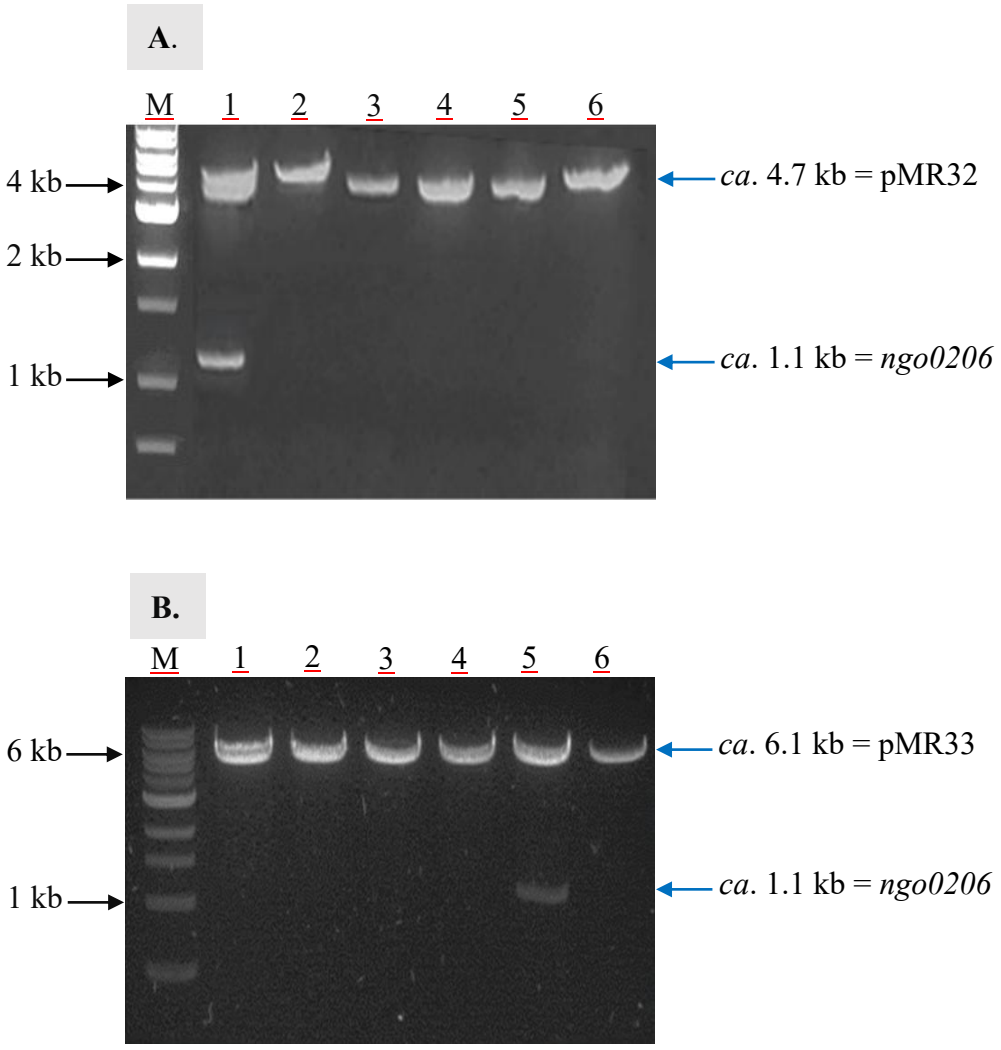

Figure 3.8. PacI and SacII double-digested plasmid DNA isolated from 12 selected *E. coli* JM109 transformant clones confirms the successful ligation of *ngo0206* into either (A) pMR32 or (B) pMR33.
The agarose gel image in panel (A) depicts the restriction profile of six independent clones harbouring the *ngo0206*::pMR32 construct. Lanes 1-6 show a 4.7 kb band corresponding to the pMR32 vector, but lane 1 contains an additional band of 1.1 kb corresponding to *ngo0206*. Panel (B) displays the corresponding analysis for six *ngo0206*::pMR33 clones. Lane 1-6 shows a 6.1 kb band corresponding to pMR33. Lane 5 shows an additional 1.1 kb band corresponding to *ngo0206*. In both gels, Lane M: 1 kb DNA ladder marker was used to indicate the size of the DNA fragments.

Following confirmation, the plasmids were renamed as pAA1 (*ngo0206* within the *iga-trpB* intergenic region under the P_{opaB} promoter) and pAA3 (*ngo0206* within the *iga-trpB* intergenic region under the *lacPOPO* promoter), respectively.

For further illustration, as shown in Figure 3.9, schematic diagrams of the pAA1 and pAA3 constructs were generated during this study.

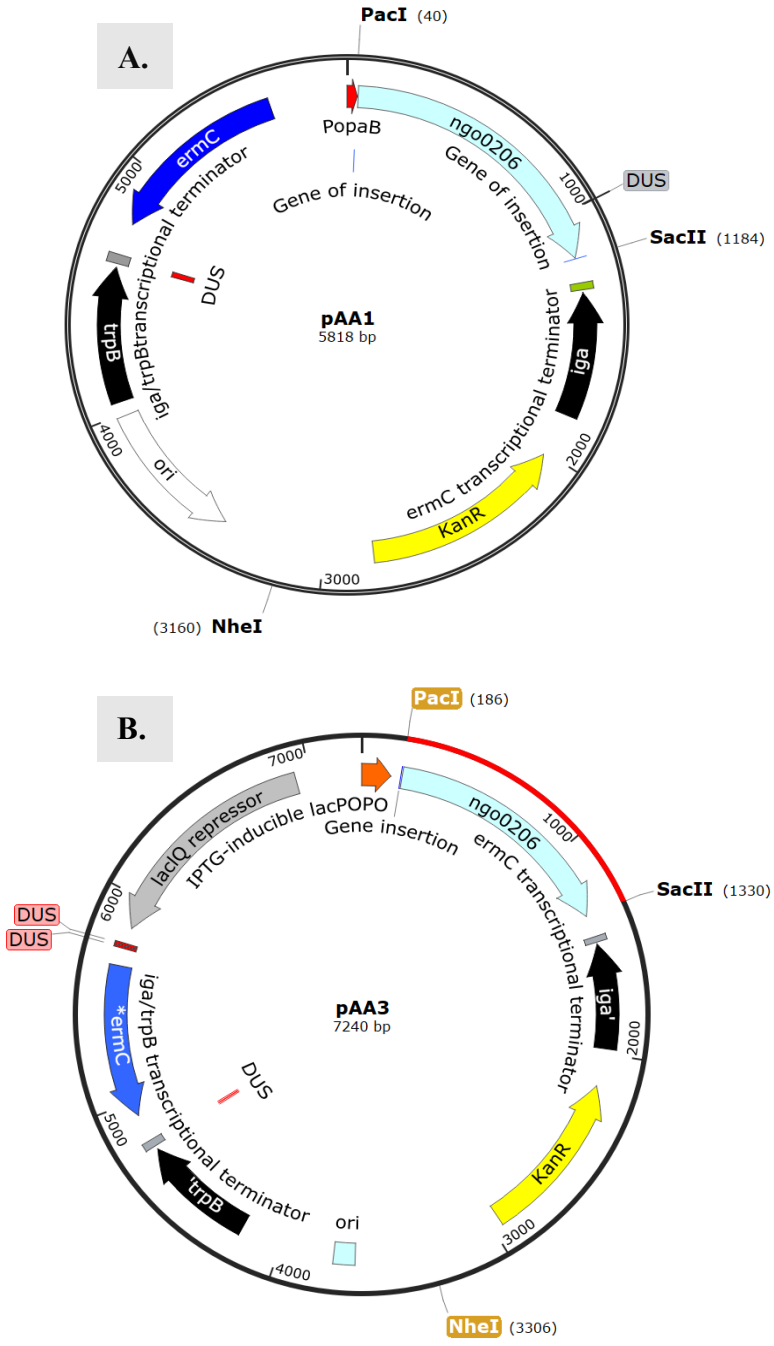

Figure 3.9. Schematic diagrams of *ngo0206* cloned into pMR32 or pMR33 vector to yield pAA1 (A) or pAA3 (B), respectively. Maps generated using SnapGene.

3.2.2.2. Natural Transformation of FA1090Δ*ngo0206* with pAA1 and pAA3

As previously, NheI-linearised pAA1 and pAA3 plasmid DNA were spotted onto a fresh Δ*ngo0206* strain grown on an agar plate containing kanamycin. Subsequently, the agar plates were incubated for 18 h at 37°C in a humidified atmosphere with 5% (v/v) CO_2.

Subsequently, the agar plates were incubated for 18 h at 37°C in a humidified atmosphere with 5% (v/v) CO_2. The following day, the growth was removed and streaked onto agar plates containing kanamycin and erythromycin for selection. Single colonies were subsequently sub-cultured, and chromosomal DNA was extracted for PCR analysis. To demonstrate the correct insertion of the gene (with promoter) and *ermC* between the *trpB* and the *iga* genes, primers *trpB*-forward and *iga*-forward were again utilised - both of which anneal to the region of *trpB* (or *iga)* present in the FA1090 chromosome, but outside the regions contained in pMR32/pMR33. These primers were used together or in combination with the *ngo0206*-specific primer to confirm successful recombination (Figures 3.10 and 3.11). However, when using the *trpB* forward primer and the NGO0206R reverse primer, a 3 kb band was obtained from colonies successfully transformed with pAA1, while a 4.5 kb band was obtained from transformants using pAA3 DNA (Figure 3.10). As expected, no band was obtained using the chromosomal DNA of Δ*ngo0206* because the *ngo0206* gene is not present downstream of *trpB.* The absence of a band in the negative control assay (no DNA template) indicated that the PCR mix was not contaminated.

Using t*rpB*-forward and *iga*-forward primers, a 4 kb band was obtained from the Δ*ngo0206* strain transformed with pAA1 DNA, and a 5.9 kb band was observed in the Δ*ngo0206* strain transformed with pAA3. As expected, a 1.4 kb band was detected in the parental Δ*ngo0206* strain (Figure 3.11). Consequently, these strains were renamed as MR320206 (Δ*ngo0206* complemented with *ngo0206* under P_{opaB} at *iga-trpB*) and MR330206 (Δ*ngo0206* complemented with *ngo0206* under *lacPOPO* at *iga-trpB*), respectively.

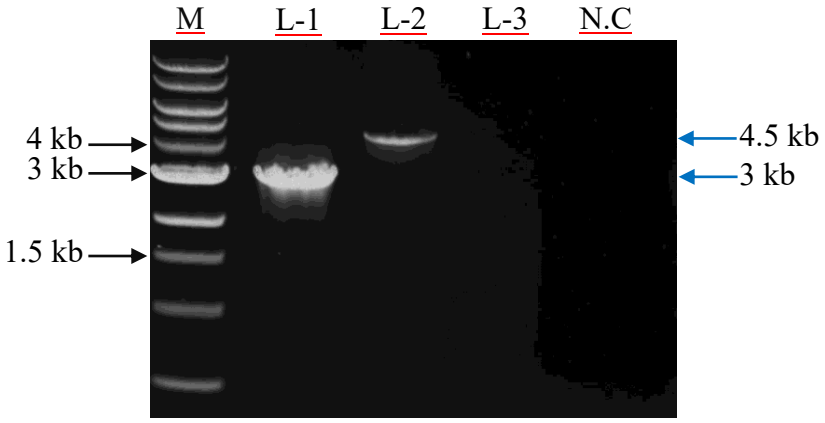

Figure 3.10. PCR products obtained using the *trpB*-forward and NGO0206R3 reverse primers confirm the insertion of *ngo0206* (with *opaB* or *lacPOPO*) promoter and *ermC* downstream of *trpB* in FA1090Δ*ngo0206*.
Lane M: 1 kb DNA ladder marker. Lane 1: shows a band of 3 kb obtained from a colony of Δ*ngo0206* transformed with pAA1. Lane 2: shows a band of 4.5 kb obtained from a colony of Δ*ngo0206* transformed with pAA3 DNA. Lane 3: Δ*ngo0206*, the absence of a band in the mutant strain results from the absence of *ngo0206* at the *trpB–iga* locus. Lane N.C: Negative control (no DNA template).

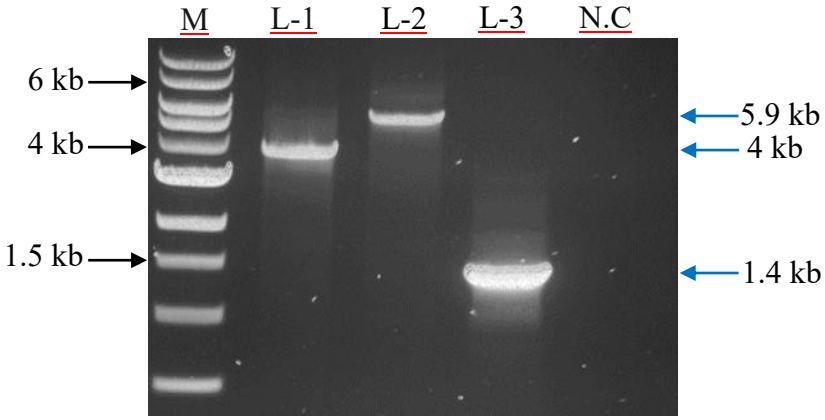

Figure 3.11. PCR products were obtained using the *trpB* forward and *iga* forward primers, which confirmed the insertion of *ngo0206*, promoter and *ermC* between *trpB* and *iga* after transforming Δ*ngo0206* with pAA1 or pAA3.
Lane M: 1 kb DNA ladder marker. Lane 1: showing a 4 kb band was obtained from a colony of Δ*ngo0206* transformed with pAA1. Lane 2: showing a band of 5.9 kb obtained from a colony of Δ*ngo0206* transformed with pAA3. Lane 3: shows a band at 1.4 kb, as expected, from the parental Δ*ngo0206* strain. Lane N.C: Negative control (no DNA template).

3.2.3. Detection of NGO1152 and NGO0206 using rabbit polyclonal antibodies

As previously mentioned, work undertaken in our laboratory has led to the generation of purified recombinant 6xHis-tagged NGO1152 and NGO0206, respectively, which were used to produce rabbit anti-NGO0206 and anti-NGO1152 polyclonal antibodies, respectively. Here, for the first time, these antisera were employed to examine the expression of the two SBPs (NGO1152 and NGO0206) in *N. gonorrhoeae* FA1090, as well as in the corresponding mutant and complemented strains.

3.2.3.1. Immunoblot detection of NGO1152 expression in FA1090 and derived strains

To investigate the expression of NGO1152 in gonococcal strains under different promoters. Whole cell lysates were prepared from WT-FA1090, Δ*ngo1152* mutant, and two complemented strains, MR321152 (*ngo1152* expressed under the constitutive *opaB* promoter) and MR331152 (*ngo1152* expressed under the inducible *lacPOPO* promoter), all of which were grown in BHI-V. For MR331152, which carries *ngo1152* under the *lacPOPO* promoter, protein expression was induced with 0.5 mM IPTG. Samples were collected at the time of induction (0 h) and subsequently at 1, 2, 3, and 4 h post-induction. These samples were compared to those from the uninduced control to assess the effects of induction over time. Subsequently, whole cell lysates were separated by SDS-PAGE and then either stained with SimplyBlue Safe stain to confirm equal sample loading, as shown in Figure 3.12A or probed with rabbit anti-NGO1152 polyclonal antibody (1:1000 dilution) to detect NGO1152 expression in Figure 3.12B. Following SDS-PAGE, the stained gel with SimplyBlue Safe stain demonstrated approximately equal loading of protein profile across all lanes, allowing subsequent comparisons of reactive band intensities detected by immunoblotting to be undertaken.

Intriguingly, the immunoblot analysis demonstrated a strong reactive band at *ca.* 30 kDa, which was present in the WT-FA1090, but absent in the Δ*ngo1152* mutant and present faintly in MR321152 (*ngo1152* under *opaB* constitutive promoter). Additionally, the reactive band at *ca.* 30 kDa appeared with low

intensity at T0 in MR331152 but became stronger at 1, 2, 3 and 4 h post-IPTG induction. The immunoblot analysis also demonstrated an additional non-specific reactive band at *ca.* 46 kDa, which was present at equal intensity in all lanes. Overall, the immunoblot analysis confirmed that NGO1152 is expressed by the WT-FA1090, but not in the Δ*ngo1152* mutant. Contrary to expectations, the MR331152 strain harbouring the *opaB* promoter exhibited low-level expression of NGO1152, whereas the MR331152 strain demonstrated rapid induction of NGO1152 expression following IPTG induction.

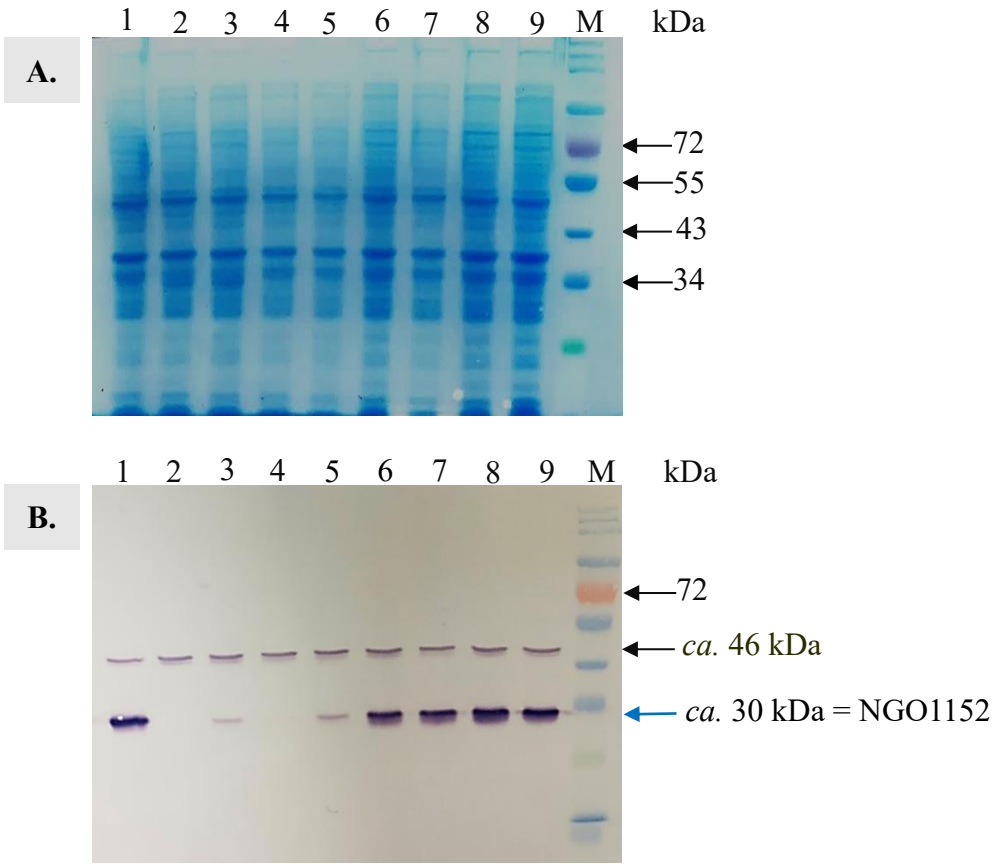

Figure 3.12. 10% SDS-PAGE gel electrophoresis stained with SimplyBlue Stain (A) and immunoblot analysis of whole cell lysates using 1:1000-diluted rabbit anti-NGO1152 (B), to investigate NGO1152 expression in WT-FA1090, Δ*ngo1152* and their complemented derivatives.
Whole cell lysates were prepared from gonococci grown in BHI-V, with samples collected from an IPTG-induced culture of MR331152 at 0 (uninduced), 1, 2, 3 and 4 h post-induction. In both panels, Lane 1: WT-FA1090; Lane 2: Δ*ngo1152*; Lane 3: MR321152; Lane 4: MR331152, no IPTG-induction. Lanes 5 to 9 MR331152 induced for 0, 1, 2, 3 and 4 h with 0.5 mM IPTG. (A) SDS-PAGE analysis demonstrated equal loading of protein across all lanes. (B) The immunoblot analysis demonstrated a strongly reactive band at *ca.* 30 kDa, which was present in the WT-FA1090, absent in the Δ*ngo1152* mutant and appeared again faintly in the MR321152 strain (*opaB* promoter). However, the reactive band at *ca.* 30 kDa appeared with low intensity at T0 of 0.5 mM IPTG-induced MR331152 (lane 5) and became stronger in lanes 6, 7, 8 and 9 at 1, 2, 3, and 4 h post-IPTG induction. An additional band at *ca.* 46 kDa in all lanes was judged to be a non-specific reaction. Lanes M in both panels; 10-250 kDa protein marker.

3.2.3.2. Immunoblot detection of NGO0206 in FA1090 and derived strains

Using an identical approach, SDS-PAGE and immunoblotting were used to confirm the presence or absence of NGO0206 in WT-FA1090, Δ*ngo0206* mutant and complemented strains. As established in prior experiments, whole cell lysates were prepared from WT-FA1090, Δ*ngo0206* mutant, and two complemented strains, MR320206 (*ngo0206* expressed under the constitutive *opaB* promoter) and MR330206 (*ngo0206* expressed under the inducible *lacPOPO* promoter), all of which were grown in BHI-V.

As established in prior experiments, for MR330206 (*ngo0206* under *lacPOPO* promoter), the strain was either uninduced or induced by IPTG for 0, 1, 2, 3, and 4 h post-induction. Subsequently, whole cell lysate samples were separated by SDS-PAGE and either stained with SimplyBlue stain or probed with rabbit anti-NGO0206 polyclonal antibody (diluted 1:1000). Protein staining confirmed equal sample loading, assisting in the interpretation of NGO0206 expression levels across different strains and/or induction conditions (Figure 3.13A).

Immunoblotting analysis with rabbit anti-NGO0206 antibody (Figure 3.13B) revealed a strongly reactive ~46 kDa band, consistent with NGO0206 (predicted molecular weight: ~41 kDa), in WT-FA1090 and IPTG-induced MR330206 lysates. This band was absent in the Δ*ngo0206* mutant strain, the MR320206 strain (expressing *ngo0206* under the constitutive *opaB* promoter), and the uninduced MR330206 complemented strain. Additional weakly reactive bands at *ca.* 30 kDa and *ca.* 72 kDa were present in all lanes and were judged to be non-specific reactions.

The immunoblot analysis confirmed that NGO0206 is expressed by WT-FA1090, and that the mutant did not express NGO0206. Unexpectedly, the MR320206 complemented strain (*ngo0206* under the control of the constitutive *opaB* promoter) demonstrated no evidence of NGO0206 expression. In contrast, the MR330206 complemented strain (*ngo0206* under the control of an IPTG-inducible promoter) showed rapid induction of NGO0206 expression, especially considering that the T0 sample was taken immediately following the addition of IPTG to the culture.

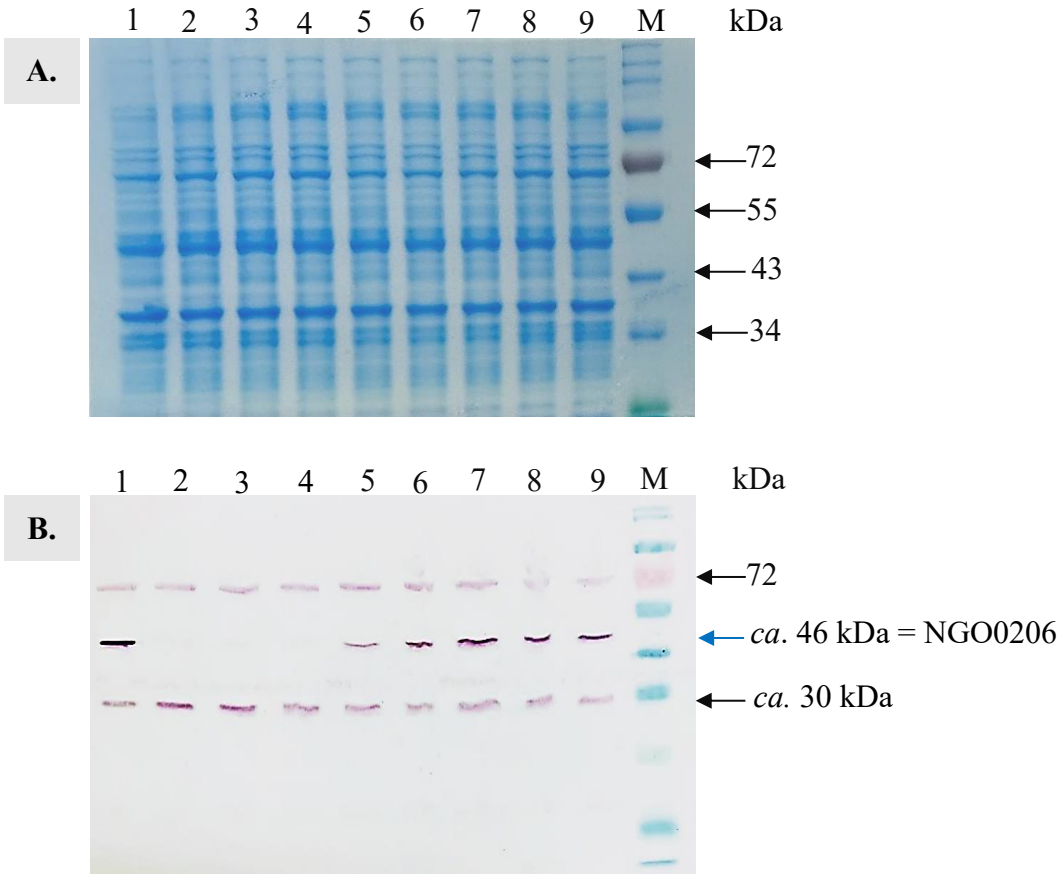

Figure 3.13. A 10% SDS-PAGE gel electrophoresis stained with SimplyBlue stain (A) and immunoblot analysis of whole cell lysates using 1:1000-diluted rabbit anti-NGO0206 (B) to investigate NGO0206 expression in WT-FA1090, Δ*ngo0206*, and complemented derivatives.
Whole cell lysates were prepared from gonococci grown in BHI-V. Additional samples were collected from an IPTG-induced culture of MR330206 at 0, 1, 2, 3 and 4 h post-induction. In both panels, Lane 1: WT-FA1090; Lane 2: Δ*ngo0206*; Lane 3: MR320206; Lane 4: MR330206; no IPTG-induction. Lanes 5 to 9; MR330206 induced for 0, 1, 2, 3 and 4 h with IPTG. Lanes M in both panels; 10-250 kDa protein marker. The SDS-PAGE analysis demonstrated equal loading of protein across all lanes of the gonococcal whole cell lysates. Immunoblotting with rabbit anti-NGO0206 demonstrated a reactive band at *ca.* 46 kDa, which was present in the WT-FA1090 and IPTG-induced MR330206 strain but absent in the Δ*ngo0206* mutant and MR320206 and uninduced MR330206 complemented strains.

3.2.4. Immunoblot optimisation and investigation of possible cross-reactivity between NGO1152 and NGO0206 antibodies

A striking observation from the immunoblots shown in Figures 3.12 and 3.13 was that both antisera detected bands at *ca.* 30 kDa and *ca.* 46 kDa, consistent with the reactive bands being NGO1152 and NGO0206, respectively.

To investigate this further, the anti-NGO1152 antisera at 1:1000 dilution was used to probe whole cell lysates from homogeneous strains of WT-FA1090, Δ*ngo1152*, MR321152 (P_{opaB}), and MR331152 (*lacPOPO*) at 4 h post-IPTG induction. As well, heterologous strains of Δ*ngo0206*, MR320206 (P_{opaB}), and MR330206 (*lacPOPO*) at 4 h post-IPTG induction.

As expected, the immunoblot analysis demonstrated a strong reactive band with an apparent molecular weight of *ca.* 30 kDa corresponding to NGO1152 in all strains expected to express NGO1152. However, a faint 46 kDa reactive band was detected in all strains except the Δ*ngo0206* mutant and the MR320206 strain, confirming its identification as NGO0206. Additional weakly reactive bands at *ca.* 72 kDa were considered to be non-specific (Figure 3.14A).

Nevertheless, subsequent increasing the dilution of the anti-NGO1152 primary antibody to 1:100,000 eliminated all non-specific reactivity, resulting in a single reactive band at approximately 30 kDa corresponding to NGO1152 in strains known to express this protein (Figure 3.14B).

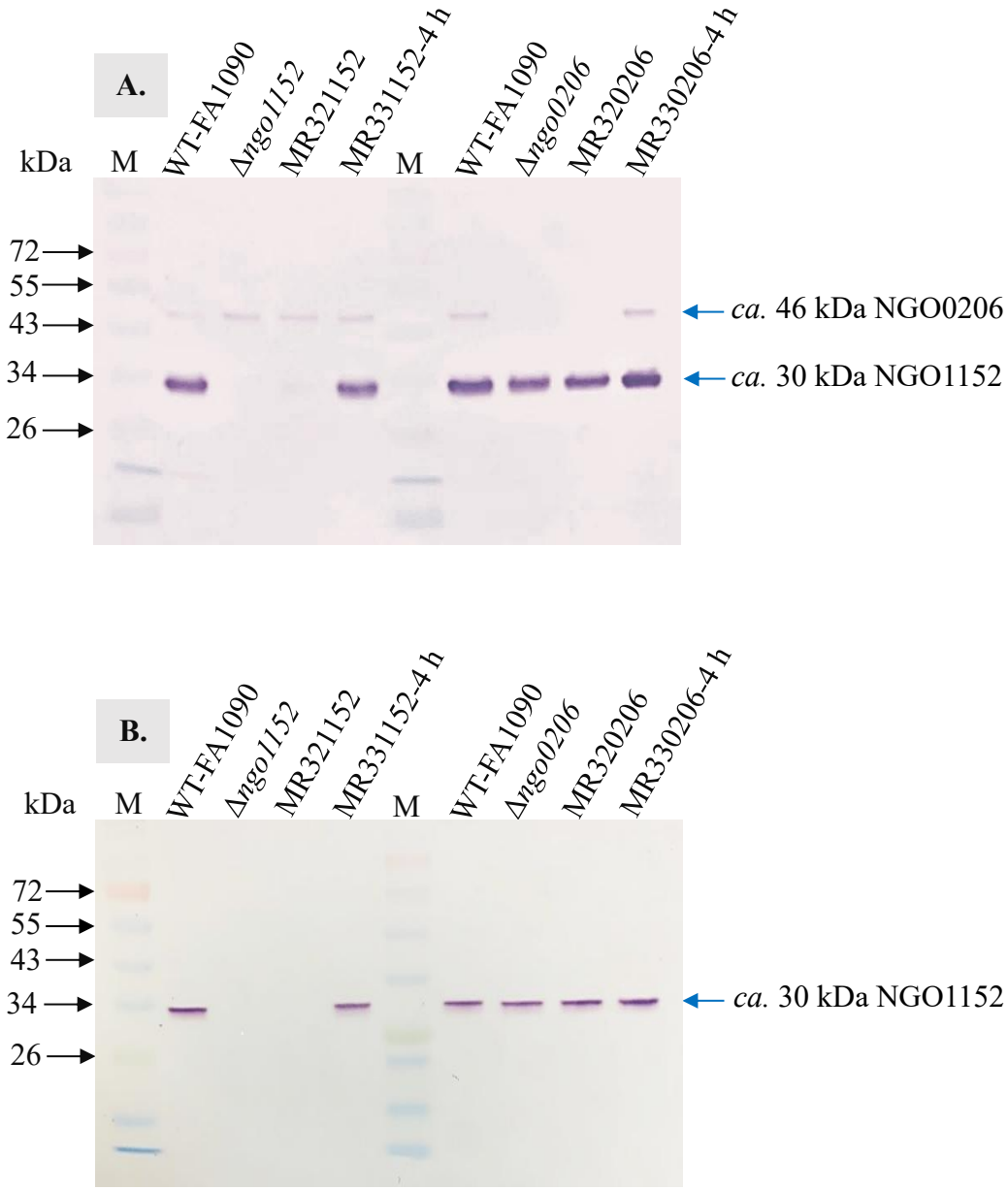

Figure 3.14. Immunoblot analysis of whole cell gonococcal lysates probed with anti-NGO1152 at 1:1000 dilution (A) or 1:100,000 dilution (B) to investigate the cross-reactive binding of anti-NGO1152 to NGO0206.
The membranes were probed with 1:1000 or 1:100,000 diluted rabbit anti-NGO1152 against gonococcal strains of WT-FA1090, Δ*ngo1152,* MR321152 (P_{opaB}), MR331152 (*lacPOPO*) induced by IPTG at 4 h, in addition, Δ*ngo0206*, MR320206 (P_{opaB}), and MR331152 (*lacPOPO*) strain induced by IPTG for 4 h. Anti-NGO1152 antibodies at (1:1000 dilution) recognised small faint bands with a molecular weight of *ca*. 46 kDa corresponded to NGO0206 in all lanes except Δ*ngo0206* and MR320206. A band at *ca*. 30 kDa appeared in all lanes except Δ*ngo1152*. The anti-NGO1152 antibodies at 1:100,000 dilution identified a *ca*. 30 kDa band in all strains except Δ*ngo1152* and MR321152 with minimal cross-reactivity to other proteins. Lanes M in both panels; 10-250 kDa protein marker.

In a complementary experiment, rabbit anti-NGO0206 polyclonal antibodies were used to probe whole cell lysates from the same strain set to determine whether the *ca*. 30 kDa non-specific reactive band identified using rabbit anti-NGO0206 at 1:1000 dilution was in fact NGO1152.

As expected, the immunoblot analysis utilised anti-NGO0206 at a 1:1000 dilution demonstrated a strong reactive band with an apparent molecular weight of *ca.* 46 kDa corresponding to the NGO0206 in the WT-FA1090 and MR330206 post-IPTG induction samples, but these bands were much less abundant in Δ*ngo0206* and MR320206. As implied, these bands were also strongly present in the NGO1152-related strains (Figure 3.15A). An apparent weakly reactive band at *ca.* 30 kDa, consistent with NGO1152, was detected in all samples except Δ*ngo1152* and MR321152. Additional weakly reactive bands at *ca.* 72 kDa were detected in all strains and were considered to be non-specific bands (Figure 3.15A). In contrast, better results were achieved after increasing the dilution of the anti-NGO0206 antibody to 1:100,000. All non-specific reactivity was eliminated, leaving only a single band reactive at *ca.* 46 kDa, equivalent to NGO0026, detected in all strains known to express this protein (Figure 3.15B).

In summary, the use of the antisera at 1:100,000 dilution in immunoblots enables the specific detection of either NGO1152 or NGO0206, respectively, in gonococcal strains.

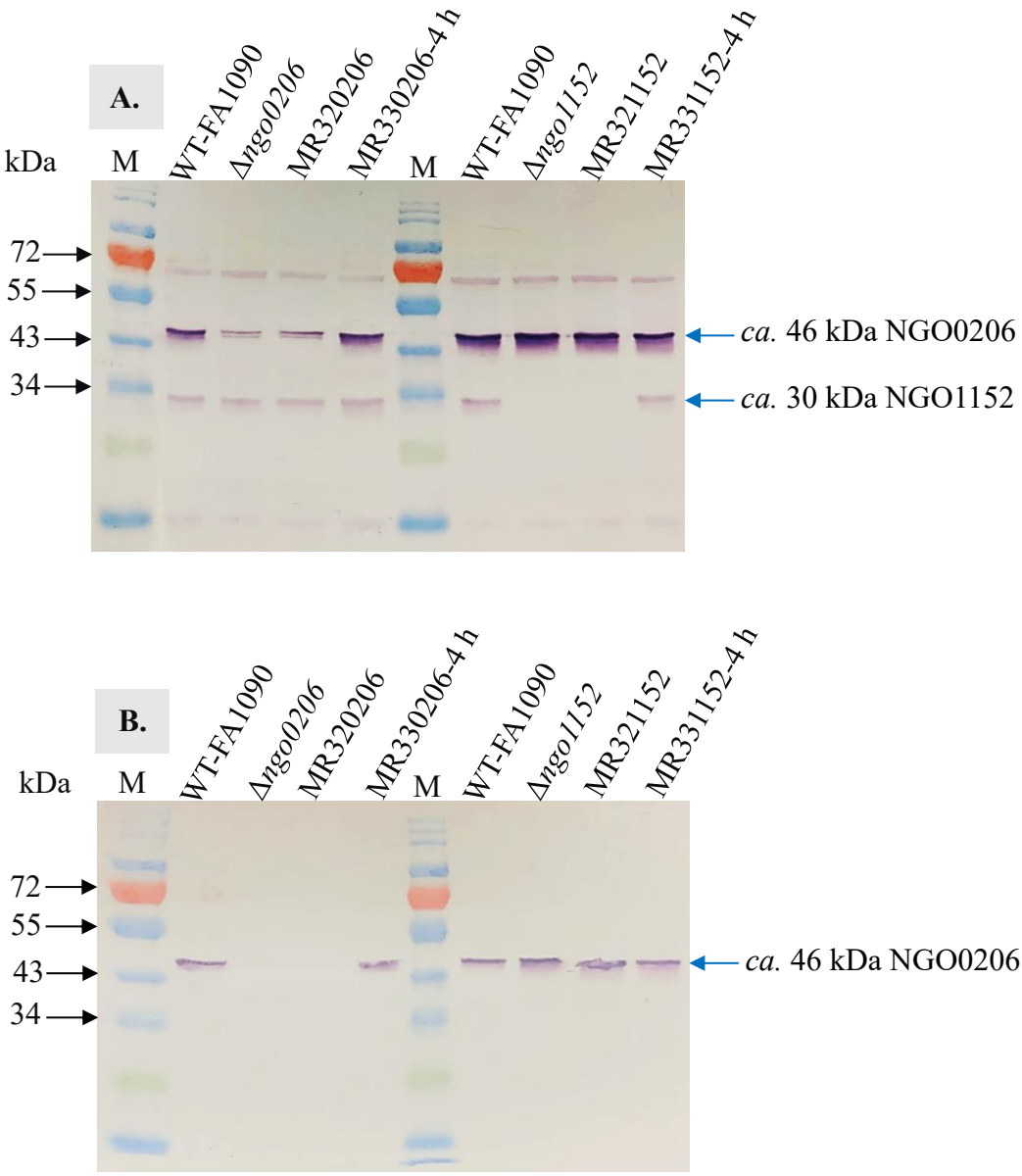

Figure 3.15. Immunoblot analysis of whole cell gonococcal lysates probed with anti-NGO0206 at 1:1000 dilution (A) or 1:100,000 dilution (B) to investigate the cross-reactive binding of anti-NGO0206 to NGO1152.
Strains utilised were WT-FA1090, Δ*ngo0206,* MR320206 (P_{opaB}), and MR330206 (*lacPOPO*) induced by IPTG for 4 h. In addition, Δ*ngo1152,* MR321152 (P_{opaB}), and MR331152 (*lacPOPO*) induced by IPTG for 4 h were also included. Lanes M in both panels; 10-250 kDa protein marker. The anti-NGO0206 antibodies at 1:1000 dilution detected reactive bands in all lanes at *ca.* 46 kDa, equivalent to NGO0206; however, the same band appeared with much-reduced intensity in Δ*ngo0206* and MR320206. Additional reactive bands at *ca*. 30 kDa corresponding to NGO1152 were detected in all strains except Δ*ngo1152* and MR321152. The band at *ca.* 72 kDa in all lanes was considered non-specific. The anti-NGO0206 antibodies at 1:100,000 dilution recognised the *ca*. 46 kDa band (NGO0206) in all strains except Δ*ngo0206* and MR320206 with no cross-reactivity evident.

3.2.5. Determining the influence of NGO1152 and NGO0206 on gonococcal growth *in vitro*

To gain insights into the impact of NGO1152 and NGO0206 on gonococcal physiology, *in vitro* growth profiles were assessed for NGO1152-related strains: [WT-FA1090, Δ*ngo1152,* MR321152 (P_{opaB}), and MR331152 (*lacPOPO*) non-induced or induced by IPTG at 4 h]. As well as NGO0206-related strains [WT-FA1090, Δ*ngo0206,* MR320206 (P_{opaB}), and MR330206 (*lacPOPO*), non-induced or induced by IPTG at 4 h. All strains were grown overnight in BHI-V at 37°C for 16 h with shaking at 250 rpm. Following growth, cultures of all gonococcal strains were diluted and equilibrated in fresh pre-warmed BHI-V media to achieve an OD_{600} of 0.2 in fresh pre-warmed BHI-V media.

Thereafter, protein expression of (NGO1152 or NGO0206) was induced at T0 by adding IPTG to a final concentration of 0.5 mM, followed by incubation with shaking at 250 rpm at 37°C. The growth rate of the gonococcal strains was evaluated by measuring the OD_{600} of the cultures at hourly intervals for 8 h.

Notably, both sets of experiments were performed in five independent replicates, on different occasions, and statistical analysis was performed by comparing the mean OD of each test strain at each time point with that of WT-FA1090.

No statistically significant differences were observed in Figures 3.16 and 3.17, indicating that NGO1152 and NGO0206 are not required for optimal growth under the conditions used.

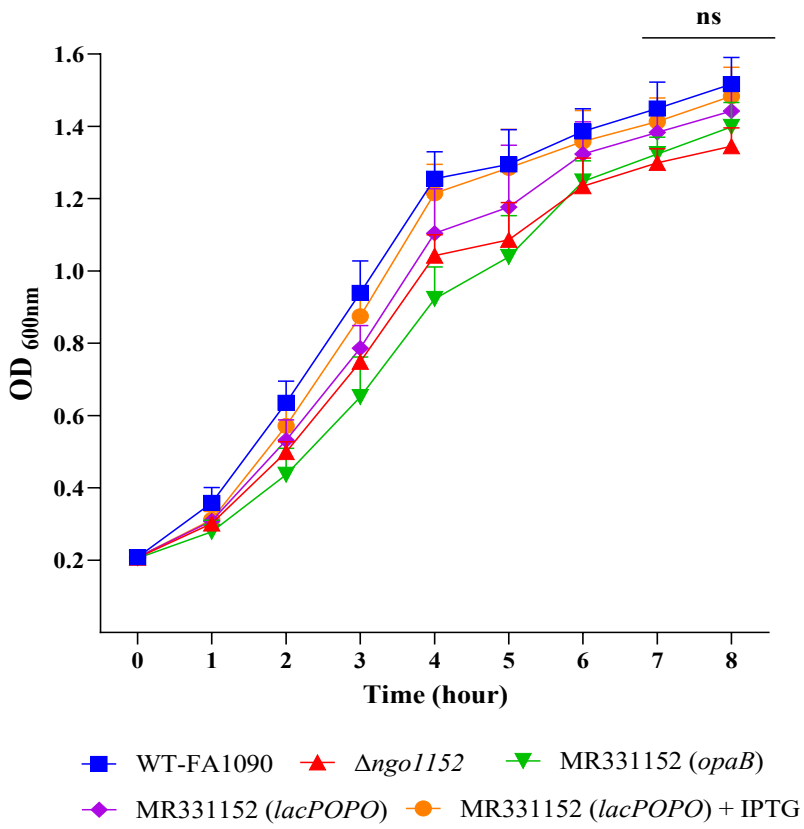

Figure 3.16. *In vitro* growth profiles of WT-FA1090, Δ*ngo1152*, MR321152 (*opaB* promoter) and MR331152 (*lacPOPO* IPTG-inducible promoter) uninduced or induced with 0.5 mM IPTG.
All gonococcal strains were grown in BHI-V media and equilibrated to an OD_{600} of 0.2. Strains were then induced (or not) with 0.5 mM IPTG at T0, and growth was monitored every hour for 8 h by measuring the OD_{600}. Mean values from five independent experiments are shown. Error bars indicate the mean ± standard deviation of a sample tested in quintuplicate. No significant differences in OD values at any time point were determined in comparison to the WT-FA1090 using two-way ANOVA.

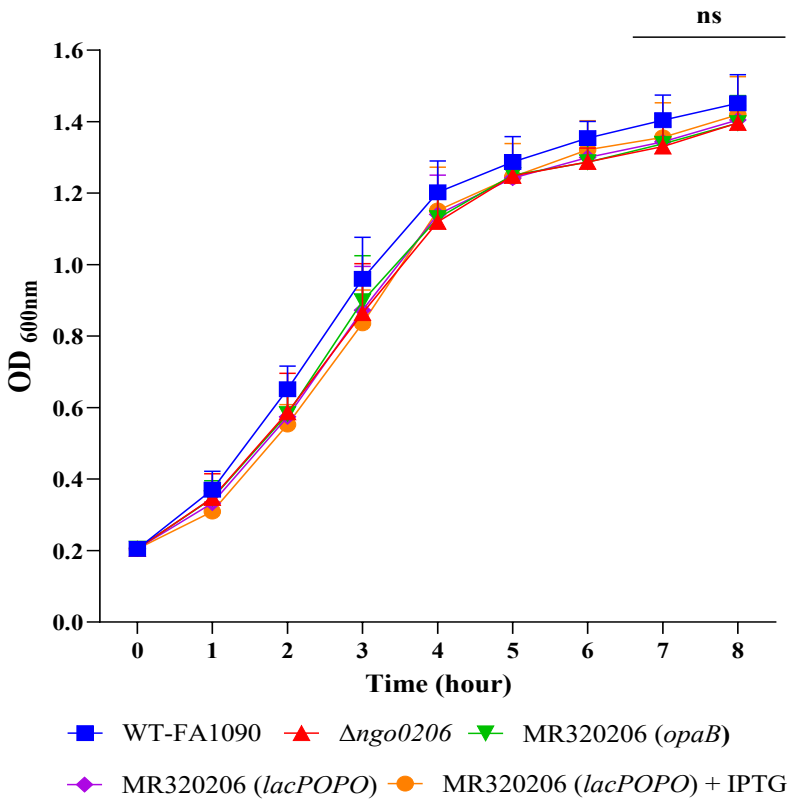

Figure 3.17. *In vitro* growth profiles of WT-FA1090, Δ*ngo0206*, MR320206 (*opaB* promoter) and MR330206 (*lacPOPO* IPTG-inducible promoter) uninduced or induced with 0.5 mM IPTG.
All gonococcal strains were grown in BHI-V media and equilibrated to an OD_{600} of 0.2. Strains were then induced (or not) with 0.5 mM IPTG at T0, and growth was monitored every hour for 8 h by measuring the OD_{600}. Mean values from five independent experiments are shown. Error bars indicate the mean ± standard deviation of a sample tested in quintuplicate. No significant differences in OD values at any time point were determined in comparison to the WT-FA1090 using two-way ANOVA.

3.3. Discussion

In prior studies in our lab, the genes *ngo1152* and *ngo0206* were knocked out and replaced with kanamycin resistance cassettes, resulting in *N. gonorrhoea* FA1090 mutant strains, Δ*ngo1152* and Δ*ngo0206*. Likewise, rabbit anti-NGO1152 and anti-NGO0206 polyclonal antisera were generated. The works described in this chapter focused on constructing complemented strains harbouring genes of interest under either strong constitutive or inducible promoters (via plasmids pMR32 and pMR33), and on optimising the application of these antisera in immunoblotting experiments. Additionally, evaluate the effects of gene deletions and their complementation on bacterial phenotype.

Hence, *ngo1152* or *ngo0206* genes were amplified and successfully ligated into the pMR32 vector, which contains the P_{opaB} promoter for strong constitutive expression in the *N. gonorrhoeae* strain FA1090. This resulted in the generation of the complemented constructs pAA2 and pAA1, respectively. As well, the respective amplicons were successfully ligated into the IPTG-inducible tandem *lac* promoter/operator (*lacPOPO*) from pMR33, along with the *lac* repressor ($lacI^q$) from pKH37 (Kohler *et al.*, 2007), generating complemented constructs of pAA4 and pAA3, respectively. This system can enhance transcript levels by 123-fold compared to wild-type *N. gonorrhoeae* (Long *et al.*, 2001).

This chapter aimed to assess the functionality of the complementation strategy and determine whether rabbit anti-NGO1152 and anti-NGO0206 antibodies successfully detected the expected expression of NGO1152 and NGO0206. Specifically, it assessed whether the constitutive (P_{opaB}) and IPTG-inducible (*lacPOPO*) promoters could restore protein expression to WT-FA1090 levels under *in vitro* conditions.

To assess NGO1152 expression from the complementation constructs, whole-cell lysates of WT-FA1090, Δ*ngo1152*, and complemented strains were subjected to SDS-PAGE and stained with SimplyBlue Safe stain (Figure 3.12A). The stained gel revealed consistent protein separation and uniform loading across all samples, indicating that the deletion and complementation did not disrupt protein expression. NGO1152 expression was assessed by immunoblot using rabbit anti-NGO1152 polyclonal antibodies (1:1000 dilution). The lysates

included WT-FA1090, Δ*ngo1152*, and complemented strains MR321152 (constitutive P_{opaB} promoter) at 0 h, and MR331152 (IPTG-inducible *lacPOPO* promoter). However, the MR331152 strain was assessed both uninduced and following IPTG induction at 0, 1, 2, 3, and 4 h to examine NGO1152 expression kinetics. Monitoring these intervals was essential to track the synthesis progression of protein synthesis and to identify any induction delays or inconsistencies that could affect experimental reliability.

Interestingly, the immunoblot analysis confirmed that anti-NGO1152 antibodies specifically detected a *ca.* 30 kDa band in WT-FA1090, consistent with NGO1152 size. This band was absent in the Δ*ngo1152* mutant, validating the knockout and confirming that NGO1152 expression was eliminated as intended.

Unexpectedly, the MR321152 strain showed only a faint *ca.* 30 kDa band for NGO1152, raising concerns about its expression (Figure 3.12B). This inconsistency, despite the typically strong *opaB* promoter, may reflect genetic variation, altered transcriptional regulation, or interference from other elements. This discrepancy indicates potential issues with the expression system, demanding further investigation. The unexpected failure of the P_{opaB} promoter in MR321152 contrasts with Ramsey *et al*. (2012), who reported that *N. gonorrhoeae* MS11 strains expressing TraWSS::′PhoA under P_{opaB} at the *iga-trpB* site (MR546) exhibited nearly threefold higher alkaline phosphatase activity than strains with *lacPO* promoter constructs (MR544, MR547) (Ramsey *et al.*, 2012). This confirmed the strong constitutive expression by P_{opaB}, which was not recapitulated in MR321152 in this study.

Following an in-depth investigation, the failure to detect robust NGO1152 expression by immunoblotting in strain MR321152 was due to the absence of a 100 bp upstream RNA transcriptional region in the *ngo1152* amplification primers (NGO1152F3 and NGO1152R3). As this region was critical for transcription initiation, it likely contained essential promoter-proximal elements necessary for effective RNA polymerase binding and transcriptional activation.

When it was absent, the P_{opaB} promoter's capacity to drive robust ngo1152 expression was impaired.

According to Ramsey *et al*. (2012), the P_{opaB} promoter was established as a strong constitutive element (Ramsey *et al.*, 2012). However, their study did not emphasise the critical requirement to include upstream regulatory sequences during the design of sequences used for amplification of the gene of interest. This omission represents a key technical oversight in the current construct design.

Nevertheless, the uninduced MR331152 strain exhibited results comparable to those of the Δ*ngo1152* mutant strain, with no protein band detected at *ca.* 30 kDa, indicating a lack of detectable NGO1152 expression. This strain was tightly regulated by the lac^q of the IPTG-inducible *lacPOPO* promoter, which effectively suppresses basal transcription in the absence of IPTG. The generation of a complemented locked *ngo1152* in the uninduced MR331152 strain confirmed that no leakage or expression of NGO1152 occurred without IPTG induction.

Upon IPTG induction, the MR331152 strain distinctly exhibited a band at 30 kDa, corresponding to the expected size of NGO1152, with a time-dependent increase in expression. The intensity of this 30 kDa band steadily increased over 0, 1, 2, 3, and 4 h post-IPTG induction. It is noteworthy that, despite lacking the RNA upstream transcription region, the MR331152 strain was still able to achieve strong expression levels comparable to those of the WT-FA1090 strain after 2 h of IPTG induction. In the MR331152 strain, expression was driven post-IPTG induction by the tandem *lac* promoter/operator (*lacPOPO*) from pMR33, alongside the $lacI^q$ repressor provided by pKH37. This system can increase transcript levels up to 123-fold compared to wild-type *N. gonorrhoeae* (Kohler *et al.*, 2007; Long *et al.*, 2001), which here significantly enhanced transcript levels of protein expression even in the absence of the 100 bp upstream region. In contrast, the efficacy of the P_{opaB} promoter is markedly reduced without this upstream sequence, as it lacks an alternative regulatory mechanism to support transcriptional initiation. Remarkably, the immunoblot analysis using anti-NGO1152 antiserum revealed additional immune cross-reactivity, demonstrated by a consistent non-specific band at *ca.* 46 kDa in all lanes of all tested strains (Figure 3.12). This band corresponds to the anticipated molecular weight of NGO0206. This finding suggests potential cross-reactivity between

anti-NGO1152 antibodies and NGO0206, highlighting the need to optimise antibody conditions to reduce cross-reactivity and achieve more specific results.

Furthermore, to assess NGO0206 expression, immunoblotting was performed using rabbit anti-NGO0206 polyclonal antibodies (1:1000 dilution). Whole-cell lysates included WT-FA1090, Δ*ngo0206*, and complemented strains MR320206 (constitutive P_{opaB} promoter at 0 h) and MR330206 (*lacPOPO* promoter). However, the MR330206 strain was assessed both uninduced and following IPTG induction at 0, 1, 2, 3, and 4 h to examine NGO0206 expression. Prior to immunoblotting, SDS-PAGE analysis (Figure 3.13A) confirmed consistent protein separation and uniform loading, validating the suitability of samples for immunodetection.

Immunoblotting analysis using rabbit anti-NGO0206 polyclonal antibodies detected a prominent band at *ca.* 46 kDa in WT-FA1090 (Figure 3.13B), despite the predicted molecular weight of ~41 kDa. This band was absent in the Δ*ngo0206* mutant, confirming its identity as NGO0206. However, in the complemented strain MR320206, where *ngo0206* expression was driven by the strong constitutive P_{opaB} promoter, NGO0206 was not detected by immunoblotting, contrasting with the clear presence observed in WT-FA1090. This unexpected absence likely results from the omission of a critical 100 bp upstream RNA transcriptional region in the NGO0206F4 and NGO0206R3 primers used for *ngo0206* amplification during complementation construct generation, as previously noted with MR321152. Although the *opaB* promoter typically drives strong constitutive expression, the absence of essential regulatory sequences in this study likely impaired transcription initiation, resulting in severely reduced transcript levels or complete transcriptional failure. This explains the undetectable NGO0206 protein expression in MR320206, which contrasts with the expression profile typically conferred by the *opaB* promoter. As predicted, the uninduced MR330206 strain did not express NGO0206, demonstrating the effectiveness of the *lacPOPO* promoter in tightly regulating gene expression and preventing leaky transcription. In the absence of IPTG, the $lacI^q$ repressor remained bound to the operator. This binding prevented transcription from the *lacPOPO* promoter. The result confirmed that gene

expression was tightly repressed under non-inducing conditions (Ramsey *et al.*, 2012).

Nonetheless, upon IPTG induction at 0, 1, 2, 3, and 4 h, the MR330206 strain displayed a time-dependent increase in NGO0206 expression, with a band appearing at *ca.* 46 kDa, corresponding to NGO0206. Expression levels progressively increased over time, with band intensity reaching WT-FA1090 levels by 2 h post-induction. These results highlight the responsiveness and utility of the *lacPOPO* system for dynamic and tightly controlled gene expression studies (Ramsey *et al.*, 2012). However, immunoblotting with anti-NGO0206 antibodies (1:1000 dilution) consistently revealed additional faint bands at *ca.* 30 kDa and 72 kDa across all samples, including WT-FA1090, Δ*ngo0206*, and complemented strains. The *ca.* 30 kDa band more likely reflects cross-reactivity with NGO1152, while the *ca.* 72 kDa band is attributed to non-specific binding. These findings suggest that further antibody titration is essential to reduce background and improve immunoblotting specificity.

Unlike the present study, where the P_{opaB} promoter failed to drive expression in MR321152 and MR320206. Juárez Rodríguez *et al*. (2024) successfully used the same promoter from pMR32 (Ramsey *et al.*, 2012) to generate a bioluminescent *N. gonorrhoeae* FA1090 strain for growth analysis (Juárez Rodríguez *et al.*, 2024). This bioluminescence-based approach has proven to be a reliable method for quantitatively assessing bacterial growth under various conditions, including during cellular infections (Brodl *et al.*, 2018; Waidmann *et al.*, 2011). By measuring the light emitted from bioluminescent bacteria, researchers can analyse growth kinetics with both high throughput and high temporal resolution (Ondari *et al.*, 2023). Since light production is ATP-dependent, bioluminescence also serves as an effective indicator of bacterial metabolic activity and viability (Gregor *et al.*, 2018).

Juárez Rodríguez *et al*. (2024) successfully engineered a bioluminescent *N. gonorrhoeae* strain (FA1090-LuxR) by using the constitutive *opaB* promoter (P_{opaB}) from pMR32. This was accomplished by inserting the *luxCDABE* operon from *Photorhabdus luminescens* into the intergenic region of the *N. gonorrhoeae* FA1090 chromosome at the *iga-trpB* locus via allelic exchange, placing it under the control of the P_{opaB} promoter (Ramsey *et al.*, 2012). The *N. gonorrhoeae iga-*

trpB locus has been used frequently for chromosomal complementation studies since the insertion of genetic elements does not affect bacterial replication (Juárez Rodríguez *et al.*, 2024). The bioluminescent output of the *Ng* FA1090-LuxR strain at various cell densities showed a strong correlation with other quantitative approaches, such as CFU counts and OD measurement, exhibiting a linear dynamic range spanning at least two orders of magnitude (Juárez Rodríguez *et al.*, 2024).

Primary immunoblotting analyses revealed that both antisera detected bands at approximately 30 kDa and 46 kDa, corresponding to the predicted sizes of NGO1152 and NGO0206, respectively. This overlap suggests potential cross-reactivity between the two antibodies and their respective antigens.

To address this, additional immunoblot analyses were conducted to optimise the specificity of the rabbit anti-NGO1152 polyclonal antibodies and minimise cross-reactivity. Whole-cell lysates from WT-FA1090, Δ*ngo1152*, MR321152 (P_{opaB}), and MR331152 (*lacPOPO*) were collected at 4 h post-IPTG induction. Furthermore, to determine whether the *ca.* 46 kDa band detected by the anti-NGO1152 antibodies corresponded to NGO0206, lysates from Δ*ngo0206*, MR320206 (P_{opaB}), and MR330206 (*lacPOPO*) were examined under the same conditions.

Lysates were probed with anti-NGO1152 antibodies at dilutions of 1:1,000 and 1:100,000 (Figure 3.14A and B). At the 1:1,000 dilution, a strong band at *ca.* 30 kDa, corresponding to NGO1152, was detected in WT-FA1090 and MR331152 but was absent in the Δ*ngo1152* strain, confirming the antibody's specificity. An additional weaker *ca.* 30 kDa band observed in MR321152 indicated reduced NGO1152 expression in this strain. However, a *ca.* 46 kDa band consistent with the molecular weight of NGO0206 was detected in WT-FA1090 and MR331152, but not in Δ*ngo0206* or MR320206, suggesting cross-reactivity of anti-NGO1152 with NGO0206. This cross-reactive band was also observed in MR330206, further supporting its identity as NGO0206 (Figure 3.14A). When the antibody dilution was increased to 1:100,000, these non-specific bands were eliminated, retaining only the band specifically corresponding to NGO1152 in relevant strains (Figure 3.14B), indicating improved specificity at higher dilution.

Parallel immunoblotting analyses using rabbit anti-NGO0206 at 1:1,000 and 1:100,000 were conducted on lysates from WT-FA1090, Δ*ngo0206*, MR320206 (P_{opaB}), and MR330206 (*lacPOPO*) to evaluate potential cross-reactivity of anti-NGO0206 with NGO1152 (Figure 3.15A and B). Lysates from Δ*ngo1152*, MR321152 (P_{opaB}), and MR331152 (*lacPOPO*) were also examined under identical conditions. At 1:1,000 dilution, a strong *ca.* 46 kDa band was observed in WT-FA1090 and MR330206, with reduced intensity in Δ*ngo0206* and MR320206. Additionally, a faint *ca.* 30 kDa band was observed in all strains except Δ*ngo1152* and MR321152, suggesting cross-reactivity with NGO1152. A consistent *ca.*72 kDa band detected across all strains was interpreted as non-specific background immunoreactivity (Figure 3.15A). However, at 1:100,000 dilution, anti-NGO0206 specifically detected only the *ca.* 46 kDa band corresponding to NGO0206 in expected strains, including WT-FA1090 and MR330206, with successful elimination of non-specific binding (Figure 3.15B). These results confirm the high specificity of anti-NGO1152 and anti-NGO0206 antibodies at the 1:100,000 dilution for their respective targets. They also highlight the importance of optimising antibody concentration to minimise cross-reactivity, particularly among structurally related SBPs.

To investigate how deletions of *ngo1152* and *ngo0206*, as well as their genetic complementation, affect the *in vitro* growth and viability of *N. gonorrhoeae* FA1090 strains. The *in vitro* growth characteristics of NGO1152-related strains [WT-FA1090, Δ*ngo0206,* MR320206 (P_{opaB}), and MR330206 (*lacPOPO*)], as well as NGO1152-related strains [WT-FA1090, Δ*ngo1152,* MR321152 (P_{opaB}), and MR331152 (*lacPOPO*)] and complemented strains, with or without IPTG, showed no significant differences compared to the WT-FA1090. This raises questions regarding the hypothesised essential roles of *ngo1152* and *ngo0206,* suggesting that their functional significance might not directly influence general growth under laboratory conditions. Hence, further investigation under diverse or stress-related conditions may be necessary to fully understand their roles.

In conclusion, complemented mutant strains were successfully constructed by reintroducing *ngo1152* or *ngo0206* into the *iga-trpB* intergenic region of pMR32 and pMR33, before reintroducing the *ngo1152* or *ngo0206* gene back into the Δ*ngo1152* or Δ*ngo0206* mutant chromosomes at the *iga-trpB* intergenic region,

under the control of either the P_{opaB} or *lacPOPO* promoter. Genotypic confirmation of the complemented strains was achieved via PCR, followed by immunoblot analysis to verify protein expression. Immunoblot results confirmed that NGO1152 (or NGO0206) was not expressed in MR321152 and MR320206 strains using the strong constitutive P_{opaB} promoter, likely due to defects in the upstream RNA transcription region. Consequently, the current study focuses on using inducible expression systems in subsequent chapters instead of relying on complemented mutants with the P_{opaB} promoter.

The immunoblot analysis confirmed the expression of NGO1152 (or NGO0206) in the WT-FA1090 and complemented derivatives, but only in MR331152 and MR330206 strains using the IPTG-inducible *lacPOPO* promoter to drive expression. IPTG induction successfully restored NGO1152 (or NGO0206) protein expression to wild-type levels within 2 h of induction. Finally, *in vitro,* growth characteristics of WT-FA1090, Δ*ngo1152* or Δ*ngo0206* mutants and their complemented strains, with or without IPTG, showed no significant differences compared to the WT-FA1090.

The next chapter will evaluate the expression of NGO1152 and NGO0206 across a panel of clinical gonococcal isolates using immunoblotting. Additionally, bioinformatics analyses will be utilised to examine the presence and conservation of NGO1152 and NGO0206-encoding sequences across thousands of *N. gonorrhoeae* strains with whole genome sequences deposited in the PubMLST database.

Chapter 4: Conservation and expression of NGO1152 and NGO0206 in clinical isolates of *N. gonorrhoeae*

4.1. Introduction

Investigating vaccine candidate proteins across diverse clinical isolates of *N. gonorrhoeae* is essential to ensure that proposed antigens are broadly conserved, consistently expressed, and representative of circulating strains (Noori Goodarzi *et al.*, 2025).

N. gonorrhoeae is a highly adaptable pathogen whose extensive genomic variability and antigenic diversity pose major challenges to vaccine development (Unemo *et al.*, 2019). Immune targets that are variably expressed or strain-specific often confer only limited or geographically restricted protection. For example, analysing clinical isolates from geographically and temporally distinct sources, researchers can assess the prevalence and expression levels of candidate OMPs to determine their potential as universal vaccine components (Zielke *et al.*, 2016). Techniques such as immunoblotting enable direct detection of these proteins in bacterial lysates or membrane fractions, allowing evaluation of their expression patterns and immunoreactivity across isolates (Sikora *et al.*, 2020). This approach strengthens antigen selection by prioritising proteins that are both immunogenic and stably expressed under physiologically relevant conditions, thereby increasing the likelihood of broad and durable vaccine efficacy (Semchenko *et al.*, 2020).

Advances in genomics, proteomics, and bioinformatics have significantly expanded the repertoire of potential *N. gonorrhoeae* vaccine candidates and accelerated antigen discovery (Baarda *et al.*, 2019; Lyu *et al.*, 2024; Zhu *et al.*, 2019). For instance, quantitative proteomic and immunoproteomic analyses have identified over 20 novel vaccine candidates. These proteins were consistently detected in the cell envelopes of 19 genetically diverse isolates, including the 2016 WHO reference strains, as well as in native OMVs derived from four widely used laboratory strains: FA1090, F62, MS11, and 1291 (El-Rami *et al.*, 2019; Zielke *et al.*, 2016). Moreover, high-throughput proteomic

profiling demonstrated their expression under host-relevant conditions such as iron limitation, anaerobiosis, and exposure to human serum (Zielke *et al.*, 2018).

In parallel, bioinformatic analyses have enabled the in-*silico* evaluation of antigen conservation across global populations of *N. gonorrhoeae*. Genomic mining of PubMLST entries allows the identification of conserved protein sequences and polymorphic variants among clinical isolates worldwide (Dijokaite-Guraliuc *et al.*, 2023). For example, Baarda *et al*. (2019) employed this approach to characterise the sequence variation, allelic distribution, and amino acid polymorphisms of multiple candidate antigens across diverse strains (Baarda *et al.*, 2019).

Assessing the expression and prevalence of NGO1152 and NGO0206 in clinical isolates represents a key step toward validating their potential as vaccine antigens. This can be effectively achieved using immunoblotting analysis of whole-cell lysates derived from a geographically and genetically diverse panel of *N. gonorrhoeae* strains. Such experimental validation complements omics and bioinformatic approaches, providing critical insight into the practical feasibility of antigen inclusion in a broadly protective gonococcal vaccine.

Additionally, the conservation and prevalence of these proteins can be examined on a global scale by leveraging genomic data available through the PubMLST database. Bioinformatic mining of all *N. gonorrhoeae* isolates deposited in PubMLST enables the identification of conserved protein sequences by comparing genetic data across a wide range of isolates (Dijokaite-Guraliuc *et al.*, 2023). For example, bioinformatics mining of all *N. gonorrhoeae* isolates deposited into the PubMLST database involved searching through genomic databases to identify alleles and single-nucleotide/amino-acid polymorphisms of the model antigens (Baarda *et al.*, 2019). This process utilised DNA/protein sequences of complete *N. gonorrhoeae* isolates that were deposited into the

The PubMLST database was used to identify model antigens, such as β-barrel assembly machinery A (BamA) and Multiple transferable resistance efflux pump protein E (MtrE), coupled with structural mapping, phylogenetic analysis, and crystal structure Studies (Baarda *et al.*, 2019).

Furthermore, PubMLST is a curated database that contains data on multi-locus sequence typing (MLST), information isolation, and a progressive increase in the number of whole genome sequences for various microorganisms, for instance, *N. meningitidis* and *N. gonorrhoeae* (Jolley *et al.*, 2004; Jolley and Maiden, 2010). Over 2500 loci, including the core *Neisseria* genome, have accessible allelic variation data (Jolley *et al.*, 2018). The fact that gene and genome sequences are deposited from research that might have intrinsic sampling biases is one of the database limitations. As a result, the frequency of a specific variant in the database does not always indicate that the variant is distributed globally. However, identifying allelic variations of protein antigens to design broadly protective vaccines could be supported by the PubMLST database, which is the largest available source of *Neisseria* genetic and genomic data information. This extensive resource could play a vital role in enabling rational vaccine formulation (Baarda *et al.*, 2019).

Nevertheless, the selection of highly conserved genes is vital for identifying long-term genetic variations, which is particularly significant in evolutionary studies. Typing systems based on multiple loci are generally superior to single-locus techniques due to the high frequency of recombination in *N. gonorrhoeae*, which can obscure the true genetic background when only one locus is analysed (ECDC, 2012). For example, among the various sequence-based typing approaches described for *N. gonorrhoeae*, PorB sequence analysis is the most widely employed. Distinguish strains by variations within the entire *PorB* gene or specific hypervariable regions. Analyses of both full-length and partial PorB sequences provide a level of discrimination that is comparable to the multi-antigen sequence typing (NG-MAST) for *N. gonorrhoeae* (Binepal *et al.*, 2024; Heymans *et al.*, 2012; Ilina *et al.*, 2010). Further differentiation can be achieved by integrating these techniques (Unemo *et al.*, 2007). PorB sequencing has been utilised to classify gonococcal types in a specific geographic region (Ilina *et al.*, 2010; Unemo *et al.*, 2007) and to examine sexual networks (Unemo *et al.*, 2002; Viscidi *et al.*, 2000) and therapy failures (Unemo *et al.*, 2011; Unemo *et al.*, 2012).

Assessing results across studies remains challenging due to inconsistencies in sequence length and the lack of a centralised database for type definition. Multi-

locus Sequence Typing (MLST) addresses that issue by assessing variation in the sequences of seven or more relatively conserved, gradually evolving genes, typically encoding housekeeping enzymes distributed throughout the genome. Each allele at these loci is assigned a specific number, and the combination of locus numbers defines an MLST type, which is both clear and transferable between research laboratories. This method is particularly suited for long-term and global epidemiological studies and for examining the dynamics of gonococcal populations, as MLST tracks slowly evolving loci.

Currently, there is no standard MLST scheme for *N. gonorrhoeae*. Nonetheless, some studies have employed an MLST scheme based on the same loci (*abcZ, adk, aroE, fumC, gdh, pdhC*, and *pgm*) used for *N. meningitidis* (Bennett *et al.*, 2007; Ilina *et al.*, 2010; Mavroidi *et al.*, 2011) while others have used additional loci (*abcZ, adk, aroE, fumC, gdh, glnA, gnd, pdhC, pgm, pilA, ppk, pyrD*, and *serC*) for greater discrimination (Pérez-Losada *et al.*, 2005). Although MLST has been utilised to study long-term epidemiology and the structure of gonococcal populations, the effectiveness of the current schemes for these purposes still requires extensive validation.

This chapter aimed to employ rabbit anti-NGO1152 and anti-NGO0206 polyclonal antisera in immunoblot analyses to investigate the prevalence and expression of NGO1152 and NGO0206 across 28 whole-cell lysates derived from genetically diverse *N. gonorrhoeae* clinical isolates collected in the UK. Bioinformatic analyses were conducted to assess the distribution, conservation, and variation of NGO1152 and NGO0206 across 7,327 *N. gonorrhoeae* isolates in the PubMLST *Neisseria* database. These isolates were collected worldwide between 2014 and 12th August 2022, and their genomic data were analysed to evaluate the prevalence, genetic variability, and potential of these loci as vaccine targets. However, these analyses were limited to isolates within this time frame due to a current restriction in the PubMLST BLAST tool, which permits interrogation of up to 10,000 isolate records at a time.

4.2. Results

4.2.1. Immunoblot analysis of NGO1152 and NGO0206 expression across a panel of clinical isolates.

To evaluate the expression profiles of NGO1152 *and* NGO0206 in *N. gonorrhoeae*, whole-cell lysates were prepared from 28 isolates, including 26 clinical strains designated 17N0001 to 17N0026. These clinical isolates were collected between 2017 and 2018 from both male and female patients attending Nottingham University Hospitals NHS Trust (UK). The samples were obtained from a range of anatomical sites, cervical, urethral, high vaginal, and rectal, to encompass potential variation in gene expression associated with site-specific or strain-specific differences. The use of diverse clinical isolates ensured both the clinical relevance of the findings and the representativeness of the study population.

In addition to the clinical isolates, whole-cell lysates were also prepared from three well-characterised *N. gonorrhoeae* reference strains to serve as comparative controls. These included: *N. gonorrhoeae* FA1090, a wild-type strain isolated in 1983 from a male patient with DGI; *N. gonorrhoeae* DGI-18, a wild-type strain isolated in 1983 from a patient with DGI; and *N. gonorrhoeae* MS11, a wild-type strain isolated in 1960 from a patient with uncomplicated gonococcal infection. Among the 28 gonococcal isolates, strains DGI-18 and MS11 were included for their well-characterised genetic backgrounds. These strains had previously been whole-genome sequenced using next-generation sequencing techniques by Dr. Neil Oldfield at UoN, UK. In contrast, the genomic sequences of the clinical isolates 17N0001–17N00027 remain uncharacterised. Including these reference strains enabled comparison of gene expression with clinical isolates, highlighting the need for vaccine candidates to show consistent expression across diverse strains.

To evaluate the expression of NGO1152 and NGO0206 across this isolate set, immunoblotting was performed using whole-cell lysates probed with rabbit anti-NGO1152 and/or anti-NGO0206 antibodies. Interestingly, the immunoblotting results confirmed that both NGO1152 and NGO0206 proteins were expressed in all tested isolates, showing bands at *ca.* 30 kDa and 46 kDa, respectively. These

molecular weights corresponded to the expected sizes of NGO1152 and NGO0206 and align with the bands observed in the WT-FA1090 strain. In contrast, these protein bands were absent in the mutant strains Δ*ngo1152* and Δ*ngo0206,* which confirms the specificity of the antisera for their respective antigens, as illustrated in Figures 4.1 and 4.2.

Nevertheless, this analysis confirmed that all isolates harboured the *ngo1152* and *ngo0206* genes and expressed functional proteins that were effectively recognised by the corresponding antisera, indicating successful expression and antigenic conservation when compared to the WT-FA1090 strain.

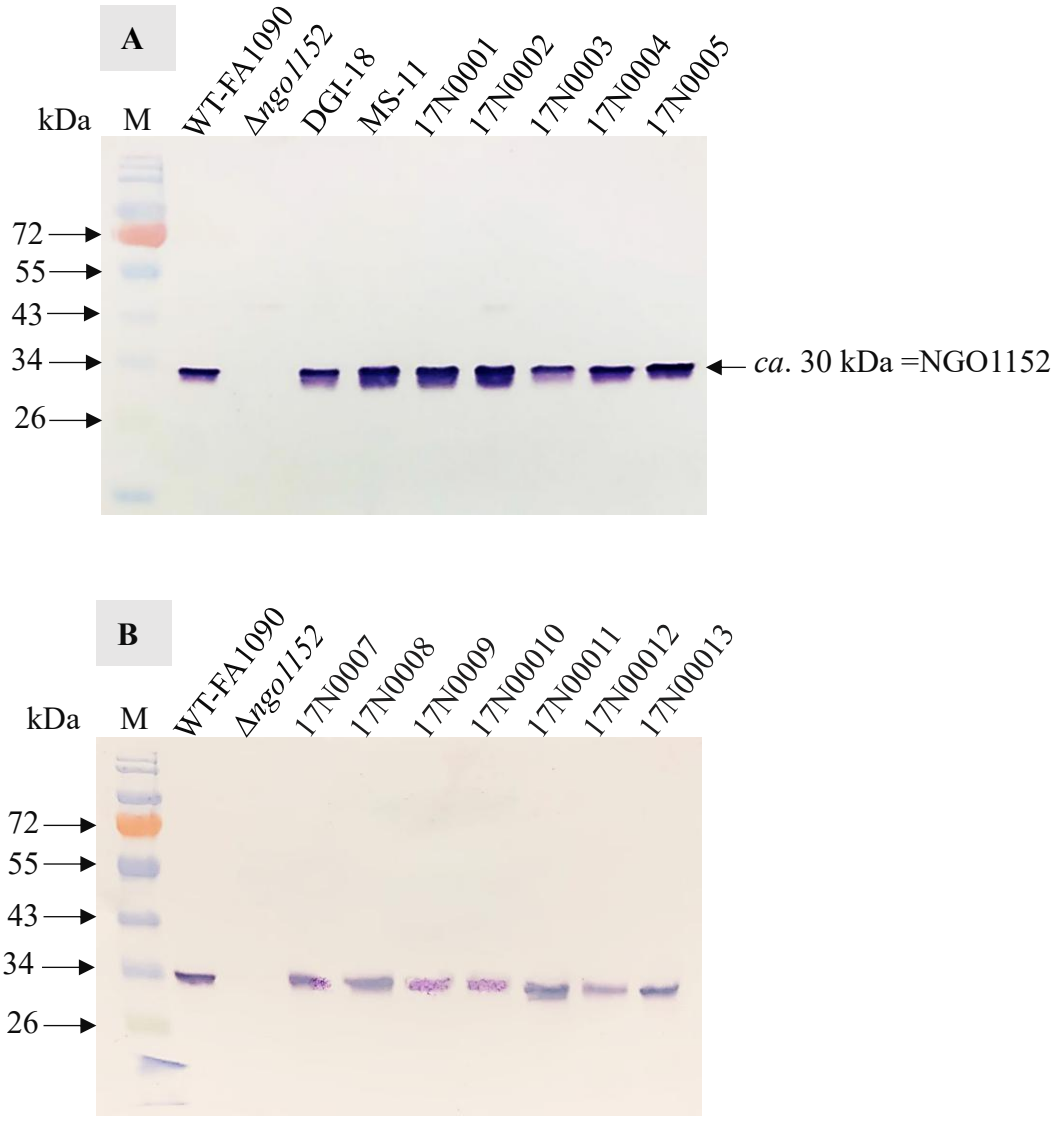

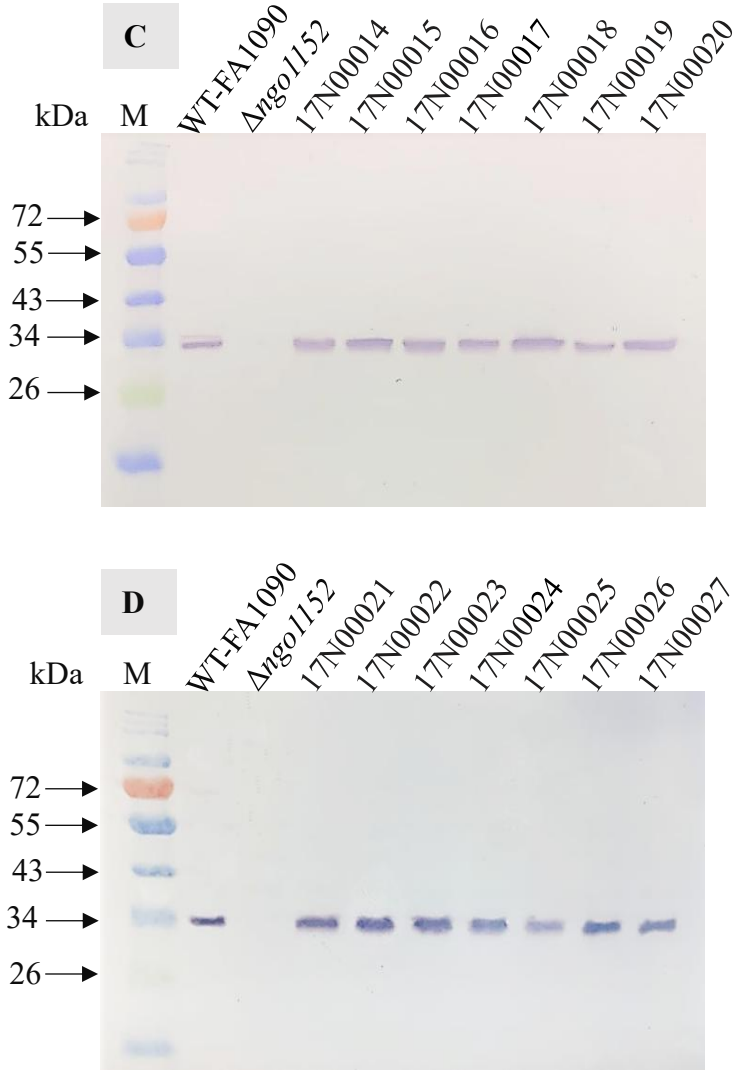

Figure 4.1. Immunoblot utilised anti-NGO1152 (1:100,000) analysis of whole cell lysates from various gonococcal clinical strains to determine the expression of NGO1152.

Whole cell lysates (equivalent to a final OD_{600} at 0.2) of clinical strains were separated by electrophoresis on 10% SDS-PAGE gels, then transferred to nitrocellulose and probed with rabbit anti-NGO1152 polyclonal antibody at a 1:100,000 dilution. The immunoblot analysis showed a strong reactive band at *ca*. 30 kDa corresponding to NGO1152, which was observed in all clinical isolates panels in (A) DGI-18 to 17N0005). (B) 17N0007 to 17N00013. (C) 17N00014 to 17N00020). (D) 17N00021 to 17N00027). Lane M: (10-250 kDa) protein marker. This confirmed the expression of the NGO1152 in the WT-FA1090 as a positive control and the absence of the band of NGO1152 in the FA1090Δ*ngo1152* as a negative control in all panels.

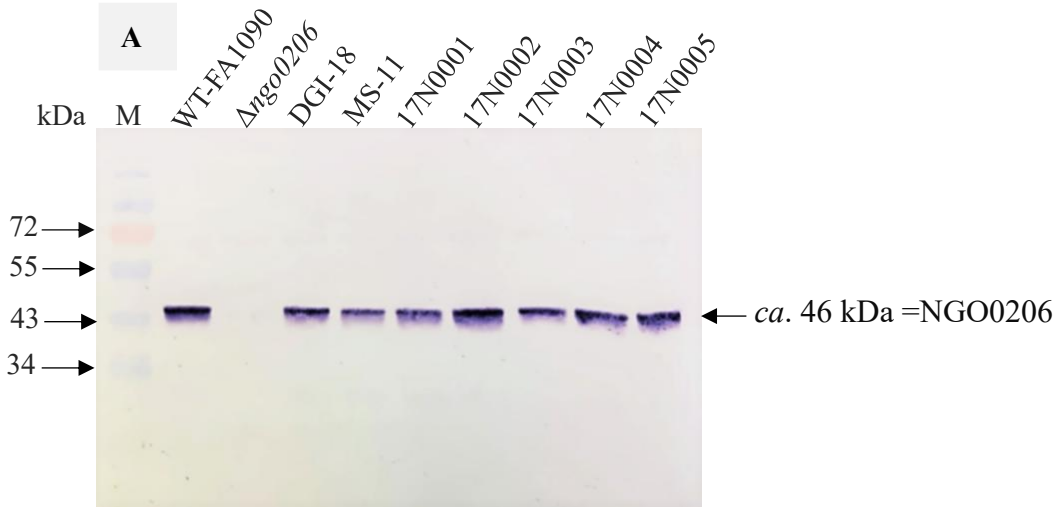
A
kDa
M
WT-FA1090
Δngo0206
DGI-18
MS-11
17N0001
17N0002
17N0003
17N0004
17N0005
72
55
43
34
ca. 46 kDa =NGO0206

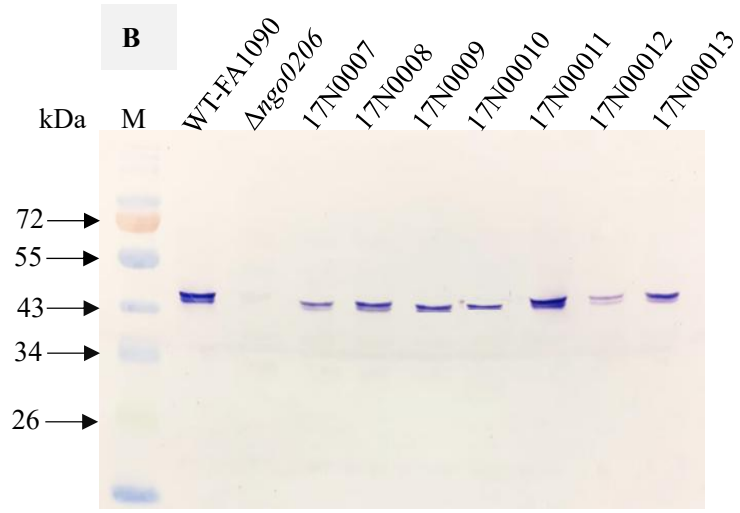
B
kDa
M
WT-FA1090
Δngo0206
17N0007
17N0008
17N0009
17N00010
17N00011
17N00012
17N00013
72
55
43
34
26

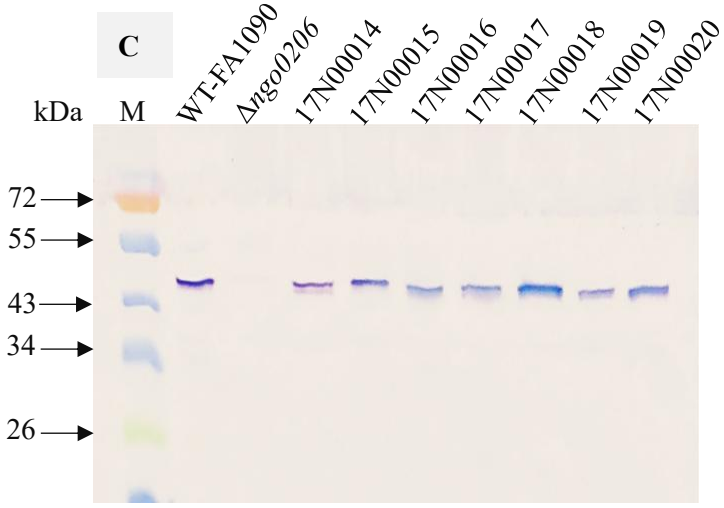
C
kDa
M
WT-FA1090
Δngo0206
17N00014
17N00015
17N00016
17N00017
17N00018
17N00019
17N00020
72
55
43
34
26

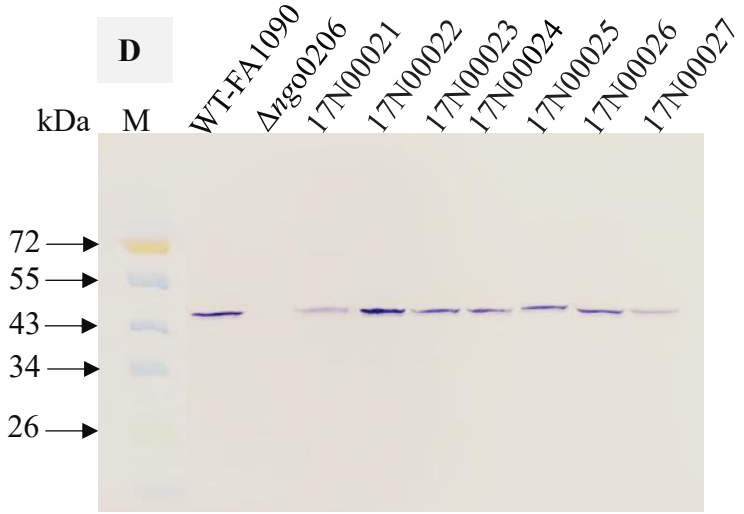

Figure 4.2. Immunoblot utilised anti-NGO0206 (1:100,000) analysis of whole cell lysate of several gonococci clinical strains to determine the expression of the NGO0206.

Whole cell lysates (equivalent to a final OD_{600} at 0.2) of clinical strains were subjected to electrophoresis on 10% SDS-PAGE gels and then transferred to nitrocellulose membranes and probed with rabbit anti-NGO1152 polyclonal antibody at a 1:100,000 dilution. Immunoblot analysis showed a strong reactive band at *ca.* 46 kDa, corresponding to the NGO0206 in clinical isolates in panels (A) DGI-18 to 17N0005. (B) 17N0007 to 17N00013. (C) 17N00014 to 17N00020. (D) 17N00021 to 17N00027. Lane M: (10-250 kDa) protein marker. This confirmed the expression of the NGO0206 in WT-FA1090 as a positive control and its absence in the FA1090Δ*ngo0206* used as a negative control in all panels.

4.2.2. Composition and diversity of the gonococcal isolate set extracted from PubMLST

The search terms utilised identified 7327 *N. gonorrhoeae* isolates with associated whole genome sequence records for bioinformatics analysis. As a prelude to the bioinformatics analysis, the metadata associated with the records were examined to gain insights into the panel of isolates.

4.2.2.1. Country of isolation

Examination of the isolate records determined that the 7327 *N. gonorrhoeae* isolates were sourced from 24 countries, as illustrated in Figure 4.3. Most isolates were collected in the UK (recorded either as UK, UK [England], UK [Wales], UK [Northern Ireland] or UK [Scotland]. Additional isolates were obtained from Sweden, the USA, Norway, New Zealand, the Netherlands, Japan, Portugal, Germany, Vietnam, Argentina, Spain, Australia, Kenya, Ghana, Ireland, Canada, Italy, Brazil, South Africa, the Philippines, China, France, and Malaysia. Overall, 4744 (64.5%) were isolated in European countries, 1181 (16.1%) were isolated in North America, 764 (10.4%) were isolated in countries in Oceania, with 432 (5.9%), 380 (5.2%) and 115 isolates (1.6%), respectively, isolated in South American, Asian, or African countries. Overall, this analysis illustrates that although the isolate panel predominantly comprises European (and mostly UK) isolates, it nonetheless contains representative isolates from all regions of the world. However, this distribution does not fully reflect the global epidemiological landscape of *N. gonorrhoeae* infections, though it still provides a valuable and diverse dataset for comparative and surveillance studies.

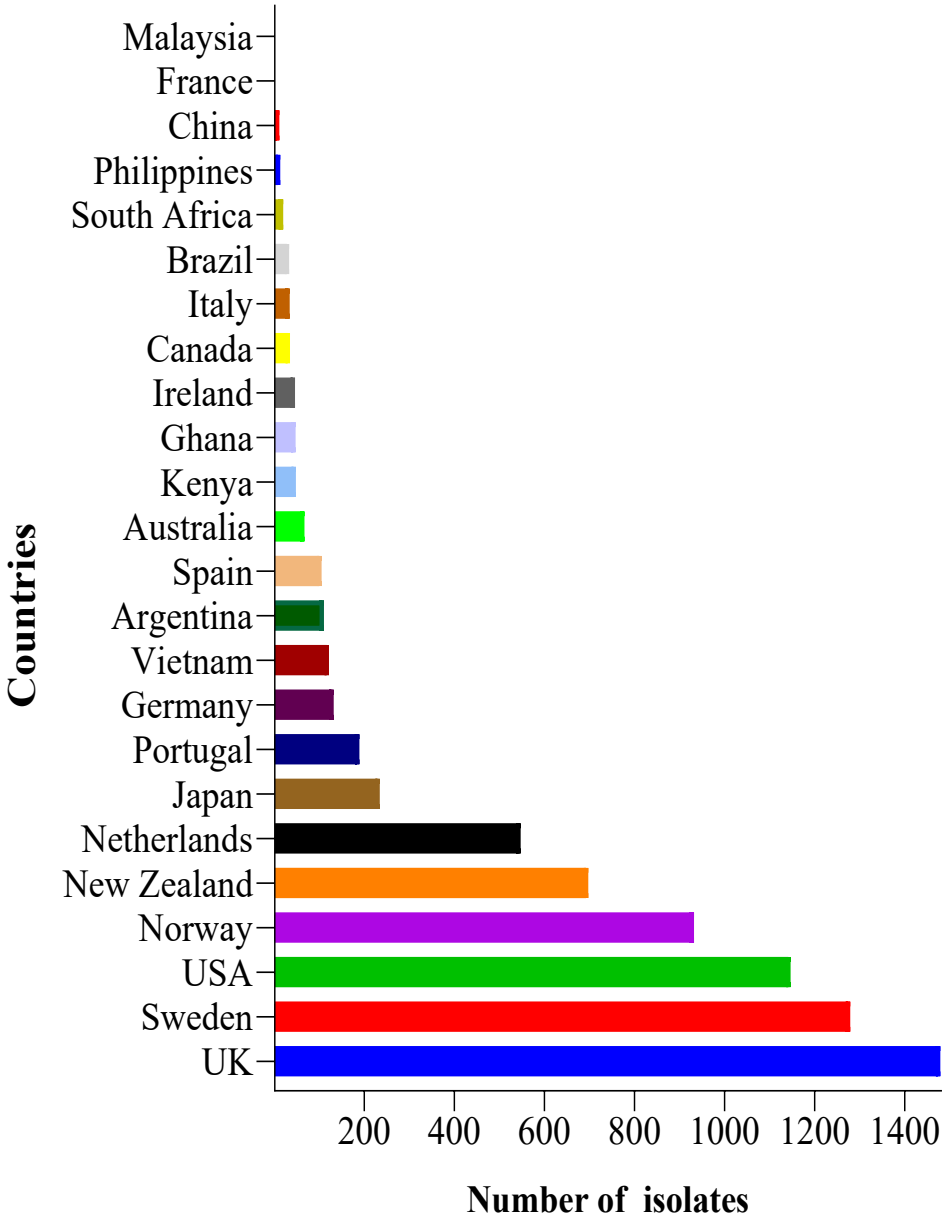

Figure 4.3. Continent-level distribution of 7,327 *N. gonorrhoeae* isolates extracted from the PubMLST database, used to assess the global prevalence and conservation of the *ngo0206* and *ngo1152* genes.
The highest numbers of isolates were reported from the UK (n = 1,479), Sweden (n = 1,279), and the US (n = 1,146). Additional isolates were recorded from Norway (n = 932), New Zealand (n = 697), the Netherlands (n = 547), Japan (n = 234), Portugal (n = 189), Germany (n = 132), Vietnam (n = 121), Argentina (n = 110), Spain (n = 105), Australia (n = 67), Kenya (n = 48), Ghana (n = 47), Ireland (n = 46), Canada (n = 35), Italy (n = 34), Brazil (n = 33), South Africa (n = 20), the Philippines (n = 13), China (n = 11), France (n = 1), and Malaysia (n = 1).

4.2.2.2. Year of isolation

Isolate records from 2014 onwards were included in this analysis, and Figure 4.4 shows the total number of isolates per year. The highest number was isolated in 2016 (n=2351), with far fewer numbers in some years (for example, 11 isolates in 2020, 7 isolates in 2021 and 6 isolates in 2022). Overall, the isolates panel predominantly spans the years 2014-2019 (n=7303; 99.7%).

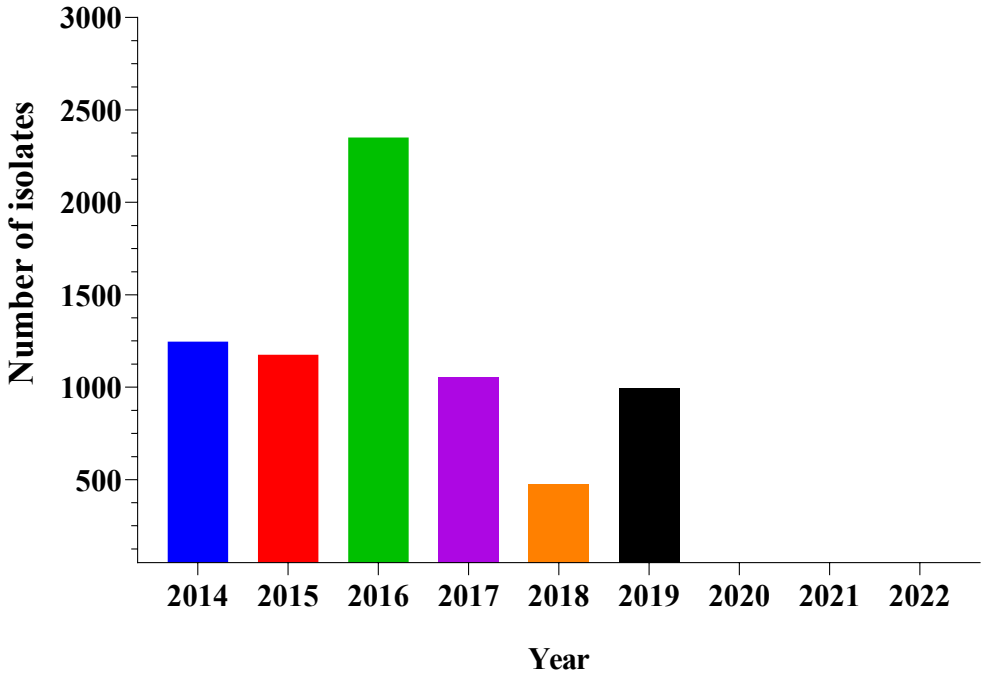

Figure 4.4. Year of isolation for 7,327 *N. gonorrhoeae* clinical isolates extracted from the PubMLST database.
The highest number of isolates was isolated in 2016 (n= 2351). In comparison, the years 2014, 2015, 2017, 2018, and 2019 exhibited relatively high and consistent numbers of isolates, ranging from 1,246 to 998 annually. A marked decline was observed in subsequent years, with only 11 isolates in 2020, 7 in 2021, and 6 in 2022.

4.2.2.3. Evaluating the gender sources of isolates

The metadata associated with 7327 gonococcal isolates was also interrogated for the gender source of the isolates. As shown in Figure 4.5, 4582 (62.5%) of isolates were isolated from males, and 772 (10.5%) were from females. However, no gender source metadata was associated with 1973 (26.9%) of the isolate records. Even if all the 1973 gonococci were, in fact, isolated from women, these data may still reflect that gonococcal infections are more likely to be symptomatic in men than women and, therefore, men are more likely to be tested for infection(Jenks *et al.*, 2022).

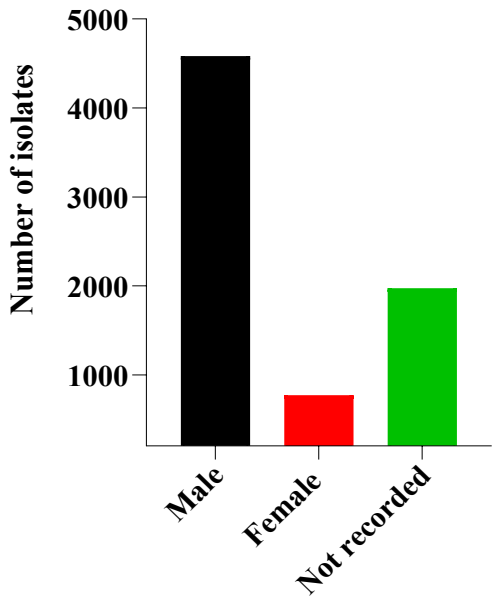

Figure 4.5. Source of 7,327 *N. gonorrhoeae* isolates categorised by patient gender, based on data extracted from the PubMLST database.
The data illustrate that 62.5% (n=4582) of isolates were isolated from men and 10.5% (n=772) from women. No gender source metadata was associated with n=1973 (26.9%) of the isolate records.

4.2.2.4. Determination of *N. gonorrhoeae* multi-sequence types (NG-STs)

A total of 450 distinct sequence types (Ledsgaard *et al.*, 2018) were identified among the 7327 isolates. However, the majority (n = 5227; 71.3%) belonged to just 26 STs, with the most common being ST-9363, ST-1901, ST-7363, and ST-8156. Collectively, these four STs accounted for 27.7% (n = 2032) of the isolates, as shown in Figure 4.6. No ST was recorded for 55 isolates (0.75%), and further examination revealed that this was due to incomplete MLST allelic profiles.

In summary, while the isolate panel demonstrates some bias toward samples from European countries, male subjects, and certain STs, it still encompasses a wide range of isolates from multiple continents and countries. Consequently, it serves as a valuable resource for examining recently circulating strains and for exploring the prevalence and conservation of potential vaccine candidates.

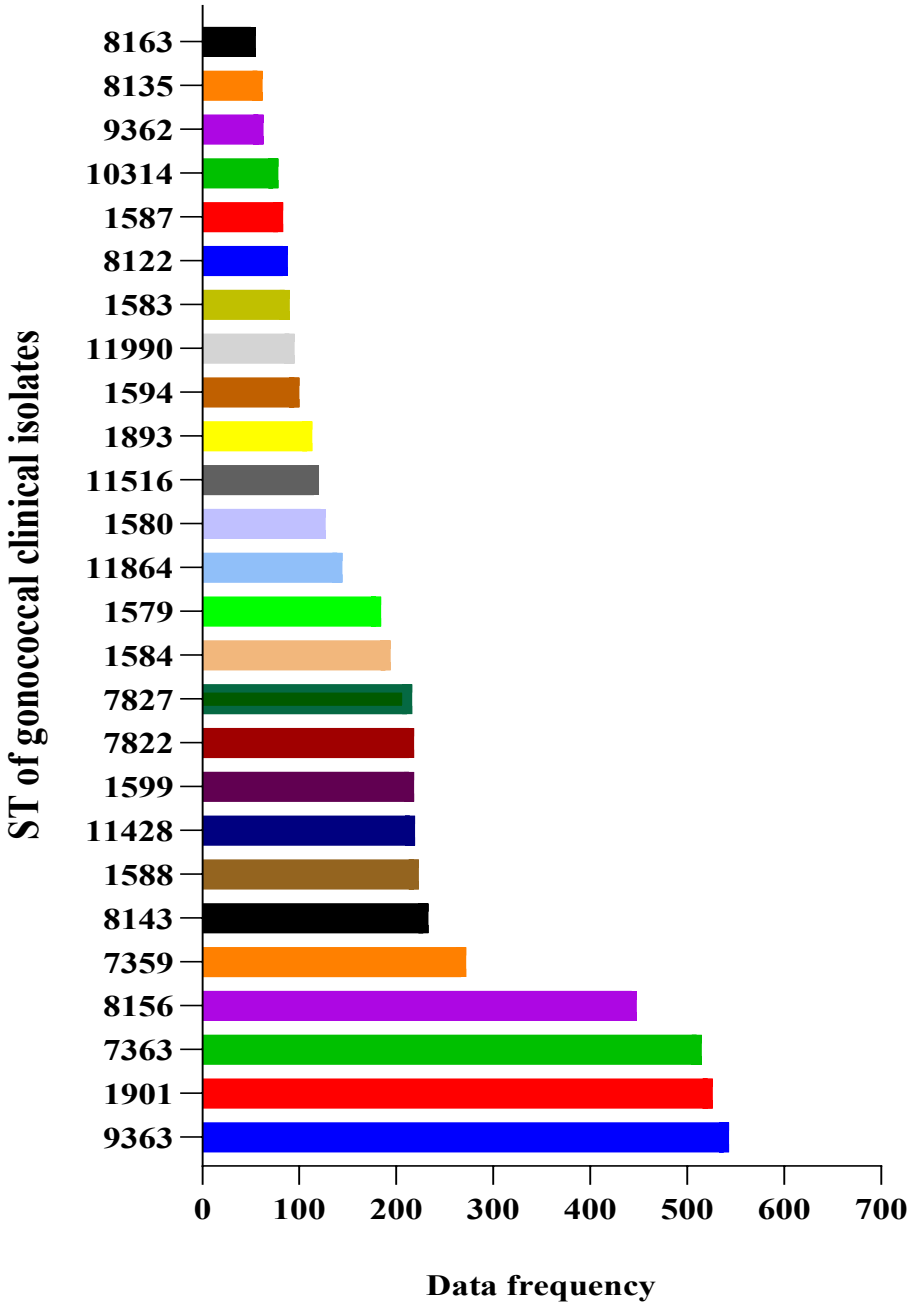

Figure 4.6. The prevalence of different STs amongst the 7327 gonococcal isolates.

Only STs present in >55 isolates are shown for clarity. ST-9363 was the most common (n=543). Other common STs (>300 isolates) included: ST-1901 (n=526), ST-7363 (n=515), and ST-8156 (n=448). Together, these four STs encompassed 27.7% (n=2032) of all isolates. The total number of isolates represented by the STs shown in the graph is 5,227, comprising 26 distinct STs. ST information was not available in the metadata for 55 isolates (0.75%).

4.2.3. Prevalence of the *ngo0206* gene and amino acid conservation of the NGO0206 protein

BLAST was used to identify regions of similarity between biological sequences by comparing a query sequence, in this case, the 378 amino acids of the NGO0206 protein from *N. gonorrhoeae* FA1090, with sequence data from 7,327 gonococcal isolates (Table 4.1). The dataset comprised whole-genome sequence data corresponding to these isolates, extracted from PubMLST. The output data, summarised in Table 4.1, revealed that 44.6% (n = 3,269) of the gonococcal isolates encode a protein substantially identical to FA1090-NGO0206 in terms of both amino acid identity and alignment length.

Full-length proteins exhibiting less than 100% identity to the query sequence were further analysed for amino acid mismatches and gaps. To accomplish this, nucleotide sequences corresponding to the BLAST hits were first translated using the ExPASy Translate tool. The resulting protein sequences were then subjected to additional BLAST searches and alignment analyses. Subsequently, the DNA sequences encoding NGO0206 from these isolates were translated and aligned against the FA1090-NGO0206 protein using multiple sequence alignment (Figure 4.7). This alignment facilitated the identification of amino acid mismatches, substitutions, and other sequence variations. For example, in BLAST analysis, it was found that 2035 isolates had an insertion of an alanine (Ala-A) residue at position 9 of the FA1090 protein, giving rise to a 379 amino acid long primary sequence, but were otherwise identical to the NGO0206 sequence. Additional isolates also encoded this insertion in combination with one or two other mismatches (Table 4.1 and Figure 4.7).

Examination of the DNA sequences from certain isolates explained the presence of evidently truncated NGO0206 proteins. These truncations resulted either from a single nucleotide change introducing a premature stop codon (*e.g.* id-107268 and id-109152) or from a frameshift mutation near the start of the gene coding sequence (id-118499). These isolates possessed the *ngo0206* gene, but they were predicted not to express a functional NGO0206 protein. Additionally, in two isolates (id-76338 and id-61813), the gene encoding NGO0206 was found to span multiple contigs, preventing accurate reassembly of the intact locus.

Consequently, these isolates were excluded from the analysis due to the inability to confidently reconstruct the full gene sequence.

However, the remaining 886 isolates examined contained hits with a considerably lower percentage identity (~60–65%) to the FA1090-NGO0206 query sequence. In these isolates, the DNA sequences encoding these hits were demonstrated not to be *ngo0206*. Therefore, 886 out of 7,325 gonococcal isolates (12.1%) were determined to lack the *ngo0206* gene.

The results of this analysis revealed that the approximate prevalence of *ngo0206* across gonococci is 87.9% (6439/7325), whereas the proportion of isolates that would be predicted to express a functional NGO0206 protein is 87.8% (6435/7325). Overall, whilst not universal, the *ngo0206* gene is highly prevalent and the NGO0206 amino acid sequence shows little variability across isolates. Notably, this analysis was restricted to isolates within a defined time frame due to a current limitation of the PubMLST BLAST tool, which permits sequence comparison against a maximum of 10,000 isolate genomes (Jolley *et al.*, 2018).

Table 4.1. Summary table for the BLAST analysis of the prevalence of the *ngo0206* and the conservation of the NGO0206 primary sequence across 7325 gonococcal isolate records from PubMLST.

% Amino acid identity	Number of isolates	Isolates %	Protein alignment length	Mismatches	Gaps	Difference in protein sequence compared to FA1090-NGO0206	Representative isolate (id)
100	3269	44.6	378	0	0	None	39081
99.736	2035	27.7	379	0	1	Insertion of Ala at position 9 of the FA1090 protein	41400
99.735	370	5.05	378	1	0	Substitution of Ala for Pro at position 212	41397
	15	0.20	378	1	0	Substitution of Pro for Ser at position 310	51668
	4	0.05	378	1	0	Substitution of Val for Ala at position 6	75919
	17	0.23	378	1	0	Substitution of Ala for Val at position 266	76370
	2	0.027	378	1	0	Substitution of Ser for Phe at position 93	78929
	2	0.027	378	1	0	Substitution of Ala for Thr at position 7	106740
	2	0.027	158	0	220	Truncated due to a single nucleotide substitution leading to the introduction of a premature stop codon	107268
	1	0.01	378	1	0	Substitution of Val for Ala at position 54	79283
	1	0.01	378	1	0	Substitution of His for Arg at position 270	86904
	1	0.01	377	1	1	Frameshift mutation at the start of the gene	118499
99.472	437	5.9	379	1	1	Insertion of Ala at position 9 and substitution of Phe for Ala at position 213	39082
	169	2.30	379	1	1	Insertion of Ala at position 9 and substitution of Ser for Phe at position 47	47774
	60	0.81	379	1	1	Insertion of Ala at position 9 and substitution of Arg for His at position 331	86610
	21	0.28	379	1	1	Insertion of Ala at position 9 and substitution of Thr for Ile at position 277	52160
	9	0.12	379	1	1	Insertion of Ala at position 9 and substitution of Arg for Cys at position 331	46927
	12	0.15	379	1	1	Insertion of Ala at position 9 and substitution of Arg for Trp at position 100	86714

	1	0.20	379	1	1	Insertion of Ala at position 9 and substitution of Ala for Thr at position 264	61797
	1	0.01	379	1	1	Insertion of Ala at position 9 and substitution of Ala for Val at position 376	76203
	1	0.01	379	1	1	Insertion of Ala at position 9 and substitution of Ala for Val at position 244	111458
	1	0.01	379	1	1	Insertion of Ala at position 9 and substitution of Ala for Val at position 342	116059
99.471	1	0.01	378	2	0	Substitution of Ala for Thr at position 91 and Phe for Ala at position 212	76042
	1		378	2	0	Substitution of Phe for Ala at position 212 and substitution of Val for Ala at position 281	115896
	1	0.01	158	1	220	Truncated due to a single nucleotide substitution leading to the introduction of a premature stop codon	109152
99.208	1	0.01	379	2	1	Insertion of Ala at position 9, substitution of Ser for Asp at position 47, and Asp for Asn at position 229	79224
99.206	3	0.04	378	3	0	Substitution of K for Asn at position 54, Ala for Phe at position 59 and Ser for Q at position 183	111443
98.945	1	0.01	379	3	1	Insertion of Ala at position 9, substitution of Thr for Ala at position 28, Met for Thr at position 66, and K for Asn at position 175	111668
64.721	2	0.027	394	123	16	Hit not NGO0206, no significant similarity was found in *N. gonorrhoeae* FA1090	56783
60.773	782	10.67	3788	139	1	Hit not NGO00206, but NGO1253 (polyamine ABC transporter substrate-binding protein)	39619
60.773	102	1.39	381	139	6	Hit not NGO00206, but NGO1253 (polyamine ABC transporter substrate-binding protein)	41391

Characterisation of dominant NGO0206 allelic variants to inform broad-coverage gonococcal vaccine design. Analysis of 7,325 *N. gonorrhoeae* isolates revealed that the NGO0206 protein is highly conserved, with two dominant allelic forms collectively present in approximately 72–75% of global circulating strains. The primary allele, identical to the FA1090-NGO0206 reference sequence (378 amino acids), was detected in 44.6% of isolates (n = 3,269).

A closely related variant, characterised by the insertion of an alanine (Ala-A) at position 9, resulting in an extended protein of 379 amino acids, was observed in 27.7% of isolates (n = 2,035). These variant shares complete sequence identity with the reference protein except for this single insertion. Additional minor variants, each representing fewer than 6% of isolates, exhibited one or two amino acid substitutions but retained over 98% sequence identity to the reference, indicating limited diversity in NGO0206.

For vaccine development, it is advisable to prioritise the two dominant allelic forms: the reference sequence and the alanine (Ala-A) insertion variant. Together, these account for approximately 72–75% of global isolates, which would maximise immunological coverage across roughly three-quarters of circulating strains. Plus, inclusion of minor variants with minimal sequence divergence may further enhance vaccine breadth, potentially extending coverage to around 80% of gonococcal isolates.

Despite the overall size of the dataset, this analysis focuses specifically on multiple sequence alignments of 105 selected NGO0206 protein variants compared to the FA1090-NGO0206 reference sequence. To facilitate clear visual identification of sequence variation, all amino acid substitutions or absence at each aligned position are highlighted in yellow, presented in bold typeface, and enclosed within black boxes (Figure 4.7).

```
47774       MKKTLVAAAILSLALTACGGGSDTAAQTPSAKPEAEQSGKLNIYNWPDYVDPETVAAFEK    60
86714       MKKTLVAAAILSLALTACGGGSDTAAQTPSAKPEAEQSGKLNIYNWSDYVDPETVAAFEK    60
46927       MKKTLVAAAILSLALTACGGGSDTAAQTPSAKPEAEQSGKLNIYNWSDYVDPETVAAFEK    60
52160       MKKTLVAAAILSLALTACGGGSDTAAQTPSAKPEAEQSGKLNIYNWSDYVDPETVAAFEK    60
86610       MKKTLVAAAILSLALTACGGGSDTAAQTPSAKPEAEQSGKLNIYNWSDYVDPETVAAFEK    60
41400       MKKTLVAAAILSLALTACGGGSDTAAQTPSAKPEAEQSGKLNIYNWSDYVDPETVAAFEK    60
39082       MKKTLVAAAILSLALTACGGGSDTAAQTPSAKPEAEQSGKLNIYNWSDYVDPETVAAFEK    60
111443      MKKTLVAA-ILSLALTACGGGSDTAAQTPSAKPEAEQSGKLNIYNWSDYVDPETVAAFEK    59
106740      MKKTLVTA-ILSLALTACGGGSDTAAQTPSAKPEAEQSGKLNIYNWSDYVDPETVAAFEK    59
78929       MKKTLVAA-ILSLALTACGGGSDTAAQTPSAKPEAEQSGKLNIYNWSDYVDPETVAAFEK    59
76370       MKKTLVAA-ILSLALTACGGGSDTAAQTPSAKPEAEQSGKLNIYNWSDYVDPETVAAFEK    59
75919       MKKTLAAA-ILSLALTACGGGSDTAAQTPSAKPEAEQSGKLNIYNWSDYVDPETVAAFEK    59
51668       MKKTLVAA-ILSLALTACGGGSDTAAQTPSAKPEAEQSGKLNIYNWSDYVDPETVAAFEK    59
39081       MKKTLVAA-ILSLALTACGGGSDTAAQTPSAKPEAEQSGKLNIYNWSDYVDPETVAAFEK    59
FA1090      MKKTLVAA-ILSLALTACGGGSDTAAQTPSAKPEAEQSGKLNIYNWSDYVDPETVAAFEK    59
41397       MKKTLVAA-ILSLALTACGGGSDTAAQTPSAKPEAEQSGKLNIYNWSDYVDPETVAAFEK    59
            ******:* ************************************ ************

47774       ETGIKMRSDYYDSNETLEAKVLTGKSGYDLTAPSIANVGRQIKAGAYQKIDKAQIPHYGN    120
86714       ETGIKMRSDYYDSNETLEAKVLTGKSGYDLTAPSIANVGWQIKAGAYQKIDKAQIPHYGN    120
46927       ETGIKMRSDYYDSNETLEAKVLTGKSGYDLTAPSIANVGRQIKAGAYQKIDKAQIPHYGN    120
52160       ETGIKMRSDYYDSNETLEAKVLTGKSGYDLTAPSIANVGRQIKAGAYQKIDKAQIPHYGN    120
86610       ETGIKMRSDYYDSNETLEAKVLTGKSGYDLTAPSIANVGRQIKAGAYQKIDKAQIPHYGN    120
41400       ETGIKMRSDYYDSNETLEAKVLTGKSGYDLTAPSIANVGRQIKAGAYQKIDKAQIPHYGN    120
39082       ETGIKMRSDYYDSNETLEAKVLTGKSGYDLTAPSIANVGRQIKAGAYQKIDKAQIPHYGN    120
111443      ETGIKMRSDYYDSNETLEAKVLTGKSGYDLTAPSIANVGRQIKAGAYQKIDKAQIPHYGN    119
106740      ETGIKMRSDYYDSNETLEAKVLTGKSGYDLTAPSIANVGRQIKAGAYQKIDKAQIPHYGN    119
78929       ETGIKMRSDYYDSNETLEAKVLTGKSGYDLTAPFIANVGRQIKAGAYQKIDKAQIPHYGN    119
76370       ETGIKMRSDYYDSNETLEAKVLTGKSGYDLTAPSIANVGRQIKAGAYQKIDKAQIPHYGN    119
75919       ETGIKMRSDYYDSNETLEAKVLTGKSGYDLTAPSIANVGRQIKAGAYQKIDKAQIPHYGN    119
51668       ETGIKMRSDYYDSNETLEAKVLTGKSGYDLTAPSIANVGRQIKAGAYQKIDKAQIPHYGN    119
39081       ETGIKMRSDYYDSNETLEAKVLTGKSGYDLTAPSIANVGRQIKAGAYQKIDKAQIPHYGN    119
FA1090      ETGIKMRSDYYDSNETLEAKVLTGKSGYDLTAPSIANVGRQIKAGAYQKIDKAQIPHYGN    119
41397       ETGIKMRSDYYDSNETLEAKVLTGKSGYDLTAPSIANVGRQIKAGAYQKIDKAQIPHYGN    119
            ********************************* ***** ********************

47774       IDKDLLKMMEAVDPGNEYAVPYFWGINTLAINTRQVQKALGTDKLPENEWDLVFKPEYTA    180
86714       IDKDLLKMMEAVDPGNEYAVPYFWGINTLAINTRQVQKALGTDKLPENEWDLVFKPEYTA    180
46927       IDKDLLKMMEAVDPGNEYAVPYFWGINTLAINTRQVQKALGTDKLPENEWDLVFKPEYTA    180
52160       IDKDLLKMMEAVDPGNEYAVPYFWGINTLAINTRQVQKALGTDKLPENEWDLVFKPEYTA    180
86610       IDKDLLKMMEAVDPGNEYAVPYFWGINTLAINTRQVQKALGTDKLPENEWDLVFKPEYTA    180
41400       IDKDLLKMMEAVDPGNEYAVPYFWGINTLAINTRQVQKALGTDKLPENEWDLVFKPEYTA    180
39082       IDKDLLKMMEAVDPGNEYAVPYFWGINTLAINTRQVQKALGTDKLPENEWDLVFKPEYTA    180
111443      IDKDLLKMMEAVDPGNEYAVPYFWGINTLAINTRQVQKALGTDKLPENEWDLVFNPEYTF    179
106740      IDKDLLKMMEAVDPGNEYAVPYFWGINTLAINTRQVQKALGTDKLPENEWDLVFKPEYTA    179
78929       IDKDLLKMMEAVDPGNEYAVPYFWGINTLAINTRQVQKALGTDKLPENEWDLVFKPEYTA    179
76370       IDKDLLKMMEAVDPGNEYAVPYFWGINTLAINTRQVQKALGTDKLPENEWDLVFKPEYTA    179
75919       IDKDLLKMMEAVDPGNEYAVPYFWGINTLAINTRQVQKALGTDKLPENEWDLVFKPEYTA    179
51668       IDKDLLKMMEAVDPGNEYAVPYFWGINTLAINTRQVQKALGTDKLPENEWDLVFKPEYTA    179
39081       IDKDLLKMMEAVDPGNEYAVPYFWGINTLAINTRQVQKALGTDKLPENEWDLVFKPEYTA    179
```

```
FA1090      IDKDLLKMMEAVDPGNEYAVPYFWGINTLAINTRQVQKALGTDKLPENEWDLVFKPEYTA  179
41397       IDKDLLKMMEAVDPGNEYAVPYFWGINTLAINTRQVQKALGTDKLPENEWDLVFKPEYTA  179
            ********************************************************:****

47774       KLKSCGISYFDSAIEQIPLALHYLGKDPNSENPEDIKAAVDMMKAVRGDVKRFSSSGYID  240
86714       KLKSCGISYFDSAIEQIPLALHYLGKDPNSENPEDIKAAVDMMKAVRGDVKRFSSSGYID  240
46927       KLKSCGISYFDSAIEQIPLALHYLGKDPNSENPEDIKAAVDMMKAVRGDVKRFSSSGYID  240
52160       KLKSCGISYFDSAIEQIPLALHYLGKDPNSENPEDIKAAVDMMKAVRGDVKRFSSSGYID  240
86610       KLKSCGISYFDSAIEQIPLALHYLGKDPNSENPEDIKAAVDMMKAVRGDVKRFSSSGYID  240
41400       KLKSCGISYFDSAIEQIPLALHYLGKDPNSENPEDIKAAVDMMKAVRGDVKRFSSSGYID  240
39082       KLKSCGISYFDSAIEQIPLALHYLGKDPNSENAEDIKAAVDMMKAVRGDVKRFSSSGYID  240
111443      KLKQCGISYFDSAIEQIPLALHYLGKDPNSENPEDIKAAVDMMKAVRGDVKRFSSSGYID  239
106740      KLKSCGISYFDSAIEQIPLALHYLGKDPNSENPEDIKAAVDMMKAVRGDVKRFSSSGYID  239
78929       KLKSCGISYFDSAIEQIPLALHYLGKDPNSENPEDIKAAVDMMKAVRGDVKRFSSSGYID  239
76370       KLKSCGISYFDSAIEQIPLALHYLGKDPNSENPEDIKAAVDMMKAVRGDVKRFSSSGYID  239
75919       KLKSCGISYFDSAIEQIPLALHYLGKDPNSENPEDIKAAVDMMKAVRGDVKRFSSSGYID  239
51668       KLKSCGISYFDSAIEQIPLALHYLGKDPNSENPEDIKAAVDMMKAVRGDVKRFSSSGYID  239
39081       KLKSCGISYFDSAIEQIPLALHYLGKDPNSENPEDIKAAVDMMKAVRGDVKRFSSSGYID  239
FA1090      KLKSCGISYFDSAIEQIPLALHYLGKDPNSENPEDIKAAVDMMKAVRGDVKRFSSSGYID  239
41397       KLKSCGISYFDSAIEQIPLALHYLGKDPNSENAEDIKAAVDMMKAVRGDVKRFSSSGYID  239
            ***.*************************** ***************************

47774       DMAAGNLCAAIGYGGDLNIAKTRAEEAANGVEIKVLTPKTGVGVWVDSFMIPRDAQNVAN  300
86714       DMAAGNLCAAIGYGGDLNIAKTRAEEAANGVEIKVLTPKTGVGVWVDSFMIPRDAQNVAN  300
46927       DMAAGNLCAAIGYGGDLNIAKTRAEEAANGVEIKVLTPKTGVGVWVDSFMIPRDAQNVAN  300
52160       DMAAGNLCAAIGYGGDLNIAKTRAEEAANGVEIKVLIPKTGVGVWVDSFMIPRDAQNVAN  300
86610       DMAAGNLCAAIGYGGDLNIAKTRAEEAANGVEIKVLTPKTGVGVWVDSFMIPRDAQNVAN  300
41400       DMAAGNLCAAIGYGGDLNIAKTRAEEAANGVEIKVLTPKTGVGVWVDSFMIPRDAQNVAN  300
39082       DMAAGNLCAAIGYGGDLNIAKTRAEEAANGVEIKVLTPKTGVGVWVDSFMIPRDAQNVAN  300
111443      DMAAGNLCAAIGYGGDLNIAKTRAEEAANGVEIKVLTPKTGVGVWVDSFMIPRDAQNVAN  299
106740      DMAAGNLCAAIGYGGDLNIAKTRAEEAANGVEIKVLTPKTGVGVWVDSFMIPRDAQNVAN  299
78929       DMAAGNLCAAIGYGGDLNIAKTRAEEAANGVEIKVLTPKTGVGVWVDSFMIPRDAQNVAN  299
76370       DMAAGNLCAAIGYGGDLNIAKTRAEEVANGVEIKVLTPKTGVGVWVDSFMIPRDAQNVAN  299
75919       DMAAGNLCAAIGYGGDLNIAKTRAEEAANGVEIKVLTPKTGVGVWVDSFMIPRDAQNVAN  299
51668       DMAAGNLCAAIGYGGDLNIAKTRAEEAANGVEIKVLTPKTGVGVWVDSFMIPRDAQNVAN  299
39081       DMAAGNLCAAIGYGGDLNIAKTRAEEAANGVEIKVLTPKTGVGVWVDSFMIPRDAQNVAN  299
FA1090      DMAAGNLCAAIGYGGDLNIAKTRAEEAANGVEIKVLTPKTGVGVWVDSFMIPRDAQNVAN  299
41397       DMAAGNLCAAIGYGGDLNIAKTRAEEAANGVEIKVLTPKTGVGVWVDSFMIPRDAQNVAN  299
            **************************.********* ************************

47774       AHRYIDYTLRPEVAAKNGSFVTYAPASRPARELLDEKYTSDASIFPTKELMEKSFIVSPK  359
86714       AHRYIDYTLRPEVAAKNGSFVTYAPASRPARELMDEKYTSDASIFPTKELMEKSFIVSPK  360
46927       AHRYIDYTLRPEVAAKNGSFVTYAPASRPACELMDEKYTSDASIFPTKELMEKSFIVSPK  360
52160       AHRYIDYTLRPEVAAKNGSFVTYAPASRPARELMDEKYTSDASIFPTKELMEKSFIVSPK  360
86610       AHRYIDYTLRPEVAAKNGSFVTYAPASRPAHELMDEKYTSDASIFPTKELMEKSFIVSPK  360
41400       AHRYIDYTLRPEVAAKNGSFVTYAPASRPARELMDEKYTSDASIFPTKELMEKSFIVSPK  360
39082       AHRYIDYTLRPEVAAKNGSFVTYAPASRPARELMDEKYTSDASIFPTKELMEKSFIVSPK  360
111443      AHRYIDYTLRPEVAAKNGSFVTYAPASRPARELMDEKYTSDASIFPTKELMEKSFIVSPK  359
106740      AHRYIDYTLRPEVAAKNGSFVTYAPASRPARELMDEKYTSDASIFPTKELMEKSFIVSPK  359
78929       AHRYIDYTLRPEVAAKNGSFVTYAPASRPARELMDEKYTSDASIFPTKELMEKSFIVSPK  359
76370       AHRYIDYTLRPEVAAKNGSFVTYAPASRPARELMDEKYTSDASIFPTKELMEKSFIVSPK  359
75919       AHRYIDYTLRPEVAAKNGSFVTYAPASRPARELMDEKYTSDASIFPTKELMEKSFIVSPK  359
51668       AHRYIDYTLRSEVAAKNGSFVTYAPASRPARELMDEKYTSDASIFPTKELMEKSFIVSPK  359
39081       AHRYIDYTLRPEVAAKNGSFVTYAPASRPARELMDEKYTSDASIFPTKELMEKSFIVSPK  359
FA1090      AHRYIDYTLRPEVAAKNGSFVTYAPASRPARELMDEKYTSDASIFPTKELMEKSFIVSPK  359
41397       AHRYIDYTLRPEVAAKNGSFVTYAPASRPARELMDEKYTSDASIFPTKELMEKSFIVSPK  359
            ********** ******************* ** ***************************

47774       SAESVKLGVKLWQGLKAGK        378
86714       SAESVKLGVKLWQGLKAGK        379
46927       SAESVKLGVKLWQGLKAGK        379
52160       SAESVKLGVKLWQGLKAGK        379
86610       SAESVKLGVKLWQGLKAGK        379
41400       SAESVKLGVKLWQGLKAGK        379
39082       SAESVKLGVKLWQGLKAGK        379
111443      SAESVKLGVKLWQGLKAGK        378
```

```
106740      SAESVKLGVKLWQGLKAGK      378
78929       SAESVKLGVKLWQGLKAGK      378
76370       SAESVKLGVKLWQGLKAGK      378
75919       SAESVKLGVKLWQGLKAGK      378
51668       SAESVKLGVKLWQGLKAGK      378
39081       SAESVKLGVKLWQGLKAGK      378
FA1090      SAESVKLGVKLWQGLKAGK      378
41397       SAESVKLGVKLWQGLKAGK      378
            ********************
```

Figure 4.7. Multiple amino acid sequence alignment of 105 distinct NGO0206 protein variants from different *N. gonorrhoeae* isolates, compared to the FA1090-NGO0206 reference sequence. Alignment was generated using Clustal Omega [https://www.ebi.ac.uk/Tools/msa/clustalo/]. Additionally, specific symbols are employed to denote the nature of the amino acid changes, substitutions, or absence at each aligned position, thus providing further resolution in interpreting the sequence variability. For example, an asterisk (*) indicates positions which are identical across all aligned sequences. A colon (:) indicates a change in the amino acid at that position to one with highly similar biochemical properties (a conservative substitution). A decimal point (.) indicates a change in the amino acid at that position to one with slightly comparable properties (a semi-conservative substitution). A space (no symbol) indicates a substitution for an amino acid with dissimilar properties. A gap (-) in the alignment represents a missing amino acid residue at that position compared to other sequences. Colours represent different residue properties: red (AVFPMILW; small hydrophobic), blue (DE; acidic), magenta (RK; with basic-H) and green (STYHCNGQ; hydroxyl, sulfhydryl, amine, and G).

4.2.3.1. Investigating gonococcal strains lacking *ngo0206*

In order to further understand why some isolates lacked the *ngo0206*, the STs of these 886 isolates were examined and compared to the STs of strains containing *ngo0206*. Only six STs accounted for the 886 isolates, including ST-13148 ($n = 2$ isolates), ST-11999 ($n = 23$ isolates), ST-11422 ($n = 37$ isolates), ST-9362 ($n = 63$ isolates) ST-11428 ($n = 219$ isolates), and ST-9363 ($n = 543$ isolates). Importantly, no isolates from these six STs were present in the 6439 *ngo0206*-positive isolates as previously described in Table 4.1.

Further examination of the MLST allelic profiles of the six STs of interest showed that two of the seven MLST loci (*adk* and *pgm*) were identical across all six STs (Table 4.2). For the remaining five MLST genes, ST-11422 and ST-9362 possessed one divergent allele compared to the most prevalent ST-9363, whilst ST-13148, ST-11999 and ST-11428 possessed two divergent alleles compared to ST-9363. Overall, these data may suggest that all six STs form a closely related genetic lineage, which appears to have lost *ngo0206* (and perhaps additional genes in close proximity) during expansion from a common ancestor.

Table 4.2. Genetic diversity at MLST loci among six STs (encompassing 886 isolates) lacking *ngo0206*. Alleles differing from ST-9363 are highlighted in bold/grey.

STs	Number of isolates	Representative isolate ID	MLST allelic profile						
			abcZ	*adk*	*aroE*	*fumC*	*gdh*	*pdhC*	*pgm*
13148	2	56782	126	39	**170**	238	**839**	153	133
11999	23	46886	126	39	67	**111**	148	**783**	133
11422	37	118126	**109**	39	67	238	148	153	133
9362	63	116503	126	39	67	238	147	153	133
11428	218	107000	126	39	**170**	238	**734**	153	133
9363	543	47753	126	39	67	238	148	153	133

N. gonorrhoeae, common housekeeping genes used in MLST include: *abcZ* - ATP-binding cassette transporter, *adk* -Adenylate kinase, *aroE* – 5-enolpyruvylshikimate-3-phosphate synthase, *fumC* – Fumarase C, *gdh* - Glutamate dehydrogenase, *pdhC* - Pyruvate dehydrogenase complex component and *pgm* – Phosphoglucomutase.

4.2.4. Prevalence of the *ngo1152* gene and amino acid conservation of the NGO1152 protein

An identical approach to that used for NGO0206 was taken to investigate the prevalence of *ngo1152* and conservation of the NGO1152 amino acid sequence (268 protein alignment length) across 7326 gonococcal isolates using tools at the PubMLST.org/*Neisseria* database.

Based on the summary in Table 4.3, one isolate (ID-76475) was excluded from the analysis because ngo1152 spanned multiple contigs, preventing accurate reassembly of the intact locus. Additionally, two isolates (ID-77388 and ID-109097) contained truncated proteins caused by nucleotide changes that introduced internal stop codons.

As shown in Table 4.3, 6107 (83%) of gonococcal isolates encoded the NGO1152 protein with 100% identity to FA1090-NGO1152 in terms of amino acid identity and alignment length. Additionally, 1219 isolates encoded NGO1152 sequences that were highly similar, but not 100% identical to FA1090-NGO1152. Among these, 149 isolates had a single mismatch, 352 had two mismatches, 1 isolate had three mismatches, 4 isolates had four mismatches, 681 had five mismatches, 1 isolate had nine mismatches, and 23 isolates had thirteen mismatches.

Ultimately, the estimated prevalence of *ngo*1152 across gonococci was 100% (7326/7326), and the proportion of isolates that would be predicted to express a functional NGO1152 protein is 99.97% (7324/7326). Therefore, NGO1152 is predicted to be almost universally expressed in *N. gonorrhoeae* strains.

Table 4.3. Summary table for the BLAST analysis of the prevalence of the *ngo1152* and the conservation of the NGO1152 primary sequence across 7326 gonococcal isolate records from PubMLST.

% Amino acid identity	Number of isolates	Percentage of total isolates	Protein alignment length	Mismatch	Gaps	Difference in protein sequence compared to FA1090-NGO1152	Representative isolate (id)
100	6107	83.3	268	0	0	None	39081
99.6	44	0.60	268	1	0	Substitution Val for Ile (at position 99)	46286
	22	0.30	268	1	0	Substitution Glu for Asp (at position 139)	51112
	21	0.28	268	1	0	Substitution Asn for Ser (at position 145)	86536
	16	0.21	268	1	0	Substitution Glu for Asp (at position 139)	39085
	9	0.12	268	1	0	Substitution Asp for Asn (at position 231)	47806
	7	0.09	268	1	0	Substitution Gly for Asp (at position 25)	46959
	5	0.06	268	1	0	Substitution Asn for Ser (at position 175)	46853
	5	0.06	268	1	0	Substitution Ala for Val (at position 15)	95818
	4	0.05	268	1	0	Substitution Gly for Arg (at position 264)	107949
	3	0.04	268	1	0	Substitution Ala for Thr (at position 33)	61848
	2	0.02	268	1	0	Substitution Ile for Val (at position 127)	76158
	2	0.02	268	1	0	Substitution Ala for Val (at position 207)	107919
	1	0.01	268	1	0	Substitution Ala for Thr (at position 20)	61869
	1	0.01	268	1	0	Substitution Cys for Gly (at position 13)	76483
	1	0.01	268	1	0	Substitution His for Phe (at position 82)	46879
	1	0.01	268	1	0	Substitution Ser for Asn (at position 195)	107274
	1	0.01	268	1	0	Substitution Val for Ile (at position 192)	111605
	1	0.01	268	1	0	Substitution Gly for Ser (at position 132)	115884
	1	0.01	268	1	0	Substitution Ala for Val (at position 26)	118096
	1	0.01	268	1	0	Substitution Ser for Asn (at position 117)	118627
	1	0.01	268	1	0	Substitution Ser for Asn (at position 99)	119226
99.3	347	4.73	268	2	0	Substitution Val for Ile (at position 99) and Glu for Asp (at position 139)	41387
	3	0.04	268	2	0	Substitution Asn for Ser (at position 175) and Asp for Asn (at position 231)	60436

	2	0.02	268	2	0	Substitution Asn for Ser (at position 164) and Asn for Ser (at position 174)	83962
98.9	1	0.01	268	3	0	Substitution Val for Ile (at position 99), Glu for Asp (at position 139), and Asn for Ser (at position 165)	56128
	2	0.02	268	3	0	Substitution Ile for Val (at position 99), Glu for Asp (at position 139), and Asn for Ser (at position 175)	111432
	1	0.01	268	3	0	Substitution Val for Ile (at position 99), Glu for Asp (at position 139), and Ser for Ala (at position 260)	111486
	1	0.01	268	3	0	Substitution Val for Ile (at position 99), E for Asp (at position 139) and His for Y (at position 153)	118019
98.5	6	0.08	268	4	0	Substitution Glu for Asp (at position 139), His for Y (at position 153), Asn for Ser (at position 165), and Asn for Ser (at position 175)	86649
	1	0.01	268	4	0	Substitution Val for Ile (at position 99), Glu for Asp (at position 139), Asn for Gly (at position 165), and Asn for Ser at position 175)	117968
98.1	680	9.28	268	5	0	Substitution Val for Ile (at position 99), Glu for Asp (at position 139), His for Y (at position 153), Asn for Ser (at position 165), and Asn for Ser (at position 175)	41393
97.9	1	0.01	202	5	66	Frameshift mutation at the start of the gene	77388
97.4	1	0.01	168	4	100	Frameshift mutation at the start of the gene	109097
96.6	1	0.01	268	9	0	Substitution Gly for Asp (at position 36), Val for Ile (at position 99), Glu for Asp (at position 139), His for Y (at position 153), Asn for Ser (at position 165), Asn for Ser (at position 175), Glu for K (at position 243), Ala for Val (at position 260) and Gly for Glu (at position 265)	107773

95.1	23	0.31	268	13	0	Substitution Leu for Ile (at position 11), Ala for Tyr (at position 17), Gly for Ser (at position 25), Pro for Thr (at position 35), Asn for Asp (at position 58), Ala for E (at position 73), Val for Thr (at position 135), E for D (at position 139), Asn for Lys (at position 143), Tyr for His (at position 153), Asn for Ser (at position 165) and Asn for Ser (at position 175).	48405

For characterisation of dominant NGO1152 allelic variants to inform broad-spectrum gonococcal vaccine design. The BLAST analysis of 7,325 *N. gonorrhoeae* isolates demonstrated that the NGO1152 protein is highly conserved, with several allelic variants of relevance for vaccine development. The primary allelic form, identical to the FA1090-NGO1152 reference sequence across all 268 amino acids, was present in 83.3% of isolates (n = 6,107). A minority of isolates (~0.6%, n = 44) exhibited a single amino acid substitution (valine (Val-V) for isoleucine (Ile-I) at position 99), while other rare substitutions, including glutamic acid (Glu-E) for aspartic acid (Asp-D) at position 139, and asparagine (Asn-N) for serine (Ser-S) at positions 145 and 175 each accounted for less than 0.3% of isolates. Isolates harbouring two or more substitutions comprised 4.73% (n = 347) of the dataset, frequently involving the valine (Val-V) /isoleucine (Ile-I) substitution at position 99 combined with the glutamic acid (Glu-E) /aspartic acid (Asp-D) substitution at position 139. More complex variants with three or more substitutions were uncommon (<0.5%) and included changes such as histidine (His-H) to tyrosine (Tyr-Y) at position 153 and asparagine (Asn-N) to serine (Ser-S) at positions 165 and 175. An exceedingly small number (<0.1%) carried frameshift mutations near the gene start, likely leading to truncated or non-functional NGO1152 proteins. To identify the most suitable amino acid sequences for broad-spectrum vaccine development, allelic analysis of NGO1152 was undertaken.

The findings indicate that inclusion of the predominant allelic form, which is 100% identical to the FA1090-NGO1152 reference sequence, alongside the most common variant (differing by one or two conservative amino acid substitutions) should be prioritised. Together, these two variants collectively represent approximately 88% of global *N. gonorrhoeae* isolates, suggesting they could confer broad immunological coverage of most circulating strains and supporting their selection as rational antigen candidates.

Again, regardless of the size of the overall dataset, this analysis presents multiple sequence alignments of a selected subset of 95 NGO1152 protein variants aligned against the FA1090-NGO1152 reference sequence. To aid clear visual identification of mutations, all amino acid changes are highlighted in yellow, displayed in bold, and enclosed within squares as shown in Figure 4.8.

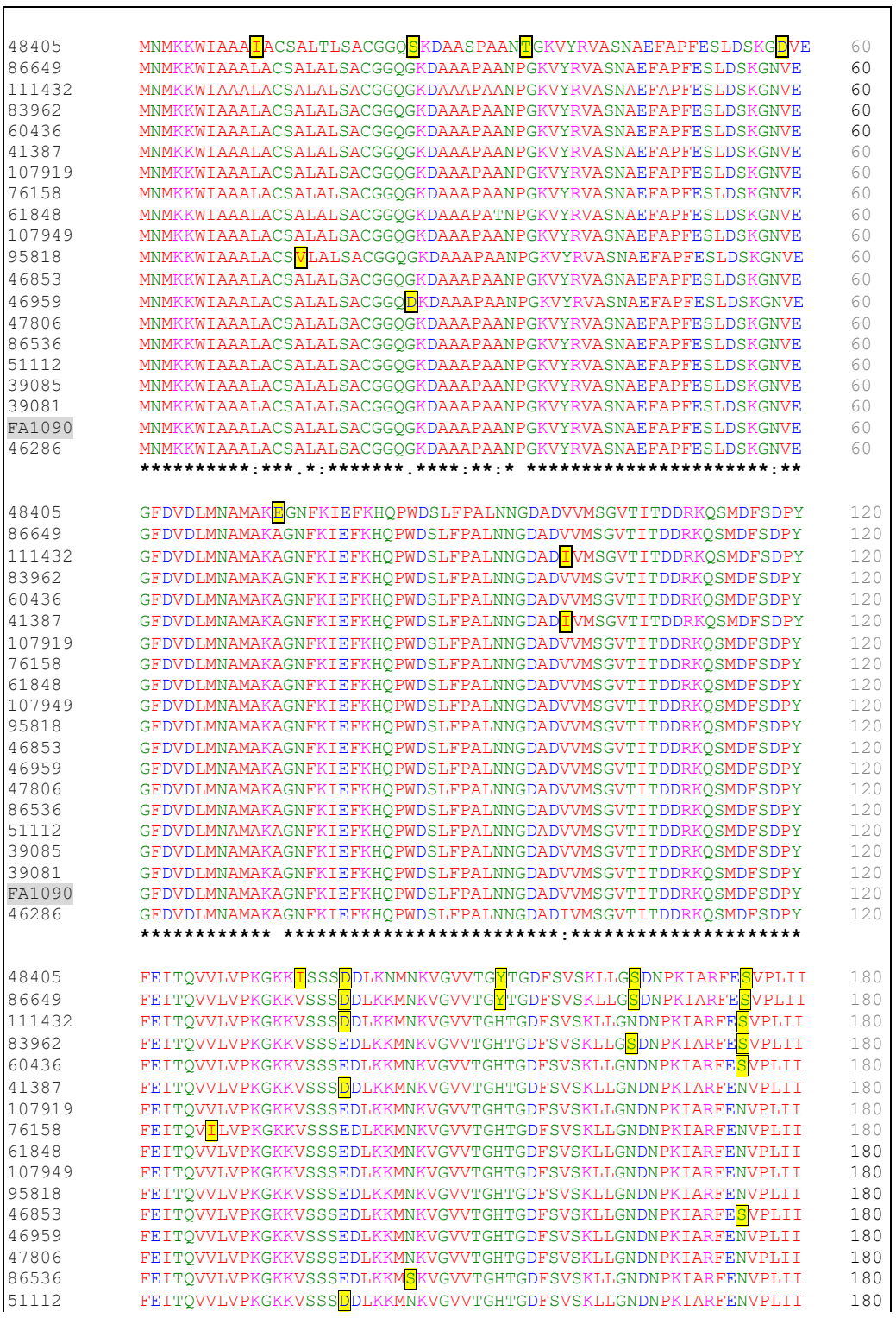

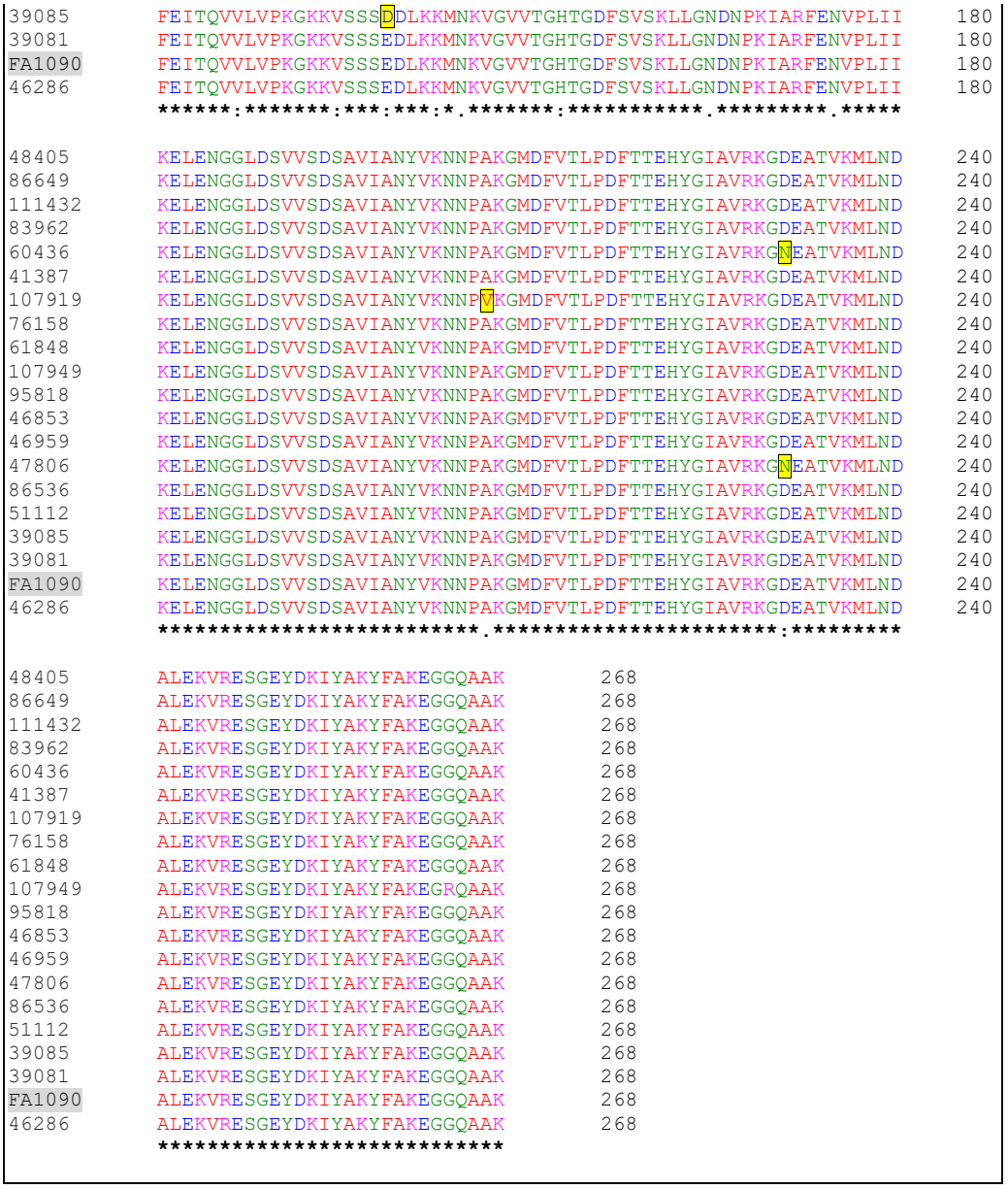

Figure 4.8. Multiple amino acid sequence alignment of 95 distinct NGO1152 protein variants from different *N. gonorrhoeae* isolates, compared to the FA1090-NGO1152 reference sequence. Alignment was generated using Clustal Omega [https://www.ebi.ac.uk/Tools/msa/clustalo/].
Additionally, specific symbols are employed to denote the nature of the amino acid changes, substitutions, or absence at each aligned position, thus providing further resolution in interpreting the sequence variability. For example, an asterisk (*) indicates positions which are identical across all aligned sequences. A colon (:) indicates a change in the amino acid at that position to one with highly similar biochemical properties (a conservative substitution). A decimal point (.) indicates a change in the amino acid at that position to one with slightly comparable properties (a semi-conservative substitution). A space (no symbol) indicates a substitution for an amino acid with dissimilar properties. Colours represent different residue properties: red (AVFPMILW; small hydrophobic), blue (DE; acidic), magenta (RK; with basic-H) and green (STYHCNGQ; hydroxyl, sulfhydryl, amine, and G).

4.3. Amino acid conservation and divergence between NGO0206 and NGO1152 and their immunological cross-reactivity

To evaluate the degree of sequence conservation between NGO0206 (378 amino acids) and NGO1152 (268 amino acids), and to investigate the molecular basis for the experimental cross-reactivity observed in immunoblotting assays between antibodies targeting NGO1152 and NGO0206 (as detailed in Chapter 3), a pairwise alignment was conducted using EMBOSS Water. This tool applies the Smith–Waterman algorithm for local sequence alignment. The alignment was performed using the EBLOSUM62 substitution matrix, with a gap opening penalty of 10.0 and a gap extension penalty of 0.5 to optimise sensitivity and accuracy.

The resulting alignment spanned 246 residues, corresponding to 65% of NGO0206 and 92% of NGO1152, with high sequence coverage but low amino acid identity (24%), as shown in Figure 4.9. The overall alignment score was 93.0, indicating limited sequence conservation between these lipoproteins and suggesting that any homology is likely confined to a shared partial domain. The EBLOSUM62 substitution matrix output revealed a low identity of 24.0% (59 out of 246 residues were identical) and a moderate similarity of 36.6% (90 residues with similar biochemical properties). The alignment also showed a high proportion of gaps (32.9%, or 81 positions out of 246), reflecting numerous insertions and deletions distributed primarily in the middle and C-terminal regions.

In contrast to the divergent central and C-terminal regions, the N-terminal signal peptide contains a conserved lipobox-like motif typical of bacterial lipoproteins. This motif terminates at the invariant cysteine (NGO0206: MKKTLVAAIL--SLALTACGG; NGO1152: MKKWIAAALACSALALSACGG), consistent with signal peptidase II processing and membrane lipidation (Figure 4.9). This conserved domain underpins membrane targeting, lipidation, and anchoring, thereby facilitating correct localisation and contributing to immune recognition. Additional conserved N-terminal motifs and short sequence elements (such as YAVPYF/FSDPYF and GFDVDL/GKSGYD) likely support shared folding and reciprocal cross-reactivity in immunoblotting, highlighting common immunological epitopes despite overall sequence divergence.

Together, the conserved N-terminal region, including the signal peptide, lipobox, and short motifs, not only supports a shared mechanism of membrane localisation but also explains the presence of shared immunogenic determinants. This provides a compelling molecular basis for the cross-reactive signals observed in immunoblotting assays (as described in Chapter 3). Specifically, anti-NGO0206 antibodies recognised both NGO0206 and NGO1152, and anti-NGO1152 antibodies likewise bound both proteins, underscoring the immunological importance of this conserved region.

Interestingly, the alignment analysis revealed that the mature sequence of NGO0206 begins at position 1, whereas NGO1152 starts at position 3, suggesting that the first two amino acids of NGO1152 may be either unannotated or removed through post-translational processing. Additionally, two deletions near positions 11–12 in NGO0206 suggest structural modifications in NGO1152's corresponding region. These observations support functional conservation of the membrane-targeting machinery despite broader sequence divergence. The conserved signal peptide suggests both proteins use similar lipoprotein transport pathways involving signal peptide cleavage and lipid modification for membrane insertion, though subtle sequence variations may affect processing, trafficking, or maturation. The central regions of NGO1152 and NGO0206 (residues 44–97 and 137–161) show pronounced divergence, with NGO1152 exhibiting deletions and NGO0206 containing insertions or domain expansions (residues 120–150). These alignment gaps likely reflect evolutionary divergence in domain architecture and functional specialisation, accounting for the observed size difference between the proteins.

Although some polar or charged residues are conserved, the alignment reveals numerous mismatches, including both conservative and non-conservative substitutions. For example, lysine (Lys-K) or alanine (Ala-A) residues in NGO0206 are often replaced by structurally distinct residues in NGO1152, potentially affecting protein folding or ligand-binding capacity. The high density of gaps and sequence variability in the middle region further supports functional divergence, possibly reflecting differences in substrate specificity or interaction partners.

Despite overall variability, several short, conserved motifs are present. For example, the segment 'YAVPYF' in NGO0206 aligns with 'FSDPYF' in NGO1152, where five out of six residues are identical or chemically similar, indicating a conserved structural element. Likewise, the NGO1152 motif 'GFDVDL' aligns with the analogous but non-identical sequence 'GKSGYD' in NGO0206, suggesting that both proteins may share β-sheet or loop structures potentially important for stability or function. This structural conservation likely underlies the shared immunological epitope recognition despite overall sequence variability. In contrast, this region also displays multiple insertions and deletions: NGO0206 contains long gaps where NGO1152 retains sequence and vice versa, reflecting their distinct sequence lengths (378 vs. 268 amino acids). Although both proteins are annotated as lipoproteins, their low sequence identity and the presence of non-overlapping insertions and deletions suggest they have undergone distinct evolutionary adaptations and are unlikely to be functionally redundant. This structural divergence carries important biological and translational implications. The high frequency of alignment gaps and region-specific variability, particularly in surface exposed areas, may underlie differences in substrate specificity, immune accessibility, and protein–protein interactions. Notably, variation within the signal peptide region can affect membrane targeting, insertion, and post-translational modifications, for example, lipidation and can ultimately shape their distinct cellular roles. However, sequence comparisons reveal that NGO0206 contains multiple insertions relative to NGO1152, especially in the middle and C-terminal regions, indicating domain expansions.

Importantly, the conserved N-terminal motifs in NGO0206 and NGO1152, potentially including β-barrel or immunoglobulin-like fold elements, preserve essential structural features that likely underpin cross-reactive antibody recognition. Although these lipoproteins are structurally divergent and functionally non-redundant, they share sufficient epitope similarity to support broad vaccine potential. Simultaneously, their distinctive regions offer opportunities for use as diagnostic or epidemiological markers, aiding strain-level differentiation. Thus, understanding their conserved and divergent features is essential for both immunological and translational applications.

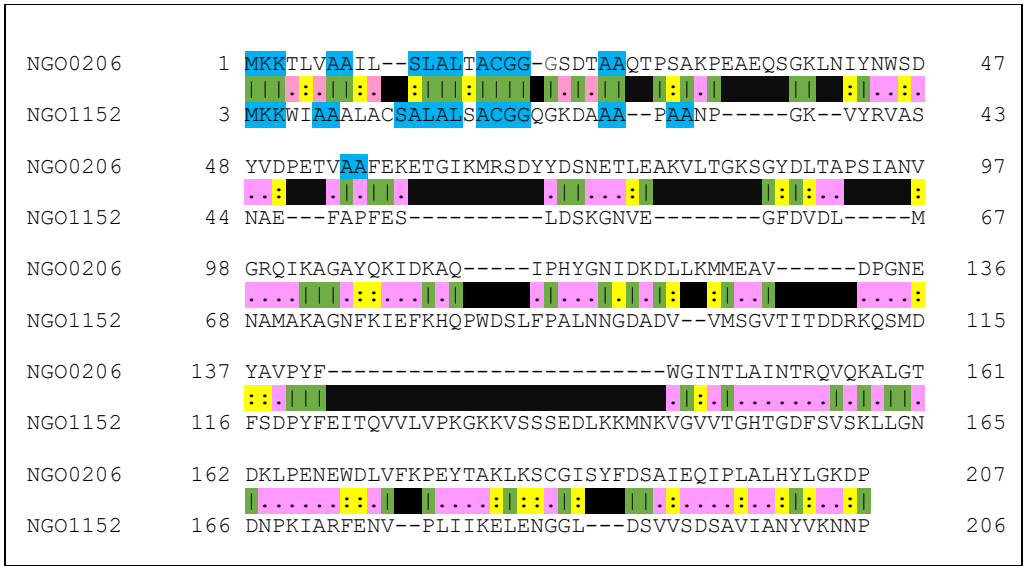

Figure 4.9. Pairwise amino acid sequence alignment analysis between FA1090-NGO0206 (378 amino acids) and FA1090-NGO1152 (268 amino acids). Alignment was generated using EMBOSS Water [https://www.ebi.ac.uk/jdispatcher/psa/emboss_water/].

The alignment reveals both conserved and divergent regions, with the following annotation symbols: Identity (| green 24.0%), residues are identical, indicating the amino acid at that position is exactly the same in both sequences. This suggests strong evolutionary conservation and likely similar structure or function. A colon (: yellow 36.6%) indicates a change in amino acid at that position to one with highly similar biochemical properties (a conservative substitution). A decimal point (. pink) indicates a change in amino acid at that position to one with slightly similar properties (a semi-conservative substitution). A gap (- black 32.9%) in the alignment represents a missing amino acid residue at that position compared to other sequences. These gaps represent insertions or deletions (indels) relative to the other sequence and may influence protein structure or function. Conserved residues were primarily restricted to the N-terminal region, with local identity observed in motifs such as MKK–AA–SALAL–ACGG (highlighted in dark blue).

4.3.1. Conservation of amino acid alignment between NGO1152 and its orthologue NMB1612 from *N. meningitidis* MC58

Bioinformatics analysis identified NGO1152 as a putative ABC transporter component in the *N. gonorrhoeae* FA1090 genome (accession number YP_208231). The gene encodes a 268-amino-acid protein with a predicted molecular weight of approximately 30 kDa. Functional predictions indicate that NGO1152 acts as SBP, likely involved in the periplasmic transport of amino acids such as glutamine, glutamate, and aspartate. It is also hypothesised to function as a histidine-binding protein, consistent with SBP subfamily classifications. It has a close orthologue to arginine-binding SBP in *N. meningitidis* strain MC58, known as NMB1612 (also referred to as NMC1533), which is similarly predicted to encode a 268-amino acid protein with a comparable function. Given the genetic and functional similarities between *Neisseria* species, it was hypothesised that NGO1152 and NMB1612 are highly conserved orthologues performing equivalent roles in their respective hosts. Establishing the degree of similarity between these proteins provides a foundation for investigating their shared structural and functional characteristics, while also offering insight into their evolutionary divergence within pathogenic *Neisseria* lineages.

To evaluate the degree of sequence conservation between NGO1152 and NMB1612, a pairwise alignment was performed using EMBOSS water, which uses the Smith-Waterman algorithm for optimal local sequence alignment.
The resulting alignment, which spanned the entire length of both proteins, demonstrated a remarkably high sequence identity of 98.1% (263 of 268 residues identical) and 98.5% similarity when including conservative substitutions. Importantly, the alignment contained no gaps, highlighting the extensive conservation and indicating highly comparable structural and functional characteristics between NGO1152 and its orthologue NMB1612. The alignment achieved a high score of 1349.0, further reflecting their strong sequence homology (Figure 4.10).

However, the alignment between NGO1152 and NMB1612 reveals five amino acid differences across their 268-residue sequences. The specific substitutions are as follows: at position 28, alanine (Ala-A) in NGO1152 is replaced by

threonine (Thr-T) in NMB1612, representing a non-conservative substitution. At position 36, glycine (Gly-G) is replaced by aspartic acid (Asp-D), also a non-conservative change. At position 143, lysine (Lys-K) is substituted with asparagine (Asn-N), a conservative substitution. At position 153, histidine (His-H) is replaced by tyrosine (Tyr-Y), representing a semi-conservative change. Finally, at position 263, glycine (Gly-G) is replaced by aspartic acid (Asp-D), another non-conservative substitution. Despite these differences, the overall sequence remains highly conserved, indicating a strong evolutionary relationship.

Collectively, the exceptionally high sequence identity of 98.1% between NGO1152 from *N. gonorrhoeae* and NMB1612 from *N. meningitidis* strongly supports their homology. This degree of conservation suggests that these proteins likely perform equivalent biological roles within their respective organisms, particularly as substrate-binding components of ABC transporters involved in *Neisseria* physiology and pathogenicity. Although minor amino acid differences, comprising only 1.9% of the sequence, may reflect strain-specific adaptations or subtle functional modulations, they are unlikely to significantly affect the protein's core structural or functional properties. Consequently, NGO1152 retains strong potential as a conserved antigenic target, relevant for both mechanistic studies and cross-species vaccine development strategies.

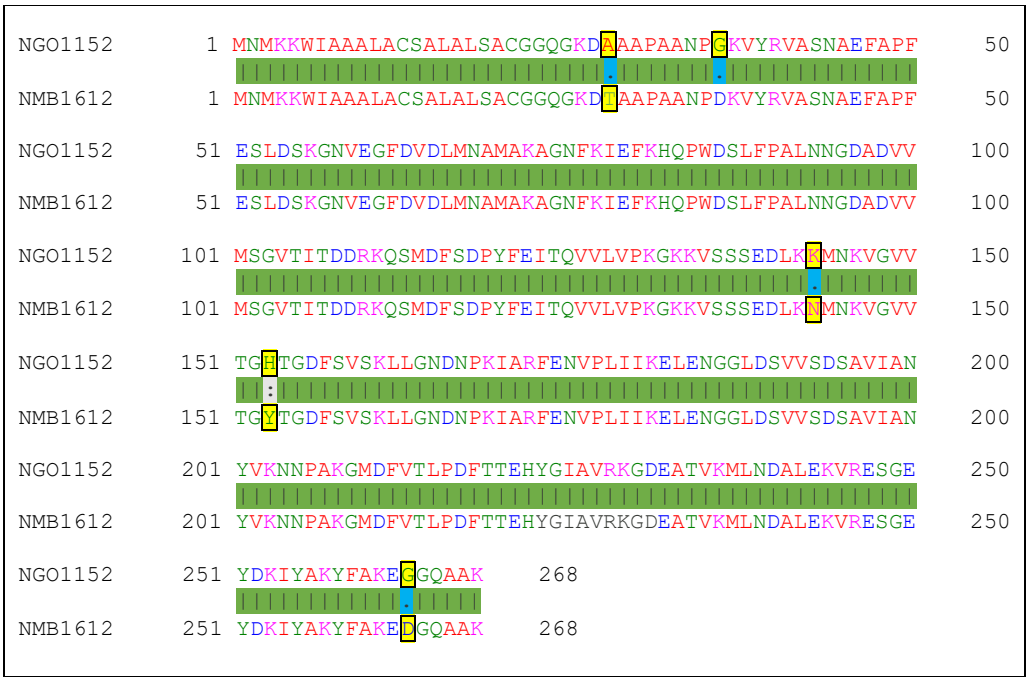

Figure 4.10. Pairwise amino acid sequence alignment analysis between NGO1152 from *N. gonorrhoeae* FA1090 and NMB1612 from *N. meningitidis* MC58 was generated using EMBOSS Water [https://www.ebi.ac.uk/jdispatcher/psa/emboss_water/].

The alignment was performed using the EMBOSS Water tool with the EBLOSUM62 substitution matrix. Residue conservation is indicated by symbols: Residue identity, similarity, and variation are indicated by alignment symbols enclosed within squares: Identity (|, green), residues are identical, indicating the amino acid at that position is exactly the same in both sequences. This suggests strong evolutionary conservation and likely similar structure or function. A colon (: grey) indicates a change in the amino acid at that position to one with highly similar biochemical properties (a conservative substitution). A decimal point (. blue) indicates a change in the amino acid at that position to one with slightly similar properties (a semi-conservative substitution). Colours represent different residue properties: red (AVFPMILW; small hydrophobic), and green (STYHCNGQ; hydroxyl, sulfhydryl, amine, and G).

4.3.1.1. Evaluate the similarity of the multiple alignment sequence between NGO0206, NGO1152, and NMB1612

Based on the finding in Figure 4.10, additional multiple sequence alignment was performed using Clustal Omega (v1.2.4) to assess sequence conservation and divergence among NGO0206 and NGO1152 from *N. gonorrhoeae* FA1090, and NMB1612 from *N. meningitidis* MC58.

The analysis revealed high sequence identity between NGO1152 and NMB1612, both of which are 268 amino acids long. In contrast to NGO0206, which exhibited notable divergence as illustrated in Figure S1 in Appendix-2. Importantly, NGO0206 is markedly longer, comprising 378 amino acids, compared to NGO1152 and NMB1612, which are both 268 residues. This length difference coincides with a striking pattern of high sequence conservation between NGO1152 and NMB1612, in contrast to the notable divergence observed in NGO0206, suggesting potential functional specialisation associated with its extended sequence.

NGO1152 and NMB1612 exhibit near-complete identity across the alignment, including conservation of the N-terminal signal peptide (residues 1–50), which contains a lipobox motif indicative of signal peptidase II processing and lipidation for periplasmic or membrane-associated localisation. Several sequence motifs, including RVASNAEFA, FESL, GNVEGFDVDLMN, and AMAKAGNFKIEFKHQPWD, are fully conserved between NGO1152 and NMB1612 but divergent in NGO0206. In contrast, NGO0206 displays only partial sequence similarity to NGO1152 and NMB1612, with the highest conservation found in the N-terminal region, where a conserved lipoprotein signal sequence suggests analogous subcellular targeting. Alignment of the N-terminal sequences revealed that all three proteins shared a lipoprotein signal motif, beginning with MKK and extending to the lipobox consensus sequence, in NGO0206, NGO1152, and NMB1612.

Despite the conserved MKK in positions 3, 4 and 5, gaps are present at positions 1 and 2 in NGO0206; these positions correspond to Methionine (Met M) and Asparagine (Asn, N) in NGO1152 and NMB1612. At position 6 in NGO0206, Threonine (Thr-T) is substituted by Tryptophan (Trp-W) in the corresponding

position of NGO1152 and NMB1612. Additionally, gaps are observed at positions 11 and 12 in NGO0206, whereas NGO1152 and NMB1612 contain Leucine (Leu-L) and Alanine (Ala-A) at these positions. These variations in the N-terminal region may influence signal peptide processing, membrane insertion, and epitope accessibility. Within the lipobox region, NGO0206 carries the sequence SLALTACG, whereas NGO1152 and NMB1612 share the closely related sequence LALSACGG. Despite the substitution of threonine (Thr-T) at position 19 in NGO0206 with serine (Ser, S) at the corresponding position in NGO1152 and NMB1612, this is a conservative change between polar residues, likely preserving the functional integrity of this motif.

Beyond this shared motif, NGO0206 exhibits substantial divergences. The central segment (~residues 150–305) contains a series of insertions and variable residues that are absent in the other two proteins. Additionally, NGO0206 possesses a unique C-terminal extension (residues 305–378) that further distinguishes NGO0206 from these homologues. These insertions likely represent additional secondary structural elements such as flexible loops or extended domains that may modulate substrate specificity, facilitate interactions with distinct molecular partners, or confer regulatory properties absent in NGO1152 and NMB1612. Such structural variations could reflect functional divergence, potentially associated with altered substrate preferences, modified membrane interactions, or distinct roles in host–pathogen dynamics. Conservation of the N-terminal signal peptide across all three proteins supports a shared membrane-targeting mechanism. However, the unique insertions and extended structure of NGO0206 point to functional divergence from NGO1152 and NMB1612. Overall, NGO1152 and NMB1612 are highly conserved orthologues, whereas NGO0206 is a structurally distinct paralogue retaining membrane-targeting capacity but likely differing in substrate binding and immune recognition. Conserved lipobox motifs suggest potential antibody recognition and vaccine inclusion, but extensive surface exposed variation in NGO0206 may limit broad cross-protection. Further structural, functional, and epitope-mapping studies are required to clarify its immunological relevance and vaccine potential.

4.4. Discussion

This chapter evaluates the prevalence and conservation of NGO1152 and NGO0206 among clinical *N. gonorrhoeae* isolates using immunoblotting and bioinformatic analyses. Demonstrating widespread expression and genetic stability of these antigens is essential for their consideration as broadly protective vaccine candidates, in line with reverse vaccinology guidelines that prioritise surface accessibility and conservation among outbreak-associated strains.

Immunoblotting of whole-cell lysates from 28 UK clinical isolates, alongside the WT-FA1090 strain, revealed immunoreactive bands at 30 kDa and 46 kDa, corresponding to NGO1152 and NGO0206, respectively. These bands were absent in the FA1090Δ*ngo1152* and FA1090Δ*ngo0206* deletion mutants, confirming the specificity of the rabbit polyclonal antisera. The expression profiles of these antigens are consistent with findings reported for NMB1612 in *N. meningitidis*, where anti-rNMB1612 sera reacted with a ~27 kDa band across all 13 meningococcal strains (Hung *et al.*, 2015). This confirms that NGO1152 and NGO0206 are highly conserved and ubiquitously expressed among circulating *N. gonorrhoeae* strains, supporting their potential involvement in pathogenesis or host interaction and their candidacy as therapeutic targets. Nonetheless, their specific functional roles, *in vivo* accessibility, and immunogenic potential remain uncharacterised. Targeted mutagenesis, host-pathogen interaction assays, and immunoproteomic profiling are required to assess their contribution to virulence and suitability for vaccine development (Baarda *et al.*, 2019; Jefferson *et al.*, 2021).

Having confirmed expression and antigenicity in a local clinical set, it was important to evaluate whether these patterns are representative across a broader, global collection of *N. gonorrhoeae* isolates. In addition to immunoblotting, bioinformatic analyses were conducted to evaluate the prevalence, antigenic variability, and sequence conservation of NGO1152 and NGO0206 across 7,327 global *N. gonorrhoeae* isolates from PubMLST. Hence, only isolates collected between 2014 and 12 August 2022 were included to ensure data recency and to remain within the current BLAST tool limit of 10,000 isolates per analysis (Jolley *et al.*, 2018). Each of these isolates was linked to curated phenotypic and

epidemiological metadata, including geographic origin, year of isolation, and host gender, enabling a contextual analysis of sequence variation.

Geographic, temporal, and demographic evaluation of the dataset revealed that most isolates originated from the UK, Sweden, the US, and Norway (Figure 4.3), while isolates from 20 other countries were markedly underrepresented. This imbalance likely reflects differences in national surveillance systems, reporting practices, diagnostic capacity, and research funding for *N. gonorrhoeae* infections (Whelan *et al.*, 2021), and it does not accurately capture global epidemiology, as many high-burden regions remain poorly represented. For instance, within the WHO African Region, only five of 47 countries contributed data to the Gonococcal Antimicrobial Resistance Surveillance Programme (GASP) (WHO, 2023). Genomic studies from Africa remain scarce (Kakooza *et al.*, 2023), leaving regional diversity and AMR patterns poorly characterised and limiting the generalisability of current findings for global control efforts.

Analysis of year-of-isolation data (Figure 4.4) revealed that 2016 experienced the highest epidemiological increase in *N. gonorrhoeae* isolates, with 2,351 cases recorded. This peak coincides with the first documented treatment failure of dual therapy (ceftriaxone and azithromycin) for pharyngeal gonorrhoea (Fifer *et al.*, 2016). This suggests a link between rising infection rates and early emergence of AMR, particularly in pharyngeal sites, which are difficult to treat due to suboptimal antibiotic penetration and frequent asymptomatic presentation (Adamson and Klausner, 2021). In comparison, data from 2014, 2015, and 2017–2019 show high and consistent isolate numbers: 1,246, 1,176, 1,057, 475, and 998 cases, respectively, indicating stable surveillance and reporting during these years. Conversely, 2020–2022 showed a sharp decline in reported cases, with only 11, 8, and 6 recorded, respectively. This decrease likely reflects disruptions in sexual health screening and surveillance during the COVID-19 pandemic rather than a true reduction in infection rates (Ivarsson *et al.*, 2022).

Alongside these temporal trends, a pronounced gender inconsistency was observed among the 7,327 isolates (Figure 4.5), with 62.5% (n = 4,582) from male patients, 10.5% (n = 772) from female patients, and 26.9% (n = 1,973) missing gender data. This likely reflects differences in symptom presentation, as 80–90% of infected men are symptomatic, whereas 50–80% of infected women

remain asymptomatic, resulting in underdiagnosis and underreporting (Rodrigues *et al.*, 2023). The high proportion of missing data underscores variability in metadata quality across countries, though stricter documentation in the UK enhances the reliability of PubMLST for AMR surveillance (UKHSA, 2024).

To assess the genetic relatedness of circulating *N. gonorrhoeae* isolates and potential clonal transmission patterns, ST analysis was performed. Among 7,327 isolates, 450 distinct STs were identified, but 5,227 isolates (71.3%) were found to be clustered within 26 dominant STs. Notably, four STs (ST-9363, ST-1901, ST-7363, and ST-8156) were particularly prevalent, collectively representing 27.7% (n = 2,032) of isolates. This clustering suggests expansion of specific clonal lineages driving transmission dynamics, consistent with prior reports linking ST-1901 to AMR and widespread dissemination (Osnes *et al.*, 2021). Crucially, ST-9363, considered a significant lineage, emerged as the most dominant in this study, emphasising its epidemiological importance. Previous research has documented the global spread of *N. gonorrhoeae* strains with reduced azithromycin susceptibility, with a particular focus on the ST-9363 core-genogroup (Joseph *et al.*, 2022). These isolates, linked to European and North American lineages, likely came from a common ancestor around 1990 and later expanded (Joseph *et al.*, 2022). This evidence shows that *N. gonorrhoeae* populations are not limited to specific regions but are clearly linked to genotype and geographic distribution.

To identify sequence hits of NGO0206 among gonococcal isolates, BLAST analysis of the 378-amino-acid NGO0206 protein from *N. gonorrhoeae* FA1090 against 7,327 gonococcal isolates in PubMLST revealed both conserved and variable regions. The observed sequence heterogeneity among isolates with less than 100% identity to the reference reflected variation in the position and biochemical properties of minor amino acid substitutions. This suggests potential for structural adaptation or functional tolerance within the protein.

However, despite this variability, a substantial proportion of isolates (44.6%, n = 3,269) encoded a protein identical to FA1090-NGO0206, exhibiting 100% amino acid identity and identical alignment length (Table 4.1). This finding

confirms that complete conservation of this protein is retained in nearly half of the circulating isolates.

Additionally, 2,035 isolates (27.7%) showed an alanine insertion at position 9 in the FA1090-NGO0206 sequence, resulting in a 379-amino-acid-long primary sequence but otherwise identical to NGO0206. These isolates exhibited an overall 99.736% amino acid identity and occasionally carried one or two additional substitutions, suggesting minor sequence variability that may influence structural dynamics without abolishing overall NGO0206 protein function (Table 4.1 and Figure 4.7).

Furthermore, three isolates were found to encode truncated variants of NGO0206. Isolate id-107268, representing two clinical isolates with 99.735% amino acid identity to FA1090-NGO0206, carried a single nucleotide substitution introducing a premature stop codon at the start of the *ngo0206* coding sequence. Similarly, isolate id-109152, corresponding to one clinical isolate, contained a single nucleotide substitution resulting in a premature stop codon. In contrast, isolate id-118499 harboured a frameshift mutation within the NGO0206 coding sequence at the start of the gene, leading to truncation. Although these isolates possessed the *ngo0206* gene, the mutations likely disrupted protein functionality. Consequently, they were predicted not to express a functional NGO0206 protein and were excluded from downstream analyses. Two further isolates (id-76338 and id-61813), the gene encoding NGO0206 was found to span/fragment across multiple contigs, thus precluding accurate reassembly of the intact complete locus. As a result, these two isolates were also excluded from the analysis due to the inability to accurately reconstruct the intact gene sequence.

Analysis of selected 105 NGO0206 variants revealed high overall conservation, consistent with functional constraint, with limited substitutions and indels predominantly in signal peptide or surface exposed regions, potentially reflecting immune-driven adaptation (Figure 4.7). Nonetheless, among the 7,325 isolates, 6,439 (87.9%) carried *ngo0206*, and 6,435 (87.8%) were predicted to encode a functional protein. This prevalence, coupled with low amino acid variability, indicates that *ngo0206* likely plays a conserved yet still uncharacterised role in *N. gonorrhoeae* biology.

In contrast, 886 isolates (12.1%) exhibited considerably lower sequence identity (~60–65%) to FA1090-NGO0206, demonstrating significant divergence from the reference sequence. These DNA sequences were confirmed not to encode *ngo0206*, indicating the complete absence of the gene. Notably, none of these 886 *ngo0206*-negative isolates overlapped with the *ngo0206*-positive group, suggesting complete segregation (Table 4.1).

Building on this, further ST analysis revealed that only six STs, including ST-13148 (n=2), ST-11999 (n=23), ST-11422 (n=37), ST-9362 (n=63), ST-11428 (n=219), and ST-9363 (n=543), accounted for all 886 *ngo0206*-negative isolates. The absence of overlap between these STs and *ngo0206*-positive isolates can support the hypothesis of a distinct, potentially clonally derived lineage (Table 4.2). Comparative MLST profiling revealed shared alleles at the *adk* and *pgm* loci across these STs, with minor allelic variations in other loci suggesting evolutionary divergence from a common ancestor, possibly accompanied by gene loss events, including *ngo0206*. The absence of *ngo0206* may coincide with broader shifts in housekeeping genes, influencing ST classification and highlighting inherent variability in *N. gonorrhoeae* populations. This is consistent with prior observations on MLST limitations (Joshi *et al.*, 2022). These isolates define a distinct evolutionary lineage, potentially reflecting adaptation to ecological niches, immune pressures, or other selective forces.

By contrast, NGO1152 was highly conserved and widely expressed. Of 7,326 isolates analysed, 6,107 (83%) encoded NGO1152, demonstrating 100% identity to NGO1152-FA1090 reference. However, the remaining 1,219 isolates (17%) displayed minor variations. Specifically, 149 isolates had one mismatch, 352 had two, 1 had three, 4 had four, 681 had five, 1 had nine, and 23 had thirteen mismatches distributed throughout the sequence (Table 4.3). Among these, one isolate (id-76475) was excluded due to fragmented locus assembly, as the *ngo1152* gene spanned multiple contigs, preventing accurate reconstruction of the intact locus. Additionally, two isolates (id-77388 and id-109097) encoded truncated proteins due to nucleotide alterations that introduced internal stop codons.

Among the 7,326 isolates expressing NGO1152, 95 selected clinical isolates showed minor amino acid differences compared to FA1090-NGO1152, with

varying numbers of substitutions. For alignment, these 95 NGO1152 protein variants were analysed (Figure 4.8). The variants exhibited only minor amino acid differences, reflecting strong conservation across circulating *N. gonorrhoeae* strains. This limited variability suggests NGO1152 is under functional constraint, with substitutions likely tolerated without disrupting overall structure or function. This high degree of conservation supports its potential as a broadly effective vaccine target.

To evaluate sequence similarity and potential immune cross-reactivity between NGO0206 and NGO1152, pairwise local alignment using EMBOSS Water (Figure 4.9) was performed. The analysis revealed a partial overlap of 246 residues (~65% of NGO0206; ~92% of NGO1152) with an alignment score of 93.0. Despite low overall identity (24%; 59/246 residues identical) and moderate similarity (36.6%; 90/246 residues with comparable biochemical properties), a high gap frequency (32.9%; 81/246 positions) highlighted substantial sequence divergence, particularly with numerous insertions in NGO0206 and deletions in NGO1152 concentrated in the central and C-terminal regions. Such variation is consistent with evolutionary divergence in lipoproteins, which often acquire specialised roles in substrate binding, cell-wall metabolism, adhesion, and signalling (Nguyen *et al.*, 2020).

In contrast, the N-terminal signal peptide and canonical lipobox motif terminating at the invariant cysteine (NGO0206: MKKTLVAAIL--SLALTACGG; NGO1152: MKKWIAAALACSALALSACGG) are highly conserved. This conservation is critical for signal peptidase II cleavage, lipidation, outer membrane targeting, and immune recognition. It likely supports similar folding and the exposure of common epitopes, providing a mechanistic basis for the reciprocal cross-reactivity observed in immunoblotting (as described in Chapter 3). Specifically, antibodies raised against NGO0206 recognised both NGO0206 and NGO1152, and anti-NGO1152 antibodies similarly bound both proteins. Additional conserved motifs, such as YAVPYF/FSDPYF and GFDVDL/GKSGYD, further suggest retention of local secondary-structure elements that could stabilise folding and expose shared surface epitopes.

Beyond the N-terminus, major sequence variation occurs in the central and C-terminal regions, including deletions in NGO1152 (residues 44–97 and 137–161), insertions in NGO0206 (residues 120–150), and multiple conservative and non-conservative substitutions. Nevertheless, several short, conserved motifs, such as 'YAVPYF' in NGO0206 aligning with 'FSDPYF' in NGO1152, and 'GFDVDL' in NGO1152 aligning with 'GKSGYD' in NGO0206, suggest structurally preserved β-strand or loop elements that may contribute to folding or stability, although their accessibility and functional relevance remain speculative without structural or experimental validation.

This conservation of the signal peptide and lipobox motif ensures identical lipidation and membrane targeting, providing a shared structural framework that underpins antibody cross-reactivity. At the same time, divergence in the central and C-terminal regions allows these proteins to retain distinct functional roles. This combination of conserved membrane-targeting domains and variable regions highlights NGO0206 and NGO1152 as promising candidates for broad-epitope vaccine development, with conserved motifs mediating cross-reactivity and variable regions offering potential discriminating markers.

Further pairwise alignment analyses revealed that NGO1152 and its *N. meningitidis* MC58 orthologue, NMB1612, are nearly identical, sharing 98.1% sequence identity without gaps across their full length. This includes complete conservation of the signal peptide and multiple SBP motifs (*e.g.* RVASNAEFA, GNVEGFDVDLMN). They differ by only five semi-conservative substitutions (1.9%), which likely reflect strain-specific adaptations or subtle functional modulations but are unlikely to affect core structural or functional properties. Collectively, these data demonstrate that NGO1152 and NMB1612 are highly conserved, supporting their functional equivalence as SBPs in ABC transporters central to *Neisseria* physiology and pathogenicity. This high conservation not only points out their shared physiological role but also identifies NGO1152 as a promising cross-species antigenic target, warranting further mechanistic studies.

The evolutionary and functional linkage of NGO1152 to NMB1612 is further supported by bioinformatic annotations. For example, NMB1612 has been identified in at least 131 *N. meningitidis* strains by the NCBI as encoding ArtJ,

a periplasmic SBP involved in L-arginine transport, based on ~41% sequence similarity with the *E. coli* ArtJ component of the ArtPIQMJ complex (Hung *et al.*, 2015). Homology is also observed with ArtJ proteins from *Geobacillus stearothermophilus* (~42% similarity; 106/231 residues), for which a crystal structure exists (Vahedi-Faridi *et al.*, 2008), as well as with ArtJ homologues from *C. trachomatis* and *C. pneumoniae* (De Boer *et al.*, 2019; Soriani *et al.*, 2010), both previously explored as vaccine candidates due to their surface accessibility and immunogenic potential (Hung *et al.*, 2015; Soriani *et al.*, 2010; Tsolakos *et al.*, 2014). In supporting these findings, recent work by Dijokaite-Guraliuc *et al*. (2023) identified NGO1152 in *N. gonorrhoeae* strain FA1090 as encoding ArtJ, consistent with UniProtKB annotations classifying it as an arginine-binding extracellular lipoprotein (Dijokaite-Guraliuc *et al.*, 2023).

To investigate evolutionary conservation and functional divergence among Neisseria lipoproteins, NGO0206 and NGO1152 were aligned with NMB1612 from *N. meningitidis* MC58. This analysis revealed near-complete sequence identity between NGO1152 and NMB1612 (both 268 amino acids), including full conservation of the N-terminal signal peptide (residues 1–50) with a canonical lipobox motif, and conserved motifs such as RVASNAEFA, FESL, GNVEGFDVDLMN, and AMAKAGNFKIEFKHQPWD. In contrast, NGO0206 shares only partial similarity with NGO1152 and NMB1612, with conservation mainly in the N-terminal region, suggesting analogous membrane targeting.

Alignment of the N-terminal sequences revealed that all three proteins contain a lipoprotein signal motif beginning with MKK and extending to the lipobox consensus. While NGO0206 carries SLALTACG, NGO1152 and NMB1612 share LALSACGG. Conservative substitutions, such as threonine (Thr) in NGO0206 for serine (Ser) in NGO1152/NMB1612, suggest retention of functional integrity. However, gaps and additional substitutions in NGO0206 may influence signal peptide processing, membrane insertion, and epitope accessibility. In this region, NGO0206 carries SLALTACG, whereas NGO1152 and NMB1612 share the closely related sequence LALSACGG. The substitution of threonine (Thr, T) in NGO0206 for serine (Ser, S) in NGO1152 and NMB1612 represents a conservative change between polar residues, suggesting

that the functional integrity of this motif is likely preserved. Despite conservation of the MKK motif at positions 3–5, NGO0206 contains gaps at positions 1 and 2, which correspond to methionine (Met, M) and asparagine (Asn, N) in NGO1152 and NMB1612. At position 6, NGO0206 has threonine (Thr, T) instead of tryptophan (Trp, W), and additional gaps occur at positions 11 and 12, where NGO1152 and NMB1612 carry leucine (Leu, L) and alanine (Ala, A), respectively. Such substitutions and deletions in the N-terminal segment may influence signal peptide processing, membrane insertion, and epitope accessibility.

Beyond this conserved motif, NGO0206 diverges substantially. Its central region (~residues 150–305) contains multiple insertions and variable residues absent from NGO1152 and NMB1612, and a unique C-terminal extension (residues 305–378) further differentiates it. These regions may form flexible loops or extended domains, potentially altering substrate specificity, molecular interactions, or regulatory properties absent in NGO1152 and NMB1612. Conserved short motifs, such as GFDVDL in NGO1152 aligning with GKSGYD in NGO0206, suggest retention of local secondary structures despite divergence.

These observed patterns for NGO0206 and NGO1152 align with broader trends in *Neisseria* lipoproteins, where sequence conservation preserves core functions, while insertions, deletions, and motif divergence drive specialised roles in substrate binding, OM processes, and host–pathogen interactions (Balasingham *et al.*, 2007; Bos *et al.*, 2014). For example, Balasingham et al. (2007) demonstrated that conserved lipoproteins such as PilP interact with secretion systems via core sequence motifs (Balasingham *et al.*, 2007). However, their function is also modulated by subtle variations in the N-terminal regions, which affect membrane localisation and the assembly of multi-protein complexes essential for pathogenicity, paralleling the substitutions observed in NGO0206. Similarly, Bos *et al*. (2014) showed that GNA2091 exhibits both evolutionary conservation and species-specific specialisation, highlighting the role of divergent domains in mediating distinct OM functions and host-pathogen interactions (Bos *et al.*, 2014). These studies collectively underscore how sequence conservation maintains essential lipoprotein functions, while indels

and motif diversification enable functional specialisation and adaptation within *Neisseria* species. This broader framework helps explain why NGO1152 remains highly conserved across gonococcal and meningococcal strains, while NGO0206 has undergone functional divergence reflecting a balance between structural conservation and adaptive specialisation in *Neisseria* lipoproteins.

In conclusion, immunoblotting confirmed the expression of NGO1152 (~30 kDa) and NGO0206 (~46 kDa) in WT-FA1090 and across all 28 clinical *N. gonorrhoeae* isolates, including NHS UK strains from 2017–2018, but both proteins were absent in their respective deletion mutants. These results validate the specificity of the antisera for NGO1152 and NGO0206 across diverse strain backgrounds and support their potential as components of a broadly protective vaccine. In support of the immunoblotting findings, complementary bioinformatic analysis of 7,325 gonococcal genomes from the PubMLST *Neisseria* spp. database. Demonstrates that *ngo0206* is present in 87.9% of isolates (6,439/7,325), with 87.8% (6,435/7,325) predicted to encode a functional protein. Although not universal, *ngo0206* is highly prevalent and exhibits minimal sequence variability across isolates. However, the *ngo0206* gene was absent in 886 of the 7,325 isolates, belonging exclusively to six STs (ST-13148, ST-11999, ST-11422, ST-9362, ST-11428, and ST-9363). These STs were completely absent in *ngo0206*-positive isolates, indicating a genetically distinct lineage. Comparative allelic profiling of the MLST loci revealed that all six STs shared identical alleles at two loci (*adk* and *pgm*), indicating a close genetic relationship and a likely common ancestor that lost *ngo0206* during evolutionary divergence. In contrast, *ngo1152* was universally present in all 7,326 isolates, with 99.97% predicted to encode a functional protein.

Nevertheless, pairwise alignment showed NGO0206 and NGO1152 share only partial similarity, with a 246-residue overlap (~65% of NGO0206, ~92% of NGO1152) but low identity (24%), moderate similarity (36.6%), and a high gap rate (32.9%), indicating substantial divergence. Most variation occurs in the central and C-terminal regions, where an extension in NGO0206 suggests evolutionary divergence and possible functional specialisation. In contrast, the N-terminal signal peptide and lipobox motif, terminating at the invariant cysteine (NGO0206: MKKTLVAAIL--SLALTACGG; NGO1152:

MKKWIAAALACSALALSACGG), are highly conserved, likely underpinning the reciprocal cross-reactivity observed in immunoblotting (Chapter 3). Where anti-NGO0206 antibodies recognised both NGO0206 and NGO1152, and anti-NGO1152 antibodies showed the same pattern. Additionally, conserved short motifs (*e.g.* YAVPYF/FSDPYF, GFDVDL/GKSGYD) suggest shared structural elements such as β-strands or loops, potentially supporting a common fold and explaining the presence of shared immunological epitopes despite overall sequence divergence. Whereas NGO1152 and NGO0206 share only limited conservation, NGO1152 and its meningococcal orthologue NMB1612 display near-complete sequence identity. Pairwise alignment showed NGO1152 and NMB1612 share 98.1% sequence identity with no gaps, differing by only five semi-conservative residues. This high conservation highlights their homologous roles as SBPs in ABC transporters and identifies NGO1152 as a promising, cross-species antigenic target.

By contrast, multiple alignment of NGO0206, NGO1152 and NMB1612 from *N. meningitidis* MC58 showed that NGO1152 and NMB1612 are near-identical sequences, sharing the N-terminal signal peptide (residues 1–50) with a canonical lipobox and full conservation of key motifs such as (RVASNAEFA, FESL, GNVEGFDVDLMN, and AMAKAGNFKIEFKHQPWD). In contrast, NGO0206 exhibited notable divergence and shared only partial sequence similarity with NGO1152 and NMB1612. The highest conservation was confined to the N-terminal region, where a conserved lipoprotein signal sequence suggests analogous subcellular targeting. Consistently, alignment of the N-terminal sequences showed that all three proteins share a signal motif beginning with MKK and extending to the lipobox consensus. Despite broader sequence variability, several short, conserved motifs (*e.g*. YAVPYF/FSDPYF and GFDVDL/GKSGYD) suggest preserved structural elements such as β-strands or loops. For instance, the motif ‘FSDPYF’ in NGO0206 aligns with ‘YAVPYF’ in NGO1152, sharing five of six chemically similar residues, while ‘GFDVDL’ in NGO1152 corresponds to the analogous but distinct ‘GKSGYD’ in NGO0206. Overall, these findings demonstrate the high conservation and widespread expression of NGO1152 and NGO0206, with NGO1152 showing

strong homology to its meningococcal orthologue, supporting their potential vaccine development.

The next chapter will examine the surface accessibility and localisation of NGO1152 and NGO0206 in *N. gonorrhoeae* strains using immuno-dot blot analysis. Subcellular localisation will be determined through cellular fractionation of WT-FA1090, mutant strains, and their uninduced/induced complemented mutant strains. Surface accessibility will be further assessed via WC-ELISAs, measuring the binding efficiency of anti-NGO1152 and anti-NGO0206 antibodies to gonococcal cell surfaces. This evaluation will extend to a panel of clinical isolates to confirm antibody recognition of conserved protein regions. Finally, the bactericidal activity mediated by these antibodies against gonococcal strains will be investigated to assess their potential as candidates for immunotherapy or vaccine development.

Chapter 5: Evaluation of surface accessibility and bactericidal activity of anti-NGO1152 and anti-NGO0206 against *N. gonorrhoeae*

5.1. Introduction

N. gonorrhoeae infection is currently managed through antibiotic therapy; however, the pathogen exhibits an exceptional capacity to develop resistance. Alarmingly, clinical isolates resistant to all classes of antibiotics used for gonorrhoea treatment have already been reported (Zhu *et al.*, 2025). In this context, vaccines represent the most promising and sustainable approach to counteract the rise of antimicrobial resistance. Among the potential vaccine targets are SBPs of ABC transporters, which are typically localised in the periplasmic space of *N. gonorrhoeae* (Rice *et al.*, 2014). Notably, although most SBPs are not exposed on the bacterial surface, several exceptions have been identified, where SBPs are surface exposed (Briles *et al.*, 2000; Otsuka *et al.*, 2016). These surface-localised SBPs may offer attractive targets for vaccine development, owing to their accessibility to host immune responses.

However, there are many uncharacterised proteins localised to the gonococcal cell envelope; some of these may have potential as novel therapeutic targets for *N. gonorrhoeae* (Huang *et al.*, 2020). In the context of *N. gonorrhoeae*, cell fractionation can be employed to isolate and analyse different components of the gonococcal cell envelope, including the outer membrane (OM), periplasmic proteins (PPs), cytoplasmic membrane, and cytoplasmic fractions. This approach aids in understanding the distribution and function of various proteins and lipids within the bacterial OM (Zielke *et al.*, 2014). Thus, these components play a critical role in establishing infections by enabling microbes to adhere to and invade host cells, mediate host tissue destruction, assist in acquiring nutrients, and cause immune response suppression (Chan *et al.*, 2012). Evaluating gonococcal vaccines remains difficult due to the lack of established correlates of protection for natural mucosal infections in humans (Rice *et al.*, 2017).

However, identifying proteins that can elicit antibodies with complement-dependent bactericidal and/or opsonic activity against gonococci is still one major goal for advancing progress in gonococcal vaccinology. The capacity of antigens to induce such functional antibodies is considered critical for protective immunity against gonococci infection and may serve as a surrogate marker for vaccine efficacy (Zhu *et al.*, 2025).

Potential protective mechanisms include antibody-dependent complement-mediated killing, such as bactericidal activity and opsonophagocytic activity, prevention by inhibition or blocking bacterial adhesion or invasion at colonisation sites, and T-cell responses. It is important to note that while these mechanisms are proposed, they have not all been fully confirmed in human studies or definitively demonstrated in experimental mouse models of gonococcal vaginal colonisation (Gottlieb and Johnston, 2017).

The SBA assay, widely used in meningococcal research, is increasingly applied as a surrogate of protection in pre-clinical gonorrhoea vaccine studies (Zhu *et al.*, 2019). As an established *in vitro* method, SBA provides a functional measure of vaccine-induced antibody efficacy (Girgis and Christodoulides, 2023; Semchenko *et al.*, 2022). The complement system is a key component of innate immunity and serves as one of the first lines of defence against Gram-negative pathogens. Beyond its direct bactericidal effects, complement activation promotes phagocytosis and triggers pro-inflammatory signalling. Complement activation occurs through three distinct pathways: alternative, classical, and lectin, which converge at the terminal pathway, leading to assembly of the C5b-9 complex, also known as Membrane Attack Complex (MAC) (Mutti *et al.*, 2018).

The alternative pathway (AP) is continuously activated on pathogen surfaces. In contrast, the classical pathway (CP) and lectin pathway (LP) are triggered by specific receptor-ligand interactions on target surfaces. The CP is initiated when antigen-antibody complexes (immune complexes, ICs) bind to C1, a complex comprising C1q, C1r, and C1s (Pryzdial *et al.*, 2022). The LP, on the other hand, is activated when lectins bind to specific sugar moieties on microbial surfaces, leading to the activation of Mannose-Binding Lectin-Associated Serine Proteases (MASPs) (Murphy and Weaver, 2016). Both CP and LP are tightly

regulated by the C1 inhibitor (C1-INH), which prevents spontaneous activation by sequestering and inhibiting C1r, C1s, and MASPs (Beinrohr *et al.*, 2008). In the absence of C1-INH, uncontrolled activation of C1 can occur. Activation of complement components results in the formation of C5 convertase, an enzyme that cleaves C5 into C5a and C5b. The C5b fragment binds to the target surface, where it sequentially recruits C6, C7, and C8, ultimately promoting the polymerisation of C9 monomers to form the MAC. This pore-forming complex integrates into lipid membranes, including the OM of Gram-negative bacteria, causing membrane disruption and cell lysis (Pryzdial *et al.*, 2022).

The complement pathways interact dynamically, forming an intricate regulatory network within the serum (Merle *et al.*, 2015). This complexity is further enhanced by the presence of additional serum bactericidal factors, which may either synergise with complement activity or function independently against invading pathogens (Merle *et al.*, 2015). As a result, dissecting the individual contributions of each pathway to serum bactericidal activity remains a challenge. This is particularly relevant for studies using human serum as a complement source, given the variability in pre-existing antibody repertoires and complement activity against human pathogens (McIntosh *et al.*, 2015).

One of the primary surface components of *N. gonorrhoeae* is LOS, whose length and composition are regulated by the *lgt* (LOS glycosyltransferase) genes. These genes undergo phase variation, leading to differences in the oligosaccharide structures within a population of gonococci, including during infection (John *et al.*, 2023). Gonococci isolated from uncomplicated urethral infections predominantly produce LOS that is capable of being sialylated. Sialylation refers to the addition of sialic acid to the terminal galactose of the LOS oligosaccharide chains, a process catalysed by the LOS sialyltransferase (Lst) (Ram *et al.*, 2017). Since *N. gonorrhoeae* cannot synthesise sialic acid, it scavenges cytidine-5′-monophosphate-N-acetylneuraminic acid (CMP-NANA) from the host. Lst is constitutively expressed (Lewis *et al.*, 2015) and is essential for efficient genital tract infection, utilising various forms of CMP-sialic acid (Gulati *et al.*, 2015).

This chapter aimed to investigate the surface accessibility and subcellular localisation of NGO1152 and NGO0206 proteins in *N. gonorrhoeae* strains using anti-NGO1152 and anti-NGO0206 antibodies. The underlying hypothesis was that NGO1152 and NGO0206 are surface exposed proteins whose localisation can be detected using specific antibodies and that they may serve as potential immune targets. To assess surface exposure, immuno-dot blot assays were initially employed on intact WT-FA1090, MR331152, and MR330206 strains under both uninduced and IPTG-induced conditions, with Δ*ngo1152* and Δ*ngo0206* mutants serving as negative controls. Subcellular localisation was determined by performing cell fractionation on WT-FA1090, Δ*ngo1152*, Δ*ngo0206*, and their complemented strains, followed by immunoblotting using the respective antibodies. To further quantify surface exposure, WC-ELISA was used to measure antibody binding to surface exposed antigens in WT-FA1090, MR331152, and MR330206 under both expression conditions. In addition, a panel of seven clinical *N. gonorrhoeae* isolates was included to evaluate whether these antibodies could recognise conserved surface exposed regions across diverse circulating strains. Finally, the potential functional relevance of these proteins was assessed by testing whether anti-NGO1152 and anti-NGO0206 antibodies could mediate human complement-dependent bactericidal activity against *N. gonorrhoeae* FA1090.

5.2. Results

5.2.1. Determine surface exposure of NGO1152 on the gonococcal cell surface

Surface exposure is essential for antibody accessibility and subsequent immune-mediated activity. An immuno-dot blot analysis was performed to assess the surface exposure of NGO1152 on *N. gonorrhoeae* and evaluate the binding specificity of anti-NGO1152 antibodies. Intact cells of WT-FA1090, Δ*ngo1152*, uninduced MR331152 and MR331152 induced with IPTG for 7 h were grown in BHI-V cultures and harvested once the OD_{600} reached ≈ 0.9. Intact gonococcal cell suspensions were spotted onto nitrocellulose membranes, dried at 37°C to fix the cells, and probed with anti-NGO1152 antibodies.

Preliminary immuno-dot blot analysis, as shown in Figure 5.1, revealed strong cross-reactivity of anti-NGO1152 antibodies with intact cells of WT-FA1090 and MR331152 that had been IPTG-induced for 7 h, suggesting significant surface exposure of NGO1152 on whole gonococcal cells. In contrast, minimal or undetectable signals were observed for the Δ*ngo1152* mutant and uninduced MR331152 strains, reflecting the absence of NGO1152 due to gene deletion or the absence of IPTG induction.

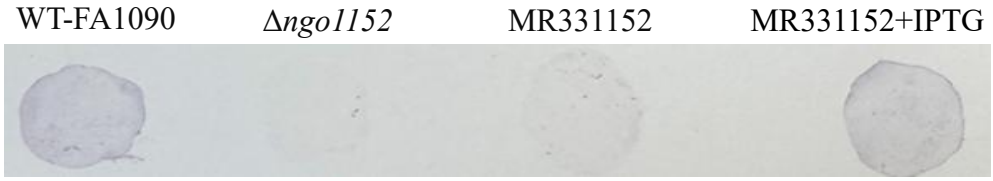

Figure 5.1. Immuno-dot blot confirming surface exposure and accessibility of NGO1152 to anti-NGO1152 antibodies on intact *N. gonorrhoeae* cells.
The immuno-dot blot image demonstrates strong cross-reactivity of anti-NGO1152 antibodies with intact cells of WT-FA1090, confirming surface exposure of NGO1152. In contrast, the Δ*ngo1152* strain exhibited faint cross-reactivity, consistent with the absence of NGO1152. The uninduced MR331152 strain displayed weak cross-reactivity, consistent with the absence of IPTG induction. After 7 h of IPTG induction, the MR331152 strain showed strong dot-blot signals indicating robust MR331152 expression.

5.2.2. Evaluate surface exposure of NGO0206 on the gonococcal cell surface

Likewise, to evaluate the surface exposure and accessibility of NGO0206 to anti-NGO0206 on intact gonococcal cells, an immuno-dot blot analysis was performed. Intact cells from WT-FA1090, Δ*ngo0206*, uninduced MR330206, and IPTG-induced MR330206 were harvested, spotted onto nitrocellulose membranes, and subsequently probed with anti-NGO0206 antibodies.

The immuno-dot blot analysis revealed significant reactivity of anti-NGO0206 antibodies with the surface of WT-FA1090 and induced MR330206 strains, indicating strong surface exposure of NGO0206. In contrast, minimal or undetectable signals were observed in the Δ*ngo0206* mutant and uninduced MR330206 strains, reflecting the absence of surface exposed NGO0206 due to gene deletion or low basal expression in the absence of IPTG induction, as shown in Figure 5.2. Remarkably, the increased cross-reactivity in the IPTG-induced MR330206 strain compared to WT-FA1090 highlights the successful upregulation of NGO0206 expression under IPTG induction, resulting in a high surface expression of the protein.

Figure 5.2. Immuno-dot blot confirming surface exposure and accessibility of NGO0206 to anti-NGO0206 antibodies on intact *N. gonorrhoeae* cells.
The immuno-dot blot image shows strong cross-reactivity of anti-NGO0206 antibodies with intact WT-FA1090 cells, confirming significant surface exposure of NGO0206. In contrast, the Δ*ngo0206* mutant and uninduced MR330206 complemented mutant strains exhibited weak or undetectable signals of NGO0206 expression. After 7 h of IPTG induction, the MR330206 strain showed strong dot-blot signals indicating robust NGO0206 expression.

5.2.3. Subcellular localisation of NGO1152 in *N. gonorrhoeae* FA1090

To examine the subcellular localisation of NGO1152, cells from WT-FA1090, Δ*ngo1152*, and MR331152 (both uninduced and induced with IPTG for 4 h or 7 h) were harvested during the mid-exponential phase. The cells were subjected to subcellular fractionation to isolate various proteome fractions, including OM-enriched and PP-enriched fractions (Dhital *et al.*, 2022), CM-enriched and C-enriched fractions (Nossal and Heppel, 1966). Gonococcal proteome fractions, along with whole-cell lysate samples derived from the same strains, were separated on 10% SDS-PAGE gels by electrophoresis.

Subsequently, SDS-PAGE gels were stained with Coomassie Brilliant Blue to visualise protein profiles. Consistent protein loading was observed across all extracted cell fractions and whole-cell lysates, as shown in Figures 5.3A, B, C and D. The consistent protein loading across all fractions ensured the reliability of subsequent comparisons of reactive band intensities in the immunoblotting analysis, as presented in Figure 5.4.

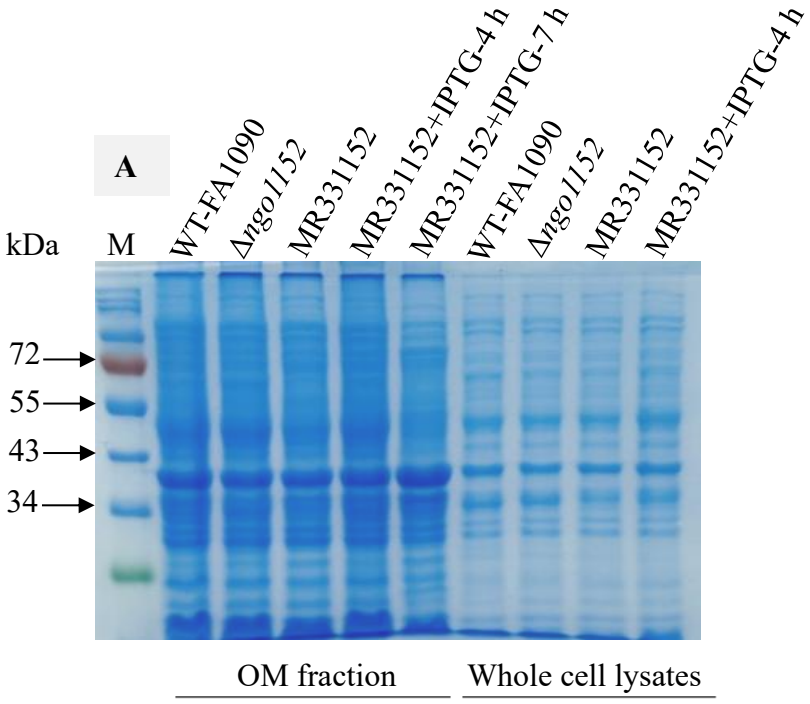

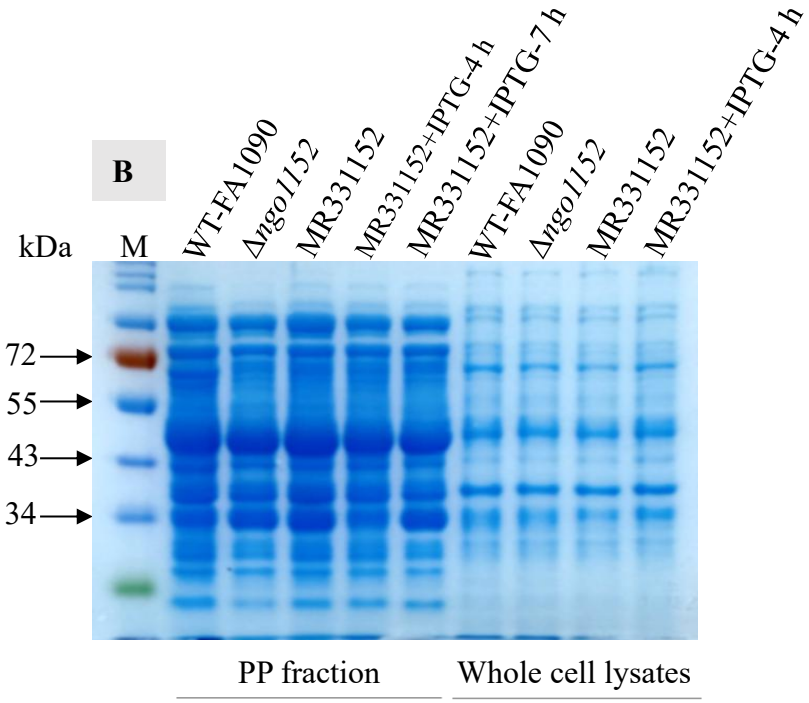
B
kDa
M
WT-FA1090
Δngo1152
MR331152
MR331152+IPTG-4 h
MR331152+IPTG-7 h
WT-FA1090
Δngo1152
MR331152
MR331152+IPTG-4 h
72
55
43
34
PP fraction
Whole cell lysates

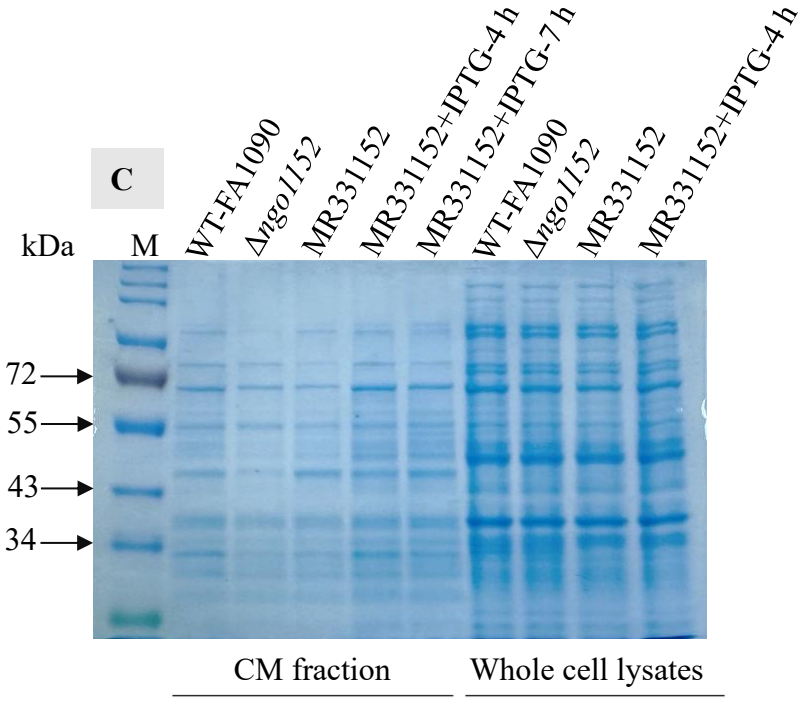
C
kDa
M
WT-FA1090
Δngo1152
MR331152
MR331152+IPTG-4 h
MR331152+IPTG-7 h
WT-FA1090
Δngo1152
MR331152
MR331152+IPTG-4 h
72
55
43
34
CM fraction
Whole cell lysates

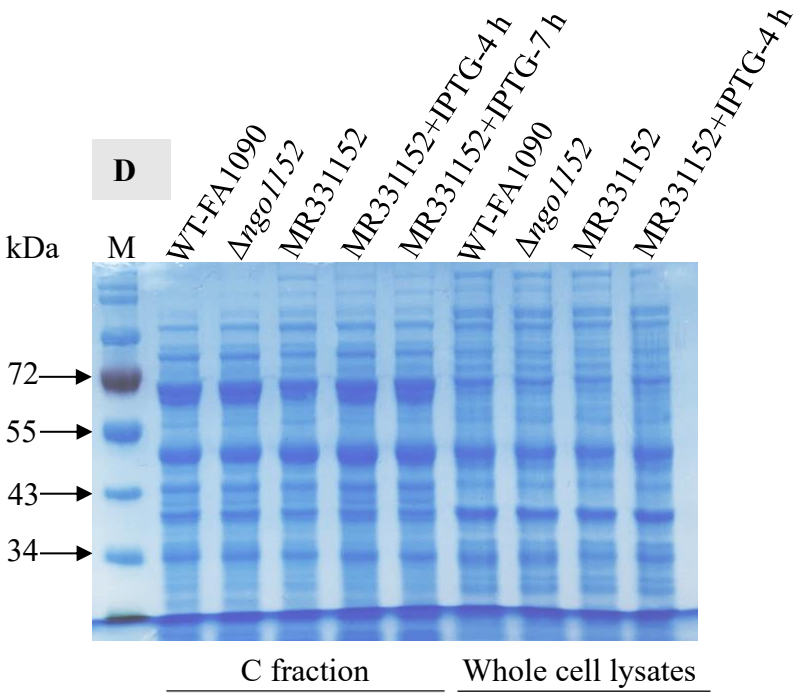

Figure 5.3. Analysis of protein profiles of subcellular fractions from gonococcal cells separated by 10% SDS-PAGE and stained with Coomassie Brilliant Blue to determine the localisation of NGO1152 (A to D).
Gonococcal strains, harvested during the mid-exponential phase, were subjected to proteome extraction to isolate the OM, PP, CM, and C fractions. Subcellular fractions from *N. gonorrhoeae*, as well as whole-cell lysates, were resolved using 10% SDS-PAGE and stained with Coomassie brilliant blue to visualise the protein profiles. The stained gels demonstrated consistent and equal protein loading across all subcellular fractions. Panels correspond to the following: (A) OM fraction, (B) PP fraction, (C) C, and (D) CM fraction. Each lane within the respective fractions corresponds to the following strains: WT-FA1090, Δ*ngo1152*, and MR331152 under both non-induced and IPTG-induced conditions (4 and 7 h). Additionally, whole cell lysates from WT-FA1090, Δ*ngo1152*, and MR331152 uninduced and induced for 4 h are included for comparison. Lanes M in all panels: 10-250 kDa protein marker.

To identify the localisation of NGO1152, immunoblotting analysis was conducted on the prepared subcellular fractions (OM, PP, CM, and C). Whole cell lysates were included as positive controls for comparison. These fractions were resolved on SDS-PAGE gels and subsequently probed with anti-NGO1152 rabbit polyclonal antibodies at a 1:100,000 dilution. As result, immunoblotting analysis of subcellular fractions revealed a single band *ca.* 30 kDa, corresponding to NGO1152, in the enriched OM, C, and CM fractions of both WT-FA1090 and IPTG-induced MR331152 at 4 and 7 h, as well as in whole cell lysates from these strains as shown in Figures 5.4A, B, C and D. The intensity of this band increased at 7 h post-IPTG induction in the enriched C and CM fractions, suggesting enhanced expression of NGO1152. In accordance with expectations, no corresponding band was observed in the Δ*ngo1152* or non-induced MR331152 strains. However, contrary to the hypothesis, the NGO1152 band was absent in the PP-enriched fractions in Figure 5.4B, challenging the assumption that the protein is localised to this compartment. This analysis confirmed that NGO1152 is a CM protein that can also be found localised to the OM of gonococci.

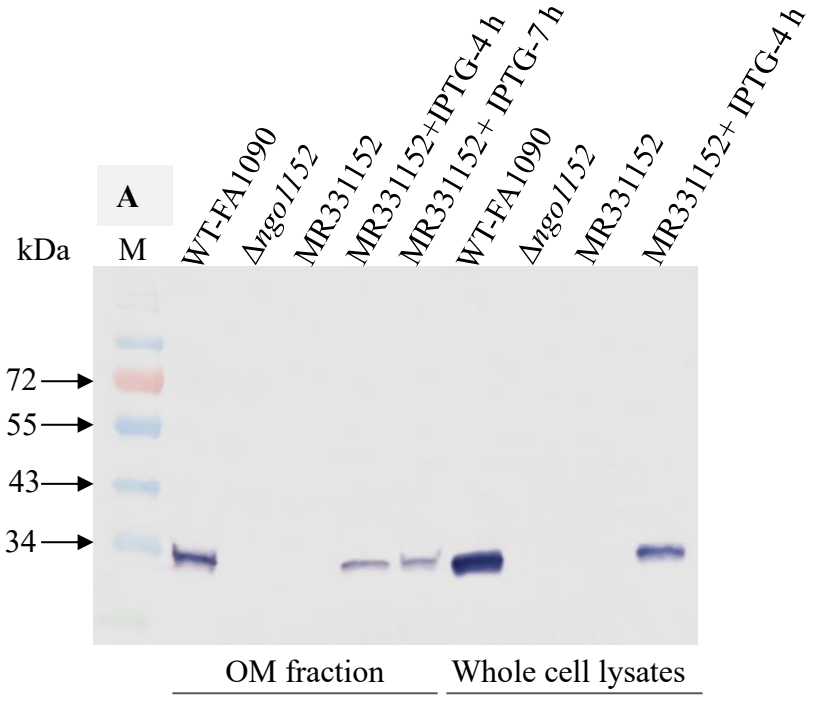

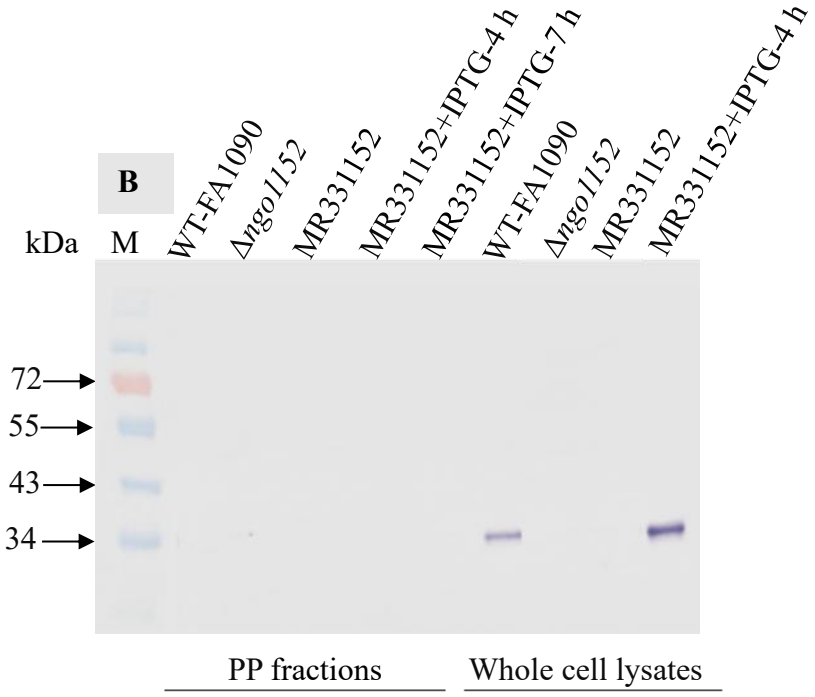
B
kDa
M
WT-FA1090
Δngo1152
MR331152
MR331152+IPTG-4 h
MR331152+IPTG-7 h
WT-FA1090
Δngo1152
MR331152
MR331152+IPTG-4 h
72
55
43
34
PP fractions
Whole cell lysates

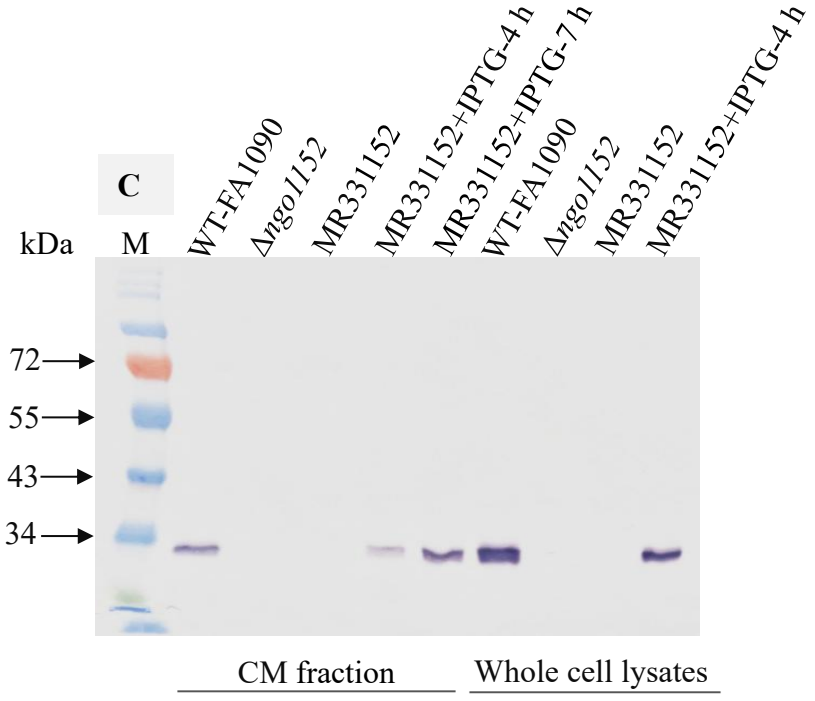
C
kDa
M
WT-FA1090
Δngo1152
MR331152
MR331152+IPTG-4 h
MR331152+IPTG-7 h
WT-FA1090
Δngo1152
MR331152
MR331152+IPTG-4 h
72
55
43
34
CM fraction
Whole cell lysates

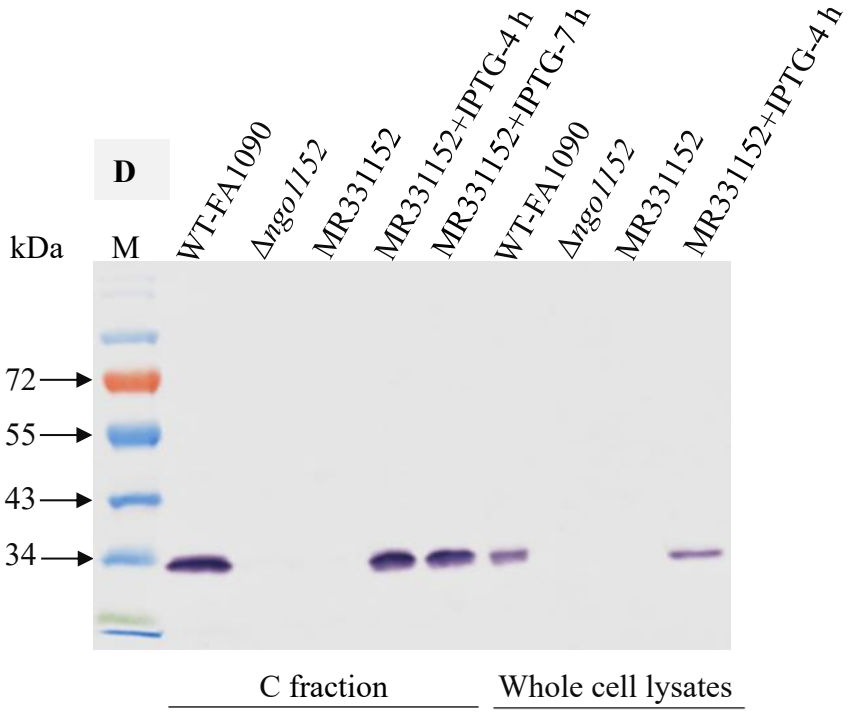

Figure 5.4. Determine Subcellular localisation of NGO1152 in gonococcal cell fractions evaluated by immunoblotting using anti-NGO1152 antibodies (A–D).

Gonococcal strains were subjected to proteome extraction to separate the OM, PP, CM, and C fractions. These fractions were resolved by SDS-PAGE and probed with anti-NGO1152 antibodies at a 1:100,000 dilution. Protein profiles of the following subcellular fractions are shown: (A) OM, (B) PP, (C) CM, and (D) C fractions. Each lane in the respective fractions corresponds to the following strains: WT-FA1090, Δ*ngo1152*, MR331152 uninduced, and MR331152 induced for 4 or 7 h. Additionally, whole cell lysates from WT-FA1090, Δ*ngo1152*, and MR331152 (uninduced and induced for 4 h) were included as positive controls. Lanes (M) in all panels contain a 10-250 kDa protein marker. The immunoblotting analysis revealed an immunodominant band at *ca.* 30 kDa, corresponding to NGO1152 in all lanes of the following samples: (A) OM, (C) CM, and (D) C for WT-FA1090, MR331152 induced for 4 and 7 h, as well as whole cell lysates of WT-FA1090 and the induced MR331152 strain. No band was observed in any of the Δ*ngo1152* and uninduced MR331152 samples. Additionally, no band was detected in the (B) PP fractions from any of the strains.

5.2.4. Subcellular localisation of NGO0206 in *N. gonorrhoeae* FA1090

Likewise, to examine the subcellular localisation of the NGO0206 in WT-FA1090, Δ*ngo0206,* and MR330206 (non-induced or induced with IPTG at 4 and 7 h) were harvested during the mid-exponential phase and subjected to sub-fractionation. Equal amounts of each cell fraction (OM, PP, CM, and C-enriched), as well as whole cell lysates from the respective strains (with MR330206 induced for 4 h), were separated by 10% SDS-PAGE. The gels were subsequently stained with Coomassie Brilliant Blue, as shown in Figure 5.5 or subjected to immunoblotting using anti-NGO0206 rabbit polyclonal antibodies, as illustrated in Figure 5.6. As a result, all the stained gels displayed consistent protein loading profiles across all extracted cell fractions and whole-cell lysates Figures 5.5A, B, C, and D.

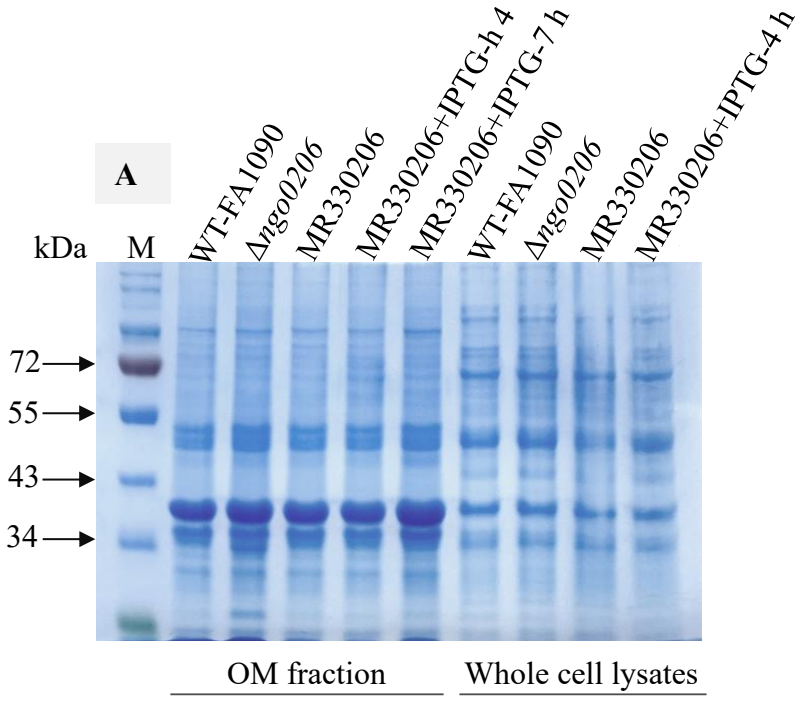

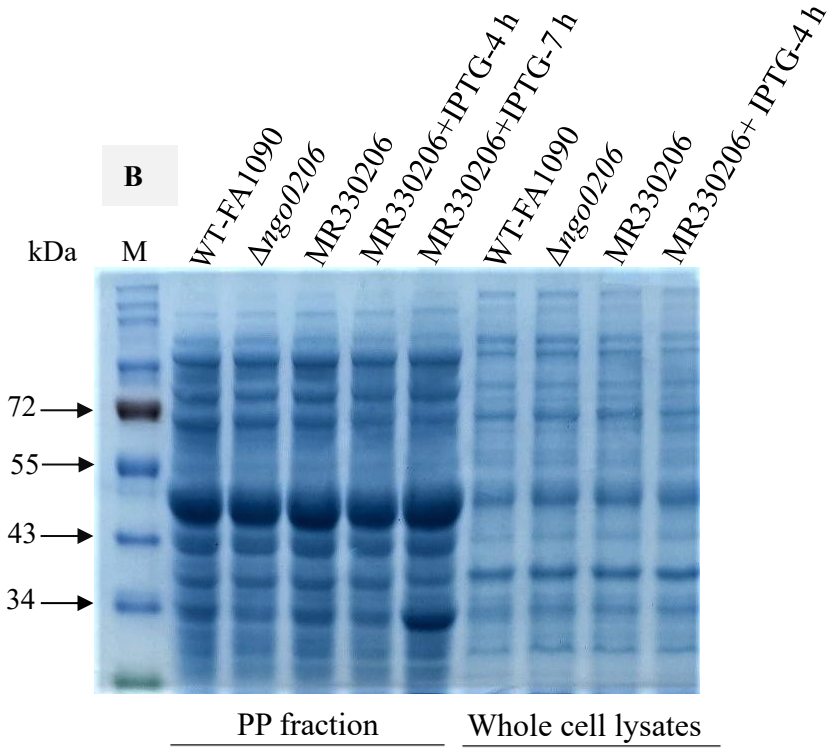
B
kDa
M
WT-FA1090
Δngo0206
MR330206
MR330206+IPTG-4 h
MR330206+IPTG-7 h
WT-FA1090
Δngo0206
MR330206
MR330206+ IPTG-4 h
72
55
43
34
PP fraction
Whole cell lysates

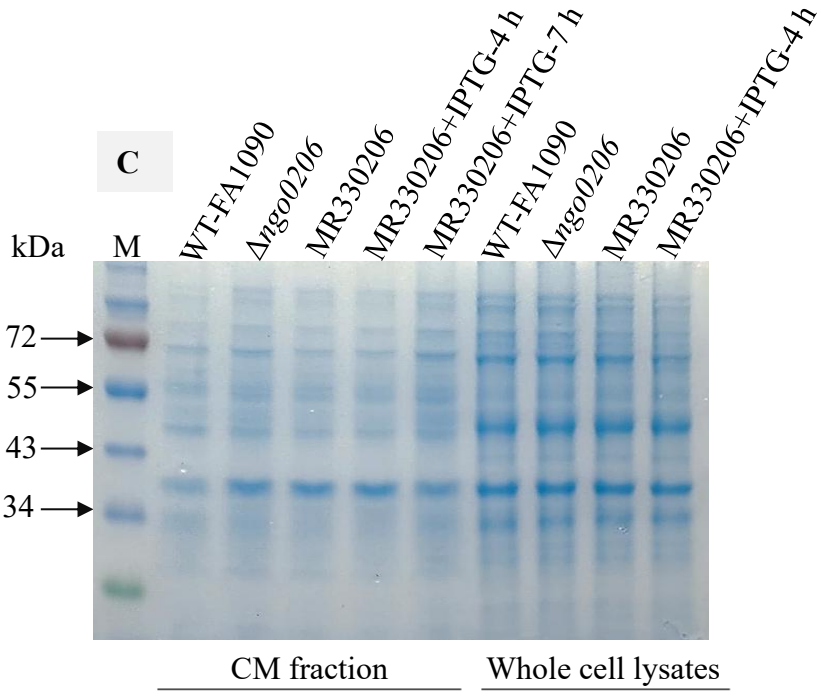
C
kDa
M
WT-FA1090
Δngo0206
MR330206
MR330206+IPTG-4 h
MR330206+IPTG-7 h
WT-FA1090
Δngo0206
MR330206
MR330206+IPTG-4 h
72
55
43
34
CM fraction
Whole cell lysates

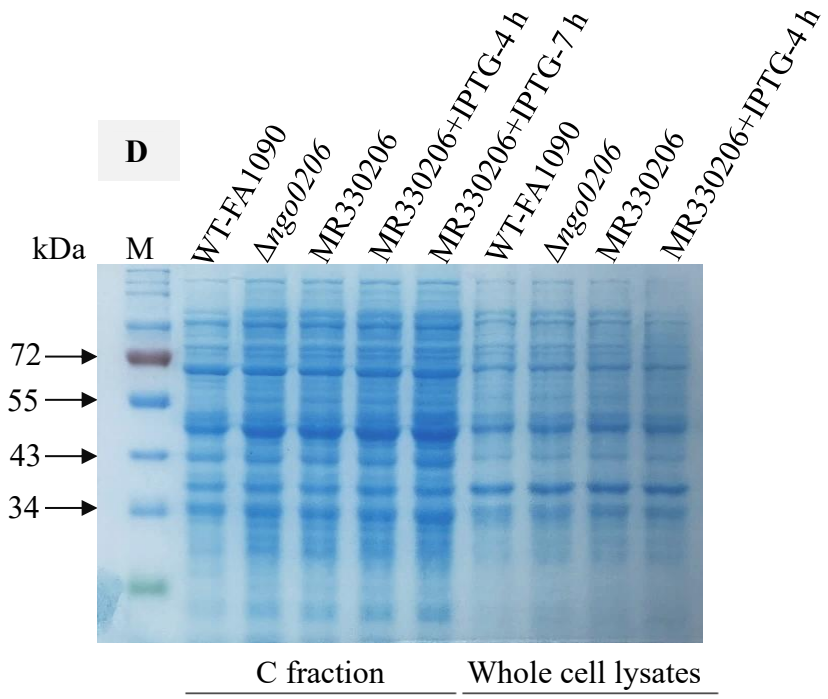

Figure 5.5. Evaluate protein profiles of subcellular fractions from gonococcal cells separated by 10% SDS-PAGE and stained with Coomassie brilliant blue to determine the localisation of NGO0206 (A to D).
Protein profiles of the following subcellular fractions are shown: (A) OM, (B) PP, (C) CM, and (D) C. Each lane in the corresponding cell fractions represents the following strains: WT-FA1090, Δ*ngo0206*, MR330206 (non-induced), and MR330206 induced for 4 and 7 h. Additionally, whole cell lysates of WT-FA1090, Δ*ngo0206*, and MR330206 (uninduced and induced for 4 h) were used as positive controls. All stained gels displayed equal protein loading profiles across all cell fractions. Lanes (M) in all panels contain a 10-250 kDa protein marker.

Similarly, immunoblotting of subcellular fractions detected a single ~46 kDa band corresponding to NGO0206. This band was present in the enriched OM, C, and CM fractions of both WT-FA1090 and IPTG-induced MR330206 at 4 and 7 h, and in whole-cell lysates from these strains (Figures 5.6A, B, C and D). As anticipated, this band was absent in the Δ*ngo0206* mutant and the non-induced MR330206 complemented mutant strains across all tested samples. However, contrary to expectations, no immunoreactive bands were detected in the PP-enriched fractions across any of the strains, as shown in Figure 5.6B. This analysis established that NGO0206 is predominantly a CM protein, with additional localisation observed at the OM of gonococci.

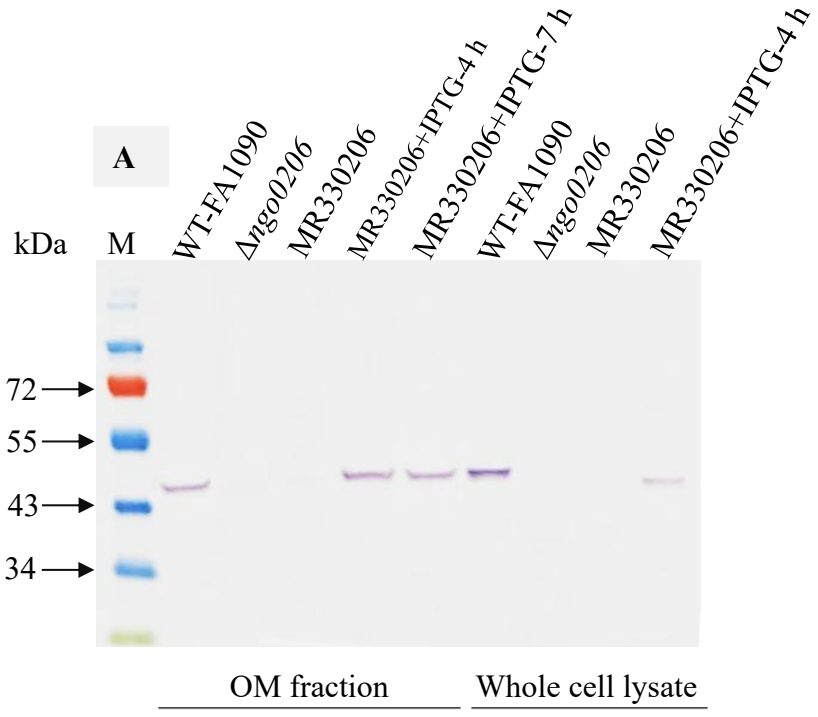

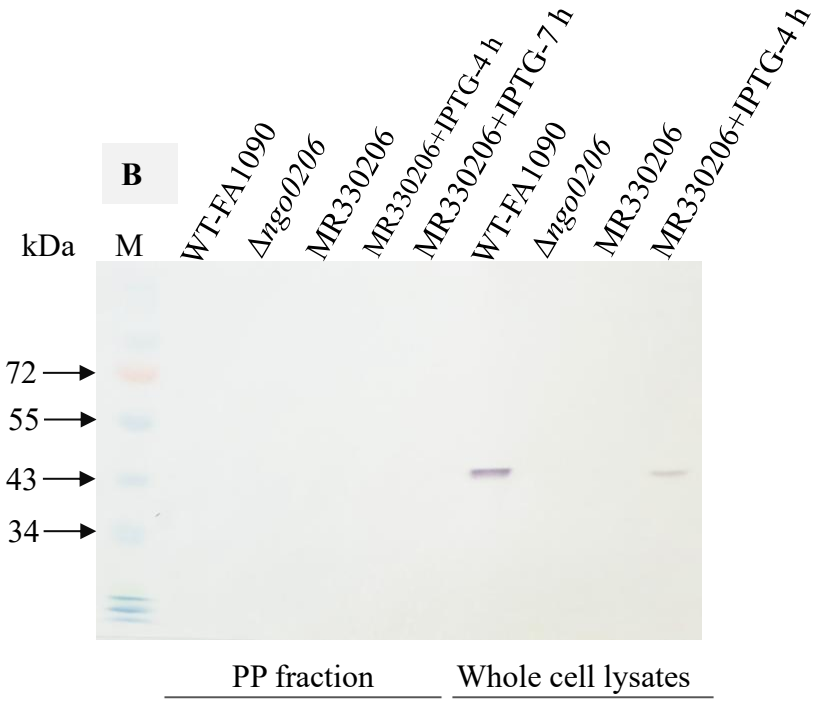
B
kDa
M
WT-FA1090
Δngo0206
MR330206
MR330206+IPTG-4 h
MR330206+IPTG-7 h
WT-FA1090
Δngo0206
MR330206
MR330206+IPTG-4 h
72
55
43
34
PP fraction
Whole cell lysates

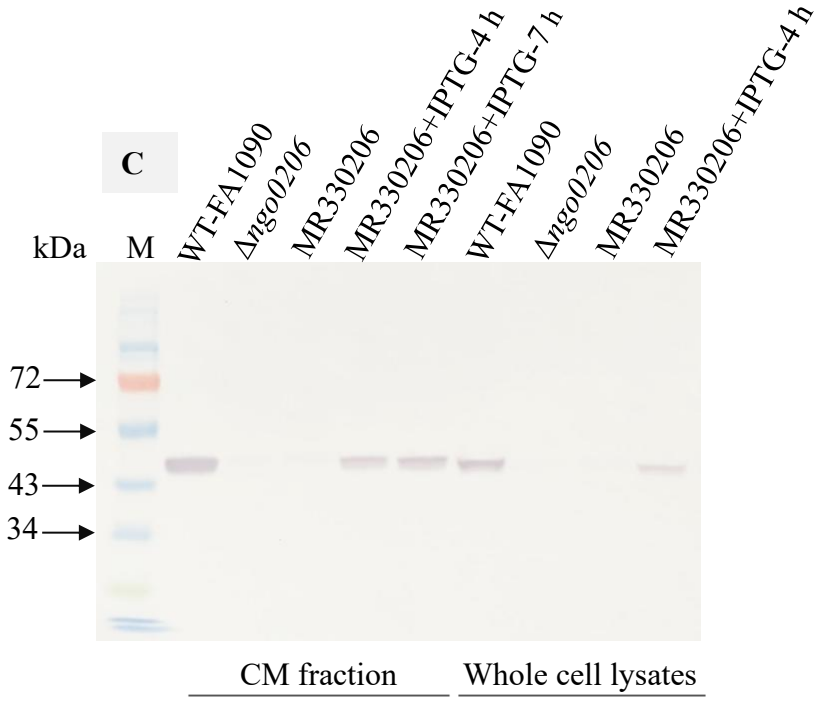
C
kDa
M
WT-FA1090
Δngo0206
MR330206
MR330206+IPTG-4 h
MR330206+IPTG-7 h
WT-FA1090
Δngo0206
MR330206
MR330206+IPTG-4 h
72
55
43
34
CM fraction
Whole cell lysates

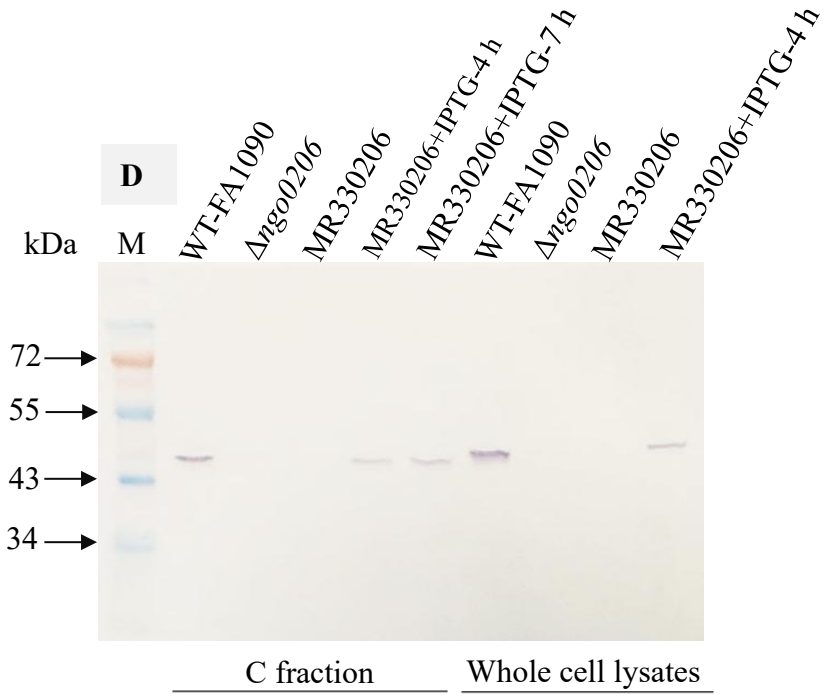

Figure 5.6. Subcellular localisation of NGO0206 in gonococcal cell fractions evaluated by immunoblotting using anti-NGO0206 antibodies (A–D).
Bacterial strains harvested during the mid-exponential phase were subjected to proteome extraction to separate the OM, PP, CM, and C fractions and resolved by SDS-PAGE and probed with anti-NGO0206 antibodies at a 1:100,000 dilution. Protein profiles of the following subcellular fractions are shown: (A) OM, (B) PP, (C) CM, and (D) C fractions. Each lane in the respective fractions corresponds to the following strains: WT-FA1090, Δ*ngo0206*, MR330206 uninduced, and MR330206 induced for 4 and 7 h. Whole cell lysates from WT-FA1090, Δng*o0206*, and MR330206 (uninduced and induced for 4 h) were included as positive controls. Lanes (M) in all panels contain a 10-250 kDa protein marker. The analysis revealed that the anti-NGO0206 antibodies detected a prominent immunodominant band at *ca.* 46 kDa, corresponding to the NGO0206 protein. This band was present in all lanes of the following samples: (A) OM, (C) CM, and (D) C fractions for WT-FA1090, MR330206 induced for 4 and 7 h, as well as whole cell lysates of WT-FA1090 and induced MR330206. No band was observed in the Δ*ngo0206* and uninduced MR330206 (*lacPOPO*) samples. Additionally, no band was detected in the (B) PP fraction.

5.2.5. NGO1152 is a surface exposed protein in *N. gonorrhoeae* FA1090

NGO1152 from *N. gonorrhoeae* FA1090 is bioinformatically predicted to function as an SBP component of an ABC transporter, typically localised to the periplasm. However, previous immunoblotting of subcellular fractions revealed that while NGO1152 is primarily associated with the CM, a smaller portion is present in the OM (Figure 5.4). Additionally, immuno-dot blot analysis (Figure 5.1) suggested that some epitopes of NGO1152 are accessible on the surface of intact gonococcal cells.

To further investigate and quantify this potential surface exposure, a direct WC-ELISA was performed to evaluate whether anti-NGO1152 antibodies could bind to intact cells. Sterile 96-well microtiter plates were coated with intact bacterial cell pellets from WT-FA1090, Δ*ngo1152*, and MR331152 (either non-induced or induced with IPTG for 4 h) at an OD_{600} of ≈ 0.3 in carbonate buffer and probed with anti-NGO1152 antibodies. Additionally, non-coated wells were utilised as negative controls, and wells coated with intact cells of WT-FA1090 were probed with rabbit anti-whole meningococcal PorA (cross-reacts with gonococcal PorB), which served as positive controls (Figure 5.7). PorA is a surface exposed protein found in *N. meningitidis* and is one of its major OMPs. In this context, PorA was utilised as a positive control in this study because of the unavailability of antibodies against specific *N. gonorrhoeae* OMP markers in our laboratory. Its prominence as a well-characterised OMP makes it a reliable reference in experiments where analogous markers for *N. gonorrhoeae* are not available (Zhu *et al.*, 2023).

The WC-ELISA results showed that rabbit anti-NGO1152 antibodies bound to WT-FA1090 and the induced MR331152 strain. In contrast, significantly less binding was observed with the Δ*ngo1152* mutant and the non-induced MR331152 strain. The residual binding to the mutant and non-induced complemented strain indicates background non-specific binding. Overall, these results confirm that anti-NGO1152 is bound to the surface of intact gonococcal cells, providing additional evidence for the surface exposure of some NGO1152 epitopes at the gonococcal cell surface under the tested conditions.

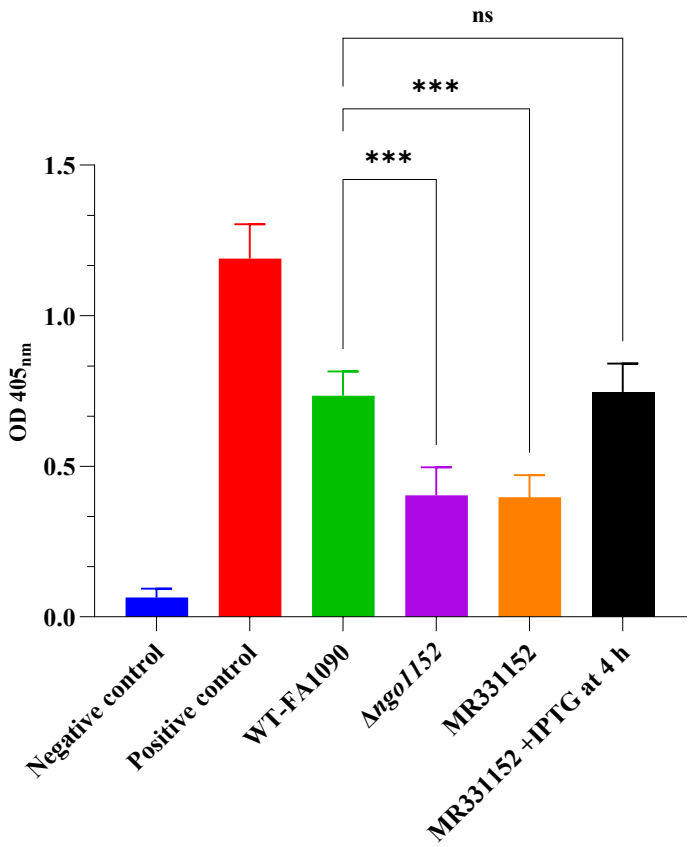

Figure 5.7. WC-ELISA using rabbit polyclonal anti-NGO1152 antibodies further confirms the surface exposure of NGO1152 in *N. gonorrhoeae* FA1090.

The 96-well plates were coated with WT-FA1090, Δ*ngo1152* and MR331152 (non-induced or induced with IPTG for 4 h) and probed with anti-NGO1152 primary antibody followed by goat anti-rabbit IgG–alkaline phosphatase conjugate secondary antibody. Colour development was achieved by adding a phosphatase substrate. The following controls were utilised: Negative control, which consists of non-coated wells used to detect any background signal. Positive Control: WT-FA1090 coated wells were probed with anti-whole meningococcal PorA antibody, which served as an OM control. This antibody cross-reacts with PorB from *N. gonorrhoeae* due to structural and epitope similarities between PorA and PorB. The graph shows the mean absorbance OD at 405 nm from four independent experiments (each experiment done in quadruplicate wells). Error bars indicate the mean ± standard deviation of a sample tested in quadruplicate. The *P*-value was calculated from the four means using two-way ANOVA tests to compare OD_{600} values from the WT-FA1090 to each of the other strains. *P*-value summary: A *p*-value of >0.05 was considered non-significant (ns), and *** indicates $P<0.001$ (two-way ANOVA). Asterisks represent statistically significant differences.

5.2.6. NGO0206 is a surface exposed protein in *N. gonorrhoeae* FA1090

Likewise, FA1090-NGO0206 was proposed to be the SBP component of a gonococcal ABC transporter and bioinformatically predicted to be localised to the periplasmic space.

Nevertheless, prior cell fractionation experiments suggested this protein was found predominantly in the CM rather than in the PP space, with some also evident in the OM fraction. Likewise, the initial immuno-dot blot experiments suggested that some epitopes of NGO0206 are accessible on the surface of intact gonococcal cells.

To expand on this, the potential surface exposure of NGO0206 was further explored using the same WC-ELISA approach that was utilised previously for NGO1152. Sterile 96-well microtiter plates were coated with intact bacterial cell pellets from WT-FA1090, Δ*ngo0206* and MR330206 (non-induced or IPTG induced for 4 h) and probed with anti-NGO0206. Non-coated wells were utilised as negative controls, and wells coated with intact cells of WT-FA1090 and subsequently treated with rabbit anti-whole meningococcal PorA as a positive control (Figure 5.8).

The findings demonstrated that rabbit anti-NGO0206 bound to WT-FA1090 and the IPTG-induced complemented strain MR330206, with statistically significantly lower binding to the Δ*ngo0206* mutant and the non-induced MR330206 complemented strain. The residual binding observed in the mutant and non-induced complemented strain suggests background non-specific binding. Collectively, these findings demonstrate that anti-NGO0206 antibodies bind to the surface of intact gonococcal cells, providing additional evidence for the surface exposure of some NGO0206 epitopes at the gonococcal cell surface.

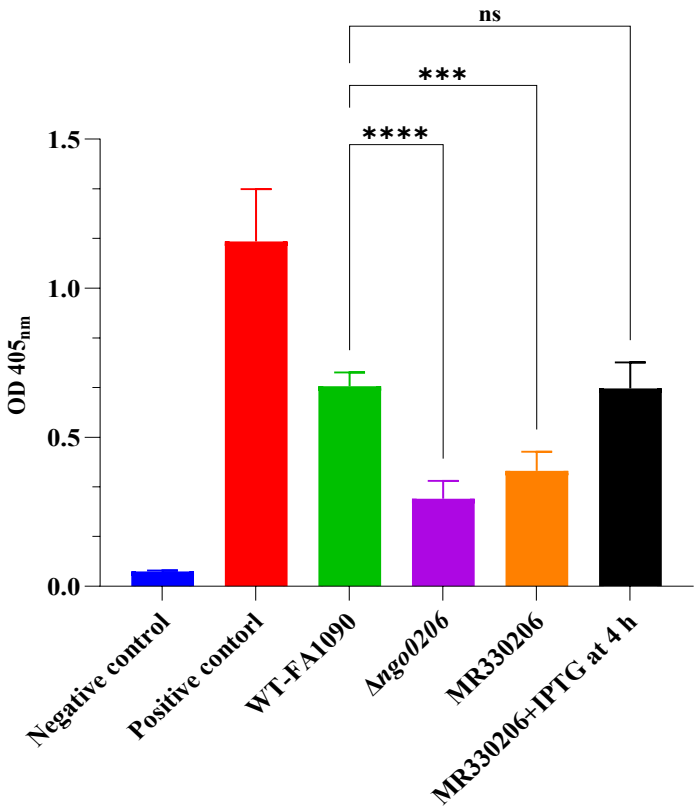

Figure 5.8. WC-ELISA using rabbit polyclonal anti-NGO0206 antibodies further confirms the surface exposure of NGO0206 in *N. gonorrhoeae* FA1090.

Sterile 96-well plates were coated with WT-FA1090, Δ*ngo0206* and MR330206 (non-induced or induced with IPTG for 4 h) and probed with anti-NGO0206 primary antibody followed by goat anti-rabbit IgG–alkaline phosphatase conjugate secondary antibody. Colour development was achieved by adding a phosphatase substrate. The following controls were utilised: positive control: wells coated with intact WT-FA1090 cells were probed with anti-whole meningococcal PorA antibody. This antibody cross-reacts with PorB from *N. gonorrhoeae* due to structural and epitope similarities between PorA and PorB. The graph illustrates the mean absorbance at OD_{405} nm from four independent experiments (each experiment done in quadruplicate wells). Error bars indicate the mean ± standard deviation of a sample tested in quadruplicate. The *P*-value was calculated from the four means using unpaired t-tests to compare OD values from the WT-FA1090 to each of the other strains. *P*-value summary: A *p*-value of >0.05 was considered non-significant (ns), *** indicates $P<0.001$, and **** indicates $P<0.0001$ (two-way ANOVA). Asterisks represent statistically significant differences.

5.2.7. NGO1152 is surface exposed in *N. gonorrhoeae* clinical isolates

Previously, the presence of the *ngo1152* gene was confirmed across a broad range of gonococcal genome sequences. Furthermore, immunoblotting of whole-cell lysates confirmed the expression of NGO1152 in a smaller subset of recent clinical isolates, as detailed in Chapter 4.

Subsequent confirming surface exposure of NGO01152 in *N. gonorrhoea*e FA1090 strains in Figure 5.7. The surface exposure of NGO1152 was investigated using WC-ELISA on a panel of strains, including MS-11, DGI-18, 17N0001, 17N0002, 17N0003, 17N0004, and 17N0005, with WT-FA1090 and Δ*ngo1152* serving as positive and negative controls, respectively (Figure 5.9). The analysis confirmed all the clinical isolates had statistically significant increases in surface exposure reactivity compared to the Δ*ngo1152* strain, indicating that NGO1152 was surface expressed in all clinical isolates.

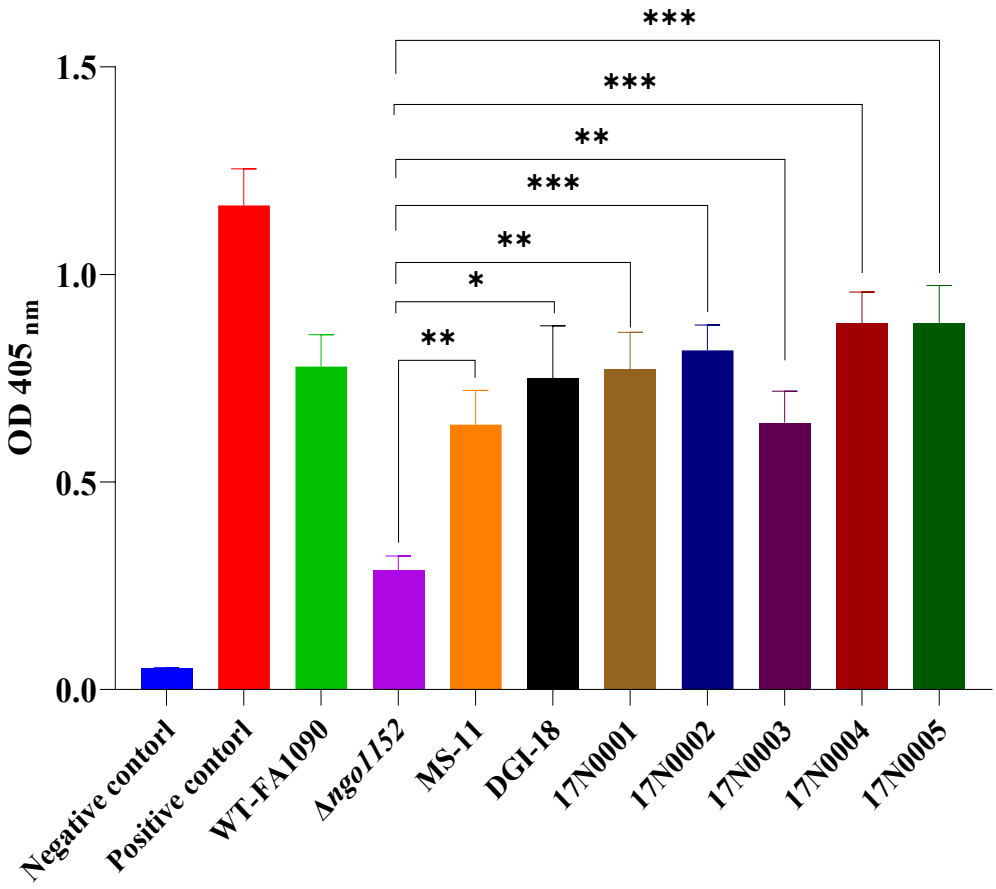

Figure 5.9. WC-ELISA using anti-NGO1152 antibodies demonstrates surface exposure of NGO1152 across a panel of *N. gonorrhoeae* clinical isolates.
Sterile 96-well plates were coated with WT-FA1090, Δ*ngo1152*, MS-11, DGI-18, 17N0001, 17N0002, 17N0003, 17N0004 and 17N0005 and probed with anti-NGO1152 primary antibody followed by goat anti-rabbit IgG–alkaline phosphatase conjugate secondary antibody. Colour development was achieved by adding a phosphatase substrate. The results for the negative control (non-coated wells) are also shown. The positive control contained WT-FA1090 probed with anti-whole meningococcal PorA-antibody. The graph shows the mean absorbance at OD_{405} nm from four independent experiments (each experiment done in quadruplicate wells). Error bars indicate standard deviation. The *P*-value was calculated by two-way ANOVA to compare Δ*ngo1152* versus MS-11, DGI-18, 17N0001, 17N0002, 17N0003, 17N0004 and 17N0005. *P* value summary: * indicates $P<0.05$, ** indicates $P<0.01$ and *** indicates $P<0.001$ (two-way ANOVA). Asterisks represent statistically significant differences.

5.2.8. NGO0206 surface exposure in *N. gonorrhoeae* clinical isolates

Likewise, previous analysis confirmed the presence of the *ngo0206* gene in a large panel of gonococcal genome sequences, and immunoblots of whole cell lysates confirmed the expression of NGO0206 in a smaller collection of recent clinical isolates, as described in Chapter 4. After confirming the surface exposure of NGO0206 cross *N. gonorrhoea* strains by WC-ELISA in Figure 5.8. Here, a panel of strains, including MS-11, DGI-18, 17N0001, 17N0002, 17N0003, 17N0004 and 17N0005 strains, were used to examine the surface exposure of NGO0206 using WC-ELISA. Additionally, WT-FA1090 and Δ*ngo0206* strains were used as positive and negative controls, respectively. The WC-ELISA analysis demonstrated significantly increased reactivity in all clinical isolates compared to the Δ*ngo0206* strain, suggesting consistent surface expression of NGO0206 across these isolates, as shown in Figure 5.10.

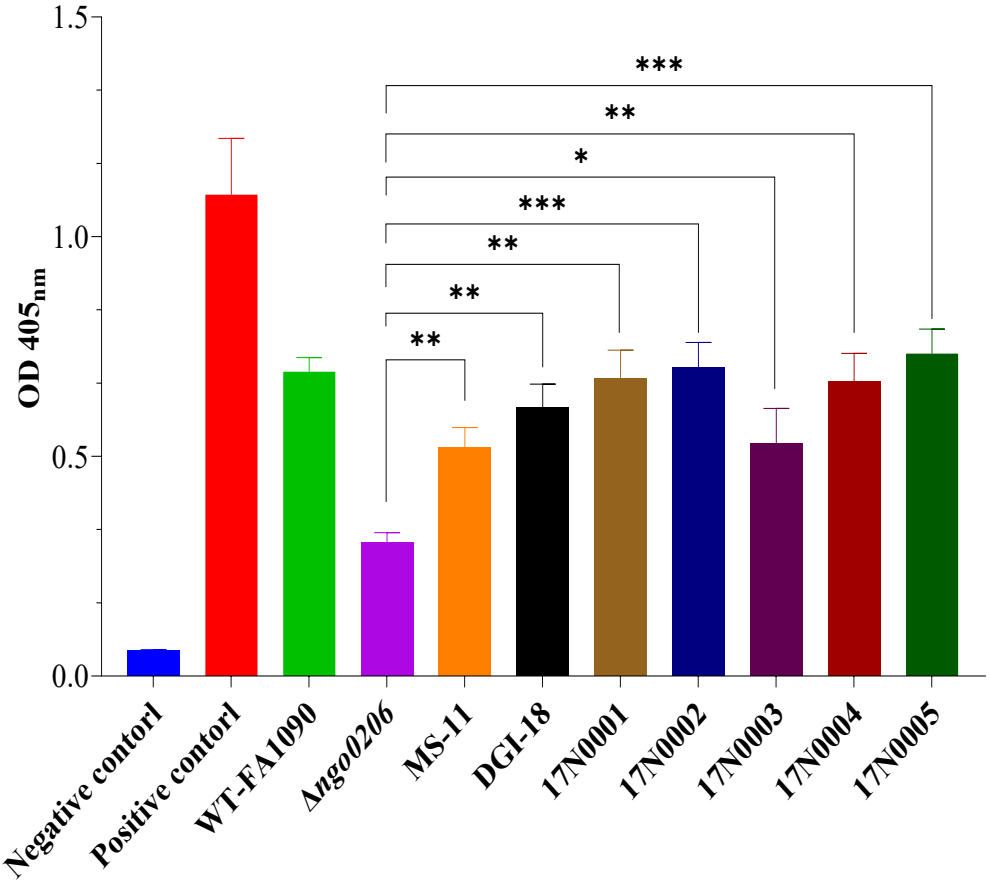

Figure 5.10. WC-ELISA using anti-NGO0206 antibodies demonstrates surface exposure of NGO0206 across a panel of *N. gonorrhoeae* clinical isolates.

Sterile 96-well plates were coated with WT-FA1090, Δ*ngo0206*, MS-11, DGI-18, 17N0001, 17N0002, 17N0003, 17N0004 and 17N0005 and probed with anti-NGO0206 primary antibody followed by goat anti-rabbit IgG–alkaline phosphatase conjugate secondary antibody. The results for the negative control (non-coated wells) are also shown. The positive control contained WT-FA1090 probed with anti-whole meningococcal PorA-antibody. The graph shows the mean absorbance at OD_{405} nm from four independent experiments (each experiment done in quadruplicate wells). Error bars indicate the mean ± standard deviation of a sample tested in quadruplicate. The *P*-value was calculated by unpaired t-tests to compare Δ*ngo0206* versus MS-11, DGI-18, 17N0001, 17N0002, 17N0003, 17N0004 and 17N0005. *P*-values greater than 0.05 were considered not statistically significant. *P* value summary: * indicates $P<0.05$, ** indicates $P<0.01$; *** indicates $P<0.001$ (two-way ANOVA). Asterisks represent statistically significant differences.

5.2.9. Bactericidal activity of the anti-NGO0206 polyclonal antibodies

To evaluate whether anti-NGO0206 antibodies mediate human complement-dependent killing of WT-FA1090 and show minimal activity against Δ*ngo0206* mutants, the SBA was performed. To better mimic *in vivo N. gonorrhoeae* infection, IgG/IgM-depleted human complement (HC; Pel-Freez Biologicals, USA) was employed to assess antibody-specific bactericidal activity while minimising interference from endogenous immunoglobulins (Roe *et al.*, 2023). Due to the absence of gonococcal-specific antibodies in our laboratory, rabbit anti-FBA meningococcal polyclonal antibodies were used as positive controls, hypothesised to cross-react with gonococcal outer membrane components and mediate complement-dependent killing of WT-FA1090. Gonococci can exhibit natural susceptibility or resistance to complement-mediated killing, which may occur even in the absence of antibodies or in the presence of antibodies alone *in vitro*. If the bacteria are excessively sensitive or resistant to complement activity, the SBA assay may yield unreliable results (Toh *et al.*, 2021).

To confirm that bactericidal activity was specifically attributable to NGO0206 as a surface exposed target rather than residual complement activity or antibody-independent effects. For this reason, WT-FA1090 and Δ*ngo0206* at ~8 × 10^4 CFU/mL were individually incubated with IgG/IgM-depleted complement (1:2), decomplemented anti-NGO0206 antibodies (1:128), or anti-FBA antibodies (1:10) alone. Bacteria alone at T0 and T30 controls, representing the initial colony count, served as a baseline for comparing CFU counts of both WT-FA1090 and Δ*ngo0206* strains after being treated or untreated with anti-NGO0206. The bactericidal titre was defined as the reciprocal of the lowest serum dilution that achieved ≥50% killing of gonococcal cells after 30 min, relative to the CFUs/T0 count.

The SBA of anti-NGO0206 was then evaluated against WT-FA1090 and the Δ*ngo0206* mutant by incubating ~8 × 10^4 CFU of each strain for 30 min with serial antibody dilutions (1:128 to 1:8192) in the presence of IgG/IgM-depleted pooled human complement in 96-well plates. After incubation, surviving bacteria rates were quantified by CFU counts, which showed reduced survival in treated samples relative to untreated controls at T0.

The analysis demonstrated that anti-NGO0206 exhibited approximately a twofold higher SBA against the WT-FA1090 strain compared to the Δ*ngo0206* mutant. Notably, the SBA titres for anti-NGO0206 ranged from 1:1024 (in three replicates) to 1:2048 (in one replicate), as illustrated by the blue dots in Figure 5.11. Each dot represents an independent experiment performed on a separate occasion, with minor variability observed across replicates.

Interaction of anti-NGO0206 with the Δ*ngo0206* mutant strain yielded a lower bactericidal titre of 1:512 across four replicates, as demonstrated by the red dots in Figure 5.11, indicating partial resistance. This reduced efficacy likely reflects the absence of NGO0206 expression, resulting in diminished antibody binding and weaker activation of the human complement cascade, leading to reduced cell lysis.

Notably, a small amount of killing was still observed, which may result from cross-reactivity of anti-NGO0206 antibodies with other gonococcal proteins. As demonstrated by immunoblotting in Chapter 3, these antibodies recognise NGO1152 at 30 kDa and an additional unidentified protein at 72 kDa. Such off-target binding can trigger non-specific complement activation, contribute to residual killing in the mutant, and reduce assay specificity. Consequently, the true effect of NGO0206 deletion on susceptibility to complement-mediated lysis may be partially masked by this antibody cross-reactivity.

The higher SBA titres strongly indicate that NGO0206 is surface expressed in *N. gonorrhoeae*, enabling recognition by anti-NGO0206 antibodies. This interaction promotes complement deposition and MAC formation, leading to bacterial killing. The minor variability observed between replicates likely reflects slight differences in experimental conditions or biological responses. Although a twofold difference in complement-dependent killing was consistently detected between WT-FA1090 and the Δ*ngo0206* mutant, this effect is relatively modest and occurred against a background of high basal activity.

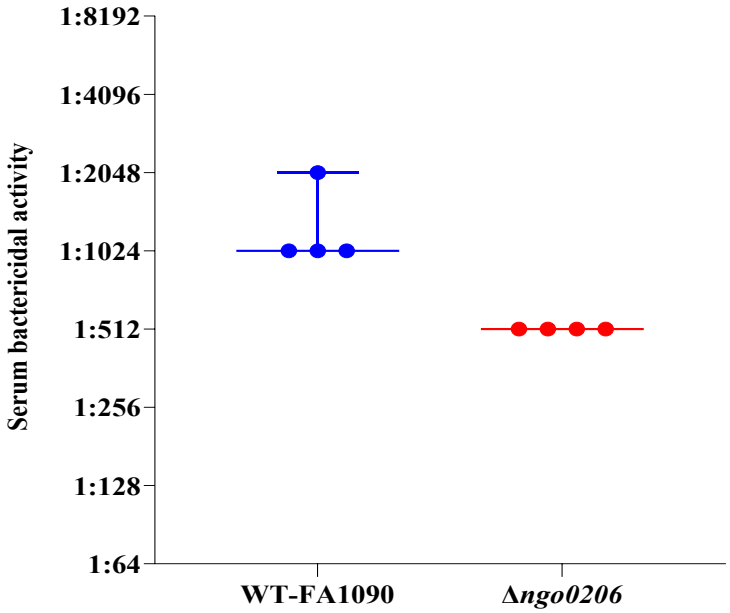

Figure 5.11. Ability of anti-NGO0206 antibodies to elicit SBA against WT-FA1090 and Δ*ngo0206* strains.
The graph displays the bactericidal titres from *n*=4 independent experiments conducted on separate occasions. Each data point represents the serum dilution of anti-NGO0206 antibodies that achieved ≥50% bacterial killing at 30 min against both the WT-FA1090 and Δ*ngo0206* mutant strains. Various control reactions were performed but are not presented in this figure, including negative controls such as bacteria alone control (T0/T30); complement alone (T30); antibody alone control (anti-NGO0206 at 1:128 dilution was incubated with WT-FA1090 and Δ*ngo0206* strains with no complement). No bacterial killing was observed in any of the negative control conditions. SBA-positive controls included: rabbit anti-meningococcal FBA antiserum (T30), which demonstrated 100% killing at 1:10 dilution when incubated with WT-FA1090 or Δ*ngo0206* mutant strains.

5.2.10. Bactericidal activity of anti-NGO1152 polyclonal antibodies

Using the same SBA approach previously applied for anti-NGO0206, it was applied to evaluate the ability of anti-NGO1152 antibodies to mediate human complement-dependent killing of *N. gonorrhoeae*.

The SBA results demonstrated that anti-NGO1152 serum effectively mediated complement-dependent killing against WT-FA1090 after 30 min of incubation, yielding a significantly higher bactericidal titre of 1:8192 across four replicates, as shown by the blue dots in Figure 5.12.

The SBA results for anti-NGO1152 against the Δ*ngo1152* strain showed significantly reduced titres, ranging from 1:512 (two replicates) to 1:2048 (two replicates), as indicated by the red dots in Figure 5.12. These titres were lower compared to the baseline CFU counts of Δ*ngo1152* at T0, indicating partial but not complete resistance to antibody-mediated killing in the absence of NGO1152.

However, a small amount of killing was still observed against the Δ*ngo1152* strain, likely reflecting background activity from cross-reactive antibodies or non-specific complement activation. This modest difference is consistent with cross-reactivity of anti-NGO1152 antibodies with other *N. gonorrhoeae* proteins, mirroring the pattern seen with anti-NGO0206. As shown by immunoblotting in Chapter 3, the anti-NGO1152 antibodies recognise both NGO1152 at 30 kDa and NGO0206 at 47 kDa. This off-target recognition may trigger non-specific complement activation, increase background killing, and reduce assay specificity, potentially causing the true impact of NGO1152 deletion on susceptibility to complement-mediated lysis to be underestimated.

The reduced bactericidal titres against Δ*ngo1152* indicate diminished antibody effectiveness due to the absence of NGO1152, resulting in decreased activation of the human complement cascade, impaired MAC formation, and reduced bacterial lysis. Collectively, these findings support that surface exposed NGO1152 is a key antigenic target for antibody binding and complement-mediated bactericidal activity.

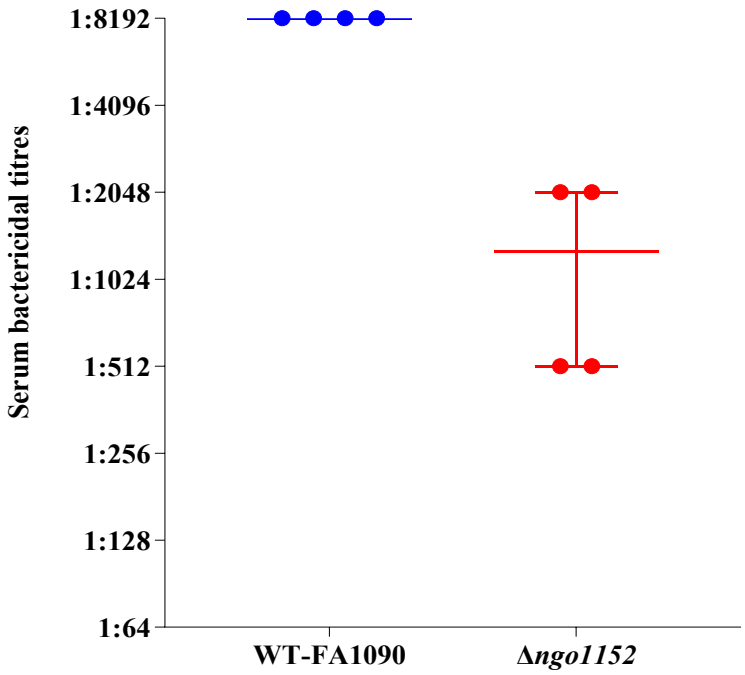

Figure 5.12. Evaluation of SBA of anti-NGO1152 polyclonal antibodies against WT-FA1090 and Δ*ngo1152* strains.
The graph shows the bactericidal titres from at least *n*=4 independent experiments. Each data point is presented as the SBA titre of anti-NGO1152 antibodies that resulted in ≥50% bacterial killing at T30. Various control reactions were performed but are not presented, including negative controls such as bacteria alone control (T0/T30); complement alone (T30); antibody alone control (anti-NGO1152 at 1:128 dilution was incubated with WT-FA1090 and Δ*ngo1152* strains with no complement). No bacterial killing was observed in any of the negative control conditions. SBA-positive controls included: Rabbit anti-meningococcal FBA Antiserum (T30), which demonstrated 100% killing at 1:10 dilution when incubated with WT-FA1090 or Δ *ngo1152* mutant strains.

5.3. Discussion

NGO1152 and NGO0206 were hypothesised to be promising vaccine candidates based on several key criteria: (I) surface accessibility; (II) high conservation across globally circulating strains with minimal phase or antigenic variation; (III) broad prevalence as confirmed in the previous chapter; (IV) the ability to elicit complement-dependent bactericidal activity; and (V) robust immunogenicity. However, the functional importance of these proteins for bacterial virulence or survival (criterion vi) was not evaluated in this study. To characterise the surface exposure, subcellular localisation, and functional relevance of NGO1152 and NGO0206 in *N. gonorrhoeae* FA1090.

A combination of immuno-dot blot, WC-ELISA, and subcellular fractionation approaches were implemented to determine protein distribution. Meanwhile, SBA was used to assess the ability of anti-NGO1152 and anti-NGO0206 antibodies to mediate complement-dependent killing of WT-FA1090 without CMP-NANA.

Protein distribution and abundance play a key role in membrane receptor function and cellular processes, which are fundamental to bacterial activity, disease development, and vaccine design (Callaghan *et al.*, 2021). *N. gonorrhoeae* exhibits phase variation, which alters surface protein expression to evade the host immune response (Walker *et al.*, 2023). Identifying antigens like NGO1152 and NGO0206, hypothesised to remain surface exposed despite this variability, supports their potential as stable vaccine targets. The surface accessibility of NGO1152 and NGO0206 was interrogated using immuno-dot blot analysis (Figures 5.1 and 5.2), which confirmed their surface localisation in line with the primary hypothesis.

An interesting finding was that anti-NGO1152 and anti-NGO0206 antibodies cross-reacted with intact WT-FA1090 and IPTG-induced complemented strains (MR331152 and MR330206), indicating that both proteins are surface accessible and maintain their native conformations. This suggests their potential as targets for antibody-mediated immunity, although further studies are needed to confirm the functional significance of this binding. In contrast, no signal was observed in the Δ*ngo1152* and Δ*ngo0206* mutants or the uninduced complemented strains,

demonstrating that surface expression of NGO1152 and NGO0206 is gene-dependent and requires active promoter induction. These findings validate their surface exposure and support their consideration as antigenic targets in vaccine development.

Once surface exposure of NGO1152 and NGO0206 was confirmed, the focus shifted to determining their localisation within the cellular compartments of *N. gonorrhoeae* FA1090 strains. To investigate the proteomic impact and subcellular localisation of NGO1152 and NGO0206, OD_{600}-normalised *N. gonorrhoeae* WT-FA1090, Δ*ngo1152*, Δ*ngo0206*, and complemented MR331152, MR330206 strains were analysed under uninduced (4 h) and IPTG-induced (4 and 7 h) conditions. SDS-PAGE and Coomassie staining of OM-, PP-, CM-, and C-enriched fractions, alongside whole-cell lysates, revealed consistent protein profiles across all strains and timepoints (Figures 5.3A-D and 5.5A-D). These findings indicate that deletion or complementation of either gene does not broadly alter global protein expression or compartmental distribution.

To immunolocalise the NGO1152. Immunoblotting analysis detected a *ca.* 30 kDa band corresponding to NGO1152 in the OM-, CM-, and C-enriched fractions of WT-FA1090 and IPTG-induced MR331152 strains at both 4 and 7 h. This band was also observed in their whole-cell lysates at 4 h and absent in Δ*ngo1152* and uninduced MR331152 strains (Figures 5.4A, C and D). However, this band was absent from the PP-enriched fractions (Figure 5.4B), contradicting the initial hypothesis of its presence in the PP. NGO1152 is predicted to be an SBP involved in ABC transporter systems, facilitating substrate capture and delivery from the cell surface to the CM via ATP hydrolysis. Additionally, NGO1152 may play roles in cellular physiology, adhesion to host cells, modulation of inflammatory responses, and delivery of virulence factors. Precise localisation is critical for maintaining the functional integrity of lipoprotein (Baarda *et al.*, 2018). The proteome-derived vaccine candidates Bame, BamG, SliC, MetQ, and NGO2054 are newly characterised as *N. gonorrhoeae* lipoproteins. NGO2111, for instance, is homologous to the *N. meningitidis* surface lipoprotein assembly modulator Slam2, which facilitates the translocation of the haemoglobin–haptoglobin utilisation protein to the cell surface (Hooda *et al.*, 2016).

Likewise, the immunoblotting with anti-NGO0206 serum detected a *ca.* 46 kDa band in OM-, CM-, and C-enriched fractions from WT-FA1090 and IPTG-induced MR330206 strains, confirming induced expression and compartmental accumulation of NGO0206 (Figures 5.6 A, C and D). However, NGO0206 was not detected in PP-enriched fractions (Figure 5.6B). Additionally, no reactive bands were observed in Δ*ngo0206* or uninduced MR330206 strains, confirming antibody specificity to NGO0206.

Subcellular localisation of NGO1152 and NGO0206 was constrained by two main factors. First, using a conventional centrifuge instead of an ultracentrifuge might lead to suboptimal compartmental separation and an increased risk of cross-contamination, which is a common issue in conventional fractionation approaches. Secondly, the absence of orthogonal control sera hindered validation of fraction purity (OM, PP, CM, and C), reducing confidence in compartment-specific enrichment. Consequently, the detection of these proteins across multiple fractions may reflect either true distribution or result from cross-contamination. To address these challenges, future studies should incorporate high-resolution centrifugation and validated markers, using specific antibodies against well-characterised proteins specific to each subcellular compartment.

In comparison of cell fractionation findings for NGO1152 and NGO0206 with a related study on lipid-modified cupredoxin azurin (Crosby and Salazar) in *N. gonorrhoeae* (Crosby and Salazar, 2015) shows similar patterns. The previous study used immunoblotting on C/PP, OM, OMV, and (SS) with use controls against the BAM complex against BAM complex components BamA (Baarda *et al.*, 2018), BamD (Sikora *et al.*, 2018), and the cytoplasmic enzyme Zwf (Wierzbicki *et al.*, 2017). The study revealed that anti-Laz antiserum primarily recognised Laz in the OM fractions, with some presence in the C/PP and OMV fractions at 25 KDa. BamA band at 75 KDa was mainly detected in CE and OMV fractions, with minor amounts in C/P, reflecting the presence of BamA polypeptide transport-associated domains residing in the periplasm (Sikora *et al.*, 2018). A distinct BamD band at 25 kDa was exclusively detected in the CE and OMV fractions, with no protein detected in the SS, highlighting distinct protein localisation patterns across subcellular compartments (Baarda *et al.*, 2019).

Further analysis by WC-ELISA demonstrated that anti-NGO1152 and anti-NGO0206 antisera consistently recognised and bound to NGO1152 and NGO0206 on the surface of intact cells of WT-FA1090, IPTG-induced MR331152 and MR330206 strains, confirming that both proteins were surface accessible on the cell surface of gonococcal (Figure 5.7 and Figure 5.8).

In contrast, both antisera exhibited significantly reduced binding to Δ*ngo1152* and Δ*ngo0206*, uninduced MR331152 and MR330206 strains, confirming decreased immune recognition due to gene deletion or lack of induction.

To broaden the investigation of NGO1152 and NGO0206 surface immunolocalisation in other strains, 7 *N. gonorrhoea* clinical isolates were selected from a pool of 28 genetically, geographically, and temporally diverse strains. Expression of both proteins was previously confirmed across all 28 isolates by immunoblotting (as described in Chapter 4). The WC-ELISA data (Figures 5.9 and 5.10) demonstrate that anti-NGO1152 and anti-NGO0206 antibodies bind with high affinity to their respective surface antigens on intact cells from MS-11, DGI-18, 17N0001, 17N0002, 17N0003, 17N0004, and 17N0005 strains. This immune cross-reactivity binding was significantly higher compared to the corresponding Δ*ngo1152* and Δ*ngo0206* mutant strains. Importantly, although all strains exhibited antigen accessibility and reactivity, only minor variation in binding magnitude was observed.

These findings indicate that NGO1152 and NGO0206 exhibit conserved surface exposed antigenic properties across genetically and geographically diverse clinical isolates, supporting their potential as broadly protective vaccine targets. WC-ELISA confirmed surface expression across strains and offers a cost-effective, scalable method for large-scale antigen screening.

However, WC-ELISA lacks single-cell resolution and is limited by background noise from non-specific binding, reducing its specificity compared to flow cytometry (Plotkin, 2020). Flow cytometry enables high-resolution, quantitative analysis of surface exposed antigens on individual bacterial cells, allowing precise detection of cell-to-cell variability and identification of subpopulations (Gray *et al.*, 2023). While more accurate, its high cost often limits routine use. This can be complemented by immunogold electron microscopy, which provides

ultrastructural localisation of antigens (Nicholson *et al.*, 2025), and by quantitative mass spectrometry, which enables molecular-level analysis of expression, localisation, and post-translational modifications.

SBA is an established correlate of protection for *N. meningitidis*, but its role in *N. gonorrhoeae* immunity remains unclear. Nonetheless, it remains a useful tool for evaluating functional antibody responses (Tzeng *et al.*, 2024). SBA assay varies across laboratories in several aspects, including the choice of assay buffers (such as PBS or HBSS), incubation timepoints (30 or 45 min), bacterial strains (F62 or FA1090), and complement sources (baby rabbit or human complement) (Matthias *et al.*, 2025). Additionally, some laboratories simulate *in vivo* conditions by inducing LOS sialylation by culture strains in the presence of the sialic acid donor cytidine-5′-monophospho-N-acetylneuraminic acid (CMP-NANA), which is incorporated into LOS by the Lst. This induction of LOS sialylation *in vitro* mimics the physiological infectious state of *N. gonorrhoeae* and increases serum resistance (Matthias *et al.*, 2025).

It was hypothesised that NGO0206 and NGO1152 are surface exposed proteins capable of inducing a complement-dependent bactericidal response. To explore this, SBA were employed to evaluate whether anti-NGO0206 and anti-NGO0206 against these targets could selectively mediate complement-dependent killing of WT-FA1090, with minimal or no effect on the respective Δ*ngo0206* and Δ*ngo1152* mutants.

Hence, bacteria can display natural susceptibility or resistance to complement-mediated killing, even in the absence of specific antibodies. When a strain is either highly sensitive or highly resistant to complement alone, the SBA assay becomes unreliable for evaluating antibody-mediated killing (Toh *et al.*, 2021). Ideally, complement should be sourced from the same species as the host to accurately reflect the immune environment during infection (Feavers and Walker, 2010). Nonetheless, baby rabbit serum is often favoured over human serum due to its natural lack of pre-existing antibodies, which minimises background interference (McIntosh *et al.*, 2015; Santos *et al.*, 2001).

To ensure that the bactericidal activity against gonococci observed in this study was not due to intrinsic killing properties of the complement source,

contaminating antimicrobial compounds, or antibody preparations. Exogenous IgG/IgM-depleted pooled human complement and decomplemented polyclonal antibodies against NGO0206, NGO1152, and meningococcal FBA were each evaluated individually against WT-FA1090, Δ*ngo0206*, and Δ*ngo1152* strains. None of these elements showed intrinsic bactericidal activity. These findings align with those of Matthias *et al*. (2025), who similarly reported no inherent killing activity using the same complement preparation against *N. gonorrhoeae* strains F62, MS11, and FA1090 (Matthias *et al.*, 2025).

During preliminary optimisation of the SBA assay, an initial 1-h incubation of anti-NGO0206 and anti-NGO1152 antibodies with bacteria in the presence of complement resulted in complete bacterial killing, preventing effective assessment of bactericidal activity. To circumvent this problem, the incubation time was reduced to 30 min, which preserved the survival of viable bacteria and demonstrated that shorter incubation was sufficient for complement-mediated killing, thereby providing a more practical approach for assay evaluation.

Herewith, it is intriguing to note that the rabbit anti-NGO0206 antibody exhibited variability in bactericidal titres, ranging from 1:1024 in three replicates to 1:2048 in one replicate against the WT-FA1090 strain (Figure 5.11).

In contrast, the Δ*ngo0206* mutant strain showed a significantly reduced SBA titre of 1:512 across four replicates following 30 min of incubation. This pronounced reduction in bactericidal activity highlights the impaired efficacy of the anti-NGO0206 antibody in the absence of its cognate antigen. Undoubtedly, the absence of NGO0206 expression in the Δ*ngo0206* strain significantly reduced the binding of anti-NGO0206 antibodies. This impaired binding weakens the initiation of the complement cascade, resulting in decreased MAC assembly and reduced bacterial cell lysis.

Similarly, anti-NGO1152 serum effectively mediated complement-dependent killing of WT-FA1090, yielding a significantly higher bactericidal titre of 1:8192. This superior activity of anti-NGO1152 serum compared to anti-NGO0206 serum highlights its capability to robustly activate the complement cascade. This enhanced bactericidal effect likely results from the binding of anti-NGO1152 immunoglobulin isotypes to a high density of NGO1152 antigens on the

bacterial surface, promoting complement deposition and MAC formation. Consequently, complement-dependent lysis and bacterial killing in WT-FA1090 were substantially greater than in the Δ*ngo1152* mutant strain, accentuating the critical role of surface antigen expression in antibody-mediated bactericidal activity. In contrast, the anti-NGO1152 response against the Δ*ngo1152* mutant strain, which lacks NGO1152 expression, exhibited a significant reduction in bactericidal titre, ranging from 1:512 to 1:2048 (Figure 5.12). Although titres against the Δ*ngo1152* strain indicated residual immune recognition, they were distinctly lower than those observed for the WT-FA1090 strain. This reduction suggests diminished serum bactericidal activity of anti-NGO1152 antibodies, likely due to the absence of NGO1152 surface expression. The lack of surface antigen reduces MAC assembly, thereby decreasing bacterial cell lysis and killing.

SBA is triggered when anti-NGO1152 and anti-NGO0206 antibodies bind in sufficient density to their respective targets, NGO1152 and NGO0206, on the gonococcal surface, enabling complement activation through multivalent antigen recognition. This process requires the formation of high-density antigen–antibody complexes, primarily involving IgM and IgG, which engage complement components upon simultaneous binding to multiple surface exposed antigens (Roe *et al.*, 2023). Complement activation occurs via three enzymatic cascades: the classical, mannan-binding lectin (MBL), and alternative pathways. The classical pathway begins when antibodies bind bacterial surface antigens, enabling C1 complex interaction with IgM or IgG Fc regions (Fantoni *et al.*, 2024). This triggers C3 convertase formation enzyme, which cleaves C3 into C3a and C3b. As Accumulated C3b on the surface, additional converts C3 convertase into C5 convertase, which cleaves C5 into C5a and C5b. C5b then associates with C6, C7, and C8 to promote C9 polymerisation, forming the MAC (Heesterbeek *et al.*, 2018). The MAC forms a ring-shaped pore that disrupts Gram-negative bacterial membranes by osmolysis, directly killing bacteria independently without immune cells' involvement (Xie *et al.*, 2020).

Importantly, immunoblotting results from Chapter 3 revealed notable cross-reactivity between anti-NGO1152 and anti-NGO0206 sera. Anti-NGO1152 sera (1:1000) bound not only to NGO1152 (~30 kDa) but also to NGO0206, indicated

by a distinct band at ~46 kDa. Conversely, anti-NGO0206 sera (1:1000) bound strongly to NGO0206 (~46 kDa) and cross-reacted with NGO1152 (~30 kDa), along with an additional, unidentified band at ~72 kDa. These findings suggest the presence of a shared or heterologous epitope that may account for the observed cross-reactivity.

This cross-reactivity likely contributed to the enhanced antigen recognition and complement activation observed in SBA assays using both antisera. While this led to increased bactericidal activity, it also elevated background activity, complicating SBA interpretation. The identity of the 72 kDa band remains unknown, and further characterisation via SDS-PAGE and mass spectrometry is recommended to clarify its role.

Despite these complexities, both antisera produced strong SBA titres and effectively mediated complement-dependent killing *in vitro*, supporting their potential for immune clearance and highlighting their promise as protective vaccine candidates. Another possible explanation for the increased SBA titres is the absence of exogenous CMP-NANA in vitro, which may have enhanced antibody-mediated killing. Under these conditions, both anti-NGO0206 and anti-NGO1152 sera showed strong bactericidal activity against WT-FA1090, with reduced killing of the Δ*ngo0206* and Δ*ngo1152* mutants.

This contrasts with findings by Almonacid-Mendoza *et al.* (2018), who reported that gonococcal sialylation inhibited bactericidal activity of antisera raised against recombinant *N. gonorrhoeae* acyl carrier protein (rNg-ACP) and OM preparations (Almonacid-Mendoza *et al.*, 2018). These findings are associated with the broader observation that assumed sialylation can inhibit immune-mediated bacterial killing. Although sialylation raises concerns regarding the inclusion of rNg-ACP and other OM antigens in future gonococcal vaccine designs. It remains noteworthy that antibodies capable of targeting unsialylated gonococci, which are encountered during infection, may still hold considerable promise for vaccine development (Almonacid-Mendoza *et al.*, 2018).

In *N. gonorrhoeae* infections, LOS sialylation is a key mechanism of immune evasion. Gonococci acquire CMP-NANA (cytidine monophosphate-N-acetylneuraminic acid, a sialic acid donor) from the human urogenital tract and

incorporate it into their LOS structure (Cardenas *et al.*, 2024). This modification increases serum resistance by reducing complement activation, thereby hindering the immune system's ability to effectively combat the infection. Sialylated LOS effectively masks the bacterial surface, reducing recognition by the host immune system, particularly by complement and antibodies (Cardenas *et al.*, 2024). To better mimic the physiological infection conditions of *N. gonorrhoeae* in humans *in vitro*, some laboratories culture gonococcal strains in the presence of CMP-NANA enhances serum resistance (Matthias *et al.*, 2025).

Future research should evaluate the SBA of anti-NGO1152 and anti-NGO0206 antibodies to determine their effectiveness against WHO reference strains and multidrug-resistant *N. gonorrhoeae* isolates. It is also important to investigate whether LOS sialylation influences antibody-mediated killing. Repeating SBA assays in the presence of CMP-NANA could help assess its impact on the bactericidal activity of both antisera. In addition to SBA, opsonophagocytic killing assays (OPAs) could (Gray *et al.*, 2023) be implemented to examine the ability of anti-NGO1152 and anti-NGO0206 antibodies to promote antibody-dependent phagocytosis and *in vitro* killing. This approach would involve incubating *N. gonorrhoeae* with antibody-treated serum, followed by the addition of human phagocytic cells such as polymorphonuclear leukocytes (PMNs) or macrophage-like cells to evaluate antibody-mediated opsonisation and bacterial clearance(Chen and Seifert, 2011).

Although *N. gonorrhoeae* is strictly a human pathogen, transient colonisation can be established in hormonally treated female BALB/c mice. Immunising these mice with anti-NGO1152 or anti-NGO0206 antibodies could help assess their protective capacity by evaluating reductions in colonisation duration or bacterial clearance. Finally, the ability of these antibodies to inhibit *N. gonorrhoeae* adherence and invasion should be explored, as blocking these antigens during early infection may enhance bacterial clearance, reduce disease severity, and offer a promising therapeutic strategy.

In conclusion, immuno-dot blot analysis provided evidence for the surface exposure and antibody accessibility of NGO1152 and NGO0206 on the surface of *N. gonorrhoeae*. Additionally, immuno-localisation further validated the

specificity of the antibody interactions with subcellular fractions, confirming that NGO1152 and NGO0206 are localised in the CM, with additional localisation observed at the OM of gonococci. The surface exposure of NGO1152 and NGO0206 was further investigated through direct WC-ELISA, which confirmed significant binding of anti-NGO1152 and anti-NGO0206 antibodies to the surface of FA1090 and a range of clinical isolates. The bactericidal activity of these antibodies was assessed using IgG/IgM-depleted pooled human complement as the active exogenous component. As a result, anti-NGO0206 antibodies exhibited SBA titres of 1:1024 to 1:2048 against WT-FA1090, while titres decreased to 1:512 for the Δ*ngo0206* mutant. Similarly, anti-NGO1152 antibodies achieved an SBA titre of 1:8192 against WT-FA1090 in comparison to SBA titres ranging from 1:512 to 1:2048 for the Δ*ngo1152* mutant. These findings collectively demonstrate that NGO1152 and NGO0206 are surface exposed, immunogenic antigens capable of eliciting complement-dependent bactericidal activity, highlighting their potential as promising candidates for future gonococcal vaccine development.

Chapter 6: General Discussion

N. gonorrhoeae causes gonorrhoea, an STI that has developed resistance to all known treatments through the acquisition of chromosomal and plasmid mutations (Unemo *et al.*, 2024). Without effective intervention, gonorrhoea can lead to serious complications, including epididymitis, endometritis, pelvic inflammatory disease, and ectopic pregnancy (Pisano *et al.*, 2024). Infection rates are rising globally, with significant disparities in disease prevalence and impact observed among different sexual, gender, racial, and ethnic groups, particularly in populations with limited access to healthcare resources (Pisano *et al.*, 2024).

Three principal challenges continue to impede gonococcal vaccine development: (i) high antigenic variability, (ii) lack of naturally acquired protective immunity or defined immune correlates of protection, and (iii) the restriction of *N. gonorrhoeae* to human hosts, limiting suitable animal models (Russell *et al.*, 2019). Despite these challenges, the success of vaccines against the closely related *N. meningitidis* offers a promising model for *N. gonorrhoeae* vaccine development (Petousis-Harris *et al.*, 2017). Effective vaccines and/or new antimicrobial treatments will be essential for controlling gonorrhoea infections (Młynarczyk-Bonikowska *et al.*, 2020).

Efforts to develop a gonococcal vaccine have been hampered by the pathogen's extensive antigenic variability. *N. gonorrhoeae* employs both phase and antigenic variation to alter its surface exposed epitopes, resulting in an ever-changing OM that hinders consistent immune recognition (Aas *et al.*, 2002).

Its cell envelope plays a central role in both pathogenesis and immune evasion, with dynamic alterations contributing to population heterogeneity (Adamczyk-Poplawska *et al.*, 2022). Moreover, the bacterium evades immune detection by residing intracellularly in epithelial cells, macrophages, and neutrophils, while actively modulating host immune responses (Gao *et al.*, 2024; Russell, 2021).

Two OM proteins, PorB and Reduction Modifiable Protein M (RmpM), are key mediators of this immune evasion. PorB, the most abundant OM protein

(constituting approximately 60% of total OM proteins), is essential for bacterial viability and facilitates ion exchange (Deo *et al.*, 2018). It possesses numerous immunomodulatory functions, including inhibition of complement-mediated killing, suppression of neutrophil and macrophage apoptosis, and modulation of T-cell responses (Jones, Jerse*, et al.*, 2024; Pisano *et al.*, 2024). RmpM further aids immune evasion by blocking antibody recognition of other surface antigens, preventing bacterial killing (Deo *et al.*, 2018).

The most promising subunit and OMV-based vaccines for *N. gonorrhoeae* employ adjuvants that promote a Th1-biased immune response, such as CpG and microencapsulated IL-12 (Sikora *et al.*, 2020; Song *et al.*, 2023).. Induction of a Th1 response is widely regarded as a critical determinant of gonococcal vaccine efficacy, as demonstrated by the intravaginal administration of IL-12, which accelerates clearance of gonococcal infection in murine models (Y. Liu *et al.*, 2013). In mice, a Th1 response is defined by interferon-γ (IFNγ) production, which drives expression of the immunoglobulin (Ig) G2a isotype. Conversely, a Th2 response is characterised by interleukin-4 (IL-4) production and is associated with IgG1 isotype expression (Snapper and Paul, 1987).

Two major antigens, PorB and RmpM, contribute to *N. gonorrhoeae* immune evasion. PorB, the most abundant and essential OMP, constitutes ~60% of the gonococcal OM and OMV proteomes (Deo *et al.*, 2018). It suppresses host immunity by recruiting complement regulators, inhibiting neutrophil, macrophage, and T cell functions, and is highly variable across strains, making it unsuitable as a vaccine antigen. RmpM is an immunosuppressive protein, with its N-terminus binding trimeric PorB in the bacteria's OM and linking it to peptidoglycan through its C-terminal domain complex (Maharjan *et al.*, 2016). Antibodies targeting RmpM have been reported to obstruct or block the recognition of other surface antigens, thereby impairing immune-mediated bacterial clearance (Rice *et al.*, 1986).

Unlike other *Neisseria* species, *N. meningitidis* expresses two major porins, PorA and PorB. Meningococcal PorB has strong immunostimulatory properties and has been used as a vaccine adjuvant because it promotes antigen-specific B- and T-cell responses (Wetzler, 2010). In contrast, *N. gonorrhoeae* PorB is largely

immunosuppressive. The PorB proteins of the two species share 60–70% amino acid sequence homology, depending on the strain (Song *et al.*, 2023)

Recent advances in gonorrhoea vaccine development highlight both academic innovation and the challenges of translating these approaches into clinically effective platforms (Jones, Ramirez-Bencomo*, et al.*, 2024).

The first notable effort from Oxford University has focused on modifying key immunomodulatory proteins of *N. gonorrhoeae*: RmpM, which can elicit blocking antibodies, and PorB, an OM porin that contributes to immunosuppression. In this strategy, gonococcal PorB was replaced with the immunostimulatory PorB from *N. meningitidis*, while RmpM was deleted to enhance immunogenicity and vesicle production. Immunisation of mice with OMVs from this modified strain elicited higher antibody titres against model antigens compared to OMVs containing native PorB. Protein microarray analysis further revealed broader IgG responses across diverse gonococcal antigens, and the immune response was skewed toward a Th1 profile, with elevated serum IgG2a and IFNγ production by splenocytes. This work demonstrates that targeted modification of OMV components can overcome gonococcal immune evasion and represents a promising next-generation platform for vaccine development, although preclinical efficacy data in infection models remain to be fully reported (Jones, Ramirez-Bencomo*, et al.*, 2024).

The MeNZB vaccine is no longer available. However, the meningococcal serogroup-B vaccine, 4CMenB Bexsero, including the MeNZB OMVs derived from the NZ-98/254 strain, plus three recombinant protein antigens: NadA NadA-NMB1994, fHbp-GNA2091, and NHBA-GNA1030, is currently licensed globally (Semchenko *et al.*, 2019). *In vitro* studies have demonstrated that NadA, fHbp, and NHBA are effective in inducing serum bactericidal antibodies against various meningococcal strains, enhanced further by fusion with accessory proteins such as GNA2091 (Bos *et al.*, 2014) and GNA1030 (Donnarumma *et al.*, 2015). Effectiveness estimates for OMV-based meningococcal vaccines against *N. gonorrhoeae* range from 31% to 46% and can persist for up to three years post-vaccination (Wang *et al.*, 2023). Given that several *Neisseria* species are capable of eliciting adaptive immune responses, it is unsurprising that

meningococcal vaccines provide partial cross-protection against gonorrhoea through shared antigens.

Encouragingly, several studies have shown that Bexsero-derived antigens elicit cross-reactive antibody responses and provide modest protection against *N. gonorrhoeae* in murine models (Craig *et al.*, 2015; Leduc *et al.*, 2020). However, these effects have not consistently translated into significant serum bactericidal activity in human studies (Beernink *et al.*, 2019). Comparative genomic and bioinformatic analyses have demonstrated important differences in the distribution of meningococcal vaccine antigens within *N. gonorrhoeae* (Williams *et al.*, 2024).

Notably, the gene encoding the NadA protein is absent in *N. gonorrhoeae* (Muzzi *et al.*, 2013). However, the gene encoding fHbp is present, but the protein is not surface exposed on the cell surface. Likewise, orthologues of NHBA, GNA2091, and GNA1030 genes were present (Muzzi *et al.*, 2013), but their specific functional and immunological characteristics remain uncharacterised. Subsequent analyses confirmed the presence of NHBA in all 17/17 examined strains of *N. gonorrhoeae* and exhibited an average similarity of 81.2% to the NHBA-2 peptide found in Bexsero (Jongerius *et al.*, 2013). In a broader dataset comparative sequence analysis using BLASTp against 438 gonococcal genomes in GenBank, coupled with Clustal alignment in MEGA7, revealed that gonococcal NHBA displays partial conservation with meningococcal homologues. Specifically, in 97 of 111 strains, *N. gonorrhoeae* NHBA exhibited 65.6% similarity to the non-vaccine NHBA-3 peptide of *N. meningitidis* MC58, showing components may be partly responsible for limited cross-protection against gonorrhoea in Bexsero-related studies (Semchenko *et al.*, 2019).

Considering the genetic and antigenic overlap between *N. gonorrhoeae* and *N. meningitidis*, with over 1,500 shared proteins (including 57 predicted to be surface expressed/OM), cross-species vaccine strategies remain an attractive prospect (Islam *et al.*, 2025). Several gonococcal antigens with known roles in nutrient acquisition and host adhesion, such as TdfF, TbpAB, LbpAB, MetQ, and NHBA, are conserved across both species, suggesting a dual-pathogen targeting strategy may be feasible (Fegan *et al.*, 2019; Kammerman *et al.*, 2020;

Maurakis *et al.*, 2019; Price *et al.*, 2007; Schryvers, 2022; Semchenko *et al.*, 2022).

Recent developments in gonococcal vaccine research have been led by GlaxoSmithKline plc (GSK), a global biopharmaceutical company headquartered in the UK, focusing on the development of vaccines and therapies for serious diseases. In June 2023, GSK announced its investigational gonococcal vaccine candidate (NgG) and initiated a combined Phase I/II clinical trial. The vaccine has also been approved in the US. FDA Fast Track designation to expedite development and review. This reflects the urgent public health need posed by gonorrhoea, the second most prevalent bacterial sexually transmitted infection worldwide, with an estimated 82 million new cases annually and rising antimicrobial resistance (GSK, 2023). The NgG vaccine was derived from GSK's $2.1 billion acquisition of Affinivax and employs a Generalised Modules for Membrane Antigens (GMMA) platform, comprising genetically detoxified OMVs from *N. gonorrhoeae* FA1090, designed to enhance immunogenicity while minimising endotoxin activity (GSK, 2023). The Phase I/II trial evaluated safety, reactogenicity, and preliminary efficacy in approximately 750 healthy adult participants aged 18–50 at risk for gonorrhoea across multiple countries, including the US, UK, France, Germany, Spain, Brazil, the Philippines, and South Africa (GSK, 2023).

Despite these initial advancements, GSK subsequently discontinued the NgG vaccine programme, citing unmet efficacy benchmarks and competitive pressures. This decision highlights the scientific and commercial challenges inherent in translating preclinical gonococcal vaccine research into viable clinical candidates (AdisInsight, 2023). More broadly, it reflects the wider landscape of gonorrhoea vaccine research: while industry efforts face significant translational hurdles, academic groups, such as those at Oxford University, continue to innovate at the preclinical level. This emphasises the ongoing need for novel approaches to overcome the biological and logistical barriers in developing effective vaccines against *N. gonorrhoeae*

In this context, our laboratory has identified NGO1152 and NGO0206 as SBP of ABC transporter as novel vaccine antigen candidates against *N. gonorrhoeae*, based on integrated bioinformatic, genetic, and immunological analyses.

ABC transporter systems represent a protein family increasingly recognised as attractive vaccine targets due to their high conservation, surface accessibility, and critical roles in nutrient acquisition (Masselot-Joubert and Di Renzo, 2025).

NGO1152 is a 268-amino acid, ~30 kDa, putative periplasmic histidine-binding lipoprotein component of an ABC transporter implicated in amino acid transport, for example, glutamine, glutamate, or aspartate.

Interestingly, NGO1152 shows strong homology to its *N. meningitidis* MC58 orthologue, NMB1612/NMC1533, as documented in PubMLST by Professor Myron Christodoulides (University of Southampton, UK), providing the basis for its characterisation. Importantly, NMB1612 has been shown to elicit bactericidal antibodies in animal models (Hung *et al.*, 2015), suggesting that NGO1152 may similarly serve as a stable cross-species vaccine target. Our analysis further confirmed that NGO1152 is highly conserved with NMB1612, sharing 98% nucleotide identity and differing by only five amino acid substitutions, highlighting its functional equivalence and potential for cross-species, broad-spectrum vaccine applicability.

By contrast, NGO0206, a ~40 kDa polyamine-binding protein within the system, exhibits greater sequence divergence than NGO1152, but NGO0206 retains conserved motifs with NGO1152 and predicted surface accessibility, supporting its immunogenic potential. NGO0206 is a component of a polyamine transporter system known as PotFGHI that contains three putative periplasmic polyamine binding proteins encoded by *potF1* (NGO0206), *potF2* (NGO1253), and *potF3* (NGO1494) (Goytia and Shafer, 2010). Additionally, Zielke *et al*. (2014) identified the NGO0206 in membrane vesicles of different strains of *N. gonorrhoeae* F62, MS11, and 1291, using the iTRAQ technique (Zielke *et al.*, 2014).

In earlier work conducted by Williams (2018), Smith (2019), and Patel (2019) in our laboratory, led to the generation of Δ*ngo1152* and Δ*ngo0206* mutants in *N. gonorrhoeae* FA1090, as well as recombinant rNGO1152 and rNGO0206, which were used to generate anti-NGO1152 and anti-NGO0206 polyclonal antibodies in rabbits.

In this research, complemented strains were generated using either a constitutive *opaB* promoter (pMR32) (Ramsey *et al.*, 2012) from *N. gonorrhoeae* strain FA1090 (P_{opaB}) or an IPTG-inducible tandem *lac* promoter/operator *lacPOPO* from pMR33 (Ramsey *et al.*, 2012), along with the *lac* repressor ($lacI^q$) from pKH37 (Kohler *et al.*, 2007). The *lacPOPO* system was used in this research because it can increase transcript levels of *ngo1152* or *ngo0206* up to 123-fold compared to wild-type *N. gonorrhoeae*, which significantly enhanced transcript levels of protein expression even in the absence of the 100 bp upstream region in both genes.

Phenotypic characterisation by immunoblotting with rabbit anti-NGO1152 and anti-NGO0206 polyclonal antibodies at 1:1000 dilution detected bands at 30 kDa for NGO1152 and 46 kDa for NGO0206 in WT-FA109, MR3311152, and MR330206 induced complement strains under the *lacPOPO* promoter. However, no bands were observed in uninduced complements or in the Δ*ngo1152* and Δ*ngo0206* mutants. Upon IPTG induction, NGO1152 and NGO0206 expression in MR3311152 and MR330206 was restored to WT-FA1090 levels within 2 h, demonstrating the effectiveness of the promoter system in driving protein expression.

Unexpectedly, MR3211152 and MR320206 strains complemented under the P_{opaB} promoter failed to express either protein, most likely due to defects in the upstream transcriptional region introduced during primer design, as ~100 bp of the native RNA regulatory sequence was missing from the amplified fragment used for complementation. At this dilution, anti-NGO0206 antibodies cross-reacted with both NGO0206 (46 kDa) and NGO1152 (30 kDa), with additional weak bands at 72 kDa considered non-specific. In contrast, anti-NGO1152 antibodies displayed the same cross-reactivity but without the 72 kDa signals. Thereafter, increasing the dilution of both antibodies to 1:100,000 eliminated non-specific bands, leaving a single clear band for NGO0206 or NGO1152, confirming that these proteins are expressed and retain their antigenic integrity.

However, sequence alignment analyses later revealed that the conserved N-terminal signal peptide, lipobox motif, and several short motifs in NGO0206 and NGO1152 likely maintain a shared fold and overlapping epitopes, providing a

structural explanation for the reciprocal antibody cross-reactivity observed in immunoblots.

To determine whether deletion or complementation of candidate antigen genes affects bacterial fitness under laboratory conditions. *In vitro* growth kinetics of mutant and complemented strains, with or without IPTG induction, were comparable to WT-FA1090, indicating that these genetic modifications do not impair fitness in nutrient-rich conditions. However, *in vitro* assays do not capture host-specific nutrient limitations, immune pressures, or microenvironmental niches encountered during infection. Nevertheless, NGO1152 and NGO0206 may be dispensable *in vitro* but could perform specialised, context-dependent roles during colonisation or pathogenesis that require *in vivo* or host-mimetic models to reveal. For example, MetQ, an ABC transporter SBP in *Neisseria,* is surface expressed and elicits bactericidal antibodies (Semchenko *et al.*, 2017), supporting SBPs as vaccine targets. Similarly, metal-binding lipoproteins such as MntC in *S. aureus* and PsaA in *S. pneumoniae* have documented roles in virulence not reflected by simple *in vitro* growth assays (Handke *et al.*, 2018).

These models highlight the requirement for host-relevant models to fully assess the functional importance and vaccine potential of NGO1152 and NGO0206. Identifying highly conserved and surface accessible antigens remains a critical challenge for gonococcal vaccine development, given the phase and antigenic variability of *N. gonorrhoeae* surface proteins (Jefferson *et al.*, 2021).

Immunoblotting confirmed that NGO1152 and NGO0206 are expressed in whole-cell lysates from 28 clinical *N. gonorrhoeae* isolates but are absent in the mutant, confirming antibody specificity and demonstrating their broad conservation. Notably, this expression pattern closely parallels findings by Hung *et al*. (2015), who reported expression of NMB1612 in *N. meningitidis*, where anti-rNMB1612 sera consistently detected a ~27 kDa band across all 13 meningococcal strains (Hung *et al.*, 2015). Collectively, these data confirm that NGO1152 and NGO0206 are highly conserved and ubiquitously expressed among circulating *N. gonorrhoeae* strains, with NGO1152 resembling NMB1612 in both structure and conservation.

In addition, comparable findings to our study were reported by Jen *et al*. (2019) in their evaluation of MsrA/B as a vaccine candidate. Using immunoblotting, MsrA/B was detected by anti-MsrA/B mouse antisera at 58 kDa in whole-cell lysates of *N. gonorrhoeae* strain 1291, and 20 clinical isolates, but was absent in the 1291*msr*::kan mutant, again confirming antibody specificity (Jen *et al.*, 2019). Furthermore, WC-ELISA demonstrated that MsrA/B is surface expressed and immunogenic across diverse isolates (Jen *et al.*, 2019). Together, these studies underscore the potential of conserved, broadly expressed antigens such as NGO1152, NGO0206, and MsrA/B for gonococcal vaccine development.

Supporting this at a broader scale, analysis of 7,327 *N. gonorrhoeae* isolates from the PubMLST database demonstrated that NGO1152 and NGO0206 are highly conserved, consistent with their predicted functional importance. Specifically, NGO1152 was present in 100% of isolates, with 99.97% predicted to encode a functional protein, whereas NGO0206 was detected in 87.9% of isolates, with 87.8% predicted to be functional. This high prevalence and limited sequence variability further highlight their potential as promising vaccine candidates.

In comparison, our findings with a study reported by Handke *et al.* (2018), who demonstrated a large-scale analysis of 34 gonococcal antigens across >5,000 5,000 clinical isolates in the *Neisseria* PubMLST database. They identified eight exceptionally conserved proteins, each represented by a single allele variant in >80% of isolates, and an additional 18 candidates represented by ≤3 alleles in >50% of isolates (Handke *et al.*, 2018). Consistent with this, NGO1152 in our study exhibits near-universal presence, aligning with the highest level of conservation (similar to ACP, AniA, BamA, MtrE, NspA, and ZnuD), whereas NGO0206, though slightly less ubiquitous, still falls within the range of broadly distributed vaccine-relevant antigens.

To explore the implications of conservation among *N. gonorrhoeae* lipoproteins, amino acid analyses of NGO0206 and NGO1152 were performed. Despite partial sequence similarity between NGO0206 and NGO1152, pairwise alignment revealed substantial divergence, with only 24% identity, 36.6% similarity, and a high gap rate of 32.9%. Most variation occurs in the central and

C-terminal regions, where an extension in NGO0206 suggests evolutionary divergence and potential functional specialisation.

In contrast, the N-terminal signal peptide and lipobox motif, terminating at the conserved cysteine (NGO0206: MKKTLVAAIL--SLALTACGG; NGO1152: MKKWIAAALACSALALSACGG, are highly preserved, likely underpinning the cross-reactivity observed in immunoblotting: antibodies against NGO0206 recognised both proteins, and the same pattern was observed with anti-NGO1152 antibodies. Moreover, several short, conserved motifs such as YAVPYF/FSDPYF and GFDVDL/GKSGYD suggest retention of key structural elements such as β-strands or loops, supporting a shared fold and partially overlapping antigenic epitopes.

Extending these findings, further analysis discovered that NGO1152 is nearly identical to its *N. meningitidis* MC58 orthologue NMB1612, sharing 98.1% sequence identity and complete conservation of the N-terminal signal peptide, lipobox, and key motifs. This high degree of conservation highlights their homologous function roles as SBPs of the ABC transporter and supports NGO1152 as a cross-species antigenic target for bactericidal antibody-based vaccine development.

Integrating comparative multiple alignment sequence analyses of NGO0206, NGO1152, and NMB1612 revealed that NGO1152 and NMB1612 are highly conserved orthologues, whereas NGO0206 represents a structurally distinct paralogue. Although NGO0206 shares partial sequence similarity with NGO1152 and NMB1612, particularly within conserved N-terminal motifs linked to membrane targeting. However, NGO0206 exhibits substantial divergence in the central and C-terminal regions. It contains unique insertions and an extended sequence. These differences suggest NGO0206 has specialised functions and may vary in substrate binding from NGO1152 and NMB1612 or immune recognition. While the broad conservation of NGO1152 supports its candidacy as a cross-species antigenic target. Meanwhile, the structural variability of NGO0206 may limit its universal applicability; nonetheless, the preserved N-terminal motifs indicate it could retain some immunological relevance.

To verify surface expression and antibody accessibility, NGO1152 and NGO0206 were assessed in intact *N. gonorrhoeae* FA1090 cells using immuno-dot blotting. This demonstrated surface exposure of both proteins in WT-FA1090 and IPTG-induced complemented strains of MR331152 and MR330206, whereas mutants and uninduced strains lacked detectable protein. Protein expression in induced complemented strains was restored to WT-FA1090 levels, validating antibody specificity and accessibility. These outcomes suggest that NGO1152 and NGO0206 could serve as potential targets to elicit bactericidal activity, which is critical for vaccine development.

To further confirm immunolocalisation, subcellular fractionation combined with immunoblotting was performed. Both proteins were detected in the OM, CM, and C fractions of WT-FA1090 and induced complemented strains (MR331152 and MR330206) and were absent in the PP fraction. Importantly, IPTG induction restored expression in complemented strains, whereas the proteins remained absent in mutants and uninduced strains.

Nevertheless, the majority of SBPs of ABC transporters are located in the periplasm of Gram-negative bacteria (Rice *et al.*, 2014). However, several SBPs have been reported to localise at the bacterial surface (Briles *et al.*, 2000; Kovacs-Simon *et al.*, 2014; Otsuka *et al.*, 2016). For instance, proteomic analyses have detected MetQ in OMP and OMV preparations of both *N. gonorrhoeae* (Zielke *et al.*, 2016) and *N. meningitidis* (Lappann *et al.*, 2013), further supporting the notion that surface localisation of SBPs is not unprecedented.

Further WC-ELISA analysis confirmed that antisera against NGO1152 and NGO0206 consistently recognised these proteins on the surface of the WT-FA1090 strains, as well as in the induced complemented strains (MR331152 and MR330206). In contrast, antibody binding was significantly reduced in Δ*ng1152* and Δ*ngo0206* deletion mutants or uninduced strains, indicating that immune recognition is directly dependent on protein expression.

To evaluate whether these findings extend beyond a single laboratory strain, WC-ELISA examined seven genetically and geographically diverse clinical isolates. Both anti-NGO1152 and anti-NGO0206 antibodies exhibited strong

binding affinity to their respective antigens across all isolates tested, although minor variations in binding were observed compared to WT-FA1090. These clinical isolates were obtained from male and female patients at a range of anatomical sites, including the cervix, urethra, high vaginal tract, rectum, and additional locations. Further isolates were obtained from individuals diagnosed with either uncomplicated or complicated DGI. Our findings confirmed that NGO1152 and NGO0206 are surface exposed antigens that possess broadly accessible antigenic properties across multiple strains and are predicted to be capable of eliciting bactericidal responses, as demonstrated below.

Importantly, these observations align with the findings of Zhu *et al*. (2019), who reported the immune recognition of six additional antigens (NGO0690, NGO1043, NGO0416, NGO0948, NGO1215, and NGO1701) across multiple strains using both immunoblotting and WC-ELISA (Zhu *et al.*, 2019). While some variability in protein expression and antibody binding was noted, the overall recognition of these antigens across different isolates reinforces the concept that certain gonococcal surface proteins possess conserved immunogenic properties (Zhu *et al.*, 2019). Taken together, both our study and that of Zhu *et al*. (2019) strengthen the rationale for prioritising surface exposed proteins as vaccine candidates with the potential to overcome strain-specific limitations.

SBA is widely recognised as the gold standard *in vitro* method for evaluating the complement-dependent bactericidal activity of antibodies, whether induced through active immunisation (McIntosh *et al.*, 2015) or administered via passive immunisation (Guachalla *et al.*, 2017). In this assay, human or rabbit serum serves as the complement source, while target bacteria are incubated with specific antibodies or immune serum. Bacterial survival is then assessed by comparing results with those obtained using a negative control antibody, non-immune serum, or an inactivated complement source (Fantoni *et al.*, 2024). Rabbit serum is often preferred over human serum, as baby rabbit sera naturally lack pre-existing antibodies, reducing potential interference (McIntosh *et al.*, 2015; Santos *et al.*, 2001). Previous studies have explored methods to deplete pre-existing antibodies from human serum using Protein G affinity purification. However, this approach has significant limitations, including the unintended

depletion of essential complement components such as C1q and C5 (Brookes *et al.*, 2013). Additionally, this method does not remove IgM or IgA, two antibody isotypes that also contribute to complement activation (Murphy and Weaver, 2016).

Bacteria can exhibit natural susceptibility or resistance to complement-mediated killing, even in the absence of antibodies. If a bacterial strain is either highly sensitive or highly resistant to complement activity, the SBA assay becomes unsuitable for evaluation (Toh *et al.*, 2021). Ideally, the complement source should originate from the same host species to accurately replicate the immune response during infection (Feavers and Walker, 2010). Therefore, when assessing bactericidal activity against human pathogens, human serum should be used as the complement source. For example, in the case of *N. meningitidis*, human complement derived from healthy donors may possess intrinsic bactericidal activity against meningococci. However, obtaining large quantities of complement with consistent haemolytic activity poses a challenge (Borrow *et al.*, 2020; Findlow *et al.*, 2022). As a result, each complement source must be validated for individual bacterial isolates to prevent assay interference.

A potential alternative is the use of a complement derived from a varied species (Plotkin, 2020). Rabbit complement is the most widely utilised and has consistently been shown to be a reliable and suitable source for serum bactericidal assays (rSBA). While rSBA has been widely applied in evaluating MenACWY vaccines, it is not suitable for MenB vaccine assessment, as rabbit complement tends to produce higher SBA titres. Consequently, only human complement (hSBA) is considered appropriate for evaluating the MenB vaccine (Plotkin, 2020).

In general, the assay involves live gonococci, usually grown until the mid-exponential phase, incubated with serially diluted sera, and an exogenous source of IgG/IgM-depleted pooled human complement. SBA is initiated when antibodies bind to specific antigens that are abundantly expressed on the bacterial cell surface. Nevertheless, the threshold density of antigen-antibody complexes needed to activate complement can also be achieved when antibodies simultaneously bind to several surface exposed antigens (Ispasanie *et al.*, 2023).

The final hypothesis in this research was addressed by performing SBA for both rabbit anti-NGO0206 and anti-NGO1152 polyclonal antibodies as a vital step in vaccine development. Specifically, the anti-NGO0206 antibody exhibited variable bactericidal titres against the WT-FA1090 strain, ranging from 1:1024 to 1:2048, in the presence of exogenous IgG/IgM-depleted pooled human complement. Conversely, the Δ*ngo0206* mutant, lacking NGO0206, exhibited a significantly reduced SBA titre of 1:512, indicating a diminished antibody effectiveness. This suggests that the absence of NGO0206 impairs the binding of anti-NGO0206 antibodies, thus hindering the initiation of the complement cascade and subsequent bacterial cell destruction. In contrast, the anti-NGO1152 serum displayed a significantly higher bactericidal titre of 1:8192, suggesting that it more effectively activates the complement system. This enhanced activity likely results from the binding of anti-NGO1152 immunoglobulin isotypes to abundant NGO1152 antigens on the bacterial surface, promoting complement cascade deposition and leading to greater complement-dependent lysis, particularly of the WT-FA1090 strain compared to the Δ*ngo1152* mutant.

Nevertheless, the findings reported in this research indicate that the anti-NGO0206 and anti-NGO1152 antibodies exhibit superior bactericidal capacity against *N. gonorrhoeae* compared to NMB1612 from *N. meningitidis* (Hung *et al.*, 2015). However, for bacterial vaccines, the SBA assay relies on intricate biological components, including live bacteria and specialised human complement, making standardisation more complex compared to antibody-binding assays (Feavers and Walker, 2010).

A recent study by Dijokaite-Guraliuc *et al*. (2023) analysed sera collected from patients with acute gonorrhoea or from sexual contacts of an index case at a hospital in the South of England during 1980–1982 (Zak *et al.*, 1984). Importantly, no information was available regarding whether these individuals had prior exposure to *N. meningitidis*, either symptomatically or asymptomatically. If such exposure had occurred, their sera may have contained antibodies against meningococcal homologs, potentially cross-reacting with gonococcal proteins such as NGO1152. Using immunoproteomic approaches, the authors identified antibodies recognising several gonococcal proteins with meningococcal homologs, specifically the surface exposed OM proteins such as

ZnuD, MIP, NalP, FbpA, ComP, and ArtJ (homologous to NGO1152 in *N. gonorrhoeae*). Although these proteins were clearly immunoreactive, the sera overall showed little or no significant complement-dependent SBA (Dijokaite-Guraliuc *et al.*, 2023). Only two of thirteen patients demonstrated ~50% killing of their homologous strain at a 1/4 serum dilution, while pooled sera achieved ~30% killing of the heterologous strain P9-17. This limited bactericidal effect may reflect the influence of blocking antibodies against proteins such as Rmp and H.8, which are known to inhibit SBA. Thus, while these surface exposed proteins are immunogenic and elicit antibody responses during natural infection, their ability to induce protective bactericidal activity was not demonstrated in this study, highlighting the likely need for additional immune mechanisms or tailored vaccine strategies (Dijokaite-Guraliuc *et al.*, 2023).

However, when compared to the SBA of anti-NGO1152 and anti-NGO0206, the trivalent vaccine antisera (Adenylate cyclase-associated protein App, NHBA, and MetQ) tested by Lu *et al*. (2024) in mice showed weaker bactericidal activity. In their study, stronger SBA responses were observed with titres ranging from 100 to 800 dilutions, particularly with the trivalent vaccine, when tested against the *N. gonorrhoeae* strains FA1090 and FA19. Bactericidal activity was reduced against sialylated gonococci when FA1090 was cultured with CMP-NANA, but no significant differences in binding to sialylated versus non-sialylated gonococci were detected in the ELISA (Lu *et al.*, 2024).

In contrast to the findings of the SBA of anti-NGO0206 and anti-NGO1152 antibodies, another study by Bagwe *et al*. (2023) investigated the immunogenicity of a whole-cell inactivated *N. gonorrhoeae* microparticle (Gc-MP) vaccine delivered transdermally via dissolving microneedles (MN) combined with adjuvant microparticles (Alhydrogel®-Alum MP and AddaVax™ MP) (Bagwe *et al.*, 2023).

Mice immunised with Gc-MP + Alum MP + AddaVax™ MP exhibited significant increases in gonococcal-specific serum IgG, IgG1, IgG2a, and vaginal mucosal IgA antibodies compared to control groups. The generated antibodies demonstrated bactericidal activity against live *N. gonorrhoeae* (Bagwe *et al.*, 2023). Additionally, immunised mice showed an enhanced clearance rate of gonococcal infection post-challenge, with complete clearance

by day 9, whereas control groups began clearing the infection around day 10. Furthermore, mice that received the full vaccine formulation displayed upregulated expression of cellular immunity markers, including CD4 and CD8 on T cells in the spleen and lymph nodes of immunised mice (Bagwe *et al.*, 2023).

These findings suggest that using microneedle-based immunisation or delivery of whole-cell inactivated gonococcal vaccines in the form of microparticles offers the advantage of inducing robust humoral, cellular, and protective immunity against gonococcal infection (Bagwe *et al.*, 2023). However, whole-cell vaccines have notable drawbacks, including potential reactogenicity due to inactivated whole-cell preparations often containing residual endotoxins like LOS, and a lack of antigen specificity, which can trigger strong inflammatory responses toward non-protective targets and reduce tolerability. Moreover, the lack of antigen specificity inherent to whole-cell vaccines means the immune system may be directed toward immunodominant but non-protective antigens, potentially compromising efficacy (Bagwe *et al.*, 2023).

Batch-to-batch variability in inactivation and formulation processes may also lead to inconsistent antigen presentation and pose challenges for quality control. In addition, whole-cell platforms are less amenable to rational vaccine design strategies, such as reverse vaccinology, which aim to selectively target conserved, surface exposed, and functionally relevant epitopes. There is also a theoretical risk of molecular mimicry, raising concerns about the potential for autoimmunity. Finally, issues related to vaccine stability and the need for cold-chain storage may hinder large-scale deployment, particularly in resource-limited settings. However, innovative delivery systems help mitigate some of these issues; whole-cell vaccines must be carefully evaluated against more refined subunit or epitope-based approaches (Bagwe *et al.*, 2023).

LOS sialylation is a well-established immune evasion mechanism in *N. gonorrhoeae* via molecular mimicry with host glycans, but NGO1152 and NGO0206 are SBPs, and there is currently no evidence that they are directly involved in LOS sialylation or glycan mimicry. Initially, sialylation was identified for its role in providing "unstable" serum resistance in gonococci recovered from urethral secretions, though this resistance did not persist

following laboratory passage (Giardina *et al.*, 2020). It has since been shown that sialylation inhibits all three complement activation pathways by reducing C1 engagement and C4b deposition while promoting factor H recruitment to the gonococcal surface (Gulati *et al.*, 2015).

Additionally, sialylated glycans allow the immune system to distinguish self from non-self, partly through interaction with sialic acid-binding immunoglobulin-like lectins (Siglecs) (Pillai *et al.*, 2012). Siglecs, expressed by various immune cells, including neutrophils - the primary immune cells involved in gonococcal infections -play a role in recognising these sialylated glycans. Siglec-5, -9, and -14 are found to be expressed on neutrophils. Both Siglec-5 and Siglec-9 contain immunoreceptor tyrosine-based inhibitory motifs (ITIMs), which recruit SH2 domain-containing phosphatases to inhibit cellular activation (Delaveris *et al.*, 2021). In contrast, Siglec-14 associates with the adapter protein DAP12, which contains an immunoreceptor tyrosine-based activating motif (ITAM). Upon phosphorylation, this motif recruits Syk kinase to initiate downstream signalling (Angata *et al.*, 2006). *Siglec-5* and *Siglec-14* genes are adjacent and are considered paired receptors due to their highly similar binding domains and glycan-binding preferences (Ali *et al.*, 2014). In certain racial and ethnic populations, 10%–70% of individuals carry a SIGLEC14/5 fusion gene, where Siglec-14 expression is absent, but Siglec-5 remains present. Thus, signalling through neutrophil Siglecs overall serves to dampen inflammatory responses. Sialylated *N. gonorrhoeae* has been shown to interact with the extracellular domains of these Siglecs, as observed with Fc chimeras proteins (Landig *et al.*, 2019). In addition to sialylation, *N. gonorrhoeae* expresses various gene products that help protect the bacteria from neutrophil antimicrobial activities (Palmer and Criss, 2018). The bacteria also modulate their ability to interact with neutrophils through the phase-variable expression of Opa proteins, which bind to one or more CEACAMs. Remarkably, binding to the granulocyte-specific CEACAM3 induces phagocytosis, reactive oxygen species production, and granule release (Ball and Criss, 2013).

Proposed future work

The outcomes of this research suggest several intriguing directions for further exploration. This research highlights several promising avenues for addressing *N. gonorrhoeae* antimicrobial resistance. One innovative strategy involves using nanocarriers in conjunction with ABC transporters to target NGO1152 and NGO0206 proteins. Nanocarriers, which are advanced nanoscale drug delivery systems, can be functionalised with anti-NGO1152 and anti-NGO0206 antibodies to deliver therapeutic agents directly to specific bacterial receptors, enabling controlled release and enhanced efficacy. Nanoparticles are particularly noteworthy for their multifunctional mechanisms, including disrupting bacterial cell walls, inhibiting protein synthesis, and altering cellular signalling pathways (Amarnani *et al.*, 2023). Their ability to increase bacterial membrane permeability and generate free radicals makes them potent agents against microbial resistance. Functionalising nanoparticles with anti-NGO1152 and anti-NGO0206 antibodies could further enhance their precision and lethality, potentially improving outcomes in gonococcal infections. Research into novel delivery methods, such as dissolving microneedles (MNs), also shows promise as discussed above.

A bivalent vaccine comprising anti-NGO1152 and anti-NGO0206 may enhance efficacy by targeting conserved, cross-reactive epitopes across *N. gonorrhoeae* strains. This multi-antigen approach mitigates risks associated with isolates that are deficient in either antigen or express non-cross-reactive variants, analogous to the strategy employed in the Bexsero meningococcal vaccine. Moreover, sustained immunogenicity is contingent upon optimal antigen accessibility to antibodies and effective engagement of immune recognition mechanisms.

Typically, this research establishes a foundation for evaluating the *in vivo* efficacy of anti-NGO1152 and anti-NGO0206 polyclonal antibodies against *N. gonorrhoeae* strains, including FA1090, DGI-18, MS11, and other clinical isolates, using a mouse vaginal colonisation model. Such a study would explore how these antibodies mediate protection, facilitate bacterial clearance, and compare the outcomes of pre- and post-infection immunisations. Adjuvants, such as MF59 and CpG-ODNs, could be used to activate immune responses.

Kim *et al*. (2020) showed that MF59 enhances antigen-specific CD8 T cell and antibody production. While CpG-ODNs mimic bacterial DNA and activate TLR9, boosting IgG responses critical for heterologous protection antibody responses (Kim *et al.*, 2020). CpG-ODNs are synthetic short single-stranded DNA molecules that contain unmethylated CpG motifs (cytosine-phosphate-guanine dinucleotides), which are common in bacterial and viral DNA but rare and usually methylated in vertebrate DNA.

To establish an *in vivo* model, female BALB/c mice treated with 17-β-estradiol and antibiotics would be used to simulate human-like gonococcal infection (Lu *et al.*, 2024). Groups of mice would be immunised via intranasal or subcutaneous routes with *N. gonorrhoeae*. Subsequently, they would be immunised with either anti-NGO0206 or anti-NGO1152 antibodies containing CpG-ODNs, or with a bivalent formulation containing both, to evaluate antigen-specific antibody responses to mediated clearance of *N. gonorrhoeae*. This combined approach may enhance efficacy by targeting conserved epitopes across *N. gonorrhoeae* strains, thereby reducing the risk of escape by non-cross-reactive variants. This strategy is analogous to the Bexsero meningococcal vaccine. Additionally, a separate group could first be immunised with either anti-NGO0206, anti-NGO1152, or the bivalent formulation, followed by infection with *N. gonorrhoeae*, to assess the potential for antibody-mediated protection against the pathogen. Further Future studies can employ NGO1152 and NGO0206, either individually or as a bivalent vaccine, in controlled human infection models (CHIMs), which could elucidate their ability to prevent disease in humans. CHIMs, despite ethical constraints limiting them to short-term studies in male volunteers, have significantly advanced our understanding of bacterial behaviour, antigenic variation, and host immunity. Evaluating these proteins in CHIMs may reveal critical insights for therapeutic development. Such research would leverage CHIMs' unique capacity to bridge preclinical and clinical studies, notwithstanding current limitations.

Upcoming research should focus on elucidating the specific biological roles of NGO1152 and NGO0206 in *N. gonorrhoeae*, particularly their contributions to adhesion and invasion of human cervical epithelial cells (ME-180) as well as their broader roles in pathogenicity and antimicrobial resistance. This could be

accomplished by comparing the Δ*ngo1152* and Δ*ngo0206* mutant strains with the WT-FA1090 strain. Such a comparison would help determine whether these mutants show reduced adhesion and invasion capabilities of these strains. Additionally, MR331152 and MR330206 complemented strains should be evaluated to see if restoring NGO1152 and NGO0206 expression could bring adhesion and invasion levels back to those seen in the WT-FA1090 strain. This would provide compelling evidence supporting the role of these proteins in mediating the attachment of *N. gonorrhoeae* to human cervical epithelial cells *in vitro* and possibly facilitating invasion.

To further validate their role in adhesion, performing antibody adhesion inhibition assays with anti-NGO1152 and anti-NGO0206 antisera is highly recommended. In this experiment, pre-incubating *N. gonorrhoeae* strains with varying concentrations of the antisera (for example, 1:20, 1:40, and 1:80) and assessing their ability to adhere to ME-180 cells would reveal whether the presence of these antibodies reduces adhesion in a concentration-dependent manner. A decrease in adhesion, when compared to the untreated WT-FA1090 strain, would offer convincing evidence for the involvement of NGO1152 and NGO0206 in the bacterial adhesion process.

Additionally, the impact of mutations in *ngo1152* and *ngo0206*, as well as the antisera treatment on *N. gonorrhoeae* colonisation, should be assessed using a female mouse model of lower genital tract infection. Mice would be intravaginally inoculated with equivalent numbers of WT-FA1090, Δ*ngo1152*, Δ*ngo0206*, MR331152, and MR330206 strains, alongside WT-FA1090 cells that have been pre-incubated with a 1:20 dilution of heat-inactivated anti-NGO1152 and anti-NGO0206 antisera. Vaginal secretions would then be collected to perform bacterial colony counts, allowing for a comparison of colonisation efficiency between the different strains. It is expected that the Δ*ngo1152* and Δ*ngo0206* strains will show significantly reduced colonisation compared to the WT-FA1090 strain. Furthermore, MR331152 and MR330206 are anticipated to restore colonisation ability to near WT-FA1090 levels. Pretreatment with anti-NGO1152 and anti-NGO0206 antisera is expected to notably inhibit the colonisation of WT-FA1090 cells.

Research summary: To date, no specific vaccine has been developed for gonorrhoea, highlighting the need for continued research into potential vaccine candidates. Therefore, developing or formulating vaccines targeting conserved antigens such as NGO1152 and NGO0206 is essential. NGO1152 and NGO0206 were found to be: (i) highly conserved in circulating clinical isolates, (ii) surface exposed antigens in *N. gonorrhoeae* and (iii) able to elicit potent complement-dependent bactericidal activity. The study's findings contribute valuable insights into the potential of NGO1152 and NGO0206 as vaccine candidates against *N. gonorrhoeae*. The development of an effective and accessible *N. gonorrhoeae* vaccine holds significant potential, offering a wide range of benefits including: (i) reducing the burden of urogenital infections on individuals and healthcare systems, (ii) improving outcomes in reproductive and neonatal health, and (iii) reducing the use of antimicrobials, which in turn could mitigate the risk of antimicrobial resistance.

References

Aas, F. E., Løvold, C., and Koomey, M. (2002). An inhibitor of DNA binding and uptake events dictates the proficiency of genetic transformation in *N. gonorrhoeae*: mechanism of action and links to Type IV pilus expression. *Molecular microbiology*, *46*(5), 1441-1450.

Abhilasha, K. V., and Marathe, G. K. (2021). Bacterial lipoproteins in sepsis. *Immunobiology*, *226*(5), 152128.

Adamczyk-Poplawska, M., Bacal, P., Mrozek, A., Matczynska, N., Piekarowicz, A., and Kwiatek, A. (2022). Phase-variable Type I methyltransferase M. NgoAV from *N. gonorrhoeae* FA1090 regulates phasevarion expression and gonococcal phenotype. *Frontiers in microbiology*, *13*, 917639.

Adamson, P. C., and Klausner, J. D. (2021). The staying power of pharyngeal gonorrhoea: implications for public health and antimicrobial resistance. In (Vol. 73, pp. 583-585): Oxford University Press US.

AdisInsight. (2023). NgG gonococcal vaccine development. Springer. [Online]. Available at: https://adisinsight.*springer.com/drugs*/800071273.

Agbodzi, B., Duodu, S., Dela, H., Kumordjie, S., Yeboah, C., Behene, E., Ocansey, K., Yanney, J. N., Boateng-Sarfo, G., and Kwofie, S. K. (2023). Whole genome analysis and antimicrobial resistance of *N. gonorrhoeae* isolates from Ghana. *Frontiers in microbiology*, *14*, 1163450.

Aggarwal, S., Singh, A. K., Balaji, S., and Ambalkar, D. (2022). Sexually transmitted infections (STIs) and its changing scenario: a scoping review. *Combinatorial Chemistry & High Throughput Screening*, *25*(10), 1630-1638.

Akhtar, A. A., and Turner, D. P. (2022). The role of bacterial ATP-binding cassette (ABC) transporters in pathogenesis and virulence: Therapeutic and vaccine potential. *Microbial pathogenesis*, *171*, 105734.

Akinbosede, D. O. (2022). *Haem scavenging by pathogenic Neisseriaceae bacteria through haemoglobin receptor HpuAB. Doctoral thesis, University of Sussex, UK.*

Ali, S. R., Fong, J. J., Carlin, A. F., Busch, T. D., Linden, R., Angata, T., Areschoug, T., Parast, M., Varki, N., and Murray, J. (2014). Siglec-5 and Siglec-14 are polymorphic paired receptors that modulate neutrophil and amnion signalling responses to group B *Streptococcus*. *Journal of Experimental Medicine*, *211*(6), 1231-1242.

Almonacid-Mendoza, H., Humbert, M., Dijokaite, A., Cleary, D., Soo, Y., Hung, M., Orr, C., Machelett, M., Tews, I., and Christodoulides, M. (2018). Structure of the recombinant *N. gonorrhoeae* adhesin complex protein (rNg-ACP) and generation of murine antibodies with bactericidal activity against gonococci. mSphere 3: e00331-18. In.

Amarnani, R., Revdekar, A., Salvi, B., and Shende, P. (2023). Potential of nanocarriers using ABC transporters for antimicrobial resistance. *Drug Discovery Today*, *28*(5), 103570.

Ambur, O. H., Frye, S. A., and Tønjum, T. (2007). New functional identity for the DNA uptake sequence in transformation and its presence in transcriptional terminators. *Journal of bacteriology*, *189*(5), 2077-2085.

Angata, T., Hayakawa, T., Yamanaka, M., Varki, A., and Nakamura, M. (2006). Discovery of Siglec-14, a novel sialic acid receptor undergoing concerted evolution with Siglec-5 in primates. *The FASEB journal*, *20*(12), 1964-1973.

Arnold, R., Galloway, Y., McNicholas, A., and O'Hallahan, J. (2011). Effectiveness of a vaccination programme for an epidemic of meningococcal B in New Zealand. *Vaccine*, *29*(40), 7100-7106.

Awate, O. A., Ng, D., Stoudenmire, J. L., Moraes, T. F., and Cornelissen, C. N. (2024). Investigating the importance of selected surface exposed loops in HpuB for haemoglobin binding and utilisation by *N. gonorrhoeae*. *Infection and immunity*, e00211-00224.

Azze, R. F. O. (2019). A meningococcal B vaccine induces cross-protection against gonorrhoea. *Clinical and experimental vaccine research*, *8*(2), 110-115.

Baarda, B. I., Martinez, F. G., and Sikora, A. E. (2018). Proteomics, bioinformatics and structure-function antigen mining for gonorrhoea vaccines. *Frontiers in immunology*, *9*, 2793.

Baarda, B. I., Zielke, R. A., Le Van, A., Jerse, A. E., and Sikora, A. E. (2019). *N. gonorrhoeae* MlaA influences gonococcal virulence and membrane vesicle production. *PLoS pathogens*, *15*(3), e1007385.

Bagwe, P., Bajaj, L., Menon, I., Gomes, K. B., Kale, A., Patil, S., Vijayanand, S., Gala, R., D'Souza, M. J., and Zughaier, S. M. (2023). Gonococcal microparticle vaccine in dissolving microneedles induced immunity and enhanced bacterial clearance in infected mice. *International Journal of Pharmaceutics*, *642*, 123182.

Balasingham, S. V., Collins, R. F., Assalkhou, R., Homberset, H. v., Frye, S. A., Derrick, J. P., and Tønjum, T. (2007). Interactions between the lipoprotein PilP and the secretin PilQ in *N. meningitidis*. *Journal of bacteriology*, *189*(15), 5716-5727.

Balboa, J., Romeu, B., Baró, M., Campa, C., Lantero, M., Sierra, G., Galindo, M., Harandi, A., Lastre, M., and Pérez, O. (2009). Mucosal approaches in *Neisseria* vaccinology. *VacciMonitor*, *18*(2), 53-55.

Ball, L. M., and Criss, A. K. (2013). Constitutively Opa-expressing and Opa-deficient *N. gonorrhoeae* strains differentially stimulate and survive exposure to human neutrophils. *Journal of bacteriology*, *195*(13), 2982-2990.

BASHH. (2019). British Association for Sexual Health and HIV (2019). UK national guideline for the management of infection with *N.*

gonorrhoeae. [Online]. Available at: https://www.bashh.org/_userfiles /pages/files/ng_guideline_251124.pdf [Accessed 3 July 2025].

BASHH. (2025). British Association for Sexual Health and HIV. (2025). UK national guideline for the management of gonorrhoea. [Online]. Available at: https://www.bashh.org/_userfiles/pages/files/gc_guideli ne_2025_final.pdf [Accessed 3 July 2025].

Bayliss, C. D., Field, D., and Moxon, E. R. (2001). The simple sequence contingency loci of *Haemophilus influensae* and *N. meningitidis*. *The Journal of Clinical Investigation*, *107*(6), 657-666.

Beernink, P. T., Ispasanie, E., Lewis, L. A., Ram, S., Moe, G. R., and Granoff, D. M. (2019). A Meningococcal Native Outer Membrane Vesicle Vaccine With Attenuated Endotoxin and Overexpressed Factor H Binding Protein Elicits Gonococcal Bactericidal Antibodies. *The Journal of Infectious Diseases*, *219*(7), 1130-1137.

Begier, E., Seiden, D. J., Patton, M., Zito, E., Severs, J., Cooper, D., Eiden, J., Gruber, W. C., Jansen, K. U., Anderson, A. S., and Gurtman, A. (2017). SA4Ag, a 4-antigen *Staphylococcus aureus* vaccine, rapidly induces high levels of bacteria-killing antibodies. *Vaccine*, *35*(8), 1132-1139.

Beinrohr, L., Dobó, J., Závodszky, P., and Gál, P. (2008). C1, MBL–MASPs and C1-inhibitor: novel approaches for targeting complement-mediated inflammation. *Trends in Molecular Medicine*, *14*(12), 511-521.

Beis, K. (2015). Structural basis for the mechanism of ABC transporters. *Biochemical Society transactions*, *43*(5), 889-893.

Bennett, J. S., Jolley, K. A., Sparling, P. F., Saunders, N. J., Hart, C. A., Feavers, I. M., and Maiden, M. C. (2007). Species status of *N. gonorrhoeae*: evolutionary and epidemiological inferences from multilocus sequence typing. *BMC biology*, *5*, 1-11.

Berntsson, R. P. A., Smits, S. H. J., Schmitt, L., Slotboom, D.-J., and Poolman, B. (2010). Addendum to "A structural classification of substrate-binding proteins" [FEBS Lett. 584 (2010) 2606–2617]. *FEBS letters*, *584*(20), 4373-4373.

Berti, F., Romano, M. R., Micoli, F., and Adamo, R. (2021). Carbohydrate-based meningococcal vaccines: past and present overview. *Glycoconjugate journal*, *38*(4), 401-409.

Bettinger, J. A., Scheifele, D. W., Halperin, S. A., Vaudry, W., Findlow, J., Borrow, R., Medini, D., Tsang, R., the members of the Canadian, F., and Program, I. M. (2013). Diversity of Canadian meningococcal serogroup B isolates and estimated coverage by an investigational meningococcal serogroup B vaccine (4CMenB). *Vaccine*, *32*(1), 124-130.

Bhattacharya, A., Bhattacharya, S., Agarwal, S., and Dasgupta, J. (2022). Structural Insights of Cobalamin and Cobinamide Uptake by ABC Importer of *Vibrio* Species. *Immune function is depressed with aging while inflammation is*, 67.

Biała, M., Pencakowski, B., Mączyńska, B., Starzyński, K., and Szetela, B. (2024). HIV-Negative MSM Infected with Two Different Isolates of Drug-Resistant *N. gonorrhoeae* Case Report. *Pathogens*, *13*(6), 497.

Biemans-Oldehinkel, E., Doeven, M. K., and Poolman, B. (2006). ABC transporter architecture and regulatory roles of accessory domains. *FEBS letters*, *580*(4), 1023-1035.

Bilitewski, U., Blodgett, J. A., Duhme-Klair, A. K., Dallavalle, S., Laschat, S., Routledge, A., and Schobert, R. (2017). Chemical and Biological Aspects of Nutritional Immunity—Perspectives for New Anti-Infectives that Target Iron Uptake Systems. *Angewandte Chemie International Edition*, *56*(46), 14360-14382.

Binepal, G., Jurga, E., Carruthers-Lay, D., Krüger, S., Zittermann, S., Minion, J., Diggle, M., Alexander, D. C., Martin, I., and Allen, V. (2024). Phenotypic diversity and shared genomic determinants among isolates causing a large incidence of disseminated gonococcal infections in Canada. *bioRxiv*, 2024.2009. 2008.611882.

Binker, M. G., Cosen-Binker, L. I., Terebiznik, M. R., Mallo, G. V., McCaw, S. E., Eskelinen, E. L., Willenborg, M., Brumell, J. H., Saftig, P., and Grinstein, S. (2007). Arrested maturation of Neisseria-containing phagosomes in the absence of the lysosome-associated membrane proteins, LAMP-1 and LAMP-2. *Cellular microbiology*, *9*(9), 2153-2166.

Bisht, N., Sharma, B., Shalini, Joshi, N., and Tewari, L. (2018). Role of microbial siderophore in Iron acquisition and amelioration of plant stress in saline soil. *Biotech Today: An International Journal of Biological Sciences*, *8*(2), 7.

Bolla, J. R., Su, C.-C., Do, S. V., Radhakrishnan, A., Kumar, N., Long, F., Chou, T.-H., Delmar, J. A., Lei, H.-T., Rajashankar, K. R., Shafer, W. M., and Yu, E. W. (2014). Crystal structure of the *N. gonorrhoeae* MtrD inner membrane multidrug efflux pump. *PloS one*, *9*(6), e97903.

Borrow, R., Taha, M.-K., Giuliani, M. M., Pizza, M., Banzhoff, A., and Bekkat-Berkani, R. (2020). Methods to evaluate serogroup B meningococcal vaccines: from predictions to real-world evidence. *Journal of Infection*, *81*(6), 862-872.

Bos, M. P., Grijpstra, J., Tommassen-van Boxtel, R., and Tommassen, J. (2014). Involvement of *N. meningitidis* lipoprotein GNA2091 in the assembly of a subset of outer membrane proteins. *Journal of Biological Chemistry*, *289*(22), 15602-15610.

Boslego, J. W., Tramont, E. C., Chung, R. C., McChesney, D. G., Ciak, J., Sadoff, J. C., Piziak, M. V., Brown, J. D., Brinton Jr, C. C., and Wood, S. W. (1991). Efficacy trial of a parenteral gonococcal pilus vaccine in men. *Vaccine*, *9*(3), 154-162.

Boyer, E., Bergevin, I., Malo, D., Gros, P., and Cellier, M. (2002). Acquisition of Mn (II) in addition to Fe (II) is required for full virulence of *Salmonella enterica serovar Typhimurium*. *Infection and immunity*, *70*(11), 6032-6042.

Bradford, P. A., Miller, A. A., O'Donnell, J., and Mueller, J. P. (2020). Zoliflodacin: an oral spiropyrimidinetrione antibiotic for the treatment of *N. gonorrhoea,* including multi-drug-resistant isolates. *ACS infectious diseases*, *6*(6), 1332-1345.

Briles, D. E., Ades, E., Paton, J. C., Sampson, J. S., Carlone, G. M., Huebner, R. C., Virolainen, A., Swiatlo, E., and Hollingshead, S. K. (2000). Intranasal immunisation of mice with a mixture of the pneumococcal proteins PsaA and PspA is highly protective against nasopharyngeal carriage of *S. pneumoniae*. *Infection and immunity*, *68*(2), 796-800.

Brodl, E., Niederhauser, J., and Macheroux, P. (2018). In situ measurement and correlation of cell density and light emission of bioluminescent bacteria. *JoVE Journal of Visualised Experiments*(136), e57881.

Brookes, C., Kuisma, E., Alexander, F., Allen, L., Tipton, T., Ram, S., Gorringe, A., and Taylor, S. (2013). Development of a large-scale human complement source for use in bacterial immunoassays. *Journal of immunological methods*, *391*(1-2), 39-49.

Bulut, H., Ma, Q., Moniot, S., Saenger, W., Schneider, E., and Vahedi-Faridi, A. (2012). Crystal structures of receptors involved in small-molecule transport across membranes. *European journal of cell biology*, *91*(4), 318-325.

Cahoon, L. A., and Seifert, H. S. (2011). Focusing homologous recombination: pilin antigenic variation in the pathogenic *Neisseria*. *Molecular microbiology*, *81*(5), 1136-1143.

Callaghan, M. M., Koch, B., Hackett, K. T., Klimowicz, A. K., Schaub, R. E., Krasnogor, N., and Dillard, J. P. (2021). Expression, localisation, and protein interactions of the partitioning proteins in the gonococcal type IV secretion system. *Frontiers in microbiology*, *12*, 784483.

Cardenas, A. J., Thomas, K. S., Broden, M. W., Ferraro, N. J., Pires, M. M., John, C. M., Jarvis, G. A., and Criss, A. K. (2024). *N. gonorrhoeae* scavenges host sialic acid for Siglec-mediated, complement-independent suppression of neutrophil activation. *MBio*, *15*(5), e00119-00124.

Carlson, M. L., Stacey, R. G., Young, J. W., Wason, I. S., Zhao, Z., Rattray, D. G., Scott, N., Kerr, C. H., Babu, M., Foster, L. J., and Van Hoa, F. D. (2019). Profiling the *E. coli* membrane protein interactome captured in peptidisc libraries. *eLife*, *8*.

Carter, E., Davis, S. A., and Hill, D. J. (2022). Rapid detection of *N. gonorrhoeae* genomic DNA using gold nanoprobes which target the gonococcal DNA uptake sequence. *Frontiers in cellular and infection microbiology*, *12*, 920447.

Cassat, James E., and Skaar, Eric P. (2013). Iron in Infection and Immunity. *Cell host & microbe*, *13*(5), 509-519.

CDC. (2022). Centres for Disease Control and Prevention (2022). Sexually transmitted disease surveillance 2020: National overview. [Online].

Available at: https://stacks.cdc.gov/view/cdc/125947 (Accessed: 6 November 2024).

Chan, C., Andisi, V. F., Ng, D., Ostan, N., Yunker, W. K., and Schryvers, A. B. (2018). Are lactoferrin receptors in Gram-negative bacteria viable vaccine targets? *Biometals*, *31*(3), 381-398.

Chan, Y. A., Hackett, K. T., and Dillard, J. P. (2012). The lytic transglycosylases of *N. gonorrhoeae*.

Chang, H., Wang, Y., Hui, L., Diao, Y., Ma, P., Li, X., and Wang, F. (2025). iTRAQ proteomic analysis of the anterior insula in morphine-induced conditioned place preference rats with high-frequency deep brain stimulation intervention. *Addiction Biology*, *30*(1), e70014.

Château, A., and Seifert, H. S. (2016). *N. gonorrhoeae* survives within and modulates apoptosis and inflammatory cytokine production of human macrophages. *Cellular microbiology*, *18*(4), 546-560.

Chen, A., and Seifert, H. S. (2011). *N. gonorrhoeae* mediated inhibition of apoptotic signalling in polymorphonuclear leukocytes. *Infection and immunity*, *79*(11), 4447-4458.

Chen, M. Y., McNulty, A., Avery, A., Whiley, D., Tabrizi, S. N., Hardy, D., Das, A. F., Nenninger, A., Fairley, C. K., and Hocking, J. S. (2019). Solithromycin versus ceftriaxone plus azithromycin for the treatment of uncomplicated genital gonorrhoea (SOLITAIRE-U): a randomised phase 3 non-inferiority trial. *The Lancet infectious diseases*, *19*(8), 833-842.

Chen, T., Grunert, F., Medina-Marino, A., and Gotschlich, E. C. (1997). Several carcinoembryonic antigens (CD66) serve as receptors for gonococcal opacity proteins. *The Journal of experimental medicine*, *185*(9), 1557-1564.

Chidiac, O., AlMukdad, S., Harfouche, M., Harding-Esch, E., and Abu-Raddad, L. J. (2024). Epidemiology of gonorrhoea: systematic review, meta-analyses, and meta-regressions, World Health Organisation European Region, 1949 to 2021. *Eurosurveillance*, *29*(9), 2300226.

Choby, J. E., and Skaar, E. P. (2016). Haem Synthesis and Acquisition in Bacterial Pathogens. *Journal of molecular biology*, *428*(17), 3408-3428.

Choi, C. C., and Ford, R. C. (2021). ATP-binding cassette importers in eukaryotic organisms. *Biological Reviews*, *96*(4), 1318-1330.

Cockerell, S. R., Rutkovsky, A. C., Zayner, J. P., Cooper, R. E., Porter, L. R., Pendergraft, S. S., Parker, Z. M., McGinnis, M. W., and Karatan, E. (2014). *Vibrio Cholerae* NspS, a homologue of ABC-type periplasmic solute binding proteins, facilitates transduction of polyamine signals independent of their transport. *Microbiology (Society for General Microbiology)*, *160*(5), 832-843.

Cole, J. G., and Jerse, A. E. (2009). Functional characterisation of antibodies against *N. gonorrhoeae* opacity protein loops. *PloS one*, *4*(12), e8108-e8108.

Colón Pérez, J., Villarino Fernández, R.-A., Domínguez Lago, A., Treviño Castellano, M. M., Pérez del Molino Bernal, M. L., Sánchez Poza, S., and Torres-Sangiao, E. (2024). Addressing Sexually Transmitted Infections Due to *N. gonorrhoeae* in the Present and Future. *Microorganisms*, *12*(5), 884.

Cornelissen, C. N. (2018). Subversion of nutritional immunity by the pathogenic *Neisseriae*. *Pathogens and disease*, *76*(1).

Cornelissen, C. N., and Hollander, A. (2011). TonB-dependent transporters expressed by *N. gonorrhoeae*. *Frontiers in microbiology*, *2*, 117.

Costa, T. R. D., Felisberto-Rodrigues, C., Meir, A., Prevost, M. S., Redzej, A., Trokter, M., and Waksman, G. (2015). Secretion systems in Gram-negative bacteria: Structural and mechanistic insights. *Nature reviews. Microbiology*, *13*(6), 343-359.

Craig, A. P., Gray, R. T., Edwards, J. L., Apicella, M. A., Jennings, M. P., Wilson, D. P., and Seib, K. L. (2015). The potential impact of vaccination on the prevalence of gonorrhoea. *Vaccine*, *33*(36), 4520-4525.

Crawford, A., and Wilson, D. (2015). Essential metals at the host–pathogen interface: nutritional immunity and micronutrient assimilation by human fungal pathogens. *FEMS yeast research*, *15*(7), fov071.

Cremieux, A., Puissant, A., Ancelle, R., and Martin, P. (1984). Bactericidal antibodies against *N. gonorrhoeae* elicited by *N. meningitidis*. *The Lancet*, *324*(8408), 930.

Criss, A. K., Kline, K. A., and Seifert, H. S. (2005). The frequency and rate of pilin antigenic variation in *N. gonorrhoeae*. *Molecular microbiology*, *58*(2), 510-519.

Crosby, R., and Salazar, L. F. (2015). Reduction of condom use errors from a brief, clinic-based intervention: a secondary analysis of data from a randomised, controlled trial of young black males. *Sexually transmitted infections*, *91*(2), 111-115.

Cyr, S. S. (2020). Update to CDC's treatment guidelines for gonococcal infection, 2020. *MMWR. Morbidity and mortality weekly report*, *69*.

Dam, V. V., and Bos, M. P. (2012). Generating knock-out and complementation strains of *N. meningitidis*. In *N. meningitidis* (pp. 55-72). Springer.

De Boer, M., Gouridis, G., Vietrov, R., Begg, S. L., Schuurman-Wolters, G. K., Husada, F., Eleftheriadis, N., Poolman, B., McDevitt, C. A., and Cordes, T. (2019). Conformational and dynamic plasticity in substrate-binding proteins underlies selective transport in ABC importers. *eLife*, *8*.

Deguchi, T., Yasuda, M., Yokoi, S., Ishida, K.-I., Ito, M., Ishihara, S., Minamidate, K., Harada, Y., Tei, K., and Kojima, K. (2003). Treatment of uncomplicated gonococcal urethritis by double-dosing of 200 mg cefixime at a 6-h interval. *Journal of infection and chemotherapy*, *9*(1), 35-39.

Delaveris, C. S., Wilk, A. J., Riley, N. M., Stark, J. C., Yang, S. S., Rogers, A. J., Ranganath, T., Nadeau, K. C., Biobank, S. C.-., and Blish, C. A. (2021). Synthetic Siglec-9 agonists inhibit neutrophil activation associated with COVID-19. *ACS central science*, *7*(4), 650-657.

Delepelaire, P. (2019). Bacterial ABC transporters of iron-ontaining compounds. *Research in microbiology*, *170*(8), 345-357.

Deo, P., Chow, S. H., Hay, I. D., Kleifeld, O., Costin, A., Elgass, K. D., Jiang, J.-H., Ramm, G., Gabriel, K., and Dougan, G. (2018). Outer membrane vesicles from *N. gonorrhoeae* target PorB to mitochondria and induce apoptosis. *PLoS pathogens*, *14*(3), e1006945.

DeRocco, A. J., and Cornelissen, C. N. (2007). Identification of Transferrin-Binding Domains in TbpB Expressed by *N. gonorrhoeae*. *Infection and immunity*, *75*(7), 3220-3232.

DeRocco, A. J., Yost-Daljev, M. K., Kenney, C. D., and Cornelissen, C. N. (2008). Kinetic analysis of ligand interaction with the gonococcal transferrin-iron acquisition system. *Biometals*, *22*(3), 439-451.

Dhital, S., Deo, P., Bharathwaj, M., Horan, K., Nickson, J., Azad, M., Stuart, I., Chow, S. H., Gunasinghe, S. D., and Bamert, R. (2022). *N. gonorrhoeae*-derived outer membrane vesicles package β-lactamases to promote antibiotic-resistance. *Microlife*, *3*, uqac013.

Dhungana, S., Taboy, C. H., Anderson, D. S., Vaughan, K. G., Aisen, P., Mietzner, T. A., and Crumbliss, A. L. (2003). The Influence of the Synergistic Anion on Iron Chelation by Ferric Binding Protein, a Bacterial Transferrin. *Proceedings of the National Academy of Sciences - PNAS*, *100*(7), 3659-3664.

Diallo, K., MacLennan, J., Harrison, O. B., Msefula, C., Sow, S. O., Daugla, D. M., Johnson, E., Trotter, C., MacLennan, C. A., and Parkhill, J. (2019). Genomic characterisation of novel *Neisseria* species. *Scientific reports*, *9*(1), 13742.

Díaz, L. M. R., González, M. d. S. L., Cuello, M., Sierra-González, V. G., Pupo, R. R., Lantero, M. I., Harandi, A. M., Black, S., and Pérez, O. (2021). VA-MENGOC-BC vaccination induces serum and mucosal anti-*N. gonorrhoeae* immune responses and reduces the incidence of gonorrhoea. *The Pediatric Infectious Disease Journal*, *40*(4), 375-381.

Dijokaite-Guraliuc, A., Humbert, M. V., Skipp, P., Cleary, D. W., Heckels, J. E., and Christodoulides, M. (2023). An immunoproteomics study of antisera from patients with gonorrhoea identifies novel *N. gonorrhoeae* proteins. *Frontiers in Bacteriology*, *2*, 1240807.

Dillard, J. P. (2011). Genetic manipulation of *N. gonorrhoeae*. *Current Protocols in Microbiology*, *23*(1), 4A. 2.1-4A. 2.24.

Dillard, J. P., and Chan, J. M. (2024). Genetic Manipulation of *N. gonorrhoeae* and Commensal *Neisseria* Species. *Current Protocols*, *4*(9), e70000.

Donnarumma, D., Golfieri, G., Brier, S., Castagnini, M., Veggi, D., Bottomley, M. J., Delany, I., and Norais, N. (2015). *N. meningitidis* GNA1030 is a ubiquinone-8 binding protein. *The FASEB journal*, *29*(6), 2260-2267.

e Silva, M. V. M. (2021). *Fitness Strategies of Fastidious Prokaryotes. Doctoral thesis, Auburn University, USA.*

ECDC. (2012). European Centre for Disease Prevention and Control, Stockholm (2012). Molecular typing of *N. gonorrhoeae*: results from a pilot study 2010–2011.

ECDC. (2019). European Centre for Disease Prevention and Control (2019). Response plan to control and manage the threat of multi-and extensively drug-resistant gonorrhoea in Europe. [Online]. Available at: https://www.ecdc.europa.eu/sites/default/files/documents/multi-andextensively-drug-resistant-gonorrhoea-response-plan-Europe-2019.pdf [Accessed 30 July 2021].

ECDC. (2023). European Centre for Disease Prevention and Control. (2023). Gonorrhoea - Annual Epidemiological Report for 2022. [Online]. Available at: https://www.ecdc.europa.eu/sites/default/files/documents/GONO_AER_2022_Report%20FINAL.pdf [Accessed 15 October 2024].

Edwards, J. L., Balthazar, J. T., Esposito, D. L., Ayala, J. C., Schiefer, A., Pfarr, K., Hoerauf, A., Alt, S., Hesterkamp, T., and Grosse, M. (2022). Potent *in vitro* and *ex vivo* anti-gonococcal activity of the RpoB inhibitor corallopyronin A. *Msphere*, *7*(5), e00362-00322.

Edwards, J. L., Jennings, M. P., Apicella, M. A., and Seib, K. L. (2016). Is gonococcal disease preventable? The importance of understanding immunity and pathogenesis in vaccine development. *Critical reviews in microbiology*, *42*(6), 928-941.

Edwards, J. L., Jennings, M. P., and Seib, K. L. (2018). *N. gonorrhoeae* vaccine development: hope on the horizon? *Current opinion in infectious diseases*, *31*(3), 246-250.

Eitinger, T., Rodionov, D. A., Grote, M., and Schneider, E. (2011). Canonical and ECF-type ATP-binding cassette importers in prokaryotes: diversity in modular organisation and cellular functions. *FEMS microbiology reviews*, *35*(1), 3-67.

El-Rami, F. E., Zielke, R. A., Wi, T., Sikora, A. E., and Unemo, M. (2019). Quantitative Proteomics of the 2016 WHO *N. gonorrhoeae* Reference Strains Surveys Vaccine Candidates and Antimicrobial Resistance Determinants*[S]. *Molecular & Cellular Proteomics*, *18*(1), 127-150.

Elendu, C., Amaechi, D. C., Elendu, I. D., Elendu, T. C., Amaechi, E. C., Usoro, E. U., Chima-Ogbuiyi, N. L., Agbor, D. B. A., Onwuegbule, C. J., and Afolayan, E. F. (2024). Global perspectives on the burden of sexually transmitted diseases: A narrative review. *Medicine*, *103*(20), e38199.

Escobar, A., Candia, E., Reyes-Cerpa, S., Villegas-Valdes, B., Neira, T., Lopez, M., Maisey, K., Tempio, F., Ríos, M., Acuña-Castillo, C., and Imarai, M. (2013). *N. gonorrhoeae* Induces a Tolerogenic Phenotype in Macrophages to Modulate Host Immunity. *Mediators of inflammation*, *2013*, 127017-127017.

Escobar, A., Rodas, P. I., and Acuña-Castillo, C. (2018). Macrophage-*N. gonorrhoeae* interactions: a better understanding of pathogen mechanisms of immunomodulation. *Frontiers in immunology*, *9*, 3044.

Eyre, D. W., Sanderson, N. D., Lord, E., Regisford-Reimmer, N., Chau, K., Barker, L., Morgan, M., Newnham, R., Golparian, D., and Unemo, M. (2018). Gonorrhoea treatment failure caused by a *N. gonorrhoeae* strain with combined ceftriaxone and high-level azithromycin resistance, England, February 2018. *Eurosurveillance*, *23*(27), 1800323.

Eyre, D. W., Town, K., Street, T., Barker, L., Sanderson, N., Cole, M. J., Mohammed, H., Pitt, R., Gobin, M., and Irish, C. (2019). Detection in the United Kingdom of the *N. gonorrhoeae* FC428 clone, with ceftriaxone resistance and intermediate resistance to azithromycin, October to December 2018. *Eurosurveillance*, *24*(10), 1900147.

Fantoni, G., Boccadifuoco, G., Verdirosa, F., Molesti, E., Manenti, A., and Montomoli, E. (2024). Current challenges and improvements in assessing the immunogenicity of bacterial vaccines. *Frontiers in microbiology*, *15*, 1404637.

Feavers, I., and Walker, B. (2010). Functional antibody assays. *Vaccine Adjuvants: Methods and Protocols*, 199-211.

Fegan, J. E., Calmettes, C., Islam, E. A., Ahn, S. K., Chaudhuri, S., Yu, R.-h., Gray-Owen, S. D., Moraes, T. F., and Schryvers, A. B. (2019). Utility of hybrid transferrin binding protein antigens for protection against pathogenic *Neisseria* species. *Frontiers in immunology*, *10*, 247.

Feinen, B., Jerse, A. E., Gaffen, S. L., and Russell, M. W. (2010). Critical role of Th17 responses in a murine model of *N. gonorrhoeae* genital infection. *Mucosal immunology*, *3*(3), 312-321.

Fifer, H., Natarajan, U., Jones, L., Alexander, S., Hughes, G., Golparian, D., and Unemo, M. (2016). Failure of dual antimicrobial therapy in treatment of gonorrhoea. *New England Journal of Medicine*, *374*(25), 2504-2506.

Findlow, J., Lucidarme, J., Taha, M.-K., Burman, C., and Balmer, P. (2022). Correlates of protection for meningococcal surface protein vaccines: lessons from the past. *Expert review of vaccines*, *21*(6), 739-751.

Fischer, F., Robbe-Saule, M., Turlin, E., Mancuso, F., Michel, V., Richaud, P., Veyrier, F. J., De Reuse, H., and Vinella, D. (2016). Characterisation in *Helicobacter pylori* of a Nickel Transporter Essential for Colonisation That Was Acquired during Evolution by Gastric *Helicobacter* Species. *PLoS pathogens*, *12*(12), e1006018.

Flemming, C. D. (2023). *A modular plasmid system for expression of genes in N. gonorrhoeae. Doctoral thesis, University of Waikato, New Zealand.*

Fung, M., Scott, K. C., Kent, C. K., and Klausner, J. D. (2007). Chlamydial and gonococcal reinfection among men: a systematic review of data to evaluate the need for retesting. *Sexually transmitted infections*, *83*(4), 304-309.

Gao, S., Gao, L., Yuan, D., Lin, X. a., and van der Veen, S. (2024). Gonococcal OMV-delivered PorB induces epithelial cell mitophagy. *Nature communications*, *15*(1), 1669.

Gasparini, R., Comanducci, M., Amicizia, D., Ansaldi, F., Canepa, P., Orsi, A., Icardi, G., Rizzitelli, E., De Angelis, G., and Bambini, S. (2014). Molecular and serological diversity of *N. meningitidis* carrier strains isolated from Italian students aged 14 to 22 years. *Journal of Clinical Microbiology*, *52*(6), 1901-1910.

Giardina, P. C., Apicella, M. A., Gibson, B., and Preston, A. (2020). Antigenic mimicry in *Neisseria* species. In *Endotoxin in Health and Disease* (pp. 55-65). CRC Press.

Girgis, M. M., and Christodoulides, M. (2023). Vertebrate and Invertebrate Animal and New *In Vitro* Models for Studying *Neisseria* Biology. *Pathogens*, *12*(6), 782.

Gokarn, K., and Pal, R. B. (2018). Activity of siderophores against drug-resistant Gram-positive and Gram-negative bacteria. *Infection and drug resistance*, 61-75.

Golparian, D., Hellmark, B., Fredlund, H., and Unemo, M. (2010). Emergence, spread and characteristics of *N. gonorrhoeae* isolates with *in vitro* decreased susceptibility and resistance to extended-spectrum cephalosporins in Sweden. *Sexually transmitted infections*, *86*(6), 454-460.

Golparian, D., Ohlsson, A., Janson, H., Lidbrink, P., Richtner, T., Ekelund, O., Fredlund, H., and Unemo, M. (2014). Four treatment failures of pharyngeal gonorrhoea with ceftriaxone (500 mg) or cefotaxime (500 mg), Sweden, 2013 and 2014. *Eurosurveillance*, *19*(30), 20862.

Golparian, D., Rose, L., Lynam, A., Mohamed, A., Bercot, B., Ohnishi, M., Crowley, B., and Unemo, M. (2018). Multidrug-resistant *N. gonorrhoeae* isolate, belonging to the internationally spreading Japanese FC428 clone, with ceftriaxone resistance and intermediate resistance to azithromycin, Ireland, August 2018. *Eurosurveillance*, *23*(47), 1800617.

Gómez-Santos, N., Glatter, T., Koebnik, R., Świątek-Połatyńska, M. A., and Søgaard-Andersen, L. (2019). A TonB-dependent transporter is required for secretion of protease PopC across the bacterial outer membrane. *Nature communications*, *10*(1), 1360.

Gottlieb, S. L., and Johnston, C. (2017). Future prospects for new vaccines against sexually transmitted infections. *Current opinion in infectious diseases*, *30*(1), 77-86.

Goytia, M., and Shafer, W. M. (2010). Polyamines can increase resistance of *N. gonorrhoeae* to mediators of the innate human host defence. *Infection and immunity*, *78*(7), 3187-3195.

GRASP. (2013). Health Protection Agency. Gonococcal Resistance to Antimicrobials Surveillance Programme (GRASP) Action Plan for

England and Wales: Informing the Public Health Response. In: Health Protection Agency, London, UK.

Gray, M. C., Thomas, K. S., Lamb, E. R., Werner, L. M., Connolly, K. L., Jerse, A. E., and Criss, A. K. (2023). Evaluating vaccine-elicited antibody activities against *N. gonorrhoeae*: cross-protective responses elicited by the 4CMenB meningococcal vaccine. *Infection and immunity*, *91*(12), e00309-00323.

Gregor, C., Gwosch, K. C., Sahl, S. J., and Hell, S. W. (2018). Strongly enhanced bacterial bioluminescence with the ilux operon for single-cell imaging. *Proceedings of the National Academy of Sciences*, *115*(5), 962-967.

GSK. (2023). GlaxoSmithKline plc receives US FDA Fast Track designation for investigational vaccine against gonorrhoe [Press release]. [Online]. Available at: https://www.gsk.com/en-gb/media/press-releases/gsk-receives-us-fda-fast-track-designation-for-investigational-vaccine-against-gonorrhoea/.

Guachalla, L. M., Hartl, K., Varga, C., Stulik, L., Mirkina, I., Malafa, S., Nagy, E., Nagy, G., and Szijártó, V. (2017). Multiple modes of action of a monoclonal antibody against multidrug-resistant *E. coli* Sequence Type 131-H 30. *Antimicrobial Agents and Chemotherapy*, *61*(11), 10.1128/aac. 01428-01417.

Guery, B., Galperine, T., and Barbut, F. (2019). *Clostridioides difficile*: diagnosis and treatments. *BMJ*, *366*.

Gulati, S., Mu, X., Zheng, B., Reed, G. W., Ram, S., and Rice, P. A. (2015). Antibody to reduction modifiable protein increases the bacterial burden and the duration of gonococcal infection in a mouse model. *The Journal of Infectious Diseases*, *212*(2), 311-315.

Gutiérrez-Preciado, A., Torres, A. G., Merino, E., Bonomi, H. R., Goldbaum, F. A., and García-Angulo, V. A. (2015). Extensive identification of bacterial riboflavin transporters and their distribution across bacterial species. *PloS one*, *10*(5), e0126124.

Hadad, R., Jacobsson, S., Pizza, M., Rappuoli, R., Fredlund, H., Olcén, P., and Unemo, M. (2012). Novel meningococcal 4 CM enB vaccine antigens–prevalence and polymorphisms of the encoding genes in *N. gonorrhoeae*. *Apmis*, *120*(9), 750-760.

Haese, E. C., Thai, V. C., and Kahler, C. M. (2021). Vaccine candidates for the control and prevention of the sexually transmitted disease gonorrhea. *Vaccines*, *9*(7), 804.

Hakenberg, O. W., Harke, N., and Wagenlehner, F. (2017). Urethritis in men and women. *European Urology Supplements*, *16*(4), 144-148.

Hamilton, H. L., Domínguez, N. M., Schwartz, K. J., Hackett, K. T., and Dillard, J. P. (2005). *N. gonorrhoeae* secretes chromosomal DNA via a novel type IV secretion system. *Molecular microbiology*, *55*(6), 1704-1721.

Handing, J. W., Ragland, S. A., Bharathan, U. V., and Criss, A. K. (2018). The MtrCDE efflux pump contributes to survival of *N. gonorrhoeae* from human neutrophils and their antimicrobial components. *Frontiers in microbiology*, *9*, 2688.

Handke, L. D., Gribenko, A. V., Timofeyeva, Y., Scully, I. L., and Anderson, A. S. (2018). MntC-dependent manganese transport is essential for *Staphylococcus aureus* oxidative stress resistance and virulence. *Msphere*, *3*(4), 10.1128/msphere. 00336-00318.

Harmsen, D., Singer, C., Rothgänger, J. r., Tønjum, T., Sybren de Hoog, G., Shah, H., Albert, J. r., and Frosch, M. (2001). Diagnostics of *Neisseriaceae* and *Moraxellaceae* by ribosomal DNA sequencing: ribosomal differentiation of medical microorganisms. *Journal of Clinical Microbiology*, *39*(3), 936-942.

Harrison, O. B., Bennett, J. S., Derrick, J. P., Maiden, M. C., and Bayliss, C. D. (2013). Distribution and diversity of the haemoglobin–haptoglobin iron-acquisition systems in pathogenic and non-pathogenic *Neisseria*. *Microbiology*, *159*(Pt_9), 1920-1930.

Haschka, D., Hoffmann, A., and Weiss, G. (2021). Iron in immune cell function and host defence. Seminars in cell and developmental biology,

Heesterbeek, D. A., Angelier, M. L., Harrison, R. A., and Rooijakkers, S. H. (2018). Complement and bacterial infections: from molecular mechanisms to therapeutic applications. *Journal of innate immunity*, *10*(5-6), 455-464.

Held, K. G., and Postle, K. (2002). ExbB and ExbD Do Not Function Independently in TonB-Dependent Energy Transduction. *Journal of Bacteriology*, *184*(18), 5170-5173.

Heppel, L. A. (1969). The effect of osmotic shock on release of bacterial proteins and on active transport. *The Journal of General Physiology*, *54*(1), 95-113.

Heymans, R., Golparian, D., Bruisten, S. M., Schouls, L. M., and Unemo, M. (2012). Evaluation of *N. gonorrhoeae* multiple-locus variable-number tandem-repeat analysis, *N. gonorrhoeae* multiantigen sequence typing, and full-length porB gene sequence analysis for molecular epidemiological typing. *Journal of Clinical Microbiology*, *50*(1), 180-183.

Higgins, C. F., and Linton, K. J. (2004). The ATP switch model for ABC transporters. *Nature structural and molecular biology*, *11*(10), 918-926.

Higgins, E. T. (1992). Achieving'shared reality'in the communication game: A social action that create; meaning. *Journal of Language and Social Psychology*, *11*(3), 107-131.

Hilligan, K. L., and Ronchese, F. (2020). Antigen presentation by dendritic cells and their instruction of CD4+ T helper cell responses. *Cellular & molecular immunology*, *17*(6), 587-599.

Holbein, B. E., Ang, M. T. C., Allan, D. S., Chen, W., and Lehmann, C. (2021). Exploiting the Achilles' heel of iron dependence in antibiotic resistant bacteria with new antimicrobial iron withdrawal agents. In *Sustainable Agriculture Reviews 49* (pp. 251-311). Springer.

Hood, M. I., and Skaar, E. P. (2012). Nutritional immunity: transition metals at the pathogen–host interface. *Nature Reviews Microbiology*, *10*(8), 525-537.

Hooda, Y., Lai, C. C.-L., Judd, A., Buckwalter, C. M., Shin, H. E., Gray-Owen, S. D., and Moraes, T. F. (2016). Slam is an outer membrane protein that is required for the surface display of lipidated virulence factors in Neisseria. *Nature microbiology*, *1*(4), 1-9.

Hook III, E. W., Golden, M. R., Taylor, S. N., Henry, E., Tseng, C., Workowski, K. A., Swerdlow, J., Nenninger, A., and Cammarata, S. (2019). Efficacy and safety of single-dose oral delafloxacin compared with intramuscular ceftriaxone for uncomplicated gonorrhoea treatment: an open-label, noninferiority, phase 3, multicenter, randomised study. *Sexually transmitted diseases*, *46*(5), 279-286.

Huang, C.-T., Yen, M.-Y., Wong, W.-W., Li, L.-H., Lin, K.-Y., Liao, M.-H., and Li, S.-Y. (2010). Characteristics and dissemination of mosaic penicillin-binding protein 2-harbouring multidrug-resistant *N. gonorrhoeae* isolates with reduced cephalosporin susceptibility in northern Taiwan. *Antimicrobial Agents and Chemotherapy*, *54*(11), 4893-4895.

Huang, J., Zhang, Q., Chen, J., Zhang, T., Chen, Z., Chen, Z., Yang, J., Wang, Y., Min, Z., Huang, M., and Min, X. (2020). *N. gonorrhoeae* NGO2105 Is an Autotransporter Protein Involved in Adhesion to Human Cervical Epithelial Cells and *in vivo* Colonisation. *Frontiers in microbiology*, *11*, 1395-1395.

Hung, M.-C., Humbert, M. V., Laver, J. R., Phillips, R., Heckels, J. E., and Christodoulides, M. (2015). A putative amino acid ABC transporter substrate-binding protein, NMB1612, from *N. meningitidis*, induces murine bactericidal antibodies against meningococci expressing heterologous NMB1612 proteins. *Vaccine*, *33*(36), 4486-4494.

Huynh, K. K., Eskelinen, E. L., Scott, C. C., Malevanets, A., Saftig, P., and Grinstein, S. (2007). LAMP proteins are required for fusion of lysosomes with phagosomes. *The EMBO journal*, *26*(2), 313-324.

Ilina, E. N., Oparina, N. Y., Shitikov, E. A., Borovskaya, A. D., and Govorun, V. M. (2010). Molecular surveillance of clinical *N. gonorrhoeae* isolates in Russia. *Journal of Clinical Microbiology*, *48*(10), 3681-3689.

Ingersol, L. J., Yang, J., Kc, K., Pokhrel, A., Astashkin, A. V., Weiner, J. H., Johnston, C. A., and Kirk, M. L. (2020). Addressing Ligand-Based Redox in Molybdenum-Dependent Methionine Sulfoxide Reductase. *Journal of the American Chemical Society*, *142*(6), 2721-2725.

Islam, E. A., Fegan, J. E., Zeppa, J. J., Ahn, S. K., Ng, D., Currie, E. G., Lam, J., Moraes, T. F., and Gray-Owen, S. D. (2025). Adjuvant-dependent

impacts on vaccine-induced humoral responses and protection in preclinical models of nasal and genital colonisation by pathogenic *Neisseria*. *Vaccine*, *48*, 126709.

Ison, C., Hussey, J., Sankar, K., Evans, J., and Alexander, S. (2011). Gonorrhoea treatment failures to cefixime and azithromycin in England, 2010. *Eurosurveillance*, *16*(14), 19833.

Ispasanie, E., Muri, L., Schmid, M., Schubart, A., Thorburn, C., Zamurovic, N., Holbro, T., Kammüller, M., and Pluschke, G. (2023). In vaccinated individuals serum bactericidal activity against B meningococci is abrogated by C5 inhibition but not by inhibition of the alternative complement pathway. *Frontiers in immunology*, *14*, 1180833.

Ivarsson, L., de Arriba Sánchez de la Campa, M., Elfving, K., Yin, H., Gullsby, K., Stark, L., Andersen, B., Hoffmann, S., Gylfe, Å., and Unemo, M. (2022). Changes in testing and incidence of Chlamydia trachomatis and *N. gonorrhoeae*, the possible impact of the COVID-19 pandemic in the three Scandinavian countries. *Infectious Diseases*, *54*(9), 623-631.

Jacobsson, S., Thulin, S., Mölling, P., Unemo, M., Comanducci, M., Rappuoli, R., and Olcén, P. (2006). Sequence constancies and variations in genes encoding three new meningococcal vaccine candidate antigens. *Vaccine*, *24*(12), 2161-2168.

Jean, S., Juneau, R. A., Criss, A. K., and Cornelissen, C. N. (2016). *N. gonorrhoeae* evades calprotectin-mediated nutritional immunity and survives neutrophil extracellular traps by production of TdfH. *Infection and immunity*, *84*(10), 2982-2994.

Jefferson, A., Smith, A., Fasinu, P. S., and Thompson, D. K. (2021). Sexually transmitted *N. gonorrhoeae* infections—update on drug treatment and vaccine development. *Medicines*, *8*(2), 11.

Jen, F. E. C., Semchenko, E. A., Day, C. J., Seib, K. L., and Jennings, M. P. (2019). The *N. gonorrhoeae* Methionine Sulfoxide Reductase (MsrA/B) Is a Surface Exposed, Immunogenic, Vaccine Candidate. *Frontiers in immunology*, *10*, 137-137.

Jenks, J. D., Hester, L., Ryan, E., Stancil, C., Hauser, Q., Zitta, J.-P., Mortiboy, M., Rayner, M., Stevens, E., and Carrico, S. (2022). Test-of-Cure After Treatment of Pharyngeal Gonorrhea in Durham, North Carolina, 2021–2022. *Sexually transmitted diseases*, *49*(10), 677-681.

Jennison, A. V., Whiley, D., Lahra, M. M., Graham, R. M., Cole, M. J., Hughes, G., Fifer, H., Andersson, M., Edwards, A., and Eyre, D. (2019). Genetic relatedness of ceftriaxone-resistant and high-level azithromycin-resistant *N. gonorrhoeae* cases, United Kingdom and Australia, February to April 2018. *Eurosurveillance*, *24*(8), 1900118.

Jerse, A. E., Wu, H., Packiam, M., Vonck, R. A., Begum, A. A., and Garvin, L. E. (2011). Estradiol-treated female mice as surrogate hosts for *N. gonorrhoeae* genital tract infections. *Frontiers in microbiology*, *2*, 107.

John, C. M., Phillips, N. J., Cardenas, A. J., Criss, A. K., and Jarvis, G. A. (2023). Comparison of lipooligosaccharides from human challenge strains of *N. gonorrhoeae*. *Frontiers in microbiology*, *14*, 1215946.

Johnson, A. (1983). The pathogenic potential of commensal species of *Neisseria*. *Journal of Clinical Pathology*, *36*(2), 213-223.

Johnson, E., Nguyen, P. T., Yeates, T. O., and Rees, D. C. (2012). Inward-facing conformations of the MetNI methionine ABC transporter: Implications for the mechanism of transinhibition. *Protein science*, *21*(1), 84-96.

Jolley, K., Bray, J., and Maiden, M. (2018). Open-access bacterial population genomics: BIGSdb software, the PubMLST. org website and their applications. *Wellcome open research*, *3*(124).

Jolley, K. A., Bliss, C. M., Bennett, J. S., Bratcher, H. B., Brehony, C., Colles, F. M., Wimalarathna, H., Harrison, O. B., Sheppard, S. K., and Cody, A. J. (2012). Ribosomal multilocus sequence typing: universal characterisation of bacteria from domain to strain. *Microbiology*, *158*(4), 1005-1015.

Jolley, K. A., Chan, M.-S., and Maiden, M. C. (2004). mlstdbNet–distributed multi-locus sequence typing (MLST) databases. *BMC bioinformatics*, *5*, 1-8.

Jolley, K. A., and Maiden, M. C. (2010). BIGSdb: scalable analysis of bacterial genome variation at the population level. *BMC bioinformatics*, *11*, 1-11.

Jomaa, M., Terry, S., Hale, C., Jones, C., Dougan, G., and Brown, J. (2006). Immunisation with the iron uptake ABC transporter proteins PiaA and PiuA prevents respiratory infection with *S. pneumoniae*. *Vaccine*, *24*(24), 5133-5139.

Jones, R. A., Jerse, A. E., and Tang, C. M. (2024). Gonococcal PorB: A multifaceted modulator of host immune responses. *Trends in microbiology*.

Jones, R. A., Ramirez-Bencomo, F., Whiting, G., Fang, M., Lavender, H., Kurzyp, K., Thistlethwaite, A., Stejskal, L., Rashmi, S., and Jerse, A. E. (2024). Tackling immunosuppression by *N. gonorrhoeae* to facilitate vaccine design. *PLoS pathogens*, *20*(11), e1012688.

Jongerius, I., Lavender, H., Tan, L., Ruivo, N., Exley, R. M., Caesar, J. J., Lea, S. M., Johnson, S., and Tang, C. M. (2013). Distinct binding and immunogenic properties of the gonococcal homologue of meningococcal factor H binding protein. *PLoS pathogens*, *9*(8), e1003528.

Jorgensen, J. H., and Turnidge, J. D. (2015). Susceptibility test methods: dilution and disk diffusion methods. *Manual of clinical microbiology*, 1253-1273.

Joseph, S. J., Thomas IV, J. C., Schmerer, M. W., Cartee, J. C., St Cyr, S., Schlanger, K., Kersh, E. N., Raphael, B. H., Gernert, K. M., and Christina, A. R. *N. g.* W. G. H. S. H. C. R. R. S. O. O. D. C. L. J. P. A.

Z. J. B. T. W. C. L. J. M. (2022). Global emergence and dissemination of *N. gonorrhoeae* ST-9363 isolates with reduced susceptibility to azithromycin. *Genome Biology and Evolution*, *14*(1), evab287.

Joshi, C. J., Ke, W., Drangowska-Way, A., O'Rourke, E. J., and Lewis, N. E. (2022). What are housekeeping genes? *PLoS computational biology*, *18*(7), e1010295.

Juárez Rodríguez, M. D., Marquette, M., Youngblood, R., Dhungel, N., Torres Escobar, A., Ivanov, S. S., and Dragoi, A.-M. (2024). Characterisation of *N. gonorrhoeae* colonisation of macrophages under distinct polarisation states and nutrients environment. *Frontiers in cellular and infection microbiology*, *14*, 1384611.

Kakooza, F., Golparian, D., Matoga, M., Maseko, V., Lamorde, M., Krysiak, R., Manabe, Y. C., Chen, J. S., Kularatne, R., and Jacobsson, S. (2023). Genomic surveillance and antimicrobial resistance determinants in *N. gonorrhoeae* isolates from Uganda, Malawi and South Africa, 2015–20. *Journal of antimicrobial chemotherapy*, *78*(8), 1982-1991.

Kammerman, M. T., Bera, A., Wu, R., Harrison, S. A., Maxwell, C. N., Lundquist, K., Noinaj, N., Chazin, W. J., and Cornelissen, C. N. (2020). Molecular insight into TdfH-mediated zinc piracy from human calprotectin by *N. gonorrhoeae*. *MBio*, *11*(3), 10.1128/mbio. 00949-00920.

Kehres, D. G., Janakiraman, A., Slauch, J. M., and Maguire, M. E. (2002). SitABCD is the alkaline Mn2+ transporter of *Salmonella enterica serovar Typhimurium*. *Journal of bacteriology*, *184*(12), 3159-3166.

Kesharwani, P., Chopra, S., and Dasgupta, A. (2020). *Drug discovery targeting drug-resistant bacteria*. Academic Press.

Kim, E. H., Woodruff, M. C., Grigoryan, L., Maier, B., Lee, S. H., Mandal, P., Cortese, M., Natrajan, M. S., Ravindran, R., and Ma, H. (2020). Squalene emulsion-based vaccine adjuvants stimulate CD8 T cell, but not antibody responses, through a RIPK3-dependent pathway. *eLife*, *9*, e52687.

Kłyż, A., and Piekarowicz, A. (2018). Phage proteins are expressed on the surface of *N. gonorrhoeae* and are potential vaccine candidates. *PloS one*, *13*(8), e0202437.

Knapp, J. S. (1988). Historical perspectives and identification of *Neisseria* and related species. *Clinical microbiology reviews*, *1*(4), 415-431.

Kohler, P. L., Hamilton, H. L., Cloud-Hansen, K., and Dillard, J. P. (2007). AtlA functions as a peptidoglycan lytic transglycosylase in the *N. gonorrhoeae* type IV secretion system. *Journal of bacteriology*, *189*(15), 5421-5428.

Koomey, J. M., Gill, R. E., and Falkow, S. (1982). Genetic and biochemical analysis of gonococcal IgA1 protease: cloning in *E. coli* and construction of mutants of gonococci that fail to produce the activity. *Proceedings of the National Academy of Sciences*, *79*(24), 7881-7885.

Kovacs-Simon, A., Leuzzi, R., Kasendra, M., Minton, N., Titball, R. W., and Michell, S. L. (2014). Lipoprotein CD0873 is a novel adhesin of Clostridium difficile. *The Journal of Infectious Diseases*, *210*(2), 274-284.

Kraus-Römer, S., Wielert, I., Rathmann, I., Grossbach, J., and Maier, B. (2022). External stresses affect gonococcal type 4 pilus dynamics. *Frontiers in microbiology*, *13*, 839711.

Kulp, A., and Kuehn, M. J. (2010). Biological functions and biogenesis of secreted bacterial outer membrane vesicles. *Annual review of microbiology*, *64*, 163-184.

Lahra, M. M., Martin, I., Demczuk, W., Jennison, A. V., Lee, K.-I., Nakayama, S.-I., Lefebvre, B., Longtin, J., Ward, A., and Mulvey, M. R. (2018). Cooperative recognition of internationally disseminated ceftriaxone-resistant *N. gonorrhoeae* strain. *Emerging infectious diseases*, *24*(4), 735.

Landig, C. S., Hazel, A., Kellman, B. P., Fong, J. J., Schwarz, F., Agarwal, S., Varki, N., Massari, P., Lewis, N. E., and Ram, S. (2019). Evolution of the exclusively human pathogen *N. gonorrhoeae*: Human-specific engagement of immunoregulatory Siglecs. *Evolutionary applications*, *12*(2), 337-349.

Lappann, M., Otto, A., Becher, D., and Vogel, U. (2013). Comparative proteome analysis of spontaneous outer membrane vesicles and purified outer membranes of *N. meningitidis*. *Journal of bacteriology*, *195*(19), 4425-4435.

Lavitola, A., Vanni, M., Martin, P., and Bruni, C. B. (1992). Cloning and characterisation of a *Neisseria* gene homologous to *hisJ* and *argT* of *E. coli* and *S. typhimurium*. *Research in microbiology*, *143*(3), 295-305.

Ledsgaard, L., Jenkins, T. P., Davidsen, K., Krause, K. E., Martos-Esteban, A., Engmark, M., Rørdam Andersen, M., Lund, O., and Laustsen, A. H. (2018). Antibody cross-reactivity in antivenom research. *Toxins*, *10*(10), 393.

Leduc, I., Connolly, K. L., Begum, A., Underwood, K., Darnell, S., Shafer, W. M., Balthazar, J. T., MacIntyre, A. N., Sempowski, G. D., Duncan, J. A., Little, M. B., Rahman, N., Garges, E. C., and Jerse, A. E. (2020). The serogroup B meningococcal outer membrane vesicle-based vaccine 4CMenB induces cross-species protection against *N. gonorrhoeae*. *PLoS pathogens*, *16*(12), e1008602-e1008602.

Lefebvre, B., Martin, I., Demczuk, W., Deshaies, L., Michaud, S., Labbé, A.-C., Beaudoin, M.-C., and Longtin, J. (2018). Ceftriaxone-resistant *N. gonorrhoeae*, Canada, 2017. *Emerging infectious diseases*, *24*(2), 381.

Lewis, D. A. (2019). New treatment options for *N. gonorrhoeae* in the era of emerging antimicrobial resistance. *Sexual health*, *16*(5), 449-456.

Lewis, L. A., Gulati, S., Burrowes, E., Zheng, B., Ram, S., and Rice, P. A. (2015). α-2, 3-sialyltransferase expression level impacts the kinetics of lipooligosaccharide sialylation, complement resistance, and the ability

of *N. gonorrhoeae* to colonise the murine genital tract. *MBio*, *6*(1), 10.1128/mbio. 02465-02414.

Lewis, L. A., Rice, P. A., and Ram, S. (2019). Role of Gonococcal *Neisserial* Surface Protein A (NspA) in Serum Resistance and Comparison of Its Factor H Binding Properties with Those of Its Meningococcal Counterpart. *Infection and immunity*, *87*(2).

Li, W., Peng, X., Lang, J., and Xu, C. (2020). Targeting mouse double minute 2: current concepts in DNA damage repair and therapeutic approaches in cancer. *Frontiers in Pharmacology*, *11*, 631.

Liu, F., Liang, J., Zhang, B., Gao, Y., Yang, X., Hu, T., Yang, H., Xu, W., Guddat, L. W., and Rao, Z. (2020). Structural basis of trehalose recycling by the ABC transporter LpqY-SugABC. *Science advances*, *6*(44), eabb9833.

Liu, G., Tang, C. M., and Exley, R. M. (2015). Non-pathogenic *Neisseria*: members of an abundant, multi-habitat, diverse genus. *Microbiology*, *161*(Pt_7), 1297-1312.

Liu, M., Bouhsira, E., Boulouis, H.-J., and Biville, F. (2013). The *Bartonella henselae* SitABCD transporter is required for confronting oxidative stress during cell and flea invasion. *Research in microbiology*, *164*(8), 827-837.

Liu, Y., Egilmez, N. K., and Russell, M. W. (2013). Enhancement of adaptive immunity to *N. gonorrhoeae* by local intravaginal administration of microencapsulated interleukin 12. *The Journal of Infectious Diseases*, *208*(11), 1821-1829.

Liu, Y., Islam, E. A., Jarvis, G. A., Gray-Owen, S. D., and Russell, M. W. (2012). *N. gonorrhoeae* selectively suppresses the development of Th1 and Th2 cells, and enhances Th17 cell responses, through TGF-β-dependent mechanisms. *Mucosal immunology*, *5*(3), 320-331.

Liuzzi, J. P., Lichten, L. A., Rivera, S., Blanchard, R. K., Aydemir, T. B., Knutson, M. D., Ganz, T., and Cousins, R. J. (2005). Interleukin-6 Regulates the Zinc Transporter Zip14 in Liver and Contributes to the Hypozincemia of the Acute-Phase Response. *Proceedings of the National Academy of Sciences - PNAS*, *102*(19), 6843-6848.

Long, C. D., Hayes, S. F., van Putten, J. P., Harvey, H. A., Apicella, M. A., and Seifert, H. S. (2001). Modulation of gonococcal piliation by regulatable transcription of pilE. *Journal of bacteriology*, *183*(5), 1600-1609.

Loss, G., Simões, P. M., Valour, F., Cortês, M. F., Gonzaga, L., Bergot, M., Trouillet-Assant, S., Josse, J., Diot, A., and Ricci, E. (2019). Staphylococcus aureus small colony variants (SCVs): news from a chronic prosthetic joint infection. *Frontiers in cellular and infection microbiology*, *9*, 363.

Lovett, A., and Duncan, J. A. (2019). Human immune responses and the natural history of *N. gonorrhoeae* infection. *Frontiers in immunology*, *9*, 3187.

Lu, Q., Yang, H., Peng, Y., Dong, Z., Nie, P., Wang, G., Luo, S., Min, X., Huang, J., and Huang, M. (2024). Intranasal trivalent candidate vaccine

induces strong mucosal and systemic immune responses against *N. gonorrhoeae*. *Frontiers in immunology*, *15*, 1473193.

Lyu, Y., Choong, A., Chow, E. P., Seib, K. L., Marshall, H. S., Unemo, M., de Voux, A., Wang, B., Miranda, A. E., and Gottlieb, S. L. (2024). Vaccine value profile for *N. gonorrhoeae*. *Vaccine*, *42*(19), S42-S69.

Mächtel, R., Narducci, A., Griffith, D. A., Cordes, T., and Orelle, C. (2019). An integrated transport mechanism of the maltose ABC importer. *Research in microbiology*, *170*(8), 321-337.

Maharjan, S., Saleem, M., Feavers, I. M., Wheeler, J. X., Care, R., and Derrick, J. P. (2016). Dissection of the function of the RmpM periplasmic protein from *N. meningitidis*. *Microbiology*, *162*(2), 364-375.

Mahdi, L. K., Van Der Hoek, M. B., Ebrahimie, E., Paton, J. C., and Ogunniyi, A. D. (2015). Characterisation of pneumococcal genes involved in bloodstream invasion in a mouse model. *PloS one*, *10*(11), e0141816.

Mancuso, A. M., Gandhi, M. A., and Slish, J. (2018). Solithromycin (CEM-101): a new fluoroketolide antibiotic and its role in the treatment of gonorrhoea. *Journal of Pharmacy Practice*, *31*(2), 195-201.

Marjuki, H., Topaz, N., Joseph, S. J., Gernert, K. M., Kersh, E. N., Group, A.-R. *N. g.* W., and Wang, X. (2019). Genetic similarity of gonococcal homologs to meningococcal outer membrane proteins of serogroup B vaccine. *MBio*, *10*(5), 10.1128/mbio. 01668-01619.

Marri, P. R., Paniscus, M., Weyand, N. J., Rendón, M. A., Calton, C. M., Hernández, D. R., Higashi, D. L., Sodergren, E., Weinstock, G. M., and Rounsley, S. D. (2010). Genome sequencing reveals widespread virulence gene exchange among human *Neisseria* species. *PloS one*, *5*(7), e11835.

Martin, D., Ruijne, N., McCallum, L., O'hallahan, J., and Oster, P. (2006). The VR2 epitope on the PorA P1. 7-2, 4 protein is the major target for the immune response elicited by the strain-specific group B meningococcal vaccine MeNZB. *Clinical and Vaccine Immunology*, *13*(4), 486-491.

Martin, P., Lavitola, A., Aoun, L., Ancelle, R., Cremieux, A., and Riou, J. (1986). A common *Neisserial* antigen evidenced by immunisation of mice with live *N. meningitidis*. *Infection and immunity*, *53*(1), 229-233.

Massari, P., Ram, S., Macleod, H., and Wetzler, L. M. (2003). The role of porins in *Neisserial* pathogenesis and immunity. *Trends in microbiology*, *11*(2), 87-93.

Masselot-Joubert, L., and Di Renzo, M. A. (2025). ATP-Binding Cassette (ABC) Transporters and Antibiotic Resistance: Specialised Systems for Capsular Polysaccharide Export in Gram-Negative Pathogens. Polysaccharides. *Polysaccharides*, *6*(2), 38.

Matthias, K. A., Reveille, A., Dhara, K., Lyle, C. S., Natuk, R. J., Bonk, B., and Bash, M. C. (2025). Development and validation of a standardised human complement serum bactericidal activity assay to measure functional antibody responses to *N. gonorrhoeae*. *Vaccine*, *43*, 126508.

Maurakis, S., Keller, K., Maxwell, C. N., Pereira, K., Chazin, W. J., Criss, A. K., and Cornelissen, C. N. (2019). The novel interaction between *N. gonorrhoeae* TdfJ and human S100A7 allows gonococci to subvert host zinc restriction. *PLoS pathogens*, *15*(8), e1007937.

Mavroidi, A., Tzelepi, E., Siatravani, E., Godoy, D., Miriagou, V., and Spratt, B. G. (2011). Analysis of emergence of quinolone-resistant gonococci in Greece by combined use of *N. gonorrhoeae* multiantigen sequence typing and multilocus sequence typing. *Journal of Clinical Microbiology*, *49*(4), 1196-1201.

McIntosh, E., Bröker, M., Wassil, J., Welsch, J., and Borrow, R. (2015). Serum bactericidal antibody assays–the role of complement in infection and immunity. *Vaccine*, *33*(36), 4414-4421.

McNeil, L. K., Zagursky, R. J., Lin, S. L., Murphy, E., Zlotnick, G. W., Hoiseth, S. K., Jansen, K. U., and Anderson, A. S. (2013). Role of factor H binding protein in *N. meningitidis* virulence and its potential as a vaccine candidate to broadly protect against meningococcal disease. *Microbiology and Molecular Biology Reviews*, *77*(2), 234-252.

Mehr, I. J., Long, C. D., Serkin, C. D., and Seifert, H. S. (2000). A homologue of the recombination-dependent growth gene, rdgC, is involved in gonococcal pilin antigenic variation. *Genetics*, *154*(2), 523-532.

Merle, N. S., Noe, R., Halbwachs-Mecarelli, L., Fremeaux-Bacchi, V., and Roumenina, L. T. (2015). Complement system part II: role in immunity. *Frontiers in immunology*, *6*, 257.

Merlin, C., Gardiner, G., Durand, S., and Masters, M. (2002). The *E. coli* metD locus encodes an ABC transporter which includes Abc (MetN), YaeE (MetI), and YaeC (MetQ). *Journal of bacteriology*, *184*(19), 5513-5517.

Miari, V. F., Bonnin, W., Smith, I. K., Horney, M. F., Saint-Geris, S. J., and Stabler, R. A. (2024). Carriage and antimicrobial susceptibility of commensal *Neisseria* species from the human oropharynx. *Scientific reports*, *14*(1), 25017.

Miethke, M., and Skerra, A. (2010). Neutrophil Gelatinase-Associated Lipocalin Expresses Antimicrobial Activity by Interfering with l-Norepinephrine-Mediated Bacterial Iron Acquisition. *Antimicrobial Agents and Chemotherapy*, *54*(4), 1580-1589.

Młynarczyk-Bonikowska, B., Majewska, A., Malejczyk, M., Młynarczyk, G., and Majewski, S. (2020). Multiresistant *N. gonorrhoeae*: a new threat in second decade of the XXI century. *Medical microbiology and immunology*, *209*, 95-108.

Mohamed, N., Wang, M. Y., Le Huec, J.-C., Liljenqvist, U., Scully, I. L., Baber, J., Begier, E., Jansen, K. U., Gurtman, A., and Anderson, A. S. (2017). Vaccine development to prevent Staphylococcus aureus surgical-site infections. *Journal of British Surgery*, *104*(2), e41-e54.

Moore, J., Bailey, S. E., Benmechernene, Z., Tzitzilonis, C., Griffiths, N. J., Virji, M., and Derrick, J. P. (2005). Recognition of saccharides by the

OpcA, OpaD, and OpaB outer membrane proteins from *N. meningitidis*. *Journal of Biological Chemistry*, *280*(36), 31489-31497.

Moreau, M. R., Massari, P., and Genco, C. A. (2017). The ironclad truth: how *in vivo* transcriptomics and *in vitro* mechanistic studies shape our understanding of *N. gonorrhoeae* gene regulation during mucosal infection. *Pathogens and disease*, *75*(5).

Muenzner, P., and Hauck, C. R. (2020). *N. gonorrhoeae* Blocks Epithelial Exfoliation by Nitric-Oxide-Mediated Metabolic Cross Talk to Promote Colonisation in Mice. *Cell host & microbe*, *27*(5), 793-808.e795.

Murphy, K., and Weaver, C. (2016). *Janeway's immunobiology*. Garland Science.

Mutti, M., Ramoni, K., Nagy, G., Nagy, E., and Szijártó, V. (2018). A new tool for complement research: *In vitro* reconstituted human classical complement pathway. *Frontiers in immunology*, *9*, 2770.

Muzzi, A., Mora, M., Pizza, M., Rappuoli, R., and Donati, C. (2013). Conservation of meningococcal antigens in the genus *Neisseria*. *MBio*, *4*(3), e00163-e00113.

Nachamkin, I., Cannon, J., and Mittler, R. (1981). Monoclonal antibodies against *N. gonorrhoeae*: production of antibodies directed against a strain-specific cell surface antigen. *Infection and immunity*, *32*(2), 641-648.

Nakayama, S.-i., Shimuta, K., Furubayashi, K.-i., Kawahata, T., Unemo, M., and Ohnishi, M. (2016). New ceftriaxone-and multidrug-resistant *N. gonorrhoeae* strain with a novel mosaic *penA* gene isolated in Japan. *Antimicrobial Agents and Chemotherapy*, *60*(7), 4339-4341.

Nguyen, M., Matsuo, M., Niemann, S., Herrmann, M., and Gotz, F. (2020). Lipoproteins in Gram-positive bacteria: abundance, function, fitness. Front Microbiol 11: 582582. In.

Nguyen, P. T., Lai, J. Y., Kaiser, J. T., and Rees, D. C. (2019). Structures of the *N. meningitides* methionine-binding protein MetQ in substrate-free form and bound tol- and d-methionine isomers. *Protein science*, *28*(10), 1750-1757.

Nguyen, P. T., Lai, J. Y., Lee, A. T., Kaiser, J. T., and Rees, D. C. (2018). Noncanonical role for the binding protein in substrate uptake by the MetNI methionine ATP-Binding Cassette (ABC) transporter. *Proceedings of the National Academy of Sciences - PNAS*, *115*(45), E10596-E10604.

Nguyen, P. T., Li, Q. W., Kadaba, N. S., Lai, J. Y., Yang, J. G., and Rees, D. C. (2015). The contribution of methionine to the stability of the *E. coli* MetNIQ ABC transporter-substrate binding protein complex. *Biological chemistry*, *396*(9), 1127-1134.

Nicholson, K. R., Yin, S., Edwards, J. L., Luan, C.-H., and Seifert, H. S. (2025). Natural compounds target the M23B zinc metallopeptidase Mpg to

modulate *N. gonorrhoeae* Type IV pilus expression. *MBio*, *16*(4), e04027-04024.

Noinaj, N., Easley, N. C., Oke, M., Mizuno, N., Gumbart, J., Boura, E., Steere, A. N., Zak, O., Aisen, P., Tajkhorshid, E., Evans, R. W., Gorringe, A. R., Mason, A. B., Steven, A. C., and Buchanan, S. K. (2012). Structural basis for iron piracy by pathogenic *Neisseria*. *Nature (London)*, *483*(7387), 53-61.

Noinaj, N., Guillier, M., Barnard, T. J., and Buchanan, S. K. (2010). TonB-dependent transporters: Regulation, structure, and function. *Annual review of microbiology*, *64*(1), 43-60.

Noori Goodarzi, N., Barzi, S. M., Ajdary, S., Chiani, M., Yekaninejad, M. S., Badmasti, F., and Pourmand, M. R. (2025). Immunogenic evaluation of LptD+ LtgC as a bivalent vaccine candidate against *N. gonorrhoeae*. *Journal of Translational Medicine*, *23*(1), 261.

Nossal, N. G., and Heppel, L. A. (1966). The release of enzymes by osmotic shock from *E. coli* in exponential phase. *Journal of Biological Chemistry*, *241*(13), 3055-3062.

Noto, J. M., and Cornelissen, C. N. (2008). Identification of TbpA Residues Required for Transferrin-Iron Utilisation by *N. gonorrhoeae*. *Infection and immunity*, *76*(5), 1960-1969.

Ohnishi, M., Golparian, D., Shimuta, K., Saika, T., Hoshina, S., Iwasaku, K., Nakayama, S.-i., Kitawaki, J., and Unemo, M. (2011). Is *N. gonorrhoeae* initiating a future era of untreatable gonorrhoea?: detailed characterisation of the first strain with high-level resistance to ceftriaxone. *Antimicrobial Agents and Chemotherapy*, *55*(7), 3538-3545.

Ohnishi, M., Watanabe, Y., Ono, E., Takahashi, C., Oya, H., Kuroki, T., Shimuta, K., Okazaki, N., Nakayama, S.-i., and Watanabe, H. (2010). Spread of a chromosomal cefixime-resistant *penA* gene among different *N. gonorrhoeae* lineages. *Antimicrobial Agents and Chemotherapy*, *54*(3), 1060-1067.

Omori, R., Chemaitelly, H., and Abu-Raddad, L. J. (2024). Understanding dynamics and overlapping epidemiologies of HIV, HSV-2, chlamydia, gonorrhoea, and syphilis in sexual networks of men who have sex with men. *Frontiers in Public Health*, *12*, 1335693.

Ondari, E., Wilkins, A., Latimer, B., Dragoi, A.-M., and Ivanov, S. S. (2023). Cellular cholesterol licenses Legionella pneumophila intracellular replication in macrophages. *Microbial Cell*, *10*(1), 1.

Ortiz, M. C., Lefimil, C., Rodas, P. I., Vernal, R., Lopez, M., Acuña-Castillo, C., Imarai, M., and Escobar, A. (2015). *N. gonorrhoeae* modulates immunity by polarising human macrophages to an M2 profile. *PloS one*, *10*(6), e0130713-e0130713.

Osnes, M. N., Dorp, L. v., Brynildsrud, O. B., Alfsnes, K., Schneiders, T., Templeton, K. E., Yahara, K., Balloux, F., Caugant, D. A., and Eldholm, V. (2021). Antibiotic treatment regimes as a driver of the

global population dynamics of a major gonorrhoea lineage. *Molecular biology and evolution*, *38*(4), 1249-1261.

Otsuka, T., Kirkham, C., Brauer, A., Koszelak-Rosenblum, M., Malkowski, M. G., and Murphy, T. F. (2016). The vaccine candidate substrate binding protein SBP2 plays a key role in arginine uptake, which is required for growth of Moraxella catarrhalis. *Infection and immunity*, *84*(2), 432-438.

Otsuka, T., Kirkham, C., Johnson, A., Jones, M. M., and Murphy, T. F. (2014). Substrate-binding protein SBP2 of a putative ABC transporter as a novel vaccine antigen of *Moraxella catarrhalis*. *Infection and immunity*, *82*(8), 3503-3512.

Palmer, A., and Criss, A. K. (2018). Gonococcal defences against antimicrobial activities of neutrophils. *Trends in microbiology*, *26*(12), 1022-1034.

Parte, A. C. (2018). LPSN–List of Prokaryotic names with Standing in Nomenclature (bacterio. net), 20 years on. *International journal of systematic and evolutionary microbiology*, *68*(6), 1825-1829.

Patel, A. J. (2019). *Investigation of novel lipoprotein (YP-207371) of N. gonorrhoeae as a potential vaccine candidate. Unpublished Master's dissertation, University of Nottingham, UK.*

Paynter, J., Goodyear-Smith, F., Morgan, J., Saxton, P., Black, S., and Petousis-Harris, H. (2019). Effectiveness of a group B outer membrane vesicle meningococcal vaccine in preventing hospitalisation from gonorrhea in New Zealand: a retrospective cohort study. *Vaccines*, *7*(1), 5.

Pérez-Losada, M., Viscidi, R. P., Demma, J. C., Zenilman, J., and Crandall, K. A. (2005). Population genetics of *N. gonorrhoeae* in a high-prevalence community using a hypervariable outer membrane porB and 13 slowly evolving housekeeping genes. *Molecular biology and evolution*, *22*(9), 1887-1902.

Pérez Medina, K. M., and Dillard, J. P. (2018). Antibiotic targets in gonococcal cell wall metabolism. *Antibiotics (Basel)*, *7*(3), 64.

Petousis-Harris, H., Paynter, J., Morgan, J., Saxton, P., McArdle, B., Goodyear-Smith, F., and Black, S. (2017). Effectiveness of a group B outer membrane vesicle meningococcal vaccine against gonorrhoea in New Zealand: a retrospective case-control study. *The Lancet*, *390*(10102), 1603-1610.

Pillai, S., Netravali, I. A., Cariappa, A., and Mattoo, H. (2012). Siglecs and immune regulation. *Annual review of immunology*, *30*(1), 357-392.

Pisano, L., Giovannuzzi, S., and Supuran, C. T. (2024). Management of *N. gonorrhoeae* infection: from drug resistance to drug repurposing. *Expert Opinion on Therapeutic Patents*(just-accepted).

Pitasi, M. A., Kerani, R. P., Kohn, R., Murphy, R. D., Pathela, P., Schumacher, C. M., Tabidze, I., and Llata, E. (2019). Chlamydia, Gonorrhoea, and Human Immunodeficiency Virus Infection Among Transgender Women and Transgender Men Attending Clinics that Provide Sexually Transmitted Disease Services in Six US Cities: Results From the

Sexually Transmitted Disease Surveillance Network. *Sexually transmitted diseases*, *46*(2), 112-117.

Pizza, M., and Rappuoli, R. (2020). Vaccinology–Editorial. Seminars in Immunology,

Pizza, M., Scarlato, Masignani, Giuliani, M. M., Arico, B., Comanducci, M., Jennings, G. T., Baldi, L., Bartolini, E., Capecchi, B., Galeotti, C. L., Luzzi, E., Manetti, R., Marchetti, E., Mora, M., Nuti, S., Ratti, G., Santini, L., Savino, S., Rappuoli, R. (2000). Identification of Vaccine Candidates against Serogroup B Meningococcus by Whole-Genome Sequencing. *Science (American Association for the Advancement of Science)*, *287*(5459), 1816-1820.

Platt, D. (1976). Carbon dioxide requirement of *N. gonorrhoeae* growing on a solid medium. *Journal of Clinical Microbiology*, *4*(2), 129-132.

Plotkin, S. A. (2020). Updates on immunologic correlates of vaccine-induced protection. *Vaccine*, *38*(9), 2250-2257.

Pogoutse, A. K., and Moraes, T. F. (2017). Iron acquisition through the bacterial transferrin receptor. *Critical reviews in biochemistry and molecular biology*, *52*(3), 314-326.

Pollard, A. J., Riordan, A., and Ramsay, M. (2014). Group B meningococcal vaccine: recommendations for UK use. *The Lancet*, *383*(9923), 1103-1104.

Poncin, T., Fouere, S., Braille, A., Camelena, F., Agsous, M., Bebear, C., Kumanski, S., Lot, F., Mercier-Delarue, S., and Ngangro, N. N. (2018). Multidrug-resistant *N. gonorrhoeae* failing treatment with ceftriaxone and doxycycline in France, November 2017. *Eurosurveillance*, *23*(21), 1800264.

Price, G. A., Masri, H. P., Hollander, A. M., Russell, M. W., and Cornelissen, C. N. (2007). Gonococcal transferrin binding protein chimeras induce bactericidal and growth inhibitory antibodies in mice. *Vaccine*, *25*(41), 7247-7260.

Pryzdial, E. L., Leatherdale, A., and Conway, E. M. (2022). Coagulation and complement: Key innate defence participants in a seamless web. *Frontiers in immunology*, *13*, 918775.

Puig, S., Ramos-Alonso, L., Romero, A. M., and Martínez-Pastor, M. T. (2017). The elemental role of iron in DNA synthesis and repair. *Metallomics*, *9*(11), 1483-1415.

Quillin, S. J., and Seifert, H. S. (2018). *N. gonorrhoeae* host adaptation and pathogenesis. *Nature Reviews Microbiology*, *16*(4), 226-240.

Raccagni, A. R., Ranzenigo, M., Bruzzesi, E., Maci, C., Castagna, A., and Nozza, S. (2023). *N. gonorrhoeae* antimicrobial resistance: The future of antibiotic therapy. *Journal of Clinical Medicine*, *12*(24), 7767.

Ram, S., Cullinane, M., Blom, A. M., Gulati, S., McQuillen, D. P., Monks, B. G., O'Connell, C., Boden, R., Elkins, C., Pangburn, M. K., Dahlbäck, B., and Rice, P. A. (2001). Binding of C4b-binding protein to porin: A

molecular mechanism of serum resistance of *N. gonorrhoeae*. *The Journal of experimental medicine*, *193*(3), 281-295.

Ram, S., Shaughnessy, J., de Oliveira, R. B., Lewis, L. A., Gulati, S., and Rice, P. A. (2017). Gonococcal lipooligosaccharide sialylation: virulence factor and target for novel immunotherapeutics. *Pathogens and disease*, *75*(4), ftx049.

Ramsey, M. E., Hackett, K. T., Kotha, C., and Dillard, J. P. (2012). New complementation constructs for inducible and constitutive gene expression in *N. gonorrhoeae* and *N. meningitidis*. *Applied and Environmental Microbiology*, *78*(9), 3068-3078.

Rappuoli, R., Alter, G., and Pulendran, B. (2024). Transforming vaccinology. *Cell*, *187*(19), 5171-5194.

Reekie, J., Donovan, B., Guy, R., Hocking, J. S., Kaldor, J. M., Mak, D. B., Pearson, S., Preen, D., Stewart, L., and Ward, J. (2018). Risk of pelvic inflammatory disease in relation to chlamydia and gonorrhoea testing, repeat testing, and positivity: a population-based cohort study. *Clinical infectious diseases*, *66*(3), 437-443.

Rees, D. C., Johnson, E., and Lewinson, O. (2009). ABC transporters: the power to change. *Nature reviews Molecular cell biology*, *10*(3), 218-227.

Remy, L., Carrière, M., Derré-Bobillot, A., Martini, C., Sanguinetti, M., and Borezée-Durant, E. (2013). The *Staphylococcus aureus* Opp1 ABC transporter imports nickel and cobalt in zinc-depleted conditions and contributes to virulence. *Molecular microbiology*, *87*(4), 730-743.

Rice, A. J., Park, A., and Pinkett, H. W. (2014). Diversity in ABC transporters: type I, II and III importers. *Critical reviews in biochemistry and molecular biology*, *49*(5), 426-437.

Rice, P. A., Shafer, W. M., Ram, S., and Jerse, A. E. (2017). *N. gonorrhoeae*: drug resistance, mouse models, and vaccine development. *Annual review of microbiology*, *71*(1), 665-686.

Rice, P. A., Vayo, H. E., Tam, M. R., and Blake, M. S. (1986). Immunoglobulin G antibodies directed against protein III block killing of serum-resistant *N. gonorrhoeae* by immune serum. *The Journal of experimental medicine*, *164*(5), 1735-1748.

Richard, K. L., Kelley, B. R., and Johnson, J. G. (2019). Haem Uptake and Utilisation by Gram-Negative Bacterial Pathogens. *Frontiers in cellular and infection microbiology*, *9*, 81-81.

Rodrigues, R., Vieira-Baptista, P., Catalão, C., Borrego, M. J., Sousa, C., and Vale, N. (2023). Chlamydial and Gonococcal Genital Infections: A Narrative Review. *Journal of Personalised Medicine*, *13*(7), 1170.

Roe, S. K., Felter, B., Zheng, B., Ram, S., Wetzler, L. M., Garges, E., Zhu, T., Genco, C. A., and Massari, P. (2023). *In Vitro* Pre-Clinical Evaluation of a Gonococcal Trivalent Candidate Vaccine Identified by Transcriptomics. *Vaccines*, *11*(12), 1846.

Rohde, K. H., and Dyer, D. W. (2003). Mechanisms of iron acquisition by the human pathogens *N. meningitidis* and *N. gonorrhoeae*. *Frontiers in bioscience*, *8*(4), d1186-1218.

Rossau, R., Van Landschoot, A., Mannheim, W., and De Ley, J. (1986). Inter- and intrageneric similarities of ribosomal ribonucleic acid cistrons of the *Neisseriaceae*. *International journal of systematic and evolutionary microbiology*, *36*(2), 323-332.

Rossau, R., Vandenbussche, G., Thielemans, S., Segers, P., Grosch, H., Göthe, E., Mannheim, W., and De Ley, J. (1989). Ribosomal ribonucleic acid cistron similarities and deoxyribonucleic acid homologies of *Neisseria, Kingella, Eikenella,* S*imonsiella, Alysiella,* and Centre for Disease Control groups EF-4 and M-5 in the emended family *Neisseriaceae*. *International journal of systematic and evolutionary microbiology*, *39*(2), 185-198.

Russell, M. W. (2021). Immune responses to *N. gonorrhoeae* challenges and opportunities with respect to pelvic inflammatory disease. *The Journal of Infectious Diseases*, *224*(Supplement_2), S96-S102.

Russell, M. W., Jerse, A. E., and Gray-Owen, S. D. (2019). Progress toward a gonococcal vaccine: the way forward. *Frontiers in immunology*, *10*, 2417.

Sabri, M., Caza, M., Proulx, J., Lymberopoulos, M. H., Brée, A., Moulin-Schouleur, M., Curtiss III, R., and Dozois, C. M. (2008). Contribution of the SitABCD, MntH, and FeoB metal transporters to the virulence of avian pathogenic *E. coli* O78 strain χ7122. *Infection and immunity*, *76*(2), 601-611.

Sabrialabed, S., Yang, J. G., Yariv, E., Ben-Tal, N., and Lewinson, O. (2020). Substrate recognition and ATPase activity of the *E. coli* cysteine/cystine ABC transporter YecSC-FliY. *Journal of Biological Chemistry*, *295*(16), 5245-5256.

Santos, G. F., Deck, R. R., Donnelly, J., Blackwelder, W., and Granoff, D. M. (2001). Importance of complement source in measuring meningococcal bactericidal titers. *Clinical Diagnostic Laboratory Immunology*, *8*(3), 616-623.

Sarkissian, C. A., Alteri, C. J., and Mobley, H. L. T. (2019). UTI patients have pre-existing antigen-specific antibody titers against UTI vaccine antigens. *Vaccine*, *37*(35), 4937-4946.

Scheepers, G. H., Lycklama A Nijeholt, J. A., and Poolman, B. (2016). An updated structural classification of substrate-binding proteins. *FEBS letters*, *590*(23), 4393-4401.

Schryvers, A. B. (2022). Targeting bacterial transferrin and lactoferrin receptors for vaccines. *Trends in microbiology*, *30*(9), 820-830.

Semchenko, E. A., Day, C. J., and Seib, K. L. (2017). MetQ of *N. gonorrhoeae* is a surface-expressed antigen that elicits bactericidal and functional blocking antibodies. *Infection and immunity*, *85*(2), 10.1128/iai. 00898-00816.

Semchenko, E. A., Day, C. J., and Seib, K. L. (2020). The *N. gonorrhoeae* vaccine candidate NHBA elicits antibodies that are bactericidal, opsonophagocytic, and that reduce gonococcal adherence to epithelial cells. *Vaccines*, *8*(2), 219.

Semchenko, E. A., Jen, F. E.-C., Jennings, M. P., and Seib, K. L. (2022). Assessment of serum bactericidal and opsonophagocytic activity of antibodies to gonococcal vaccine targets. *Bacterial Vaccines: Methods and Protocols*, 363-372.

Semchenko, E. A., Tan, A., Borrow, R., and Seib, K. L. (2019). The serogroup B meningococcal vaccine Bexsero elicits antibodies to *N. gonorrhoeae*. *Clinical infectious diseases*, *69*(7), 1101-1111.

Shah, P., and Swiatlo, E. (2006). Immunisation with polyamine transport protein PotD protects mice against systemic infection with *S. pneumoniae* (vol 74, pg 5888, 2006). *Infection and immunity*, *74*(12), 7046-7046.

Shams, F., Oldfield, N. J., Lai, S. K., Tunio, S. A., Wooldridge, K. G., and Turner, D. P. (2016). Fructose-1, 6-bisphosphate aldolase of *N. meningitidis* binds human plasminogen via its C-terminal lysine residue. *Microbiologyopen*, *5*(2), 340-350.

Sharaf, N. G., Shahgholi, M., Kim, E., Lai, J. Y., VanderVelde, D. G., Lee, A. T., and Rees, D. C. (2021). Characterisation of the ABC methionine transporter from *N. meningitidis* reveals that lipidated MetQ is required for interaction. *eLife*, *10*, e69742.

Shewell, L. K., Ku, S. C., Schulz, B. L., Jen, F. E. C., Mubaiwa, T. D., Ketterer, M. R., Apicella, M. A., and Jennings, M. P. (2013). Recombinant truncated AniA of pathogenic *Neisseria* elicits a non-native immune response and functional blocking antibodies. *Biochemical and biophysical research communications*, *431*(2), 215-220.

Shi, X., Chen, M., Yu, Z., Bell, J. M., Wang, H., Forrester, I., Villarreal, H., Jakana, J., Du, D., Luisi, B. F., Ludtke, S. J., and Wang, Z. (2019). In situ structure and assembly of the multidrug efflux pump AcrAB-TolC. *Nature Communications*, *10*(1), 2635-2636.

Siburt, C. J. P., Mietzner, T. A., and Crumbliss, A. L. (2012). FbpA—A bacterial transferrin with more to offer. *Biochimica et Biophysica Acta (BBA)-General Subjects*, *1820*(3), 379-392.

Sica, A., and Mantovani, A. (2012). Macrophage plasticity and polarisation: *in vivo* veritas. *The Journal of Clinical Investigation*, *122*(3), 787-795.

Sikora, A. E., Gomez, C., Le Van, A., Baarda, B. I., Darnell, S., Martinez, F. G., Zielke, R. A., Bonventre, J. A., and Jerse, A. E. (2020). A novel gonorrhea vaccine composed of MetQ lipoprotein formulated with CpG shortens experimental murine infection. *Vaccine*, *38*(51), 8175-8184.

Sikora, A. E., Wierzbicki, I. H., Zielke, R. A., Ryner, R. F., Korotkov, K. V., Buchanan, S. K., and Noinaj, N. (2018). Structural and functional insights into the role of BamD and BamE within the β-barrel assembly

machinery in *N. gonorrhoeae*. *Journal of Biological Chemistry*, *293*(4), 1106-1119.

Silale, A. v. d. B., Bert. (2023). TonB-dependent transport across the bacterial outer membrane. *Annual review of microbiology*, *77*(1), 67-88.

Singh, R., Liechti, G., Slade, J. A., and Maurelli, A. T. (2020). Chlamydia trachomatis oligopeptide transporter performs dual functions of oligopeptide transport and peptidoglycan recycling. *Infection and immunity*, *88*(5), 10.1128/iai. 00086-00020.

Slotboom, D. J. (2014). Structural and mechanistic insights into prokaryotic energy-coupling factor transporters. *Nature reviews. Microbiology*, *12*(2), 79-87.

Smith, E. L. (2019). *Characterisation of two outer membrane lipoproteins of N. gonorrhoeae as potential vaccine antigens. Unpublished Master's dissertation, University of Nottingham, UK.*

Snapper, C. M., and Paul, W. E. (1987). Interferon-γ and B cell stimulatory factor-1 reciprocally regulate Ig isotype production. *science*, *236*(4804), 944-947.

Solger, F., Kunz, T. C., Fink, J., Paprotka, K., Pfister, P., Hagen, F., Schumacher, F., Kleuser, B., Seibel, J., and Rudel, T. (2020). A Role of Sphingosine in the Intracellular Survival of *N. gonorrhoeae*. *Frontiers in cellular and infection microbiology*, *10*, 215.

Song, S., Wang, S., Jiang, X., Yang, F., Gao, S., Lin, X. a., Cheng, H., and van der Veen, S. (2023). Th1-polarized MtrE-based gonococcal vaccines display prophylactic and therapeutic efficacy. *Emerging Microbes & Infections*, *12*(2), 2249124.

Song, W., Yu, Q., Wang, L.-C., and Stein, D. C. (2020). Adaptation of *N. gonorrhoeae* to the Female Reproductive Tract. *Microbiology insights*, *13*, 1178636120947077-1178636120947077.

Soriani, M., Petit, P., Grifantini, R., Petracca, R., Gancitano, G., Frigimelica, E., Nardelli, F., Garcia, C., Spinelli, S., and Scarabelli, G. (2010). Exploiting antigenic diversity for vaccine design: the chlamydia ArtJ paradigm. *Journal of Biological Chemistry*, *285*(39), 30126-30138.

Sritharan, M. (2016). Iron homeostasis in Mycobacterium tuberculosis: mechanistic insights into siderophore-mediated iron uptake. *Journal of bacteriology*, *198*(18), 2399-2409.

Steichen, C. T., Cho, C., Shao, J. Q., and Apicella, M. A. (2011). The *N. gonorrhoeae* biofilm matrix contains DNA, and an endogenous nuclease controls its incorporation. *Infection and immunity*, *79*(4), 1504-1511.

Steichen, C. T., Shao, J. Q., Ketterer, M. R., and Apicella, M. A. (2008). Gonococcal cervicitis: a role for biofilm in pathogenesis. *The Journal of Infectious Diseases*, *198*(12), 1856-1861.

Stohl, E. A., Brockman, J. P., Burkle, K. L., Morimatsu, K., Kowalczykowski, S. C., and Seifert, H. S. (2003). *E. coli* RecX inhibits RecA

recombinase and coprotease activities *in vitro* and *in vivo*. *Journal of Biological Chemistry*, *278*(4), 2278-2285.

Strange, H. R., Zola, T. A., and Cornelissen, C. N. (2011). The fbpABC Operon is required for Ton-Independent utilisation of xenosiderophores by *N. gonorrhoeae* strain FA19. *Infection and immunity*, *79*(1), 267-278.

Subashchandrabose, S., and Mobley, H. L. (2015). Back to the metal age: battle for metals at the host–pathogen interface during urinary tract infection. *Metallomics*, *7*(6), 935-942.

Sun, Y.-H., Bakshi, S., Chalmers, R., and Tang, C. M. (2000). Functional genomics of *N. meningitidis* pathogenesis. *Nature medicine*, *6*(11), 1269-1273.

Sverzhinsky, A., Chung, J. W., Deme, J. C., Fabre, L., Levey, K. T., Plesa, M., Carter, D. M., Lypaczewski, P., and Coulton, J. W. (2015). Membrane protein complex ExbB4-ExbD1-TonB1 from *E. coli* demonstrates conformational plasticity. *Journal of bacteriology*, *197*(11), 1873-1885.

Tanabe, M., Atkins, H. S., Harland, D. N., Elvin, S. J., Stagg, A. J., Mirza, O., Titball, R. W., Byrne, B., and Brown, K. A. (2006). The ABC Transporter Protein OppA Provides Protection against Experimental *Yersinia pestis* Infection. *Infection and immunity*, *74*(6), 3687-3691.

Tanaka, K. J. (2019). *The Multifunctional Role of Substrate-Binding Proteins in Haem Uptake and Antimicrobial Resistance. Doctoral thesis, Northwestern University, USA.*

Tanaka, K. J., Song, S., Mason, K., and Pinkett, H. W. (2018). Selective substrate uptake: the role of ATP-binding cassette (ABC) importers in pathogenesis. *Biochimica et Biophysica Acta (BBA)-Biomembranes*, *1860*(4), 868-877.

Tanaka, M., Nakayama, H., Huruya, K., Konomi, I., Irie, S., Kanayama, A., Saika, T., and Kobayashi, I. (2006). Analysis of mutations within multiple genes associated with resistance in a clinical isolate of *N. gonorrhoeae* with reduced ceftriaxone susceptibility that shows a multidrug-resistant phenotype. *International journal of antimicrobial agents*, *27*(1), 20-26.

Taniguchi, M., and Lindsey, J. S. (2023). Absorption and fluorescence spectra of open-chain tetrapyrrole pigments–bilirubins, biliverdins, phycobilins, and synthetic analogues. *Journal of Photochemistry and Photobiology C: Photochemistry Reviews*. *55*, 100585.

Tapsall, J. W., Ndowa, F., Lewis, D. A., and Unemo, M. (2009). Meeting the public health challenge of multidrug-and extensively drug-resistant *N. gonorrhoeae*. *Expert review of anti-infective therapy*, *7*(7), 821-834.

Taylor, B. D., Ness, R. B., Darville, T., and Haggerty, C. L. (2011). Microbial correlates of delayed care for pelvic inflammatory disease. *Sexually transmitted diseases*, *38*(5), 434-438.

ter Beek, J., Duurkens, R. H., Erkens, G. B., and Slotboom, D. J. (2011). Quaternary Structure and Functional Unit of Energy Coupling Factor

(ECF)-type Transporters. *The Journal of biological chemistry*, *286*(7), 5471-5475.

Terkelsen, D., Tolstrup, J., Johnsen, C. H., Lund, O., Larsen, H. K., Worning, P., Unemo, M., and Westh, H. (2017). Multidrug-resistant *N. gonorrhoeae* infection with ceftriaxone resistance and intermediate resistance to azithromycin, Denmark, 2017. *Eurosurveillance*, *22*(42), 17-00659.

Thomas, C., and Tampé, R. (2018). Multifaceted structures and mechanisms of ABC transport systems in health and disease. *Current opinion in structural biology*, *51*, 116-128.

Thomas, C., and Tampé, R. (2020). Structural and Mechanistic Principles of ABC Transporters. *Annual review of biochemistry*, *89*(1), 605-636.

Toh, Z. Q., Higgins, R. A., Mazarakis, N., Abbott, E., Nathanielsz, J., Balloch, A., Mulholland, K., and Licciardi, P. V. (2021). Evaluating functional immunity following encapsulated bacterial infection and vaccination. *Vaccines*, *9*(6), 677.

Tramont, E. C., and Boslego, J. W. (1985). Pilus vaccines. *Vaccine*, *3*(1), 3-10.

Tsolakos, N., Brookes, C., Taylor, S., Gorringe, A., Tang, C. M., Feavers, I. M., and Wheeler, J. X. (2014). Identification of vaccine antigens using integrated proteomic analyses of surface immunogens from serogroup B *N. meningitidis*. *Journal of proteomics*, *101*, 63-76.

Tzeng, Y.-L., Sannigrahi, S., Borrow, R., and Stephens, D. S. (2024). *N. gonorrhoeae* lipooligosaccharide glycan epitopes recognised by bactericidal IgG antibodies elicited by the meningococcal group B-directed vaccine, MenB-4C. *Frontiers in immunology*, *15*, 1350344.

UKHSA. (2023). UK Health Security Agency (2023). English surveillance programme for antimicrobial utilisation and resistance (ESPAUR) report 2022 to 2023. GOV.UK. [Online]. Available at: https://iris.who.int/bitstream/handle/10665/44863/9789241503501_eng.pdf [Accessed 3 February 2025].

UKHSA. (2024). UK Health Security Agency. (2024). Antibiotic-resistant gonorrhoea cases are on the rise. GOV.UK. [Online]. Available at: https://www.gov.uk/government/news/antibiotic-resistant-gonorrhoea-cases-are-on-the-rise [Accessed 6 December 2024].

UKHSA. (2025). UK Health Security Agency (2025). Ceftriaxone-resistant *N. gonorrhoeae*: Increasing cases, including transmission associated with sex workers, Briefing Note 2025/017. GOV.UK. [Online]. Available at: https://frimley.icb.nhs.uk/doclink/20250617-bn2025-017-ceftriaxone-resistantn-gonorrhoeae-v01-00/eyj0exaioijkv1qilcjhbgcioijiuzi1nij9.eyjzdwiioiiymdi1mdyxny1ibjiwmjutmde3lwnlznryawf4b25llxjlc2lzdgfudg4tz29ub3jyag9lywutdjaxltawiiwiawf0ijoxnzuwmzi3nzm3lcjlehaioje3nta0mtqxmzd9.soved-nwqv6dwtifue61hm5c78onpblvvak9ps-dm0e [Accessed 3 Jul. 2025].

Unemo, á., Golparian, D., and Hestner, A. (2011). Ceftriaxone treatment failure of pharyngeal gonorrhoea verified by international recommendations, Sweden, July 2010. *Eurosurveillance*, *16*(6), 19792.

Unemo, M. (2015). Current and future antimicrobial treatment of gonorrhoea - the rapidly evolving *N. gonorrhoeae* continues to challenge. *BMC infectious diseases*, *15*(1), 364.

Unemo, M., Golparian, D., Nicholas, R., Ohnishi, M., Gallay, A., and Sednaoui, P. (2012). High-level cefixime-and ceftriaxone-resistant *N. gonorrhoeae* in France: novel penA mosaic allele in a successful international clone causes treatment failure. *Antimicrobial Agents and Chemotherapy*, *56*(3), 1273-1280.

Unemo, M., Golparian, D., Syversen, G., Vestrheim, D., and Moi, H. (2010). Two cases of verified clinical failures using internationally recommended first-line cefixime for gonorrhoea treatment, Norway, 2010. *Eurosurveillance*, *15*(47), 19721.

Unemo, M., and Jensen, J. S. (2017). Antimicrobial-resistant sexually transmitted infections: Gonorrhoea and Mycoplasma genitalium. *Nature reviews. Urology*, *14*(3), 139-152.

Unemo, M., Lahra, M. M., Cole, M., Galarza, P., Ndowa, F., Martin, I., Dillon, J.-A. R., Ramon-Pardo, P., Bolan, G., and Wi, T. (2019). World Health Organisation Global Gonococcal Antimicrobial Surveillance Program (WHO GASP): review of new data and evidence to inform international collaborative actions and research efforts. *Sexual health*, *16*(5), 412-425.

Unemo, M., Lahra, M. M., Escher, M., Eremin, S., Cole, M. J., Galarza, P., Ndowa, F., Martin, I., Dillon, J.-A. R., and Galas, M. (2021). WHO global antimicrobial resistance surveillance for *N. gonorrhoeae* 2017–18: a retrospective observational study. *The Lancet Microbe*, *2*(11), e627-e636.

Unemo, M., Olcén, P., Berglund, T., Albert, J., and Fredlund, H. (2002). Molecular epidemiology of *N. gonorrhoeae*: sequence analysis of the porB gene confirms presence of two circulating strains. *Journal of Clinical Microbiology*, *40*(10), 3741-3749.

Unemo, M., Sánchez-Busó, L., Golparian, D., Jacobsson, S., Shimuta, K., Lan, P. T., Eyre, D. W., Cole, M., Maatouk, I., and Wi, T. (2024). The novel 2024 WHO *N. gonorrhoeae* reference strains for global quality assurance of laboratory investigations and superseded WHO *N. gonorrhoeae* reference strains phenotypic, genetic and reference genome characterisation. *Journal of antimicrobial chemotherapy*, dkae176.

Unemo, M., and Shafer, W. M. (2014). Antimicrobial resistance in *N. gonorrhoeae* in the 21st century: past, evolution, and future. *Clinical microbiology reviews*, *27*(3), 587-613.

Unemo, M., Vorobieva, V., Firsova, N., Ababkova, T., Leniv, I., Haldorsen, B., Fredlund, H., and Skogen, V. (2007). *N. gonorrhoeae* population in

Arkhangelsk, Russia: phenotypic and genotypic heterogeneity. *Clinical Microbiology and Infection*, *13*(9), 873-878.

Vahedi-Faridi, A., Eckey, V., Scheffel, F., Alings, C., Landmesser, H., Schneider, E., and Saenger, W. (2008). Crystal structures and mutational analysis of the arginine-, lysine-, histidine-binding protein ArtJ from *Geobacillus stearothermophilus*. Implications for interactions of ArtJ with its cognate ATP-binding cassette transporter, Art (MP) 2. *Journal of molecular biology*, *375*(2), 448-459.

Vallely, L. M., Egli-Gany, D., Wand, H., Pomat, W. S., Homer, C. S., Guy, R., Silver, B., Rumbold, A. R., Kaldor, J. M., and Vallely, A. J. (2021). Adverse pregnancy and neonatal outcomes associated with *N. gonorrhoeae*: systematic review and meta-analysis. *Sexually transmitted infections*, *97*(2), 104-111.

Van der Heide, T., and Poolman, B. (2002). ABC transporters: one, two or four extracytoplasmic substrate-binding sites? *EMBO reports*, *3*(10), 938-943.

Van Der Pol, L., Stork, M., and van der Ley, P. (2015). Outer membrane vesicles as platform vaccine technology. *Biotechnology journal*, *10*(11), 1689-1706.

Vermont, C. v. d. D., Germie. (2002). *N. meningitidis* serogroup B: laboratory correlates of protection. *FEMS immunology and medical microbiology*, *34*(2), 89-96.

Viola, A., Munari, F., Sánchez-Rodríguez, R., Scolaro, T., and Castegna, A. (2019). The Metabolic Signature of Macrophage Responses. *Frontiers in immunology*, *10*, 1462.

Viscidi, R. P., Demma, J. C., Gu, J., and Zenilman, J. (2000). Comparison of sequencing of the por gene and typing of the opa gene for discrimination of *N. gonorrhoeae* strains from sexual contacts. *Journal of Clinical Microbiology*, *38*(12), 4430-4438.

Waidmann, M. S., Bleichrodt, F. S., Laslo, T., and Riedel, C. U. (2011). Bacterial luciferase reporters: the Swiss army knife of molecular biology. *Bioengineered bugs*, *2*(1), 8-16.

Walker, E., Van Niekerk, S., Hanning, K., Kelton, W., and Hicks, J. (2023). Mechanisms of host manipulation by *N. gonorrhoeae*. *Frontiers in microbiology*, *14*, 1119834.

Wang, B., Giles, L., Andraweera, P., McMillan, M., Almond, S., Beazley, R., Mitchell, J., Ahoure, M., Denehy, E., and Flood, L. (2023). 4CMenB sustained vaccine effectiveness against invasive meningococcal B disease and gonorrhoea at three years post programme implementation. *Journal of Infection*, *87*(2), 95-102.

Wang, G., Zhao, J., Zhang, X., Li, S., Sun, C., and Gu, G. (2025). Immunological studies of Burkholderia multivorans O-antigen oligosaccharide-rsScpA193 conjugates as potential candidates for vaccine development. *International Journal of Biological Macromolecules*, *287*, 138570.

Wang, J., Xiong, K., Pan, Q., He, W., and Cong, Y. (2021). Application of TonB-Dependent Transporters in Vaccine Development of Gram-Negative Bacteria. *Frontiers in cellular and infection microbiology*, *10*, 589115-589115.

Wang, S., Xue, J., Lu, P., Ni, C., Cheng, H., Han, R., and van der Veen, S. (2018). Gonococcal MtrE and its surface-expressed Loop 2 are immunogenic and elicit bactericidal antibodies. *The Journal of infection*, *77*(3), 191-204.

Warner, D. M., Folster, J. P., Shafer, W. M., and Jerse, A. E. (2007). Regulation of the MtrC-MtrD-MtrE Efflux-Pump System Modulates the *In Vivo* Fitness of *N. gonorrhoeae*. *The Journal of Infectious Diseases*, *196*(12), 1804-1812.

Warner, D. M., Shafer, W. M., and Jerse, A. E. (2008). Clinically relevant mutations that cause derepression of the *N. gonorrhoeae* MtrC-MtrD-MtrE Efflux pump system confer different levels of antimicrobial resistance and *in vivo* fitness. *Molecular microbiology*, *70*(2), 462-478.

Watkins, R. R., Thapaliya, D., Lemonovich, T. L., and Bonomo, R. A. (2023). Gepotidacin: a novel, oral,'first-in-class' triazaacenaphthylene antibiotic for the treatment of uncomplicated urinary tract infections and urogenital gonorrhoea. *Journal of Antimicrobial Chemotherapy*, *78*(5), 1137-1142.

Weerasinghe, A. J., Amin, S. A., Barker, R. A., Othman, T., Romano, A. N., Parker Siburt, C. J., Tisnado, J., Lambert, L. A., Huxford, T., Carrano, C. J., and Crumbliss, A. L. (2013). Borate as a Synergistic Anion for Marinobacter algicola Ferric Binding Protein, FbpA: A Role for Boron in Iron Transport in Marine Life. *Journal of the American Chemical Society*, *135*(39), 14504-14507.

Wetzler, L. M. (2010). Innate immune function of the neisserial porins and the relationship to vaccine adjuvant activity. *Future microbiology*, *5*(5), 749-758.

Whalan, R. H., Funnell, S. G. P., Bowler, L. D., Hudson, M. J., Robinson, A., and Dowson, C. G. (2005). PiuA and PiaA, iron uptake lipoproteins of *S. pneumoniae*, elicit serotype independent antibody responses following human *pneumococcal* septicaemia. *FEMS immunology and medical microbiology*, *43*(1), 73-80.

Whelan, J., Abbing-Karahagopian, V., Serino, L., and Unemo, M. (2021). Gonorrhoea: a systematic review of prevalence reporting globally. *BMC infectious diseases*, *21*(1), 1152.

Whelan, J., Kløvstad, H., Haugen, I. L., van Beest, M. R.-D. R., and Storsaeter, J. (2016). Ecologic study of meningococcal B vaccine and *N. gonorrhoeae* infection, Norway. *Emerging infectious diseases*, *22*(6), 1137.

Whiley, D. M., Jennison, A., Pearson, J., and Lahra, M. M. (2018). Genetic characterisation of *N. gonorrhoeae* resistant to both ceftriaxone and azithromycin. *The Lancet infectious diseases*, *18*(7), 717-718.

WHO. (2012). World Health Organisation. (2012). Global action plan to control the spread and impact of antimicrobial resistance in *N. gonorrhoeae*. [Online]. Available at: https://iris.who.int/bitstream/handle/10665/44863/9789241503501_eng.pdf [Accessed 6 November 2024].

WHO. (2016). World Health Organisation (2016). Global health sector strategy on sexually transmitted infections, 2016–2021. [Online]. Available at: https://www.who.int/publications/i/item/WHO-RHR-16.09 (Accessed: 6 November 2024).

WHO. (2021). World Health Organisation (2021). Global progress report on HIV, viral hepatitis and sexually transmitted infections, 2021. [Online]. Available at: https://www.who.int/publications/i/item/9789240027077 (Accessed: 31 July 2024).

WHO. (2023). World Health Organisation. (2023). Enhanced Gonococcal Antimicrobial Surveillance Programme (EGASP): Surveillance report 2023. [Online]. Available at: https://www.who.int/publications/i/item/9789240102927 (Accessed: 15 November 2024).

WHO. (2024). World Health Organisation (2024). Multi-drug-resistant gonorrhoea. [Online]. Available at: https://www.who.int/news-room/fact-sheets/detail/multi-drug-resistant-gonorrhoea (Accessed: 31 July 2024).

Wierzbicki, I. H., Zielke, R. A., Korotkov, K. V., and Sikora, A. E. (2017). Functional and structural studies on the *N. gonorrhoeae* GmhA, the first enzyme in the glycero-manno-heptose biosynthesis pathways, demonstrate a critical role in lipooligosaccharide synthesis and gonococcal viability. *Microbiologyopen*, *6*(2), e00432.

Williams, A. D. N., Wood, F., Gillespie, D., Couzens, Z., Hughes, K., and Hood, K. (2022). The relationship between HIV pre-exposure prophylaxis, sexually transmitted infections, and antimicrobial resistance: a qualitative interview study of men who have sex with men. *BMC Public Health*, *22*(1), 2222.

Williams, E., Seib, K. L., Fairley, C. K., Pollock, G. L., Hocking, J. S., McCarthy, J. S., and Williamson, D. A. (2024). *N. gonorrhoeae* vaccines: a contemporary overview. *Clinical microbiology reviews*, *37*(1), e00094-00023.

Williams, J. (2018). *Expression and purification of outer membrane lipoproteins of N. gonorrhoeae as potential vaccine antigens. Unpublished Master's dissertation, University of Nottingham, UK.*

Williams, J. N., Skipp, P. J., O'Connor, C. D., Christodoulides, M., and Heckels, J. E. (2009). Immunoproteomic analysis of the development of natural immunity in subjects colonised by *N. meningitidis* reveals potential vaccine candidates. *Infection and immunity*, *77*(11), 5080-5089.

Winer, D. A., Winer, S., Shen, L., Wadia, P. P., Yantha, J., Paltser, G., Tsui, H., Wu, P., Davidson, M. G., and Alonso, M. N. (2011). B cells promote insulin resistance through modulation of T cells and production of pathogenic IgG antibodies. *Nature Medicine*, *17*(5), 610-617.

Wise, J. (2020). Gonorrhoea cases in England hit highest level since records began. *BMJ*, *370*, m3425-m3425.

Wolfgang, M., van Putten, J. P., Hayes, S. F., Dorward, D., and Koomey, M. (2000). Components and dynamics of fibre formation define a ubiquitous biogenesis pathway for bacterial pili. *The EMBO journal*, *19*(23), 6408-6418.

Xie, C. B., Jane-Wit, D., and Pober, J. S. (2020). Complement membrane attack complex: new roles, mechanisms of action, and therapeutic targets. *The American Journal of Pathology*, *190*(6), 1138-1150.

Xue, Y., and Ha, Y. (2013). Large Lateral Movement of Transmembrane Helix S5 Is Not Required for Substrate Access to the Active Site of Rhomboid Intramembrane Protease. *The Journal of biological chemistry*, *288*(23), 16645-16654.

Yadav, R., Noinaj, N., Ostan, N., Moraes, T., Stoudenmire, J., Maurakis, S., and Cornelissen, C. N. (2020). Structural Basis for Evasion of Nutritional Immunity by the Pathogenic *Neisseriae*. *Frontiers in microbiology*, *10*, 2981-2981.

Yang, M., Johnson, A., and Murphy, T. F. (2011). Characterisation and Evaluation of the *Moraxella catarrhalis* Oligopeptide Permease A as a Mucosal Vaccine Antigen. *Infection and immunity*, *79*(2), 846-857.

Yang, Y., Zhao, J., Morgan, R. L., Ma, W., and Jiang, T. (2010). Computational prediction of type III secreted proteins from gram-negative bacteria. *BMC bioinformatics*, *11*(1), S47-S47.

Yokoi, S., Deguchi, T., Ozawa, T., Yasuda, M., Ito, S.-i., Kubota, Y., Tamaki, M., and Maeda, S.-i. (2007). Threat to cefixime treatment for gonorrhoea. *Emerging infectious diseases*, *13*(8), 1275.

Young, E. C., Baumgartner, J. T., Karatan, E., and Kuhn, M. L. (2021). A mutagenic screen reveals nsps residues important for regulation of *Vibrio Cholerae* biofilm formation. *Microbiology (Society for General Microbiology)*, *167*(3).

Yu, S., Lee, N. Y., Park, S.-J., and Rhee, S. (2011). Crystal structure of toll-like receptor 2-activating lipoprotein IIpA from *Vibrio vulnificus*. *Proteins, structure, function, and bioinformatics*, *79*(3), 1020-1025.

Yuen, R., Kuniholm, J., Lisk, C., and Wetzler, L. M. (2019). Neisserial PorB immune-enhancing activity and use as a vaccine adjuvant. *Human vaccines & immunotherapeutics*, *15*(11), 2778-2781.

Zackular, J. P., Chazin, W. J., and Skaar, E. P. (2015). Nutritional Immunity: S100 Proteins at the Host-Pathogen Interface. *The Journal of biological chemistry*, *290*(31), 18991-18998.

Zafar, H., and Saier Jr, M. H. (2018). Comparative genomics of transport proteins in seven Bacteroides species. *PloS one*, *13*(12), e0208151.

Zak, K., Diaz, J.-L., Jackson, D., and Heckels, J. (1984). Antigenic variation during infection with *N. gonorrhoeae*: detection of antibodies to surface

proteins in sera of patients with gonorrhea. *Journal of Infectious Diseases*, *149*(2), 166-174.

Zariri, A., van Dijken, H., Hamstra, H.-J., van der Flier, M., Vidarsson, G., van Putten, J. P. M., Boog, C. J. P., van den Dobbelsteen, G., and van der Ley, P. (2013). Expression of human CEACAM1 in transgenic mice limits the Opa-specific immune response against meningococcal outer membrane vesicles. *Vaccine*, *31*(47), 5585-5593.

Zhu, T., McClure, R., Harrison, O. B., Genco, C., and Massari, P. (2019). Integrated bioinformatic analyses and immune characterisation of new *N. gonorrhoeae* vaccine antigens expressed during natural mucosal infection. *Vaccines*, *7*(4), 153.

Zhu, W., Cardenas-Alvarez, M. X., Tomberg, J., Little, M. B., Duncan, J. A., and Nicholas, R. A. (2023). Commensal *Neisseria* species share immune suppressive mechanisms with *N. gonorrhoeae*. *PloS one*, *18*(4), e0284062.

Zhu, W., Tomberg, J., Knilans, K. J., Anderson, J. E., McKinnon, K. P., Sempowski, G. D., Nicholas, R. A., and Duncan, J. A. (2018). Properly folded and functional PorB from *N. gonorrhoeae* inhibits dendritic cell stimulation of CD4+ T cell proliferation. *The Journal of biological chemistry*, *293*(28), 11218-11229.

Zhu, W., Waltmann, A., Little, M. B., Connolly, K. L., Matthias, K. A., Thomas, K. S., Gray, M. C., Sikora, A. E., Criss, A. K., and Bash, M. C. (2025). Protection against *N. gonorrhoeae* induced by OMV-based Meningococcal Vaccines are associated with cross-species directed humoral and cellular immune responses. *Frontiers in immunology*, *16*, 1539795.

Zielke, R. A., Gafken, P. R., and Sikora, A. E. (2014). Quantitative Proteomic Analysis of the Cell Envelopes and Native Membrane Vesicles Derived from Gram-Negative Bacteria. *Current Protocols in Microbiology*, *34*(1), 1F. 3.1-1F. 3.16.

Zielke, R. A., Le Van, A., Baarda, B. I., Herrera, M. F., Acosta, C. J., Jerse, A. E., and Sikora, A. E. (2018). SliC is a surface-displayed lipoprotein that is required for the anti-lysozyme strategy during *N. onorrhoeae* infection. *PLoS pathogens*, *14*(7), e1007081.

Zielke, R. A., Wierzbicki, I. H., Baarda, B. I., Gafken, P. R., Soge, O. O., Holmes, K. K., Jerse, A. E., Unemo, M., and Sikora, A. E. (2016). Proteomics-driven antigen discovery for development of vaccines against gonorrhea. *Molecular & Cellular Proteomics*, *15*(7), 2338-2355.

Zughaier, S. M., Kandler, J. L., and Shafer, W. M. (2014). *N. gonorrhoeae* modulates iron-limiting innate immune defences in macrophages. *PloS one*, *9*(1), e87688-e87688.

Appendices

Appendix-1: Solution and reagents

Agarose Gel Preparation: Agarose gel was prepared by dissolving 1 g of agarose powder (Sigma-Aldrich, UK) in 100 mL of 1× TAE buffer and melting the mixture. After complete dissolution, 10 µL of SYBR™ Safe DNA Gel Stain (Invitrogen™) was added.10% SDS Solution: A 10% SDS solution was prepared by dissolving 1 g of SDS in 100 mL of dH_2O.

Lysogeny Broth (LB) and LB Agar: 18 g of LB powder (standard components: tryptone 10 g/L, yeast extract 5 g/L, NaCl 10 g/L) (Oxoid, Thermo Fisher Scientific, UK) was dissolved in deionised water (dH_2O). For LB broth, the solution was autoclaved at 121 °C for 15 min, cooled to ~50–60 °C, and, if required, kanamycin was added to a final concentration of 80 µg/mL before inoculating *E. coli*. For LB agar, agar (15 g/L) was included, and after autoclaving and cooling to ~50–60 °C, kanamycin (80 µg/mL, if required) was added. The LB agar was poured into Petri dishes within a biosafety cabinet and allowed to solidify. All media were stored at 4 °C until use.

Gonococci Agar Media: A 7.3% (w/v) solution was prepared by suspending 14.4 g of GC agar from Thayer Martin Medium Agar (Thermo Fisher, UK) in 196 mL of dH_2O and mixing thoroughly to ensure complete dissolution. The mixture was sterilised by autoclaving at 121 °C for 15 min and allowed to cool to 50–60 °C. At this temperature, 200 mL of soluble haemoglobin and 4 mL of Vitox supplement were added. Antibiotics were included if required: kanamycin (400 µL of an 80 µg/mL stock) or erythromycin (16 µL of a 50 µg/mL stock). The agar mixture was then carefully poured into Petri dishes inside a biosafety cabinet to minimise contamination. Once solidified, the plates were stored at 4 °C until use**.**

Soluble Haemoglobin Solution: A 2% (w/v) solution was prepared by dissolving 4 g of soluble haemoglobin powder (Thermo Fisher, UK) in 200 mL of warm distilled water, with continuous stirring using a magnetic stirrer on a hot plate set to 70 °C. The mixture was heated and stirred for 1 h to ensure complete solubilisation and was then sterilised by autoclaving.

Vitox Supplement: Oxoid Vitox Supplement liquid (Catalogue number: SR0090A, Oxoid, UK) was mixed with the powdered components according to the manufacturer's instructions. The prepared Vitox Supplement was stored at −20 °C. Aseptically, 4 mL (1% v/v) of the Vitox Supplement was added to 400 mL of sterile BHI broth or to 200 mL of cooled GC agar containing 200 mL of soluble haemoglobin.

Brain Heart Infusion (BHI) broth: This was prepared by dissolving 14.4 g of BHI powder (Oxoid, Thermo Fisher Scientific, UK) in 400 mL of dH_2O, autoclaving at 121 °C for 15 min, and allowing it to cool to RT. The medium was pre-warmed to 37 °C before inoculation with *N. gonorrhoeae*. At this stage, 4 mL of Vitox supplement (1% v/v) was added to enhance bacterial growth, and IPTG was incorporated to a final concentration of 0.005% (v/v) when induction of gene expression was required.

IPTG: A 1 M IPTG stock solution was prepared by dissolving 0.238 g of IPTG (Isopropyl β-D-1-thiogalactopyranoside) in 1 mL of dH_2O. The solution was sterilised by filtration through a 0.22 µm filter and stored at −20 °C.

Table S1. Preparation of Antibiotic Stock Solutions

Antibiotic	Stock Concentration (mg/mL)	Solvent
Kanamycin	80	dH_2O
Streptomycin	200	dH_2O
Erythromycin	2	Ethanol

All antibiotics were purchased from Sigma-Aldrich, UK and prepared according to the manufacturer's instructions, sterilised through a 0.2 µm filter and stored at 4 °C until use.

Preparation of Sodium Dodecyl Sulfate (SDS) Buffers

Buffer A: This buffer was prepared by dissolving 181.7 g of Tris base and 40 mL of 10% (w/v) SDS in 100 mL of dH_2O. The final volume was brought to 1 L with dH_2O, and the pH was then adjusted to 8.8 by adding HCl dropwise while stirring continuously with a magnetic stirrer.

Buffer B: This buffer was prepared by dissolving 60.6 g of Tris base and 40 mL of 10% (w/v) SDS in dH_2O, and the final volume of the buffer was brought to 1 L with dH_2O. The pH was adjusted to 6.8 by adding HCl dropwise,

10% Sodium Dodecyl Sulfate (SDS): 10 g of SDS ($NaC_{12}H_{25}SO_4$, MW: 288.38 g/mol) was dissolved in 100 mL of dH_2O. For the preparation of Buffer A or Buffer B, 20 mL of this 10% SDS solution was added to achieve a final concentration of 0.4%.

SDS-Running Buffer (10×): This buffer was prepared by dissolving 30.3 g (w/v) of Tris base, 144 g (w/v) of glycine, and 10 g (w/v) of SDS in dH_2O, and adjusting the final volume to 1 L.

Table S2. Preparation of mini gel (10%).

Component	Resolving (separating) gel (10% acrylamide) strength	Stacking gel
Buffer A	2.5 mL	-
Buffer B	-	1.3
Acrylamide (30%)	3.3 mL	1
dH_2O	4.1 mL	2.7
10% Ammonium persulfate (APS) for polymerisation	45 µL	35 µL
Tetramethyl ethylenediamine (TEMED)	45 µL	35 µL

Coomassie Blue stock: was prepared by mixing 250 mL of 50% methanol, 51 mL of acetic acid, and 10 mL of Coomassie Blue (1.2 g/L).

Destaining Solution: A destaining solution was prepared by adding 10 mL of 10% (v/v) methanol/acetic acid to 80 mL of dH_2O.

TAE Buffer (50× Stock): This buffer was prepared by dissolving 242 g (w/v) of Tris base (Life Technologies), 18.6 g (w/v) of EDTA, and adding 57.1 mL (v/v) of glacial acetic acid (Fisher Chemicals) in dH_2O to a final volume of 1 L. The pH was adjusted to 8.0 by the dropwise addition of HCl while the solution was continuously mixed using a magnetic stirrer.

Table S3. 5× SDS-PAGE sample buffer.

Component	Amount	Details
2M Tris-HCl (pH 6.8)	7.8125 mL	From a 2M stock solution
5% SDS	1.25 g	-
25% Glycerol	6.25 mL	-
12.5% β-Mercaptoethanol	3.125 mL	-
0.002% Bromophenol Blue	A small spatula tip	Adjust to 0.002% final concentration
dH_2O	15.625 mL	Adjust to 25 mL final volume

Preparation of Western Blotting Buffers and Reagents

Western Transfer Buffer (WTB): WTB was prepared by dissolving 5.82 g of Tris base and 2.9 g of glycine in 100 mL of dH_2O. Then, 3.75 mL of 10% (w/v) SDS (sodium dodecyl sulfate) was added, followed by 200 mL of methanol (v/v). Then, the solution was brought up to a final volume of 1 L with dH_2O. The WTB was used for the transfer of proteins during the Western blotting procedure.

Ammonium Persulfate (APS): A 10% (w/v) APS solution was prepared by dissolving 1 g of APS in 10 mL of dH_2O. Subsequently, the solution was filtered through a 0.22 µm sterilised filter and stored at 4 °C. APS was used as an accelerator for the polymerisation of acrylamide gels.

N**,N,N',N'-Tetramethyl Ethylenediamine (TEMED):** UltraPure™ pre-made solutions (Sigma-Aldrich, UK) are commonly used as an accelerator for the polymerisation of acrylamide gels. For preparation, 45 µL of TEMED was used with Buffer A and 35 µL with Stack Buffer B.

SDS-PAGE Running Buffer (1 ×): To prepare a 1X SDS-PAGE running buffer, 200 mL of the 10 × Thermo Scientific Tris-glycine-SDS running buffer (pH 8.3) was added to 1800 mL of dH_2O.

Protein Markers: 7 µL of Colour-Plus Pre-stained Standard, Broad Range P7719S (10–250 kDa) (NEB, UK), was loaded onto a 10–20 % SDS-PAGE gel.

Protein Transfer to the Nitrocellulose Membrane: Subsequent protein samples were separated on 10% SDS-PAGE gels **at** 124 V and 400 mA until complete protein separation in an Invitrogen Mini Gel Tank (Invitrogen™, Fisher Scientific, UK). The transfer sandwich was prepared as follows: filter

papers were soaked in Western Blot Transfer Buffer and placed on the flat surface of the Trans-Blot® SD Semi-Dry Transfer Cell apparatus (Bio-Rad, USA), and a laminating or rubber roller was used to press the filter papers or membrane evenly. The nitrocellulose membrane (Amersham™ Protran™ 0.2 µm, Cytiva, USA) was equilibrated in transfer buffer and placed on top of the first filter paper. The gel was then carefully positioned on the membrane, followed by a second pre-soaked filter paper. The entire assembly was gently rolled with a rubber roller to remove excess buffer and air bubbles, ensuring uniform contact. The completed sandwich was placed into the Trans-Blot® SD Semi-Dry Transfer Cell apparatus, maintaining the correct orientation from **cathode (–) to anode (+)** as follows: pre-soaked filter paper → gel → membrane → pre-soaked filter paper. Proteins were transferred using the Trans-Blot® SD Semi-Dry Transfer Cell (Bio-Rad, USA) with the PowerPac™ HC High-Current Power Supply (Bio-Rad, USA) set to 12 V and 400 mA for 12 min.

Phosphate Buffered Saline Solution (PBS): PBS was prepared by dissolving one tablet of phosphate-buffered saline (Dulbecco A, Oxoid) in 100 mL of dH_2O. The solution was then sterilised by filtration through a 0.22 µm membrane filter and autoclaved.

Blocking Buffer Solution: The buffer was prepared as a 0.5% (w/v) solution by dissolving 0.100 g of skimmed milk powder in 20 mL of PBS containing 0.05% (v/v) Tween 20 and was used for blocking non-specific binding sites during immunodetection procedures.

Washing Phosphate-Buffered Saline Solution with Tween 20 (PBS-T): The PBS-T washing buffer was prepared by adding 250 µL of Tween 20 (v/v) to 400 mL of sterilised and filtered PBS.

Primary Antibodies:

Anti-rabbit-NGO1152 and anti-rabbit-NGO0206 polyclone antibodies were used at a 1:100,000 (v/v) dilution. Briefly, 2 µL of antibody was added to 198 µL of PBS-T, and then 20 µL of this dilution was added to 20 mL of blocking buffer solution.

Secondary Antibodies:

Bio-Rad Blotting Guard Affinity-Purified Goat Anti-Rabbit IgG (H+L)-

AP Conjugate: This antibody was used at a 1:10,000 (v/v) dilution by adding 2 µL of the secondary antibody to 20 mL of blocking buffer.

Goat Anti-Rabbit IgG (Conjugated) Alkaline Phosphatase: This antibody was initially diluted 1:1,000 and then further diluted to 1:10,000 (v/v) in 20 mL of blocking buffer (Sodium Dodecyl Sulfate; Sigma-Aldrich, USA)

BCIP®/NBT-Blue Liquid Substrate System for Membranes: This pre-made alkaline phosphatase substrate system consists of 5-bromo-4-chloro-3-indolyl phosphate (BCIP) and nitro blue tetrazolium (NBT) liquid substrate (Sigma, USA). The BCIP stock solution was stored at 4 °C in a brown bottle to protect it from light. For each assay, 2 mL of the substrate solution was used for immunoblotting detection.

Bactericidal activity assay:

Blocking Buffer: A blocking buffer containing 1–5% (w/v) bovine serum albumin (BSA; Sigma-Aldrich, UK) was prepared by dissolving 1–5 g of BSA in 100 mL of sterile PBS, followed by filtration through a 0.22 µm membrane filter for sterilisation.

Bactericidal Buffer: The bactericidal buffer was prepared by dissolving 0.5 g of BSA-free immunoglobulin (IgG, A3059; Sigma-Aldrich, USA), free from protease and globin, in 100 mL of pre-made Dulbecco's Phosphate Buffered Saline (1× DPBS, pH 7.4) to obtain a final concentration of 0.5% (w/v). The buffer was supplemented with $MgCl_2$ and $CaCl_2$ (Sigma-Aldrich, UK), heated at 56 °C for 15 min to inactivate any residual complement activity, then filtered through a sterile 0.2 µm membrane filter, and stored at −20 °C.

Appendix-2: Multiple alignment sequences

Supplement 1. Evaluate the similarity of the multiple alignment sequence between NGO0206, NGO1152, and NMB1612 from *N. meningitidis* MC58

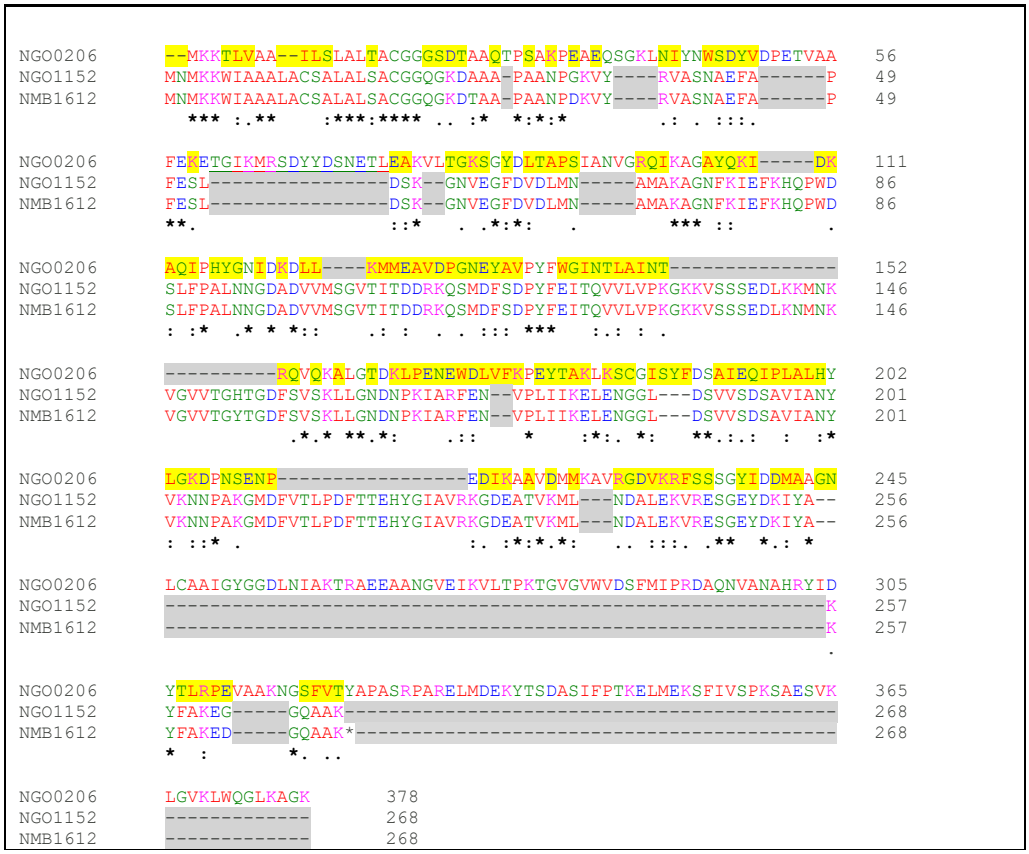

Figure S1. Multiple amino acid sequence alignment analysis between FA1090-NGO0206 (378 amino acids), NGO1152-FA1090 (268 amino acids), and NMB1612 (268 amino acids), as a putative amino acid-binding lipoprotein transporter from *N. meningitidis* MC58. Alignment was genera ted using Clustal Omega [https://www.ebi.ac.uk/Tools/msa/clustalo/].
Additionally, specific symbols are employed to denote the nature of the amino acid changes, substitutions, or absence at each aligned position, thus providing further resolution in interpreting the sequence variability. For example, an asterisk (*) indicates positions which are identical across all aligned sequences. A colon (:) indicates a change in the amino acid at that position to one with highly similar biochemical properties (a conservative substitution). A decimal point (.) indicates a change in the amino acid at that position to one with slightly comparable properties (a semi-conservative substitution). A gap (-) in the alignment represents a missing amino acid residue at that position compared to other sequences. A space (no symbol) indicates a substitution for an amino acid with dissimilar properties. Colours represent different residue properties: red (AVFPMILW; small hydrophobic), blue (DE; acidic), magenta (RK; with basic-H) and green (STYHCNGQ; hydroxyl, sulfhydryl, amine, and G).